

Postglacial paleoenvironmental history of the Southern Patagonian Fjords at 53°S

Inaugural-Dissertation

zur

Erlangung des Doktorgrades

der Mathematisch-Naturwissenschaftlichen Fakultät

der Universität zu Köln



vorgelegt von

Jean P. Francois S.

aus Santiago de Chile

Köln, 2014

Berichtersteller: Prof. Dr. Frank Schäbitz
Prof. Dr. Olaf Bubenzer

Vorsitzender der
Prüfungskommission: Prof. Dr. Martin Melles

Tag der mündlichen Prüfung: 7. Juli. 2014

A mi familia

Abstract

Southern Patagonia (50°-56°S) is a key region for paleoenvironmental studies, in particular, for addressing fundamental paleoclimatic and paleoecological questions. This is due to a number of physical and biotic characteristics of the region: (i) its location allows to examine and reconstruct changes of the Southern Westerly Wind (SWW) belt, (ii) the presence of the Andes, which intercepts the flux of the SWWs creating a strong orographic precipitation gradient on a west-east axis, and (iii) consequently the development and succession of distinct ecosystems along this gradient.

This thesis aims to investigate the vegetational history of Southern Patagonia through space and time and assess the various physical parameters that shaped these environments. Therefore, a comprehensive study of the modern vegetation and pollen rain in the Fjords at 53°S was undertaken. Additionally, a new paleoenvironmental record was acquired from the Tamar Lake (52°54'S; 73°48'W) and was analyzed using geochemistry and pollen analysis. Lastly, the Tamar and other regional paleorecords located along a west-east transect at 53°S were compared using multivariate analyses (PCA, DCCA, rarefaction) in order to develop a comprehensible postglacial history of S. Patagonian ecosystems.

The main vegetation types (i.e. Magellanic Moorland, Evergreen forest, Deciduous forest and Patagonian Steppe) occurring along this west-east transect are clearly identified in the modern pollen rain. Redundancy analysis suggests that modern pollen spectra from the different ecosystems are closely linked with the precipitation and temperature gradient occurring at 53°S. The pollen record from Tamar covering the last 16,000, indicates the development of a heath and grassland between 16 – 13.6 kyr BP, followed by the spread of scrublands and *Nothofagus* woodlands after 13.6 kyr BP, suggesting a shift from cold/dry to a more warm/wet climate. The Holocene is characterized by a succession of distinctive forest types, which begins with the development of *Nothofagus* forests (~11.8 – 8.5 kyr BP), followed by *Nothofagus-Drimys* forests (~10.3 – 6.2 kyr BP), and culminating in mixed temperate evergreen forests (~6.2 kyr BP to present). These changes in vegetation suggest a shift in the intensity of the SWWs and in temperature during the postglacial, accounting for a windy/warm early Holocene. Mass wasting events, well-developed soils and dense vegetation are characteristic for this period. Finally, the findings from the paleoecological reconstruction along Southern Patagonia, reveal substantial differences in the vegetation history (i.e. compositional changes, turnover and palynological richness) of the ecosystems located west and east of the Andes during the postglacial. The response of the ecosystems to environmental forcing (climatic and non-climatic) differs significantly along this transect.

This study reveals the complex interplay between abiotic and biotic factors (e.g. temperature, precipitation, soil development, species competition) in the evolution of the ecosystems of Southern Patagonia over time. The ecosystems respond sensitively to environmental (climatic and non-climatic) forcing, but differ significantly in their resilience depending on intrinsic characteristics. In light of increasing anthropogenic impact and ongoing climate change, these findings offer important insights in the evolution of regional ecosystems that could be used in planning conservation projects.

Kurzzusammenfassung

Süd-Patagonien (50°-56°S) ist eine Schlüsselregion für Paläoumwelt-Studien, insbesondere im Fokus grundlegender paläoklimatischer und paläoökologischer Fragestellungen. Dies liegt an einer Reihe von typischen physisch-geographischen und biotischen Merkmalen der Region: (i) ihre Lage gestattet die Überprüfung und Rekonstruktion der Änderungen der latitudinalen Position der südlichen Westwindzone (SWW), (ii) der Andenkordilliere, die für die SSW eine Barriere darstellt und für einen starken orographischen Niederschlagsgradienten entlang einer West-Ost-Achse sorgt, und folglich, (iii) der Entwicklung und Sukzession unterschiedlicher Ökosysteme entlang dieses Gradienten.

Ziel dieser Arbeit ist die raum-zeitliche Untersuchung der Vegetationsgeschichte von Süd-Patagonien und die Bewertung von verschiedenen natürlichen Parametern, die diese Umwelt prägt. Dazu wurde eine umfassende Studie über die rezente Vegetation und den rezenten Pollenniederschlag in den Fjorden auf 53°S vorgenommen. Zusätzlich wurde ein neuer Paläoumwelt-Datensatz aus Seesedimenten des Tamar-Sees (52°54'S , 73°48'W) mittels Geochemie und Pollenanalyse ausgewertet. Anschließend wurden die Tamar-Daten mit anderen regionalen Paläo-Datensätzen entlang eines West-Ost-Transektivs auf 53°S unter Anwendung multivariater Analysen (PCA, DCCA, rarefaction) verglichen, um einen Überblick zur nacheiszeitlichen Entwicklungsgeschichte süd-patagonischer Ökosysteme zu erstellen.

Die Hauptvegetationstypen (u.a. Magellanisches Moorland, immergrüne Wälder, laubwerfende Wälder und patagonische Steppe), die entlang dieses West-Ost-Transektivs auftreten, prägen sich deutlich im rezenten Pollenniederschlag aus. Redundanz-Analysen deuten darauf hin, dass rezente Pollenspektren aus den verschiedenen Ökosystemen eng mit dem Niederschlags- und Temperaturgefälle auf 53°S zusammenhängen. Der Pollennachweis des Tamar-Sees für die letzten 16,000 Jahre zeigt die Entwicklung von Heide- und Grasland zwischen 16 bis 13.6 kyr BP, gefolgt von der Ausbreitung von Buschland und *Nothofagus*-Wäldern nach 13.6 kyr BP, was auf eine Verschiebung von kalt / trockenem zu einem wärmeren / feuchten Klima schließen lässt. Das Holozän ist durch die Entwicklung einer Reihe von markanten Waldtypen gekennzeichnet. Anfänglich durch die Ausdehnung von *Nothofagus*-Wäldern charakterisiert

(~11.8 – 8.5 kyr BP), folgt auf diese Phase die Ausbreitung von *Nothofagus-Drimys*-Wäldern (~10.3 bis 6.2 kyr BP), welche schließlich zu den heutigen gemäßigten, immergrünen Mischwäldern führt (~6.2 kyr BP bis heute). Diese Veränderungen in der Vegetation deuten auf eine Verschiebung der Intensität der SWW und der Temperatur im Postglazial hin, gefolgt von einem windigen / warmen Frühholozän. Hangrutschungen, gut entwickelte Böden und dichte Vegetationsbedeckung sind charakteristisch für diesen Zeitraum. Zusammenfassend ergeben die Erkenntnisse aus der Paläoumwelt-Rekonstruktion in Süd-Patagonien, dass sich die nacheiszeitliche Vegetationsgeschichte (d.h. Änderungen der Vegetationszusammensetzung, Artenwechsel und Pollen-Diversität) der Ökosysteme westlich und östlich der Anden erheblich voneinander unterscheiden. Die Reaktion der Ökosysteme auf Umweltveränderungen (klimatischer und nicht-klimatischer Natur) unterscheidet sich signifikant entlang des Transektivs.

Diese Studie verdeutlicht das komplexe Zusammenspiel zwischen abiotischen und biotischen Faktoren (z.B. Temperatur, Niederschlag, Bodenentwicklung, Konkurrenz) in der Evolution der Ökosysteme von Süd-Patagonien über einen langen Zeitraum hinweg. Die Ökosysteme reagieren empfindlich auf Umweltveränderungen (klimatischer und nicht-klimatischer Natur). Abhängig von ihren intrinsischen Merkmalen, unterscheiden sich aber deutlich in ihrer Anpassungsfähigkeit. Angesichts des zunehmenden anthropogenen Eingriffs und dem fortschreitenden Klimawandel, liefern diese Erkenntnisse wichtige Einblicke in die Entwicklung der regionalen Ökosysteme, was für die Planung von Naturschutzprojekten Beachtung finden sollte.

Acknowledgments

First of all, I would like to thank my supervisor, Prof. Dr. Frank Schäbitz (University of Cologne) who provided me the support during all these years of thesis work. Likewise, my gratitude is extended to Prof. Dr. Rolf Kilian (University of Trier) for sharing data from Tamar Lake but more important for his advice and big influence in my work, without which it would not have been possible to make this thesis. I thank the Deutscher Akademischer Austausch Dienst (DAAD) and the Comisión Nacional de Investigación Científica y Tecnológica (CONICYT) for funding this my thesis (DAAD-CONICYT Stipendium, 07-DOCDAAAD-08), and Prof. Dr. Olaf Bubenzer for agreeing to review this thesis.

I also whist thanks to the Drs. Frank Lamy (AWI Bremerhaven), Helge Arz, Jerome Kaiser (Leibniz Institute for Baltic Sea Research, Warnemünder) and Flavia Quintana (University of Bariloche) for their helpful ideas to my work. In addition, I would like to thank all colleagues and friends from the Laboratory of Palynology and the department of Geographie und Ihre Didaktik of the Universität zu Köln: Karsten Schitteck, Jonathan Hense, Verena Foerster, Jan Wowrek, Tsige Gebru-Kassa, Maria Papadopoulou, Mark Bormann, Jonas Urban, Wilfried Schulz, Michael Wille, Steffi Reusch, René Kabacinski, Carina Casimir, Markus Dzakovic and Dominik Berg for stimulating conversations, bright ideas, its invaluable help in the laboratory and for numerous extra curriculum activities. In special I would like to express my deepest gratitude to Konstantinos Panagiotopoulos for his friendship and support all along my thesis. Also thanks to Oscar Baeza, Francisco Rios and Sonja Breuer from the University of Trier for its friendship and help during the sampling time in Trier. Thanks also to Marcelo Arevalo, Anne Marx and Corinna Wagner for assistance in fieldwork.

I also wish to thanks my friends from Cologne city, people that helped to survive outside the University life. First of all my deepest gratitude to AAFUMAK my Chess group, and in special to Manuel Vasquez, David "Negro" Martinez, Luciano "Lucho" Lagos, Juan Chapuis, and Francisco Muñoz alias "Pancho Poeta". Also to Francisco Pinto and Anna Marczak, and Miguel Alvarez and Kerstin for its beautiful and sincere friendship.

How to forget my Chilean friends from Juan Gomez Millas which by beautiful coincidences meet up in Germany, in special Natalia Marquez and Jaime Martinez, and its kids Luna and Eru Martinez, alto to Camila Villavicencio, Rene Quispe and the little Ernesto Quispe. Thank you for all this tons of laughs and love that we passed in Berlin, München and Kreta.

Last but not least I would like to express my sincerest gratitude to my wife Loreto Ramirez, and all my family in Chile for their unreserved support.

Table of Contents

Abstract	i
Kurzzusammenfassung	ii
Acknowledgments	iii
List of Figures	vi
List of Tables	xiv
1. INTRODUCTION	1
1.1. Background	1
1.2. Research questions and thesis objectives	6
2. STUDY AREA	10
2.1. Geology, climate and vegetation across Southern Patagonia at 53°S	10
2.1.1. Regional geology	10
2.1.2. Climate	11
2.1.3. Vegetation.	14
3. MATERIALS AND METHODS	18
3.1. Vegetation and modern pollen-rain.	18
3.1.1. Sampling	18
3.1.2. Pollen analyses	18
3.1.3. Numerical analyses	19
3.1.3.1. Cluster analyses and Principal Component Analysis (PCA)	19
3.1.3.2. Canonical analyses	20
3.2. Sediment cores	25
3.2.1. Coring locations	25
3.2.2. Core analyses	27
3.2.2.1. Non-destructive analysis, core correlation and geochemical analysis	27
3.2.2.2. Radiocarbon and age model	27
3.2.2.3. Pollen analyses	29
3.2.3. Numerical analysis	29
3.2.3.1. Cluster analysis (CONISS) and Principal Component Analysis (PCA)	29
3.2.3.2. Turnover and Richness.	30
4. RESULTS	31
4.1. Vegetation and modern pollen-rain.	31
4.1.1. Vegetation and modern pollen-rain in the Southern Patagonian Fjords	31
4.1.1.1. Cluster analyses and Principal Component Analysis (PCA)	35
4.1.2. Pollen rain in a regional context.	37
4.1.2.1. Cluster analysis	37
4.1.2.2. Principal Component Analysis (PCA)	40
4.1.2.3. Canonical ordination	40
4.2. Paleoenvironmental reconstruction of Tamar catchment	43

4.2.1. Physical environment and vegetation within the Lake Tamar catchment	43
4.2.2. Tamar Lake Sediment cores	46
4.2.2.1. Core stratigraphy and chronology	46
4.2.2.1.1. Lithological sections	46
4.2.2.1.2. Age-depth model	50
4.2.2.1.3. Light-colored deposits (LCD's)	51
4.2.2.1.4. Event chronology	54
4.2.2.2. Pollen record	56
4.2.2.2.1. Percentages	56
4.2.2.2.2. Concentrations	57
4.2.2.3. Numerical Analyses	61
4.2.2.3.1. Principal Component Analysis (PCA)	61
4.2.2.3.2. Palynological Turnover and Richness	63
4.2.2.4. Numerical Analyses performed in additional pollen record located along a west- east transect	64
4.2.2.4.1. Gran Campo Nevado (GCN).	66
4.2.2.4.2. Rio Rubens	68
4.2.2.4.3. Lago Guanaco	70
4.2.2.4.4. Potrok Aike	72
5. DISCUSSION	73
5.1. Vegetation and modern pollen-rain.	73
5.1.1. Vegetation and modern pollen-rain in the Southern Patagonian Fjords	73
5.1.1.1. Distribution of main plant communities within the Fjords (53°S)	73
5.1.2. Modern pollen-rain within the Fjords and vicinity areas	81
5.1.3. Modern pollen-rain and vegetation at regional scale (53°S)	84
5.1.4. Pollen assemblages and environmental variables.	87
5.2. Examining the postglacial history of the Southern Patagonian Fjords at 53°S	88
5.3. Main vegetation changes along a west-east transect in Southern Patagonia at 53°S during the Postglacial	99
6. CONCLUSIONS	103
7. BIBLIOGRAPHY	105
8. APPENDIX	120
8.1. Appendix A. Figures and Tables	121
8.2. Appendix B. Transfer functions.	140
8.3. Bibliography appendix A & B	151
Erklärung	152
Lebenslauf	153

List of Figures

- Figure 1. Global map showing the average wind (annual mean) at 850 mb during the period 1949-2013. The arrows indicate the prevalent wind direction, and the background colors the wind speed (m/s) (Image provided by the NOAA/ESRL Physical Sciences Division, <http://www.esrl.noaa.gov/psd/>). The Southern Patagonia territories (50°-56°S) are indicated by the purple color square. 3
- Figure 2. (Above) Topographic map based on a digital elevation model (SRTM, 30 arc-sec resolution; 90m) of Southern Patagonia territories (50°-56°S) and, (Below) schematic transect along the west-east axis (white line on the upper figure) denoting the precipitation gradient and the succession of main plant communities. 4
- Figure 3. Map of Southern Patagonia showing the location of pollen records (Table 1) and the likely extension of the Patagonian Ice Sheet during the Last Glacial Maximum (LGM). The colour for each pollen site regards to the main vegetation occurring in the study area after the Figure 2. The star indicates the pollen record studied in this thesis (Tamar Lake). 5
- Figure 4. Geological map of southern Patagonia (after SERNAGEOMIN 2003, Ghiglione et al. 2009; Fosdick et al. 2011) and inferred glacial limits during the LGM (after McCulloch et al. 2005; Coronato et al. 2008; Kaplan et al. 2008; Sagredo et al. 2011; Garcia et al. 2012). 10
- Figure 5. Composite means for the period 1949-2013 illustrating the annual and seasonal (winter and summer) patterns of zonal wind speed (above) and Sea Level Pressures (middle) occurring in the Southern Hemisphere, and its repercussions in the precipitation patterns along southern South America (below). The images were produced utilizing the online data provided by the NOAA/ESRL Physical Sciences Division, Boulder Colorado (<http://www.esrl.noaa.gov/psd/>). 12
- Figure 6. Composite means for the period 1949-2013 illustrating the annual and seasonal (winter and summer) temperatures of the air (above) and surface (below) in the southern South America. The images were produced utilizing the online data provided by the NOAA/ESRL Physical Sciences Division, Boulder Colorado (<http://www.esrl.noaa.gov/psd/>). 13
- Figure 7. Digital Elevation Model (DEM) and location of weather stations present in the study area (53°S). Please note the under-represent values occurring during the winter months (MJJ) in the weather station of Gran Campo because the solid precipitation (snow). 15
- Figure 8. General map of Southern Patagonia, indicating the main plant formations occurring at regional-scale (after Schmithüsen 1956 and Gajardo 1994). 17
- Figure 9. Map of the study area (Southwest Patagonian Fjords, at 53°S) indicating the localities visited (n=7) where vegetation surveys and soil sampling were performed for the study of modern pollen-rain. The information into the rectangles refers to the name of the site and code for the samples retrieved (parenthesis) after Table 2. Rectangles in red indicate locations where additional samples from surface sediments (two lakes and one bay) were obtained. More details in the text. 19
- Figure 10. Vegetation map (after Figure 8) showing the location of samples utilized to the study of the modern pollen-rain that include the main plant formations occurring along a west-east transect in Southern Patagonia. The information into

the rectangles (this thesis) and circles (previous studies) indicates the codes of the samples provided in the Tables 2 & 3. 20

Figure 11. (A) General map of the Southwest Patagonian territories at 53°S (left) indicating the location of the study site at Tamar Island (right). The yellow area in the georeferenced orthophoto denotes the lake catchment. (B) Oblique view (orthophoto+DEM) of the Tamar Lake catchment and elevation contour lines. (C) Bathymetry map of Tamar Lake (left) indicating the location of the piston core (circle) and the performed echosounder tracks. The bold line denotes the track of the seismic profile plotted on the right. 26

Figure 12. Modern vegetation map (after figure 8) where is indicated the location of pollen sites (rectangles) utilized to (i) examine changes in the plant community composition (turnover and richness) along a west-east gradient (at 53°S) and (ii) develop quantitative climatic reconstructions (transfer functions, see appendix section 8.2) for the postglacial. Locations for modern surface samples (pollen-rain) are also indicated. For more details see the text. 30

Figure 13. Pollen diagram (relative percentage) from soil samples used to characterize the pollen rain of the dominant plant communities occurring in Southwest Patagonia. Samples are grouped according to main vegetal formations and altitude. In addition, surface sediment samples (gravity cores) from Lake Tamar, Lake Desolacion and Chids Bay are included at the end. The locations of the study sites are indicated in the Table 2 and Figure 9. Black points indicates values <5%. 33

Figure 14. Cluster analysis (Edward & Cavalli-Sforza's chord distance method) of the modern pollen spectra from the Southern Patagonian Fjords. The analysis was performed using the samples obtained from soils and surface sediment (gravity cores). The name and colours indicates the main plant communities previously discussed (Figure 13). Grey rectangles indicate outliers. Sample codes are in parenthesis (Table 2). 35

Figure 15. Principal Component Analysis for the main pollen types (>2%) on the first two axes, using the samples obtained from soils and surface sediment (gravity cores) from the Southern Patagonian Fjords. 36

Figure 16. Pollen diagram (relative percentage) from surface samples used to characterize the west-to-east modern pollen-rain along a broad biogeographic gradient (Figure 10 & Table 2). Colors indicate main groups defined by means of cluster analysis. Black points indicates values <5%. 38

Figure 17. Principal Component Analysis (PCA) for the main pollen types (>2%) present on surface samples used to characterize the west-to-east modern pollen-rain along a broad biogeographic gradient (Figure 10 & Table 2). Colors indicate main groups defined previously by means of cluster analysis (Figure 16). 41

Figure 18. Biplot showing the first two axes of the RDA ordination for modern surface samples and selected taxa. Significant climatic variables Pann and Tann are denoted in red. Correlation and probability values are in the Table 6 42

Figure 19. Main physic features (elevation, aspect and slope) from the Tamar Lake catchment 43

Figure 20. Maps of the most relevant physical features occurring within of Lake Tamar

catchment: A) elevation, B) aspect, and C) gradient slope. Below (D), vegetation mapping of Tamar Lake catchment. The images positioned left and right, represent the aerial and 3D perspective (respectively) view for each categorized maps. 45

Figure 21. Composite image of the sediment core TML, showing: the position of radiocarbon dates, a descriptive lithology column and the lithological sections discussed in the text, including the position of the different types of light-colored deposits (LCD's). In the right are show the parameters of magnetic susceptibility and gray scale intensity 48

Figure 22. Grayscale, magnetic susceptibility, and geochemical data from core TML1 versus composite core depth (cm) and age (cal. yr BP). Color bars blue, red and green denotes the stratigraphic position of light-colored deposits (LCDs) Types 1-3 (respectively), while grey bars mark the two tephra originating from eruptions of Mt.-Burney. Red diamonds not line-connected on the geochemical parameters, indicates data points retrieved from LCDs. 49

Figure 23. Age-depth model and sedimentation rates (mm yr^{-1}) for the composite sediment core TML. The reliability of the model is constrained to the core sections where organic pelagic sedimentation occurs (lithological section II-IV). Note that the model is plotted against a corrected depth (without light-colored deposits and tephra layers). For more details see the text 50

Figure 24. Close-up sections for the four different types of light-colored deposit (LCD's) present in the composite sediment core TML, indicating: length (cm), lithology, and the outcome of the parameters of grayscale and magnetic susceptibility for each one of them. 53

Figure 25. Chronology, thickness and frequency (per 1000 years) of events, based on individualized light-colored deposits (LCD's), present in the TML sedimentary record. Taking into account the differences observed among the LCD's (e.g. internal structure and distribution along the core), in the graph above (A) are plotted only the events corresponding to LCD's types 1-3, while in the graph below (B) are plotted the events associated to the LCD's type 4. Arrows in the graph B indicate periods when the recurrence among events is <100 years (sub-centennial time scales). 55

Figure 26. Percentage diagram of selected taxa from Core TML, plotted against the calibrated calendar age. The secondary y-axis displays the composite depth scale (cm). Dashed lines represent the boundaries of pollen zones after the cluster analyses (CONNIS) in the right. Gray area (outside the curves) indicates an exaggeration factor x5. 59

Figure 27. Concentration diagram (grains/cc) of selected taxa from the pollen record of Tamar Lake. On the right of the graph are included the total concentration of terrestrial plants, ferns and aquatics. Please note the differences in the concentration scale among the taxa. 60

Figure 28. (Above) Biplot of Principal Component Analysis (PCA) for the pollen record TML, performed on a re-calculated dataset containing only taxa >5%. The respective pollen zone for each sample is indicated. (Below) Sample scores for the Axis 1 and 2, plotted against age. Pollen zones are also indicated. Results for the DCCA (Turnover) and the palynological rarefaction analysis (Richness)

performed on the pollen record. The estimated palynological richness is based on the minimum number of pollen taxa (Tn). In order to highlight the major trends in the palynological turnover and richness, a Loess smoother (solid lines) has been fitted to the raw data, utilizing a sampling span of 1.5 and rejecting the outliers.62

Figure 29. (Above) Biplot of Principal Component Analysis (PCA) for the pollen record GCN, performed on a re-calculated dataset containing only taxa >5%. The respective pollen zone for each sample is indicated. (Below) Sample scores for the Axis 1 and 2, plotted against age. Pollen zones are also indicated. Results for the DCCA (Turnover) and the palynological rarefaction analysis (Richness) performed on the pollen record. The estimated palynological richness is based on the minimum number of pollen taxa (Tn). The results are plotted against age. Pollen zones are indicated on the middle of the graph. In order to highlight the major trends in the palynological turnover and richness, a Loess smoother (solid lines) has been fitted to the raw data, utilizing a sampling span of 1.5 and rejecting the outliers.65

Figure 30. (Above) Biplot of Principal Component Analysis (PCA) for the pollen record Rio Rubens, performed on a re-calculated dataset containing only taxa >5%. The respective pollen zone for each sample is indicated. (Below) Sample scores for the Axis 1 and 2, plotted against age. Pollen zones are also indicated. Results for the DCCA (Turnover) and the palynological rarefaction analysis (Richness) performed on the pollen record. The estimated palynological richness is based on the minimum number of pollen taxa (Tn). The results are plotted against age. Pollen zones are indicated on the middle of the graph. In order to highlight the major trends in the palynological turnover and richness, a Loess smoother (solid lines) has been fitted to the raw data, utilizing a sampling span of 1.5 and rejecting the outliers.67

Figure 31. (Above) Biplot of Principal Component Analysis for the pollen record Laguna Guanaco, performed on a re-calculated dataset containing only taxa >5%. The respective pollen zone for each sample is indicated. (Below) Sample scores for the Axis 1 and 2, plotted against age. Pollen zones are also indicated. Results for the DCCA (Turnover) and the palynological rarefaction analysis (Richness) performed on the pollen record. The estimated palynological richness is based on the minimum number of pollen taxa (Tn). The results are plotted against age. Pollen zones are indicated on the middle of the graph. In order to highlight the major trends in the palynological turnover and richness, a Loess smoother (solid lines) has been fitted to the raw data, utilizing a sampling span of 1.5 and rejecting the outliers.69

Figure 32. (Above) Biplot of Principal Component Analysis for the pollen record Potrok Aike, performed on a re-calculated dataset containing only taxa >5%. The respective pollen zone for each sample is indicated. (Below) Sample scores for the Axis 1 and 2, plotted against age. Pollen zones are also indicated. Results for the DCCA (Turnover) and the palynological rarefaction analysis (Richness) performed on the pollen record. The estimated palynological richness is based on the minimum number of pollen taxa (Tn). The results are plotted against age. Pollen zones are indicated on the middle of the graph. In order to highlight the major trends in the palynological turnover and richness, a Loess smoother (solid lines) has been fitted to the raw data, utilizing a sampling span of 1.5 and rejecting the outliers.71

Figure 33.	Schematic profile indicating the distribution of main plant communities identified and described in this thesis, as the most characteristic in the Southern Patagonia Fjords (53°S). For each plant community the most representative taxa is indicated, while rare taxa are marked with a “+”. Main characteristics of the physical environment where each plant community occurs are also indicated on the left upper corner of the figure.	76
Figure 34.	Images from Sub-alpine environments present in the Southern Patagonian Fjords at 53°S. Left. General view of the vegetal landscape at ~300 m.a.s.l. Right. Detail of regolith formation in a wind exposed area at ~350 m.a.s.l. The red dashed line indicates the approximate elevation where sub-alpine environments take place. Both photographs from Chids Island (for location see figure 9)	77
Figure 35.	Above. Analysis of the correlation between elevation and slope parameters for two studied locations, Tamar Island and Chids Island (for location see Figure 9). The analysis was performed using GIS, utilizing a grid of 100 m extracted from a DEM (SRTM, 3 arc-sec resolution; 90m). The red line represents the linear regression, and the blue the best fit-curve (quadratic). The yellow bar indicates the mid-elevations. Below. Basic conceptual diagram indicating the main stages and mechanisms involved in the transition from soil-mantled landscapes to bedrock-dominated landscapes in the Southern Patagonian Fjords. For details see text.	79
Figure 36.	Observed geomorphological context where forest communities occurs in the visited areas on the Southern Patagonian Fjords	80
Figure 37.	Process of natural destruction of cushion-bogs observed in the visited areas.	80
Figure 38.	Above. Comparison between summary pollen diagram (left) and PCA Axis 1 (right) from the modern pollen-rain samples retrieved in the Fjords and vicinity areas. Below. Boxplots for percentages corresponding to the different plant communities identified and studied, and linear regression between PCA Axis 1 and soil cover classes. The box encloses the middle half of the data between the first and third quartiles. The central line denotes the value of the median. The horizontal line extending from the top and bottom of the box indicates the range of typical data values. Outliers are displayed as “o” for outside values and “*” for far outside values	83
Figure 39.	Left. Comparison between summary pollen diagram, PCA Axis 1 and cluster analyses. Right. Boxplots of percentages for the main plant formations studied in this thesis located along the west-east transect. The box encloses the middle half of the data between the first and third quartiles. The central line denotes the value of the median. The horizontal line extending from the top and bottom of the box indicates the range of typical data values. Outliers are displayed as “o” for outside values and “*” for far outside values	86
Figure 40.	Map of the study area at 53°S indicating the locations of paleoenvironmental proxies discussed in the text. The star shows the location of Tamar Island and TML core. Glaciers are marked in orange and inferred ice limits in yellow. Minimum ages corresponding to ice retreat are also provided.	89
Figure 41.	Summary figure for main geochemical and palynological results from the TML core, and selected paleoclimatic proxies	90

Figure 42. Left. View of the Lake Tamar catchment and surrounding vegetation. Lake bathymetry and lithology of gravity cores are shown.	93
Figure 43. Summary figure of main abiotic and biotic proxies from the TML core	96
Figure 44. Summary figure for abiotic (geochemical) and biotic (pollen) from TML and selected paleoclimatic proxies. For location see figure 40	97
Figure 45. Summarized pollen concentration diagram of tree taxa, indicating its shade tolerance. The red arrow indicates the point when the taxon becomes abundant in the record.	98
Figure 46. Comparison of the results obtained from the principal component analysis (PCA), detrended canonical correspondence analysis (Turnover) and Rarefaction analysis (Richness) performed at the four additional pollen records located along the west-east transect in Southern Patagonia (Figure 12). In all the cases, the results are plotted against time. The data from Turnover and Richness were smoothed utilizing a 0.2 lowess spline (solid line). The estimated palynological richness was calculated based on the minimum number of pollen taxa (Tn) at each site. Also selected paleoclimatic proxies are provided.	101
Figure 47. Schematic evolution of the main vegetation types of Southern Patagonia during the Postglacial.. . . .	102
Appendix figure 1. Co-occurrence network from the quantitative content analysis performed on a dataset that include only scientific publications (n=29) related with Quaternary palynological issues of Southern Patagonia (see table 1 for references). The results (co-occurrence networks) are representing words (nodes) from the texts (excluding the bibliography) from the analysed pollen publications-dataset. Two methods and analysed in terms of: sentences (left) and paragraphs (right). The resulting co-occurrence network was measured utilizing a community-modularity clustering method (Clauset <i>et al.</i> 2004). The position of the nodes was calculated use Fruchterman-Reingold algorithm (Fruchterman and Reingold).	121
Appendix figure 2. Idealized wind behaviour scenarios in a landscape with and without topography. Above. Cross section along the landscape in where is indicated with red lines the wind behaviour in a scenario without topography, and with blue lines the wind behaviour in the presence of a mountain (grey). Below. Graph for wind speed versus height along three profiles (a,b,c). The first (a) characterizes the idealized behaviour of the wind speed along the height in the absence of topography. On the contrary the profiles a and b denotes the effect of the topography. Notice the increase of the flow (wind speeds) in response to the topography because the compression of the flux in the top of the hill, and the presence of a wind-sheltered zone on the leeward (Modified from several sources)..	122
Appendix figure 3. (Above) Hanging vegetation occurring in coastal areas and, (Below) an example of the observed absence of vegetation probably related to characteristics of rock type.	123
Appendix figure 4. Images showing the area affected by a recent landslide in the area of Bahía Bahamondes, being appreciable the soil covered by <i>Gunnera magellanica</i>	124
Appendix figure 5. Panoramic view of Tamar lake, Chids bay and Desolacion lake.	125

Appendix figure 6. Boxplots of modern pollen rain percentages for selected taxa arranged by dominant plant formations occurring in Southern Patagonia. The box encloses the middle half of the data between the first and third quartiles. The central line denotes the value of the median. The horizontal line extending from the top and bottom of the box indicates the range of typical data values. Outliers are displayed as “o” for outside values and “*” for far outside values. Note changes in scale. 126

Appendix figure 7. Detail of the magnetic susceptibility results from the Tamar lake sediment core indicating in gray the basal section of the record where predominates clays (light gray) and sandy layers (dark gray). 127

Appendix figure 8. Boxplots of selected geochemical parameters for pelagic sediments (matrix) and LCD’s (types 2-4) present within of the sediment core from Tamar lake . The box encloses the middle half of the data between the first and third quartiles. The central line denotes the value of the median. The vertical line extending from the top and bottom of the box indicates the range of typical data values. Outliers are displayed as “o”. 128

Appendix figure 9. Percentage diagram of the pollen record from Tamar of lake, where are included the samples (in red) associated to mass wasting deposits or light-colored deposits (LCDs). Colour bars blue, red and green denotes the stratigraphic position of LCDs Types 1-3 (respectively). 129

Appendix figure 10. Plant macrorest found in the mass wasting deposits of Tamar lake sediment core. 130

Appendix figure 11. Leaves of *Nothofagus betuloides* found in the mass wasting deposits of Tamar lake sediment core. 131

Appendix figure 12. Concentration diagram (grains/cc) including all the taxa from the pollen record of Tamar Lake. 132

Appendix figure 13. Percentages pollen diagram from Gran Campo Nevado sediment core. 133

Appendix figure 14. Percentages pollen diagram from Rio Rubens sediment core. 134

Appendix figure 15. Percentages pollen diagram from Lago Guanaco sediment core. . . . 136

Appendix figure 16. Percentages pollen diagram from Potrok Aike sediment core.. . . . 137

Appendix figure 17. Scatter plot of the predicted precipitation values versus the observations (upper panel) and its respective residuals (lower panel), for the WAPLS and MAT models. 141

Appendix figure 18. Boxplots of estimated precipitation (Pann) from the transfer function models (MAT and WAPLS) for each of the pollen records utilized in this thesis in order to perform quantitative paleoprecipitation reconstructions along a west-east transect at ~53°S (Figure 12). The box encloses the middle half of the data between the first and third quartiles. The central line denotes the value of the median. The vertical line extending from the top and bottom of the box indicates the range of typical data values. Outliers are displayed as “o”. 143

Appendix figure 19. (Left) Reconstructed annual precipitation (Pann) parameter from the pollen record of Tamar lake, utilizing the transfer functions WAPLS (red) and MAT (blue). The green arrow and dashed line indicate the modern Pann at the

study site. (Right) Results from a simple subtraction operation (expressed in mm) performed among the transfer functions, in order to visualize more easily divergences between the curves. The solid-hard line on the graphs correspond to a Loess smoother, have been fitted to the raw data in order to highlight the major trends, utilizing a sampling span of 1.5 and rejecting the outliers. 144

Appendix figure 20. (Left) Reconstructed annual precipitation (Pann) parameter from the pollen record of GCN, utilizing the transfer functions WAPLS (red) and MAT (blue). The green arrow and dashed line indicate the modern Pann at the study site. (Right) Results from a simple subtraction operation (expressed in mm) performed among the transfer functions, in order to visualize more easily divergences between the curves. The solid-hard line on the graphs correspond to a Loess smoother, have been fitted to the raw data in order to highlight the major trends, utilizing a sampling span of 1.5 and rejecting the outliers. 145

Appendix figure 21. (Left) Reconstructed annual precipitation (Pann) parameter from the pollen record of Rio Rubens, utilizing the transfer functions WAPLS (red) and MAT (blue). The green arrow and dashed line indicate the modern Pann at the study site. (Right) Results from a simple subtraction operation (expressed in mm) performed among the transfer functions, in order to visualize more easily divergences between the curves. The solid-hard line on the graphs correspond to a Loess smoother, have been fitted to the raw data in order to highlight the major trends, utilizing a sampling span of 1.5 and rejecting the outliers. 147

Appendix figure 22. (Left) Reconstructed annual precipitation (Pann) parameter from the pollen record of Lago Guanaco, utilizing the transfer functions WAPLS (red) and MAT (blue). The green arrow and dashed line indicate the modern Pann at the study site. (Middle) Results from a simple subtraction operation (expressed in mm) performed among the transfer functions, in order to visualize more easily divergences between the curves. The solid-hard line on the graphs correspond to a Loess smoother, have been fitted to the raw data in order to highlight the major trends, utilizing a sampling span of 1.5 and rejecting the outliers. Notice that reconstructed annual precipitation (Pann) utilizing the MAT transfer functions is plotted as single graph in the right of the figure.. . . . 148

Appendix figure 23. (Left) Reconstructed annual precipitation (Pann) parameter from the pollen record of Potrok Aike, utilizing the transfer functions WAPLS (red) and MAT (blue). The green arrow and dashed line indicate the modern Pann at the study site. (Right) Results from a simple subtraction operation (expressed in mm) performed among the transfer functions, in order to visualize more easily divergences between the curves. The solid-hard line on the graphs correspond to a Loess smoother, have been fitted to the raw data in order to highlight the major trends, utilizing a sampling span of 1.5 and rejecting the outliers. 150

List of Tables

Table 1. Summary table indicating the code (number), name, location and altitude of palynological studies performed in Southern Patagonia (Figure 3). Note that sites are ordered according to the dominant plant formation present on each of the study sites.	9
Table 2. Codes and main geographical characteristics (coordinates/elevation, site name and dominant plant formations) of the surface samples collected in this thesis to study the modern pollen-rain within the Southern Patagonian Fjords.	22
Table 3. Additional surface sample locations (Quintana 2009) utilized to develop a comprehensive study of the modern pollen-rain along a broad west-to-east transect in Southern Patagonia (53°S). For more details see the text.	24
Table 4. Radiocarbon dates for the Tamar Lake composite core, indicating corrected depths after be subtracted all the layers related to events of instantaneous deposition (e.g. tephra, mass flows). Radiocarbon samples have been calibrated using Calib 6.1.0 and the Southern Hemisphere calibration curve (SHCal04). For ages beyond the SHCal04 calibration curve were used the IntCal04 calibration curve. Median and 1 sigma of distribution for each calibrated radiocarbon date are provided. The age of tephra layers are based on previously reported results (Kilian et al. 2003). For more details see the text.	28
Table 5. Climatic and geographic variables used in the ordination analysis (RDA). Variables in bold are significant at p-value<0.005.	41
Table 6. Correlations and inter-correlations between significant climatic variables and RDA axis.	42
Table 7. Total and relative areal cover of the main plant communities identified within the Tamar Lake catchment, and the physical features characterizing the areas where they occur.	44
Table 8. Summary of principal component analysis (PCA) and detrended canonical correspondence analyses (DCCA), measure of trends in turnover (beta-diversity), total inertia (total variance in each sequence), and the first eigenvalue (λ_1) measure of the contribution of the first axis to total variance at the four study sites, using both all samples and only those samples covering the period in common (12,750 cal yr BP to present).	64
Table 9. Main ecological traits for tree taxa involved in the postglacial forest succession in the Tamar pollen record	99
Appendix table 1. Chronology of events associated to light-colored deposits (LCDs) present in the sediment core of Tamar Lake	138
Appendix table 2. Performance of the reconstruction models, indicating: the coefficient of determination between predicted and observed climate values (R^2), the maximum bias (Max. bias), root mean square error of prediction (RMSEP) and the percentage of change among the components (%Change). The best model within each set of algorithms are indicated in color, namely: MAT (Modern analogue technique), WA (weighted averaging) and WAPLS (Weighted averaging partial least squares regression). For more details see the text.	141

Appendix table 3. Basic statistic parameters for each of the reconstructions (WAPLS and MAT) performed on selected pollen records located along a west-east transect at ~53°S. 142

1. INTRODUCTION

1.1. Background

The configuration of modern ecosystems, in terms of its distribution and composition, is the result of complex processes tied inherently to particular environmental forcings in time (Delcourt *et al.* 1983, Delcourt and Delcourt 1988, Seppä and Bennett 2003, Willis and Birks 2006, Davies and Bunting 2010, Rull 2010, Willis *et al.* 2010, Vegas-Vilarrubia *et al.* 2011). Today it is broadly accepted that climate exerts a key control over the distribution of the world's major ecosystems (Holdridge 1947, Whittaker 1975), and therefore past climate changes must have also been imprinted through changes in biota (Bennett 1997, Lieberman 2000)¹. A classic example which illustrates the role of climate as a key environmental forcing are the profuse and coeval changes observed in the distribution and composition of terrestrial and marine ecosystems (Coope and Wilkins 1994, Hewitt 2000, Willis *et al.* 2004, MacDonald *et al.* 2008) during the successive glacial-interglacial cycles which characterize the Quaternary (<2.6 Ma) (Pillans and Naish 2004, Gibbard *et al.* 2009). Nevertheless, this apparent synchronicity and correlation between changes in climate and biota lessen in importance when the spatial-temporal scale decreases, giving way to a new level in which ecological factors acquire relevance (Delcourt *et al.* 1983, Delcourt and Delcourt 1988). In other words, environmental forcing functions and biotic responses vary according to the temporal and spatial scales investigated.

The palynology as a proxy for the study of past plant communities

Palynology or pollen analysis; the study of fossil pollen and spores, is the principal technique utilized to perform vegetational reconstructions at various timescales (Fægri and Iversen 1989). Since its development by Von Post (Mantel 1967), palynological studies have provided significant contributions to Quaternary sciences, being utilized largely as a paleoclimatic proxy². Nevertheless, even when climate strongly influences the geographical distribution of plants and vegetation types (Woodward 1987), the evidence also indicates that vegetation changes are not always in equilibrium with it (Webb 1986). For example, the observed time lag (~1500 yr) between climate change and postglacial spread of temperate trees in northern Europe has been interpreted as result of deficient soil development in areas previously covered by ice (Pennington 1986). In comparison, in areas not covered by ice during the last glacial maximum the process is reversed, beginning with the forest arrival and then the development and maturation of soils (Willis *et al.* 1997). Other examples illustrating the participation of non-climatic mechanisms in the reconstructed changes and patterns (e.g. succession) of the vegetation involve dispersal mechanisms (Wilkinson 1997), interspecific competition (Bennett and Lamb 1988), disturbance mediated by wildfires (Bond *et al.* 2005), pathogens attack (Waller 2013) and human activities (Edwards and MacDonald 1991).

In recent years, several studies have highlighted the relevance of including a long-term perspective for conservation strategies and policies (Willis and Birks 2006, Davies and Bunting 2010, Willis *et al.* 2010, Vegas-Vilarrubia *et al.* 2011, Birks 2012). In this context, palynological studies provide a robust tool to examine the biotic responses to environmental forcing (climatic and non-climatic) along different spatial-temporal scales. Paleoenvironmental information inferred from pollen records is not solely restricted to vegetation reconstructions. Nowadays, owing to the

¹ The notion of climate as the main control in the distribution of global biota, was first mentioned in the 18th century by Carl Linnaeus "On the increase of the habitable Earth" (*Oratio de Telluris habitabilis incremento*, 1744). Nevertheless, it was only during the 19th century when the idea of climate changes conducting changes on the biota with time was conceived. This invaluable contribution to the science is discussed of two classic works of the epoch: "Principles of Geology (1837)" of Charles Lyell "and "The origin of the species (1859)" of Charles Darwin.

² For more details refer to section: Pollen records, in the Encyclopedia of Quaternary Science (Brewer *et al.* 2007).

development of new statistical tools and numerical analysis, it is possible to estimate qualitative changes in the diversity and composition of the ecosystems on various scales (Odgaard 2007)³. Consequently, ecological thresholds and resilience⁴ of plant communities to environmental forcing over different timescales can be examined (Birks and Birks 1980, Delcourt *et al.* 1983, Prentice 1986, Delcourt and Delcourt 1988, Delcourt and Delcourt 1991, MacDonald and Edwards 1991, Huntley 1996, Seppä and Bennett 2003, Rull 2010, Willis *et al.* 2010, Birks 2012).

Rationale: Southern Patagonia as a case study

Southern Patagonia (50°-56°S) is key region for paleoenvironmental studies addressing complex paleoclimatic and paleoecological questions, due to a number of physical and biotic singularities that characterize local environments. Firstly, Southern Patagonia located at the tip of South America is the only continental landmass extending south of 38°S (Australia) and the most austral continuous land south of 46°S (New Zealand; Figure 1)⁵. The absence of significant landmasses in mid and high latitudes of the Southern Hemisphere, allows the development of a symmetric behaviour in the flux of the Southern Westerly Wind belt (SWW), a key component of the coupled atmosphere-ocean system (Garreaud *et al.* 2009)(Figure 1). Several studies have highlighted the importance of examining the dynamics of the SWW (e.g. strength and position) through time, due to its influence on climate of mid-high latitudes of the Southern Hemisphere. The SWW are linked with the global climate due to its role in the active upwelling mechanism of deeper Antarctic Circumpolar Current (ACC) waters and the subsequent repercussions for CO₂ degassing from the Southern Ocean (Thompson and Solomon 2002, Shulmeister *et al.* 2004, Varma *et al.* 2012, Razik *et al.* 2013). Therefore, the Southern Patagonia territories are a key location for undertaking paleoenvironmental studies to reconstruct and examine changes in the dynamic of the SWW at various timescales.

A further noteworthy characteristic of the Southern Patagonia territories is the succession of distinct biophysical environments along the west-east axis (Figure 2). This feature, result of million of years of tectonic history and evolution of biota⁶, can be summarized to: (i) a main cordillera dividing dissimilar landscapes occurring in the west (Fjords) and the east (plains and tablelands), (ii) creating a strong orographic precipitation gradient along the west-east axis, and with (iii) the consequent occurrence of hyper-humid climates in the west and semi-desert in the east (Endlicher and Santana 1988, Schneider *et al.* 2003, Coronato *et al.* 2008, Garreaud *et al.* 2013)(Figure 2). The vegetation follows this natural west-east gradient, with the dominance of Moorlands ecosystems in the western Fjords, Evergreen and Deciduous Forest in the Andean region, and extensive grasslands ecosystems (Steppe) along the eastern plains(Schmithüsen 1956, Oberdorfer 1960, Pisano 1977, Boelcke *et al.* 1985, Gajardo 1994)(Figure 2).

³ Whittaker *et al.* (2001) offers a coherent discussion about changes in the species diversity along different spatial-temporal scales, proposing a hierarchical schema that distinguishes five main diversity tiers: community (α -diversity), between-community (β -diversity), landscape (γ -diversity), between-landscape (δ -diversity), and regional (ϵ -diversity).

⁴ The ecological threshold refers to the point at which there is an abrupt change in the properties or structures of an ecosystem, whereas the ecological resilience regards with the ability of the (eco)systems to tolerate disturbances (i.e environmental forcings) and still maintain the properties or structures similar to the pre-disturbance state (for more details see Groffman *et al.* 2006).

⁵ This observation excludes the Antarctic territories and the subantarctic islands (Auckland, Kerguelen, Falkland and South Georgia, among others).

⁶ Geologic and paleobotanic information suggest that the first stages of the differentiation between the biogeographic subregions of Subantarctic (west) and Patagonia (east), are closely related with the progressive uplift of Patagonian Andean Cordillera during the Late Miocene (14-10 Ma) and the Early Pliocene (5 Ma), and the subsequent develop of the rain-shadow effect (Hinojosa and Villagrán 1997; Villagrán and Hinojosa 2005; Ortiz-Jaureguizar and Cladera 2006). Thereby, these antecedents highlight the ancient roots of the physical and environmental gradient studied in this thesis..

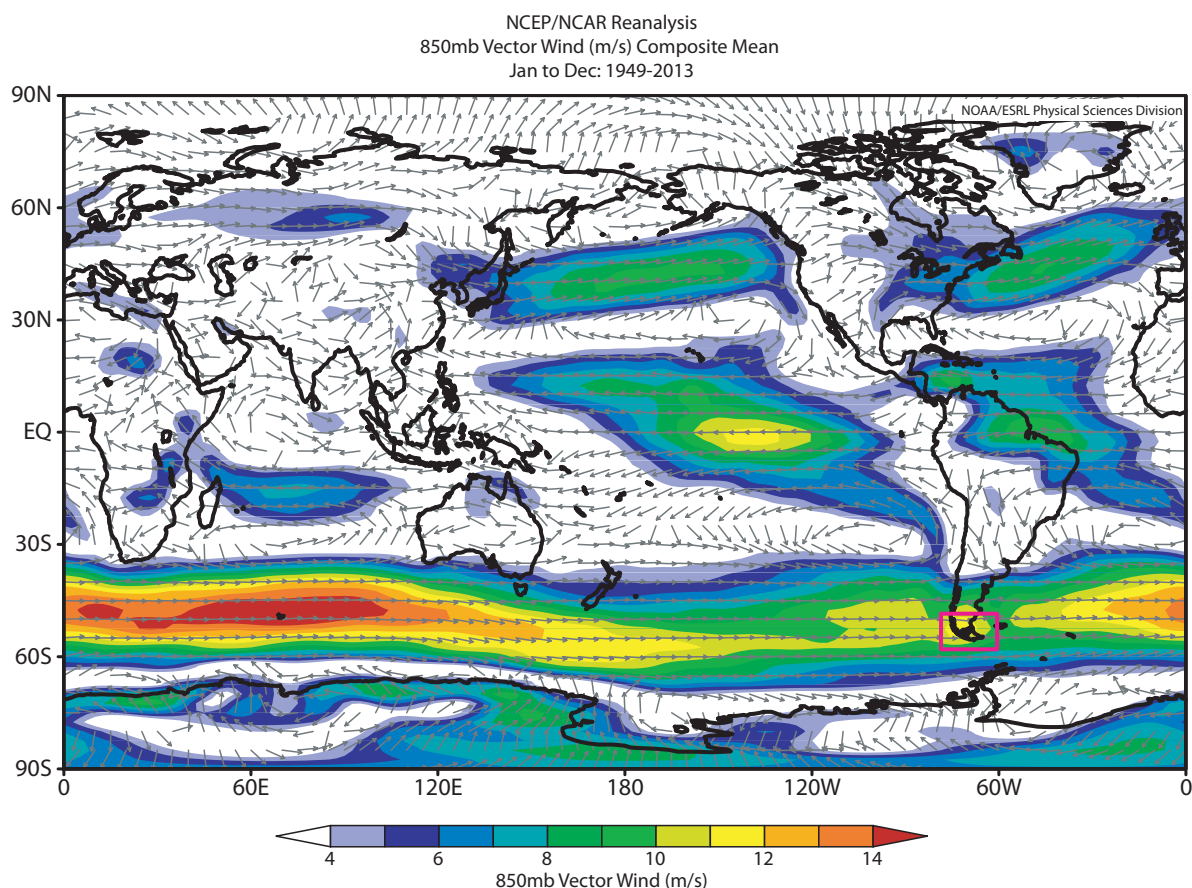


Figure 1. Global map showing the average wind (annual mean) at 850 mb during the period 1949-2013. The arrows indicate the prevalent wind direction, and the background colors the wind speed (m/s) (Image provided by the NOAA/ESRL Physical Sciences Division, <http://www.esrl.noaa.gov/psd>). The Southern Patagonia territories (50°-56°S) are indicated by the purple color square.

Several paleoenvironmental studies have been conducted within this biophysical gradient, using different kinds of archives and proxies (Kilian and Lamy 2012). The findings, which indicate significant changes in the biotic and abiotic components of the reconstructed paleoenvironments, suggest important transformations in the ecosystems under the action of environmental forcing. Pollen studies, the most common paleoenvironmental proxy utilized in Southern Patagonia (Kilian and Lamy 2012), have been largely used to reconstruct past climate changes and specifically changes in the SWW dynamic, but hardly to address paleoecological questions (Appendix figure 1)⁷. For example, a well-know feature observed in all pollen records is the increase of tree pollen percentages during the postglacial, denoting the spread of forest communities through the region (Markgraf 1993, McCulloch and Davies 2001, Mancini 2002, Heusser 2003, Fesq-Martin *et al.* 2004, Huber *et al.* 2004, Villa-Martinez and Moreno 2007, Mancini 2009, Wille and Schäbitz 2009, Markgraf

⁷ As a direct way to exemplify the observed lack of non-climatic topics in the main discussions of palynological studies, a quantitative text analysis content was performed over a dataset that included all palynological publications published until present. The analysis was performed using co-occurrence networks, a common statistical technique utilized in quantitative content analysis to determine the presence of certain words, concepts, themes, phrases, characters, or sentences within texts or sets of texts and to quantify this presence in an objective manner (Danowski 1993). In this case, the co-occurrence network approach was used to identify the main focus or trends, and the correlations among concepts. The results highlighted the lack paleoecological topics in the text, and the strong correlation among the concepts pollen-record and climate. More information is provided in the appendix section (Appendix figure 1).

and Huber 2010, Moreno *et al.* 2010, Ponce *et al.* 2011). The timing and structure of this change is site-dependent, suggesting a complex history in forest expansion and establishment through the region during the postglacial. Absence of dispersal agents, insufficient soil development, intra- and interspecific competition, and/or features related with the distance from refugial areas and physical barriers in the routes of migration, are some of the plausible factors able to modify the dynamic of colonization and spread of tree taxa (Giesecke 2007). However, in most palynological studies interpret these changes are interpreted only in terms of precipitation changes associated with the SWW dynamics.

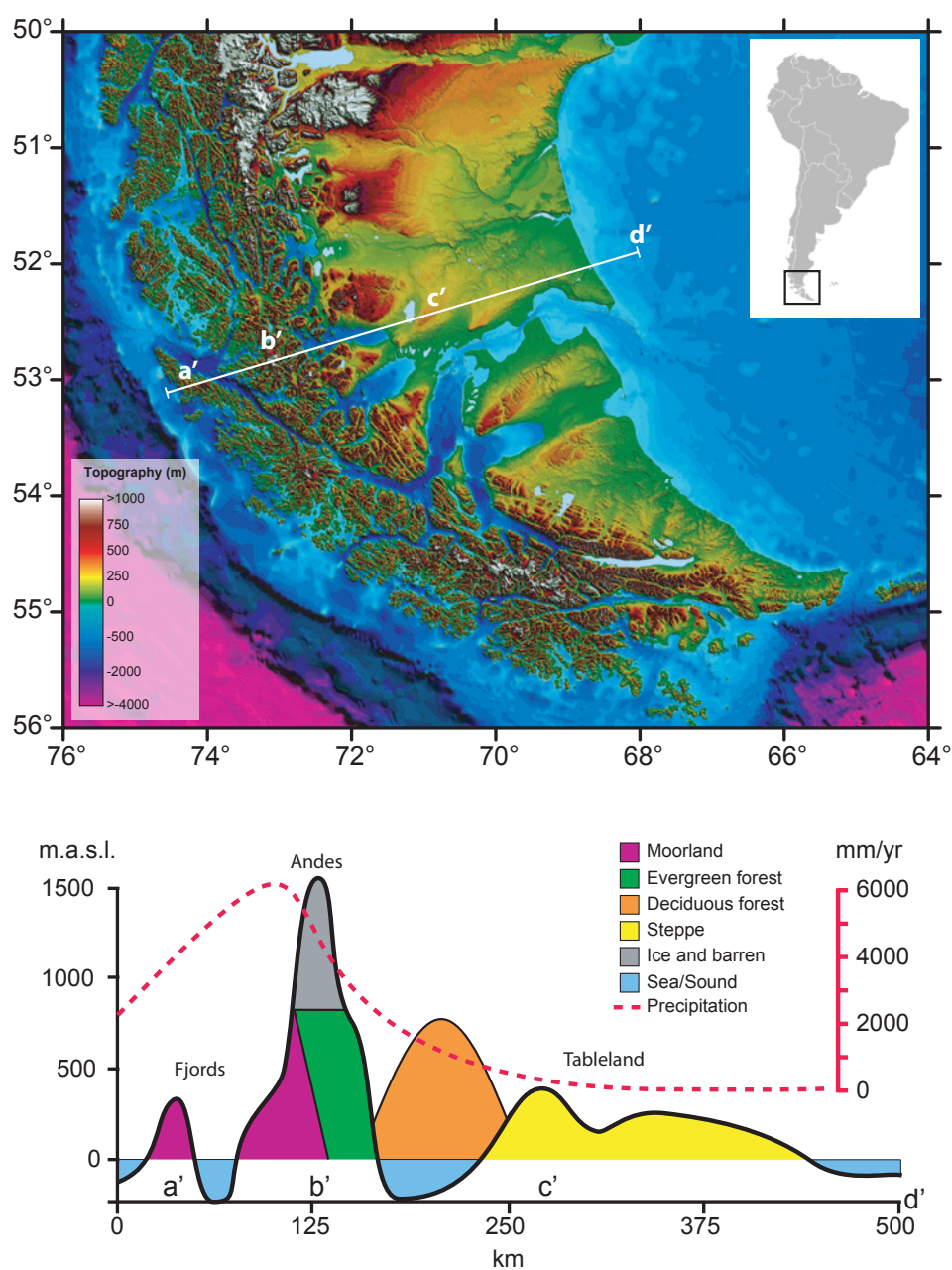


Figure 2. (Above) Topographic map based on a digital elevation model (SRTM, 30 arc-sec resolution; 90m) of Southern Patagonia territories (50°-56°S) and, (Below) schematic transect along the west-east axis (white line on the upper figure) denoting the precipitation gradient and the succession of main plant communities.

Additionally, it is important to mention the anomalous conglomeration of pollen records along the Andes and adjacent territories, and the resulting low representation of the steppe and moorland environments in paleoenvironmental studies (Figure 3). This is partly due to the lack of suitable locations to acquire paleoenvironmental records in the east (due to the prevalent dry climatic conditions) and due to logistic difficulties in accessing western locations⁸ (Kilian and Lamy 2012). The lack of data in the west (i.e. Channels and Fjords) is can be also seen in the sparse vegetation surveys (Luebert and Plissock 2006) undertaken and the absence of pollen-rain studies (Schäbitz *et al.* 2013) both prerequisites for the interpretation of pollen records (Fægri and Iversen 1989).

In light of the above, this study aims to investigate these ecological issues such as the actual distribution and composition of main plant communities occurring in Western Patagonia, as well as the representation of these plant communities in the modern pollen rain. The relationships between pollen assemblages (i.e. vegetation types) and key environmental variables (i.e. climate, altitude, etc) have been not studied by previous studies concerning the modern pollen-rain (Mancini 1998, Prieto *et al.* 1998, Heusser 2003, Trivi *et al.* 2006, Mancini *et al.* 2012). Hence, with the development of a modern pollen-rain study in the fjords is possible solve the sampling bias exhibited by previous studies, and to perform quantitative analyses to explore the relationship between pollen assemblages and environmental variables along a range which includes all the main plant formations from Southern Patagonia (Figure 2).

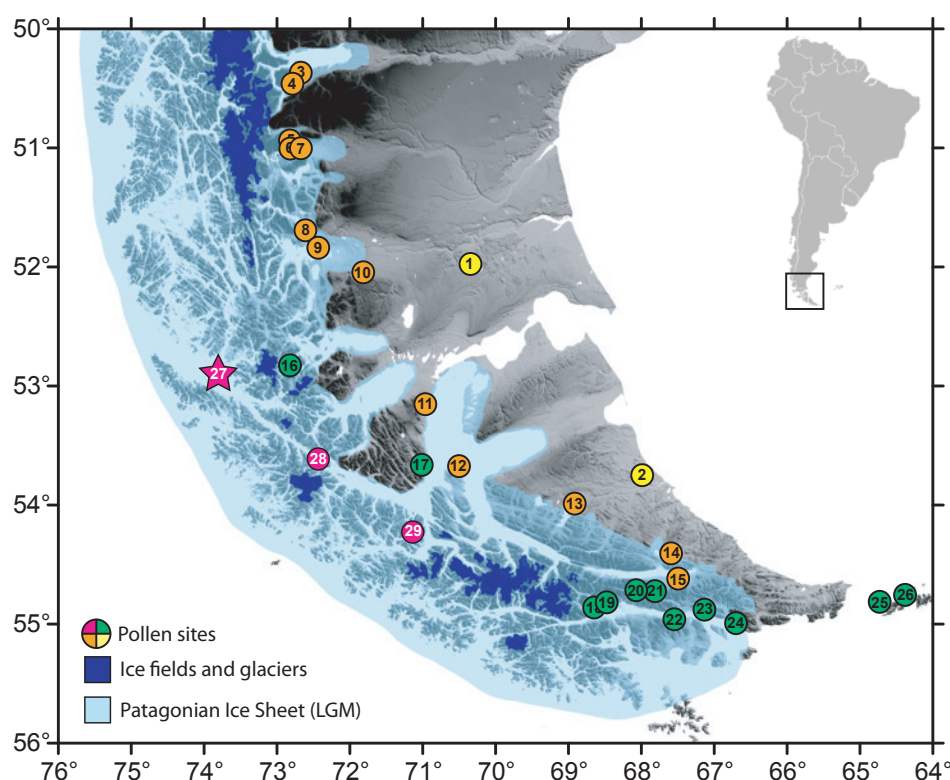


Figure 3. Map of Southern Patagonia showing the location of pollen records (Table 1) and the likely extension of the Patagonian Ice Sheet during the Last Glacial Maximum (LGM). The colour for each pollen site regards to the main vegetation occurring in the study area after the Figure 2. The star indicates the pollen record studied in this thesis (Tamar Lake).

⁸ The Southern Patagonian Fjords are one of the most isolated and unpopulated areas in southernmost South America (estimated demographic density <0.01 inhabitant/km², source INE). This explains why its territories, at present, contain several pristine ecosystems, making some areas of the western Andes particularly important in terms of conservation (Martínez-Harms and Gajardo 2008).

1.2. Research questions and thesis objectives

As mentioned above, paleoenvironmental studies, and more specifically palynological studies, performed in Southern Patagonia are characterized by a lack of paleoecological issues or non-climate related focus in the research questions and subsequent discussions. Thus, fundamental questions such as when did the establishment of the modern phytogeographic gradient that characterizes Southern Patagonia take place, What changes in diversity and composition were experienced by the vegetal ecosystems during the postglacial and how stable are these plant communities through time and space remain open. Further to this, by taking in account the fact that during the last ice age vast areas of the territory were covered by ice (Sugden *et al.* 2005; Figure 3), questions such as: how and when did plant colonization occur following ice retreat, is this process comparable (in its character and timing) with the vegetational successions that take place today, for example, on recently ice free areas, and what role do migration routes, dispersal mechanisms and soil development play in colonization and successional stages after the ice retreat? are also important to address. Finally, questions with regards to understanding the impact of environmental changes (i.e. climate) on the regional biogeography of Southern Patagonia territories such as whether the communities respond along the west-east transect as a whole or individually to particular environmental changes, which ecosystems are more sensitive, or which ecosystems respond more gradually or abruptly to environmental changes and what is the expected time lag between climate change and ecological change are a challenge. In order to address these questions, it is necessary to keep in mind that data from pollen records tell us about past vegetation or past environment, but not both. Further to this, circular argumentation could occur making it difficult to deduce organism-environment relationships. As a result, the use of an independent proxy to verify the hypothesis is integral for the validation of this study. On the other hand, questions regards to the vegetation and the modern pollen-rain, such as what are the characteristic vegetation communities occurring in the Southern Fjords of Patagonia and what environmental factors can explain their distribution, as well as which environmental variables (climatic and non-climatic) can explain the variation observed in the modern pollen-rain assemblages along the west-east transect and which taxa are under-represented and over-represented in the pollen rain are also important and must be addressed.

Based on the arguments and questions exposed before, four main objectives are addressed in this Thesis

1. Characterize the phytogeography occurring in the Fjords (and vicinity areas). More specifically:
 - Identify the main plant communities and its characteristic taxa occurring in the Fjords and vicinity areas.
 - Examine the distribution of main plant communities as a function of the basic features of their surrounding physical environment (i.e. elevation, slope, aspect, soil characteristics).

2. Develop a comprehensive study of the modern pollen-rain in order to calibrate the pollen diagrams. More specifically:
 - Identify the main plant communities occurring in the Fjords (and vicinity areas) and, examine their distribution as a function of the basic features of their surrounding physical environment (i.e. elevation, slope, aspect, soil characteristics).
 - Establish how the main plant communities present along the west-east transect are represented in the pollen-rain, and identify by means of multivariate analyses the most distinctive taxa characterizing each community.
 - Identify and determine, using multivariate analyses, which environmental variables (climatic and non-climatic) explain the main changes (variability) experienced by modern pollen assemblages and the most distinctive taxa that characterize it.

3. Contribute to the understanding of paleoecology of the Southern Patagonian Fjords by means of the development of a new paleoenvironmental record. More specifically:
 - Determine the timing and nature of deglaciation in the area of Tamar Island, and the evolution of the physical environment during the postglacial through geochemical analysis of the sedimentary record.
 - Reconstruct a history of vegetation (colonization, succession and, changes and ecosystem interactions) since the last ice retreat in the area of Tamar Island, through pollen analysis of the sedimentary record.
 - Determine and differentiate between a number of environmental forcing factors which could potentially influence past changes of plant communities and/or physical environment, through the constructed of a paleoenvironmental record from Tamar Island and use of independent proxies related to key environmental forcings (climatic and non-climatic) with local-to-regional implications.

4. Examine the transformations (ecological properties) experienced by the main plant communities along the west-east gradient of Southern Patagonia during the postglacial. More specifically:

Summarize the compositional changes and transformations experiences by the main plant communities during the postglacial, through the use of multivariate analyses performed on selected pollen records located along the west-east biogeographic gradient.

- Identify the ecological thresholds and resilience of distinctive plant communities to particular environmental forcings (climatic and non-climatic) through comparison between the outcomes of qualitative analysis (diversity and compositional turnover) performed on selected pollen records along the west-east biogeographic gradient and independent proxies related to key environmental forcings (climatic and non-climatic) with local-to-regional implications.

Finally, paleoclimatic pollen-based reconstructions are performed on selected pollen records located along the west-east gradient utilizing quantitative analyses (Appendix B). The main objective is to identify and discuss the positive aspects and limitations for the application of this analysis, taking in account in pollen records to a new region (Tonello *et al.* 2009, Schäbitz *et al.* 2013). Therefore, a comparison between different methods is conducted on each pollen record, in order to identify bias associated with the models utilized. Later the results are compared with other quantitative paleoclimatic reconstructions performed in the region in order to identify possible trends.

Table 1. Summary table indicating the code (number), name, location and altitude of palynological studies performed in Southern Patagonia (Figure 3). Note that sites are ordered according to the dominant plant formation present on each of the study sites.

Dominant plant formation	N°	Site	Long	Lat	Altitude (m.a.s.l.)	References
Steppe						
	1	Potrok Aike*	70.38	51.96	113	(Wille <i>et al.</i> 2007)
	2	La Mision	68.04	53.72	60	(Auer 1958, Markgraf 1993)
Deciduous Forest						
	3	Cerro Frias	72.70	50.40	200	(Mancini 2009)
	4	Brazo Sur	72.92	50.59	198	(Wille and Schäbitz 2009)
	5	Vega Ñandu	72.77	50.93	200	(Villa-Martinez and Moreno 2007)
	6	Lago Guanaco*	72.83	51.03	185	(Francois 2009, Moreno <i>et al.</i> 2010)
	7	TDP	72.69	51.00	90	(Heusser 1995)
	8	Lago Eberhard	72.67	51.58	68	(Cárdenas 2006, Moreno <i>et al.</i> 2012)
	9	Dumestre	72.44	51.80	77	(Moreno <i>et al.</i> 2012)
	10	Rio Rubens*	71.87	52.04	220	(Huber and Markgraf 2003)
	11	Pta. Arenas	70.95	53.15	85	(Heusser 1995)
	12	Est. Esmeralda	70.50	53.61	60	(McCulloch and Davies 2001)
	13	Onamonte	68.97	53.95	190	(Heusser 1993)
	14	Lago Yehuín	67.66	54.35	110	(Markgraf 1983)
	15	Lago Fagnano	67.49	54.62	65	(Heusser 1994)
Evergreen Forest						
	16	GCN*	72.92	52.81	70	(Fesq-Martin <i>et al.</i> 2004)
	17	Pto. Hambre	70.94	53.61	6	(Heusser 1995, Heusser <i>et al.</i> 2000, McCulloch and Davies 2001)
	18	Lapataia	68.59	54.85	18	(Heusser 1998)
	19	Ushuaia-2	68.37	54.81	80	(Heusser 1998)
	20	Las Cotorras	68.05	54.69	420	(Borromei <i>et al.</i> 2010)
	21	Paso Garibaldi	67.84	54.71	420	(Markgraf and Huber 2010)
	22	Caleta Robalo	67.64	54.94	20	(Heusser 1989)
	23	Pto. Haberton	67.20	54.89	20	(Heusser 1990, Markgraf 1991)
	24	Bahia Moat	66.78	54.95	20	(Heusser 1995)
	26	Lago Galvarne	64.33	54.74	2	(Björck <i>et al.</i> 2012)
	25	Isla Estados	64.64	54.85	27	(Ponce <i>et al.</i> 2011)
Moorland						
	27	Lake Tamar*	73.80	52.90	35	This thesis
	28	Lake Ballena	72.48	53.58	70	(Fontana and Bennett 2012)
	29	Isla Clarence	71.20	54.18	35	(Auer 1958, Auer 1974)

* Study sites used to estimate changes in plant community composition (turnover and richness) and to perform quantitative climatic reconstructions (Pann and Tann; Appendix B), along a west-east gradient during the postglacial.

2. STUDY AREA

2.1. Geology, climate and vegetation across Southern Patagonia at 53°S

2.1.1. Regional geology

Three main geological provinces are found in the study area. In the west, deep and linear valleys carved into the bedrock as result of the glacial erosion and tectonic activity characterizes the Patagonian Fjords province (Glasser and Ghiglione 2009). Its rock basement consists mainly in granodiorites and granites from the Patagonian Batholith (Cretaceous), nevertheless volcanic sequences from the Paleozoic (Carboniferous-Permian) are present in islands located to the west (SERNAGEOMIN 2003)(Figure 4). In contrast, eastern territories are comprised of basaltic plateaus and outwashplains, and characterize the denominated Patagonian Tableland or Patagonian Plain province (Coronato *et al.* 2008). Both units (basaltic plateaus and outwashplains) are of Tertiary-Quaternary age and overlie marine Cretaceous sequences of the Austral Magallanes basin (Ghiglione *et al.* 2009). Finally, dividing the previous geological provinces (Fjords and Tableland-Plains) emerges the Patagonian Andean province with mountains reaching altitudes over the 1000 m.a.s.l. It is here that temperature and precipitation conditions are appropriate for ice accumulation (positive mass balance) resulting in the occurrence of glaciers (Casassa *et al.* 2007)(Figure 4). The Andean orogenesis is closely linked with subduction occurring in the west flank of the continent, causing uplift and deformation of Cretaceous sequences in the east (fold thrust belt) and the Patagonian Batholith in the west (Ramos and Ghiglione 2008, Ghiglione *et al.* 2009, Fosdick *et al.* 2011).

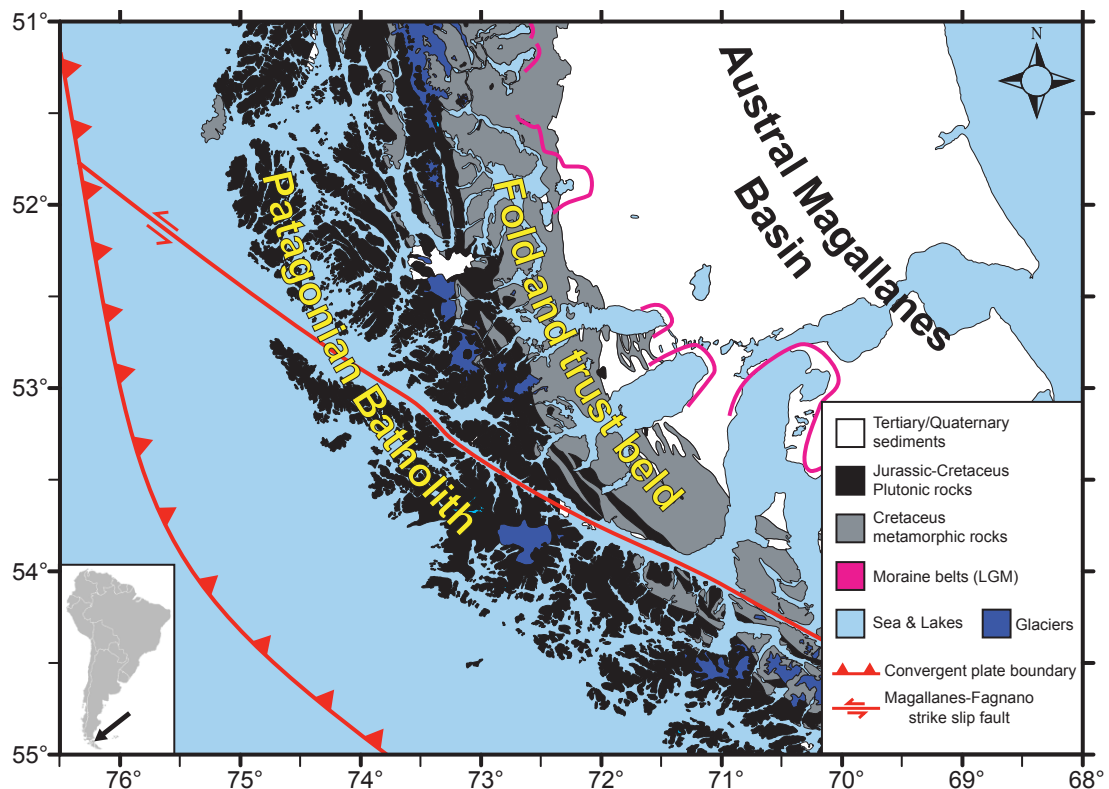


Figure 4. Geological map of southern Patagonia (after SERNAGEOMIN 2003, Ghiglione *et al.* 2009; Fosdick *et al.* 2011) and inferred glacial limits during the LGM (after McCulloch *et al.* 2005; Coronato *et al.* 2008; Kaplan *et al.* 2008; Sagredo *et al.* 2011; Garcia *et al.* 2012).

Well-preserved moraine belts occur to the east of the main Cordillera, denoting the flux of ice lobes towards lowlands during the numerous Pleistocene ice ages (Caldenius 1932). Geomorphological studies provide valuable information to determine the ice limits during the Last Glacial Maximum (LGM) in east flank of the Andes (McCulloch *et al.* 2005, Coronato *et al.* 2008, Kaplan *et al.* 2008, Sagredo *et al.* 2011, García *et al.* 2012)(Figure 4). On the contrary, the glacial history of western territories (chronology and extension) is limited, with the available information suggesting that most of the Fjords were ice covered during the LGM (Coronato *et al.* 2008).

2.1.2. Climate

The climate of Southern Patagonia is strongly influenced by the Southern Westerly Winds (SWWs), responsible for the temporal and spatial precipitation patterns occurring in the region (Figure 1 and Figure 5) (Miller 1976, Endlicher and Santana 1988, Schneider *et al.* 2003, Garreaud *et al.* 2013). Its dynamic is closely correlated with changes in the strength and position of the South Pacific Anticyclone (SPA) around the year (Miller 1976). Thus, during the austral summer (DJF) when the SPA is expanded and displaced to the south of its mean location (30°S), the northern margin and the core of SWW are forced to move poleward (45°-55°S). On the contrary, during the austral winter (MJJ) when the SPA is weak and situated to the north of its mean position, the SWW's northern margin and core is displaced towards to equatorward (Schneider *et al.* 2003, Garreaud *et al.* 2009, Garreaud *et al.* 2013)(Figure 5). These changes experienced by the SWW throughout the year result in important variations in its flux, with a strengthening during the austral summer and a weakening during the austral winter. Consequently, the precipitation patterns over the Southern Patagonia territories follow this trends (Figure 5)(Schneider *et al.* 2003, Garreaud *et al.* 2009).

The temperatures regimes throughout the year are closely related with the amount of incoming radiation and sunshine hours, both controlled by the latitude (Coronato *et al.* 2008). Values close to 180W/m² (annual average) are registered in the northern territories of Southern Patagonia (50°S), whereas in its southern rim (56°S) the values of incoming radiation reach 100W/m² (Coronato *et al.* 2008). The thermal amplitude also experience a change along the latitudinal gradient, exhibiting mean values of 16°C in the northern territories and 8°C in the south. This decreasing trend in thermal amplitude towards to the South Pole is a result of continental narrowing and a subsequent increase in the oceanic influence on the climate (Coronato *et al.* 2008). In addition, the proximity to the Antarctic continent and the Antarctic Circumpolar Current (ACC) have a strong influence on the climate, producing a decrease in the mean temperatures over the region (Figure 6), resulting in the regional mean annual air temperature of below 7°C.

Climatic fluctuations at decadal to sub-decadal timescales are observed in several hydro-meteorological records of Southern Patagonia, and can be attributed to the action of two mechanism: the Southern Annular Mode (SAM) [also called the Antarctic Oscillation] and El Niño Southern Oscillation (ENSO) (Thompson and Wallace 2000, Thompson and Solomon 2002, Schneider and Gies 2004, Garreaud *et al.* 2009, Garreaud *et al.* 2013, Villalba *et al.* 2013). The most prominent mechanism affecting the climate of Southern Patagonia is the SAM, which is related to changes in the pressure gradient at sea level (SLP) between mid and high latitudes (Thompson and Wallace 2000, Thompson and Solomon 2002). During the positive phase of SAM decreased (increased) surface pressure and geopotential heights over Antarctica (midlatitudes) are observed, resulting in a strengthening and poleward shift of the SWW. During the negative phase of SAM, the SWW experiences a weakening as result of the decrease in the pressure gradient between mid- and high latitudes (Garreaud *et al.* 2009). The impact of ENSO phenomenon in the Southern Patagonia climate, as yet, not fully understood, nevertheless it is apparent that during its positive phase (El

NCEP/NCAR Reanalysis
Composite means 1949-2013

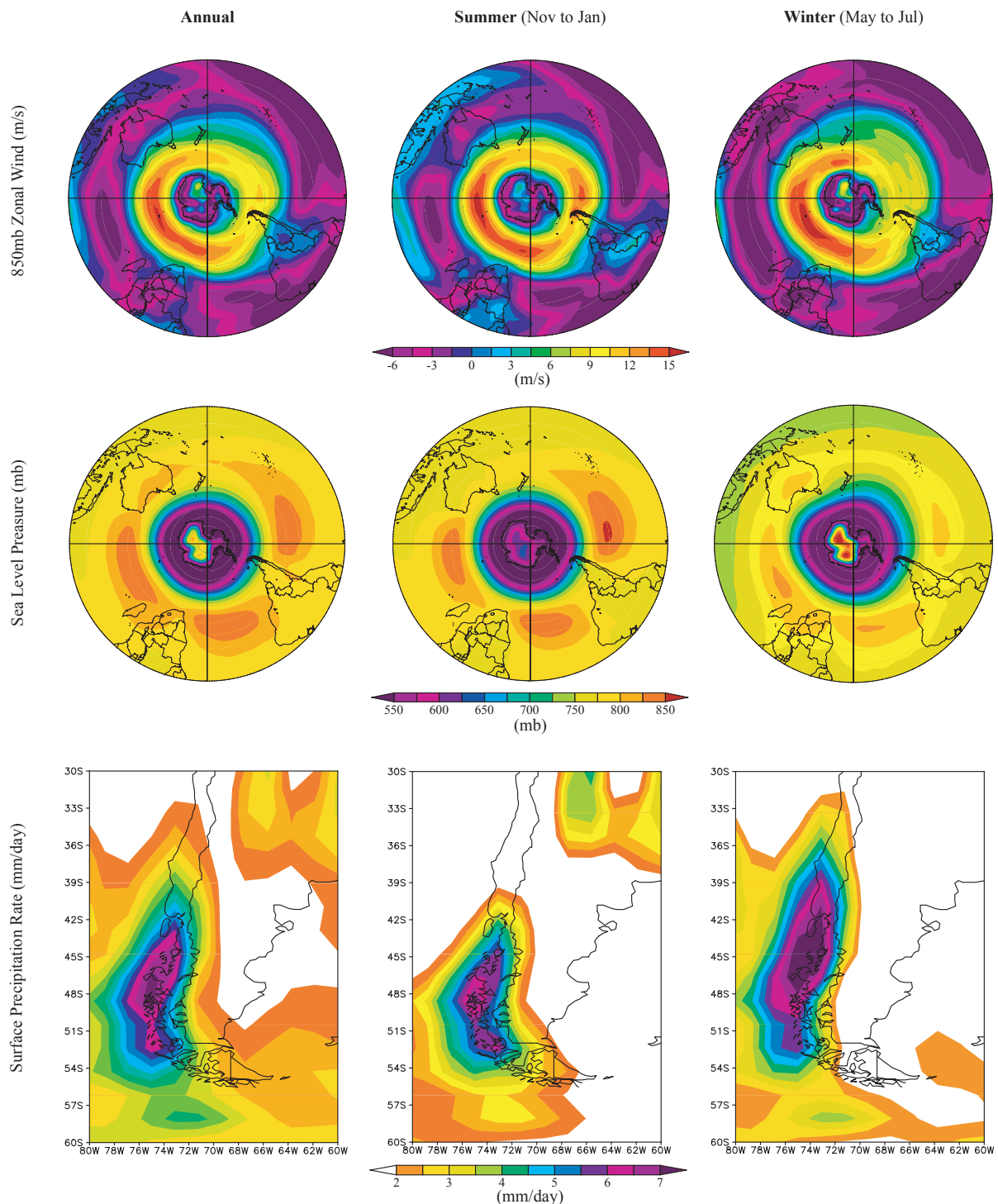


Figure 5. Composite means for the period 1949-2013 illustrating the annual and seasonal (winter and summer) patterns of zonal wind speed (above) and Sea Level Pressures (middle) occurring in the Southern Hemisphere, and its repercussions in the precipitation patterns along southern South America (below). The images were produced utilizing the online data provided by the NOAA/ESRL Physical Sciences Division, Boulder Colorado (<http://www.esrl.noaa.gov/psd/>).

NCEP/NCAR Reanalysis
Composite means 1949-2013

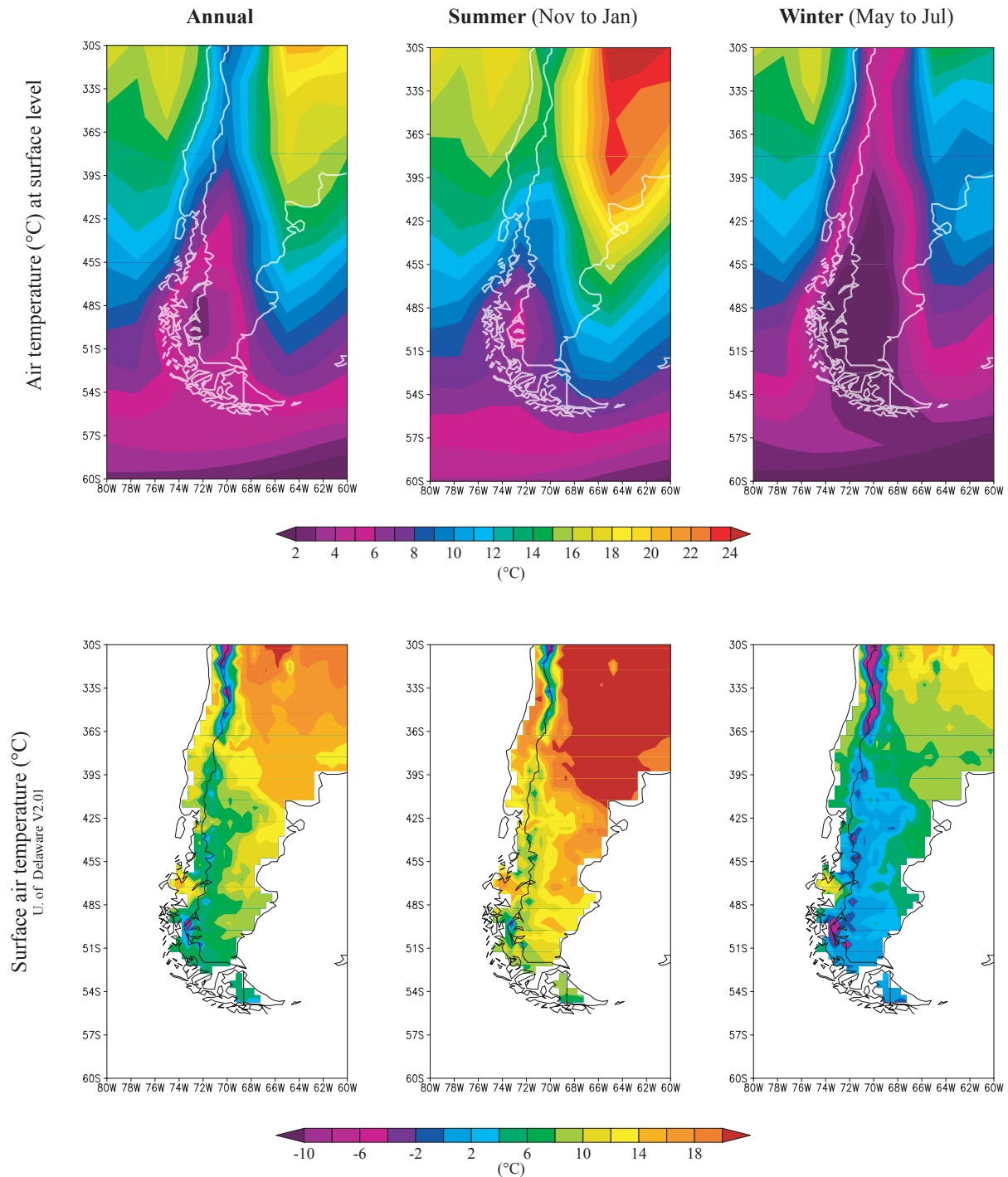


Figure 6. Composite means for the period 1949-2013 illustrating the annual and seasonal (winter and summer) temperatures of the air (above) and surface (below) in the southern South America. The images were produced utilizing the online data provided by the NOAA/ESRL Physical Sciences Division, Boulder Colorado (<http://www.esrl.noaa.gov/psd/>).

Niño) decrease in the level of precipitation occurs, especially in the west (Schneider and Gies 2004). This is related to the reduction in wind speed during the El Niño phase, caused by a decrease of the meridional SLP gradient (Schneider and Gies 2004).

The regional topography produces a strong influence on the precipitation and temperature regimes along the west-to-east transect (Miller 1976, Endlicher and Santana 1988, Schneider *et al.* 2003, Garreaud *et al.* 2013). High levels of precipitation are measured over the Andes (~6000 mm/yr) and the Fjords (~2500 mm/yr), as a result of the orographically-induced uplift of moist air masses advected from the west (Figure 2 & Figure 7). On the contrary, to the east of the main divide of the mountains, the air masses become drier because of the Foehn Effect, with a decrease in precipitation values on the Patagonia plains (~500 mm/yr) and at the Atlantic coast (<250 mm/yr) (Endlicher and Santana 1988, Schneider *et al.* 2003) (Figure 2 & Figure 7). The Foehn Effect is also found to strengthen during periods of enhanced (reduction) westerlies, resulting in an increase in the amount of precipitation to the west of the Andes and a decrease in the east (leeward). The opposite occurs during periods of reduction in the westerlies flux, with a weakening in the foehn effect and a diminishing of the west-east precipitation gradient (Schneider *et al.* 2003, Garreaud *et al.* 2013). Intra-annual variations in the precipitation regime are also observable along the west-east transect, with a slightly but significant increased in the seasonality towards the east (Endlicher and Santana 1988, Schneider *et al.* 2003).

Changes in the mean annual temperature regime are also recorded along the west-to-east gradient (Coronato and Bisigato 1998, Schneider *et al.* 2003). The ocean influences this gradient, which retains heat and causes mild temperatures along the coasts and adjacent areas. This results in low annual temperature amplitudes along the coast, whereas into the continent the temperature amplitude is more pronounced (Coronato and Bisigato 1998, Schneider *et al.* 2003, Garreaud *et al.* 2013). Also, with altitude, temperatures decrease, allowing the presence of ice caps and glaciers at altitudes over 1000 m.a.s.l (Figure 7).

2.1.3. Vegetation

Phytosociological and ecological studies indicate a distinct change in the vegetation structure and composition along the west-to-east gradient (Schmithüsen 1956, Oberdorfer 1960, Pisano 1977, Boelcke *et al.* 1985, Gajardo 1994). At least four major regional vegetation types or vegetal formations can be recognized along this gradient (Figure 2 & Figure 8).

The Magellanic Moorland is comprised of several plant communities including cushion/peat bog and outliers elements of evergreen forest. The shrub/herbaceous components are diverse with characteristic species including *Chiliotrichum diffusum* (Asteraceae), *Gaultheria mucronata* (Ericaceae), *Empetrum rubrum* (Ericaceae) and *Escallonia serrata* (Escalloniaceae) in well drained soils, and *Schoenus antarcticus* (Cyperaceae), *Marsippospermum grandiflorum* (Juncaceae), *Donatia fascicularis* (Donatiaceae), *Astelia pumila* (Liliaceae), *Caltha appendiculata* (Ranunculaceae) and *Gunnera magellanica* (Gunneraceae) in swamp soils. The arboreal elements are few, composed by *Nothofagus antarctica*, *Nothofagus betuloides* (Fagaceae), *Drimys winteri* (Winteraceae), *Desfontainia spinosa* (Desfontainiaceae), *Tepualia stipularis* (Myrtaceae), and *Pilgerodendron uviferum* (Cupressaceae). A number of edaphic and topographic features control the occurrence and distribution of the different vegetation types. At coastal and waterlogged locations *Tepualia stipularis* and *Pilgerodendron uviferum* prevail. Whereas, the small forest are primarily composed of *Nothofagus betuloides* and *Drimys winteri* which grow on steeper slopes at altitudes below 430 m, characterized by well- drainage, thinner soils, and in locations protected from the persistent, cold

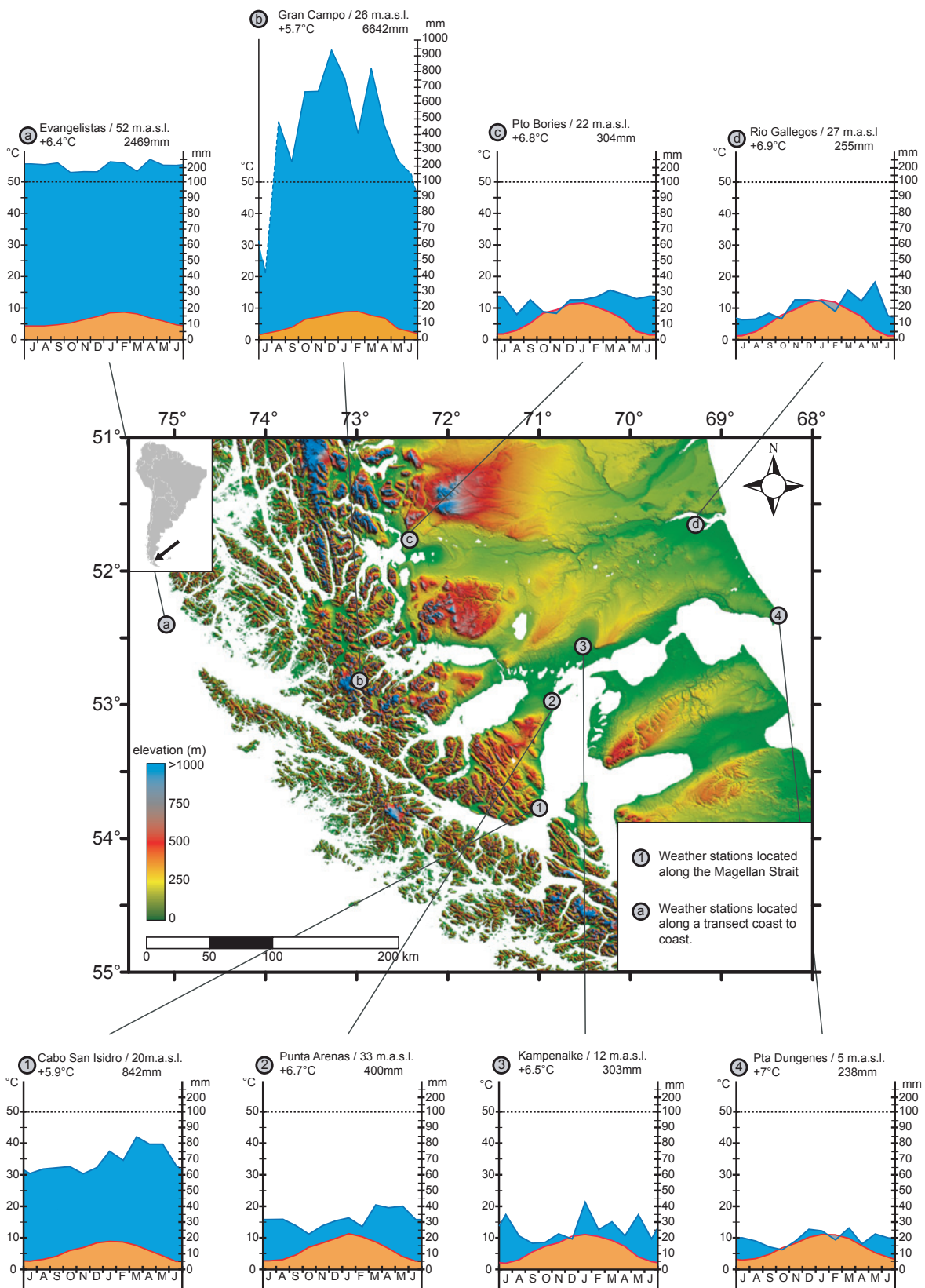


Figure 7. Digital Elevation Model (DEM) and location of weather stations present in the study area (53°S). Please note the under-represent values occurring during the winter months (MJJ) in the weather station of Gran Campo because the solid precipitation (snow).

and wet conditions, often including gale-force storms. The treeline is comprised of crooked and stunted (Krummholz) individuals of *Nothofagus antarctica* which also occurs in areas of high wind.

The **Subantarctic Evergreen Forest** is found at the foot of the Andes. The arboreal stratum (>5 m) is complex and encompasses species such as *Nothofagus betuloides*, *Nothofagus antarctica*, *Drimys winteri*, *Tepualia stipularis*, *Lomatia ferruginea* (Proteaceae), *Raukaua laetevirens* (Araliaceae) and *Maytenus magellanica* (Celastraceae). The shrub/herbaceous stratum is also diverse and includes taxa such as *Gaultheria mucronata*, *Desfontainia spinosa*, *Gunnera magellanica*, *Marsippospermum grandiflorum*, *Lebetanthus myrsinites* (Epacridaceae), *Philesia magellanica* (Philleciaceae) and *Berberis ilicifolia* (Berberidaceae). A number of fern species grow on the forest floor and on tree trunks, most of which are epiphytes from the Hymenophyllaceae family.

The **Subantarctic Deciduous Forest** is positioned inland of the Subantarctic Evergreen Forest, penetrating further in to the continent. At low altitudes *Nothofagus pumilio* and *Nothofagus antarctica* are the dominant or co-dominant arboreal components, forming tall (>30 m) and close-canopy stands. The understory is poor or absent, only occurring in canopy gaps where *Chilotrimum diffusum* and *Osmorhiza chilensis* (Apiaceae) become dominant. *Misodendrum* sp, a woody hemiparasite infecting several species of *Nothofagus*, is a common element in the forest canopy. Upslope, at the treeline, the *Nothofagus* species acquires the form of Krummholz, denoting the effect of altitude (decrease) on temperatures.

To the east the **Deciduous Forest** becomes shorter and open, and is often present as isolated stands with few individuals, resulting in a park-like landscape known as the Forest-Steppe Ecotone. The shrub and herb strata are increasingly significant, merging with Patagonian elements from the steppe to the forest (patch) edge. Typical woody elements are *Nothofagus pumilio*, *Nothofagus antarctica*, *Gaultheria mucronata*, *Empetrum rubrum*, *Chilotrimum diffusum*, *Berberis microphylla* (Berberidaceae), *Nardophyllum obtusifolium* (Asteraceae), *Baccharis magellanica* (Asteraceae), *Anarthrophyllum desideratum* (Fabaceae), *Mulinum spinosum* (Apiaceae), and *Adesmia boronioides* (Papilionaceae). Predominantly, these taxa are present as cushions in a grass matrix dominated by *Festuca gracillima* (Poaceae), along with *Acaena integerrima* (Rosaceae), *Valeriana carnososa* (Valerianaceae). Anthropogenically produced fires and cattle breeding play a significant role in vegetation, causing modifications to the species present and adding exotic species such as *Taraxacum officinale* (Asteraceae), *Rumex acetosella* (Polygonaceae), *Trifolium repens* (Papilionaceae), *Hypochaeris* sp. (Asteraceae), *Cirsium* sp. (Asteraceae).

The **Patagonian Steppe** occurs farther to the east again, reaching the Atlantic coast. This vegetation type corresponds to a grass steppe dominated by *Festuca gracillima*. Following Roig *et al.* (1985), this steppe can be divided into a humid grass steppe to the west and a xeric grass steppe to the east. The humid type comprises of a number of shrubby species including *Empetrum rubrum*, *Chilotrimum diffusum* and *Berberis microphylla* whereas, the xeric type is predominantly characterized by *Festuca gracillima* and *Nardophyllum bryoides* (Asteraceae). According to León *et al.* (1998), both humid and xeric steppes extend from the south of Santa Cruz, Argentina, towards the north of Tierra del Fuego, including throughout the Patagonian plateaus in Chile (52°–53°S) (Pisano 1981)

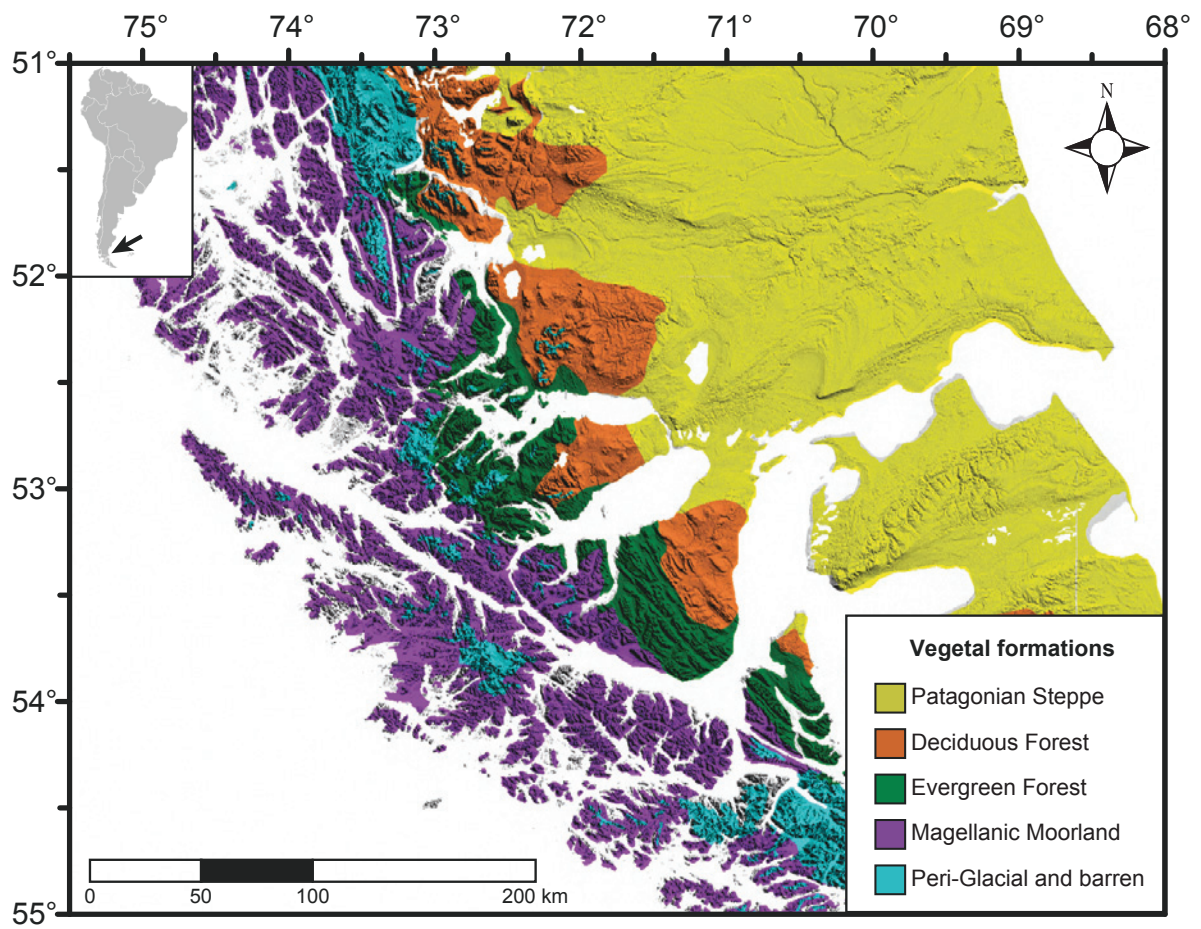


Figure 8. General map of Southern Patagonia, indicating the main plant formations occurring at regional-scale (after Schmithüsen 1956 and Gajardo 1994).

3. MATERIALS AND METHODS

3.1. Vegetation and modern pollen-rain

As mentioned previously, one limitation in the development of pollen records in western areas of Southern Patagonia (*sensu* Southern Patagonian Fjords) is the lack of information with regards to vegetation and its pollen-rain. Therefore, the initial aim of this thesis was develop a basic but comprehensive study of the relationship between the vegetation and pollen-rain for the most distinctive plant communities and the vegetation gradients occurring in the western territories of Southern Patagonia.

3.1.1. Sampling

Due to the characteristics of the study area (Fjords) the sampling was conducted onboard the Research Vessel “Gran Campo II” (Kilian *et al.* 2013), during the spring (September to October) of 2010. During the field campaign a total of seven localities distributed along a west-east transect were visited, in order to characterize the main vegetation and obtain samples to study the modern pollen-rain (Table 2 & Figure 9). The first step performed at each visited locality was to identify the most distinctive plant communities and/or a vegetation gradient (e.g. altitudinal) in order to design the sampling survey (Mueller–Dombois and Ellenberg 1974). Later utilizing the classic relevé method, vegetation characteristics (e.g. abundance and cover) and environmental features (e.g. slope, facing, altitude) were registered (Mueller–Dombois and Ellenberg 1974). In total twenty-three soil samples were collected by hand from well-defined plant communities occurring in the survey areas, following the method of multiple samples (Adam and Mehringer 1975, Hicks *et al.* 1998)(Table 2). In addition, three undisturbed surface sediment from two lakes (Lake Tamar and Desolacion) and one smaller bay (Chids Bay) were retrieved using a gravity corer (Table 2 & Figure 9).

Special attention was paid to the site on Tamar Island (Figure 9), where multiples sediment cores were retrieved from an unnamed lake (Lake Tamar) and later analysed in order to reconstruct the local paleoenvironmental history (this thesis). Therefore, a vegetation mapping was developed for the catchment surrounding the lake through interpretation of aerial photographs (orthophotos scale 1:70.000) and data collected in the field. Later, the developed vegetation map was plotted over a Digital Elevation Model (SRTM, 30 arc-sec resolution; 90m), in order to estimate the extents of the most distinguish plant communities occurring in the catchment. In addition, the physical features of altitude, slope and aspect were determined for consideration in the implications on plant community distribution within the Lake Tamar catchment. The physical features, alongside the lake and catchment boundaries, were determined by a combination of GPS measurements in the field and Geographical Information Systems (GIS).

3.1.2. Pollen analyses

Approximately 10 g samples of soil and 2 cc of the upper centimeters (0-1 cm) from the sedimentary sequences were collected for the study of modern pollen-rain. In both cases the samples were processed following the standard pollen preparation techniques which includes the use of HCl (10%, dissolution of carbonates), KOH (10%, deflocculation), sieving (<120 μ m), ZnCl₂ (recovery the organic matter by flotation), HF (40%, silica removal), and acetolysis (cellulose removal) (Fægri and Iversen 1989). In addition, tablets of exotic *Lycopodium* spores were added to allow calculation of pollen and spore concentration (Stockmarr 1971). The residues obtained were mounted on slides and counted under the microscope. A total of >300 pollen grains including trees,

shrubs, cushion plants and herbs were identified and counted in each sample (terrestrial pollen). The abundance of pteridophytes and paludal/aquatic taxa were calculated in separated sums called: 'total terrestrial pollen and spores' (terrestrial pollen+pteridophytes) and 'total pollen and spores' (terrestrial pollen+pteridophytes+paludal/aquatics). Reference pollen material and specialized literature were consulted for pollen identification (Heusser 1971, Markgraf and D'Antoni 1978).

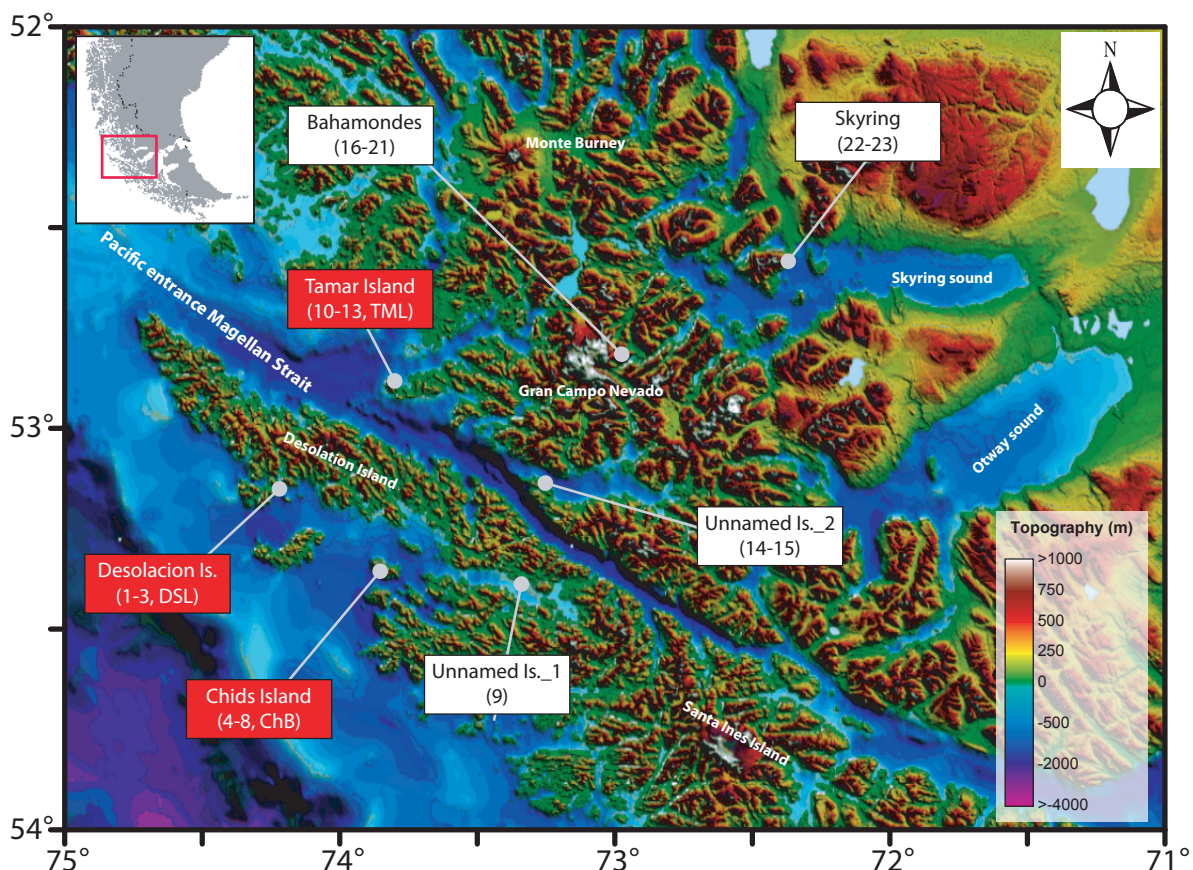


Figure 9. Map of the study area (Southwest Patagonian Fjords, at 53°S) indicating the localities visited ($n=7$) where vegetation surveys and soil sampling were performed for the study of modern pollen-rain. The information into the rectangles refers to the name of the site and code for the samples retrieved (parenthesis) after Table 2. Rectangles in red indicate locations where additional samples from surface sediments (two lakes and one bay) were obtained. More details in the text.

3.1.3. Numerical analyses

3.1.3.1. Cluster analyses and Principal Component Analysis (PCA)

In order to examine and obtain a direct measure of degree of similarity/dissimilarity among modern pollen assemblages from soil and gravity samples, unconstrained cluster analysis was performed on a dataset composed by taxa with values over 2% (27 taxa) (Overpeck *et al.* 1985). The percentages of the selected taxa were re-calculated and later the dissimilitude coefficients were measured using the Edward & Cavalli-Sforza's chord distance method (Grimm 1987). Principal Component Analysis (PCA) was utilized as a complementary data analysis technique to explore the correlation between pollen samples and taxonomic composition (ter Braak and Prentice 1988),

using the same dataset as used in the cluster analysis. This procedure (cluster analysis and PCA) was also used to estimate the degree of correspondence between the samples from western Patagonia (this thesis) and adjacent samples from the east (Quintana 2009) (Figure 10). In both cases exotic (e.g. *Rumex*) and long-distance transport pollen types (e.g. Mimosaceae and Anacardiaceae) which do not occur in Southern Patagonia were excluded from the analysis.

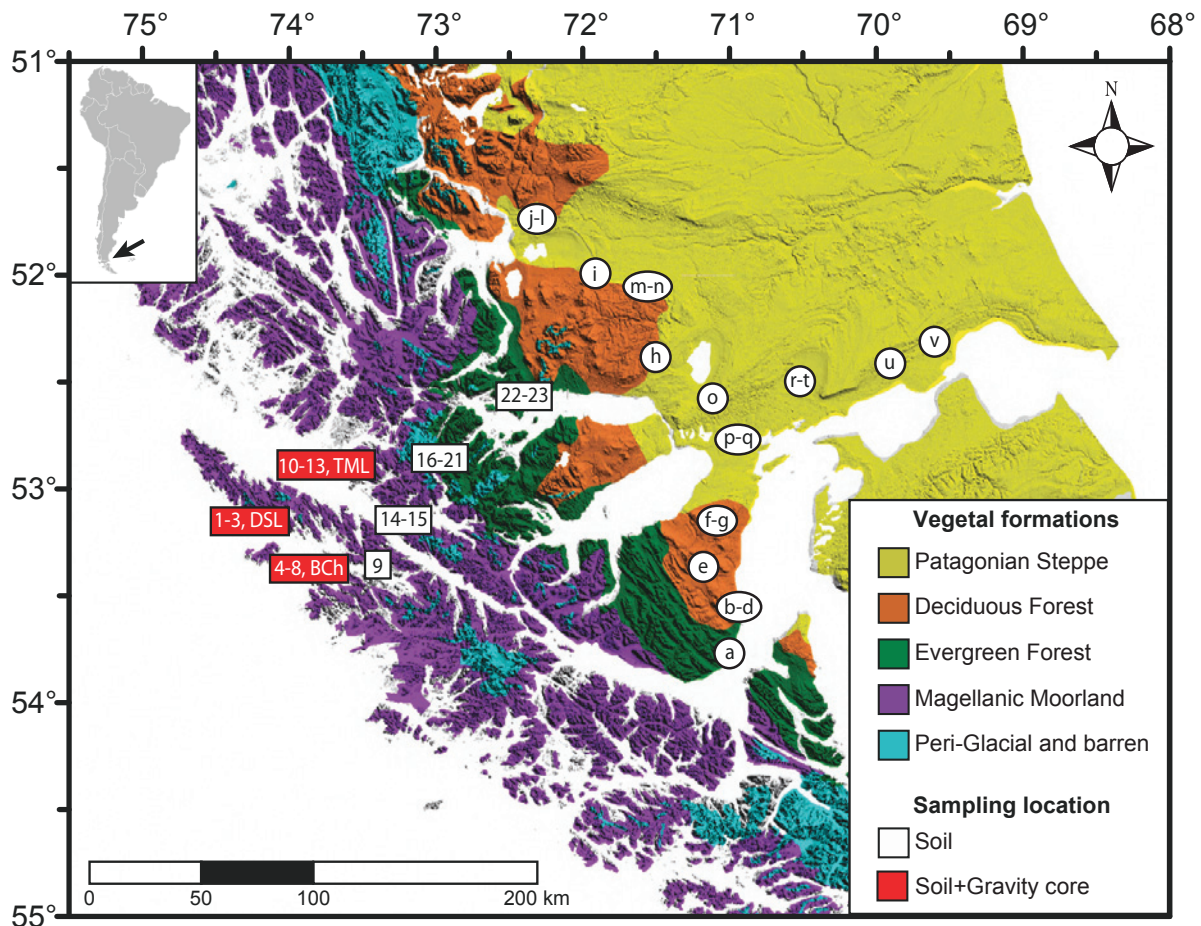


Figure 10. Vegetation map (after Figure 8) showing the location of samples utilized to the study of the modern pollen-rain that include the main plant formations occurring along a west-east transect in Southern Patagonia. The information into the rectangles (this thesis) and circles (previous studies) indicates the codes of the samples provided in the Tables 2 & 3.

3.1.3.2. Canonical analyses

Using the dataset used in the cluster analysis to examine the west-east pollen rain, canonical ordination analysis was carried out to determine the climatic variables with the best fit to the pollen data (ter Braak and Prentice 1988). Detrended Correspondence Analysis (DCA) was performed a priori to estimate the gradient length. This exploratory analysis indicated that the gradient lengths of the first axis are less than 2.4 standard deviations, suggesting that underlying responses are linear (Legendre and Birks 2012). As a result, Redundancy Analysis (RDA) was selected to assess the relationship between pollen assemblages and climatic variables. The pollen dataset was square-root transformed and treated with chord transformation, followed by calculation of the Euclidean distance (Legendre and Gallagher 2001).

Since meteorological stations are scarce in the study area, interpolated data from the WorldClim dataset (1-km spatial resolution) was used (Hijmans *et al.* 2005). In order to determine the influence of climatic factors on surface pollen distribution (Table 2 & Table 3), annual Precipitation (Pann) and mean annual Temperatures (Tann) were selected as external variables for the RDA. In addition, the geographical parameters of longitude, latitude and altitude were also included. Data skewness was reduced through the application of a logarithmic transformation, and standardized using an interval-scale ranging transformation (Legendre and Birks 2012). The significance of climatic and geographical variables was estimated using unrestricted Montecarlo permutations (n=999). Climatic and geographical parameters with variance inflation factor (VIF) values over 10 were removed to avoid inflation in the canonical coefficients variance due to co-linearity among the explanatory variables.

Table 2. Codes and main geographical characteristics (coordinates/elevation, site name and dominant plant formations) of the surface samples collected in this thesis to study the modern pollen-rain within the Southern Patagonian Fjords.

Code	Latitude	Longitude	Elevation (m.a.s.l.)	Location/Dominant plant formation	Local vegetation
1	53.12	74.24	2	Desolacion Island/Magellanic Moorland	Coastal graminoid heath ^{2,4,5}
2	53.12	74.24	78	Desolacion Island/Magellanic Moorland	Cushion-Bog ^{1,3,4,5}
3	53.12	74.24	78	Desolacion Island/Magellanic Moorland	Cushion-Bog ^{1,3,4,5}
4	53.34	73.84	378	Chids Island/Magellanic Moorland	Montane cushion community ^{2,4}
5	53.35	73.83	2	Chids Island/Magellanic Moorland	Coastal Scrub ^{1,4}
6	53.34	73.84	324	Chids Island/Magellanic Moorland	Montane cushion community ^{2,4}
7	53.35	73.83	70	Chids Island/Magellanic Moorland	<i>Nothofagus betuloides</i> dwarf forest ^{2,3,4}
8	53.35	73.83	12	Chids island/Magellanic Moorland	<i>Nothofagus - Drimys</i> Forest ^{1,3,4}
9	53.36	73.36	26	Unnamed Island_1/Magellanic Moorland	<i>Nothofagus betuloides</i> dwarf forest ^{2,3,4}
10	52.90	73.81	290	Tamar island/Magellanic Moorland	Montane cushion community ^{2,4}
11	52.91	73.80	30	Tamar island/Magellanic Moorland	Cushion-Bog ^{1,3,4,5}
12	52.90	73.81	256	Tamar island/Magellanic Moorland	Montane cushion community ^{2,4}
13	52.90	73.80	155	Tamar island/Magellanic Moorland	<i>Nothofagus betuloides</i> evergreen heath ^{2,4}
14	53.14	73.26	6	Unnamed Island_2/Magellanic Moorland	Cyperaceous-bog ^{3,4,5}
15	53.14	73.26	30	Unnamed Island_2/Magellanic Moorland	<i>Pilgerodendron uviferum</i> Scrub ^{1,4}
16	52.81	72.94	411	Bahamondes/Subantarctic Evergreen Forest	Montane cushion community ^{2,3,4}
17	52.81	72.93	90	Bahamondes/Subantarctic Evergreen Forest	Cushion-Bog ^{1,3,4,5}
18	52.81	72.93	13	Bahamondes/Subantarctic Evergreen Forest	Juncaceous-bog ^{3,4,5}
19	52.81	72.93	22	Bahamondes/Subantarctic Evergreen Forest	Cushion-Bog ^{1,3,4,5}
20	52.81	72.94	53	Bahamondes/Subantarctic Evergreen Forest	Disturbed <i>Nothofagus - Drimys</i> Forest ^{1,3,4}
21	52.80	72.92	12	Bahamondes/Subantarctic Evergreen Forest	<i>Nothofagus betuloides - Drimys winteri</i> Forest ^{1,3,4}
22	52.58	72.36	4	Skyring/Subantarctic Evergreen Forest	Coastal Scrub ^{1,4}
23	52.58	72.36	14	Skyring/Subantarctic Evergreen Forest	Coastal <i>Nothofagus betuloides</i> forest ^{1,3,4}

Table 2. Continue

Code	Latitude	Longitude	Elevation (m.a.s.l.)	Location/Dominant plant formation	Local vegetation
TML	52.91	73.80	35	Tamar island/Magellanic Moorland	--
BCh	53.35	73.83	--	Chids Island/Magellanic Moorland	--
DSL	53.12	74.23	39	Desolacion Island/Magellanic Moorland	--

References: ¹Pisano 1977; ²Pisano 1982; ³Pisano 1983; ⁴Roig *et al.* 1985b; ⁵Kleinebecker *et al.* 2007

Table 3. Additional surface sample locations (Quintana 2009) utilized to develop a comprehensive study of the modern pollen-rain along a broad west-to-east transect in Southern Patagonia (53°S). For more details see the text.

Code	Latitude	Longitude	Elevation (m.a.s.l.)	Dominant plant formation	Local vegetation
a	53.75	70.97	4	Subantarctic Evergreen Forest	Evergreen forest of the Brunswick Peninsula ⁶
b	53.60	70.95	48	Subantarctic Evergreen Forest	Coastal open areas ⁶
c	53.62	70.92	0	Subantarctic Evergreen Forest	Evergreen forest of the Brunswick Peninsula ⁶
d	53.62	70.92	11	Subantarctic Evergreen Forest	Coastal open areas ⁶
e	53.40	71.25	317	Subantarctic Deciduous Forest	<i>Nothofagus pumilio</i> and <i>Nothofagus antarctica</i> deciduous forest ⁶
f	53.16	71.02	348	Subantarctic Deciduous Forest	<i>Nothofagus pumilio</i> and <i>Nothofagus antarctica</i> deciduous forest ⁶
g	53.16	71.02	317	Subantarctic Deciduous Forest	<i>Nothofagus pumilio</i> and <i>Nothofagus antarctica</i> deciduous forest ⁶
h	52.27	71.33	254	Forest-Steppe ecotone	<i>Festuca gracillima</i> humid grass steppe and <i>Nothofagus antarctica</i> deciduous forest ⁴
i	51.97	72.02	185	Forest-Steppe ecotone	<i>Festuca gracillima</i> humid grass steppe and <i>Nothofagus antarctica</i> deciduous forest ⁴
j	51.78	72.17	134	Forest-Steppe ecotone	<i>Festuca gracillima</i> humid grass steppe and <i>Nothofagus antarctica</i> deciduous forest ⁴
k	51.75	72.22	173	Forest-Steppe ecotone	<i>Festuca gracillima</i> humid grass steppe and <i>Nothofagus antarctica</i> deciduous forest ⁴
m	52.05	71.50	180	Forest-Steppe ecotone	<i>Festuca gracillima</i> humid grass steppe and <i>Nothofagus antarctica</i> deciduous forest ⁴
l	51.72	72.27	257	Patagonian Steppe	<i>Festuca gracillima</i> humid grass steppe ^{4,7}
n	52.09	71.37	203	Patagonian Steppe	<i>Festuca gracillima</i> humid grass steppe ^{4,7}
o	52.57	71.18	208	Patagonian Steppe	<i>Festuca gracillima</i> humid grass steppe ^{4,7}
p	52.85	70.95	58	Patagonian Steppe	Disturbed <i>Festuca gracillima</i> humid grass steppe ^{4,7}
q	52.72	70.95	16	Patagonian Steppe	<i>Festuca gracillima</i> humid grass steppe ^{4,7}
r	52.53	70.75	97	Patagonian Steppe	Disturbed <i>Festuca gracillima</i> humid grass steppe ^{4,7}
s	52.60	70.57	35	Patagonian Steppe	Disturbed <i>Festuca gracillima</i> humid grass steppe ^{4,7}
t	52.58	70.32	33	Patagonian Steppe	<i>Festuca gracillima</i> xeric grass steppe ⁴
u	52.47	69.82	30	Patagonian Steppe	<i>Festuca gracillima</i> xeric grass steppe ⁴
v	52.32	69.65	63	Patagonian Steppe	<i>Festuca gracillima</i> xeric grass steppe ⁴

References: ⁴ Roig *et al.* 1985a; ⁶ Pisano, 1973; ⁷ Endlicher y Santana 1988

3.2. Sediment cores

3.2.1. Coring locations

Lake Tamar (52°54'22"S; 73°48'11"W) is a closed hydrological system located in the south area of the homonymous island, close to the Pacific entrance of Magellan Strait (Figure 11a). The lake is located at 35 m.a.s.l. and reaches a maximum water depth of 22 m (Breuer *et al.* 2013)(Figure 11c). The surrounding catchment includes hills with maximum altitudes of ~350 m.a.s.l. to the north and open sea to the south sea (Figure 11). Its lithology includes Lower Cretaceous granites, granodiorites and Tonalites (SERNAGEOMIN 2003), whereas the vegetation type includes bogs over flat areas and forests and scrubs over steeper slopes. More information about the physical environment and vegetation types occurring within the Lake Tamar catchment are presented and discussed in detail in Section 4.2.1

Multiple long and gravity cores were retrieved during the field campaign 2006 by Prof. Dr. Rolf Kilian (University of Trier) and co-workers, utilizing a UWITEC corer facility. Coring locations were selected after the development of systematic bathymetry and seismic profiles using a Parametric Echosounding System SES 2000 from Innomar (Wunderlich and Mueller 2003). Following extraction, the cores were packed and shipped to the University of Trier where they were stored at 4°C. The studied sedimentary sequence corresponds to the most complete, retrieved from the deepest lake portion (22 m water depth), and consist of two long piston-cores with an overlap of ~1m (LT-I; 0-493 cm and LT1-II; 400-764 cm) and one gravity-core (LaTM; 0-111cm).

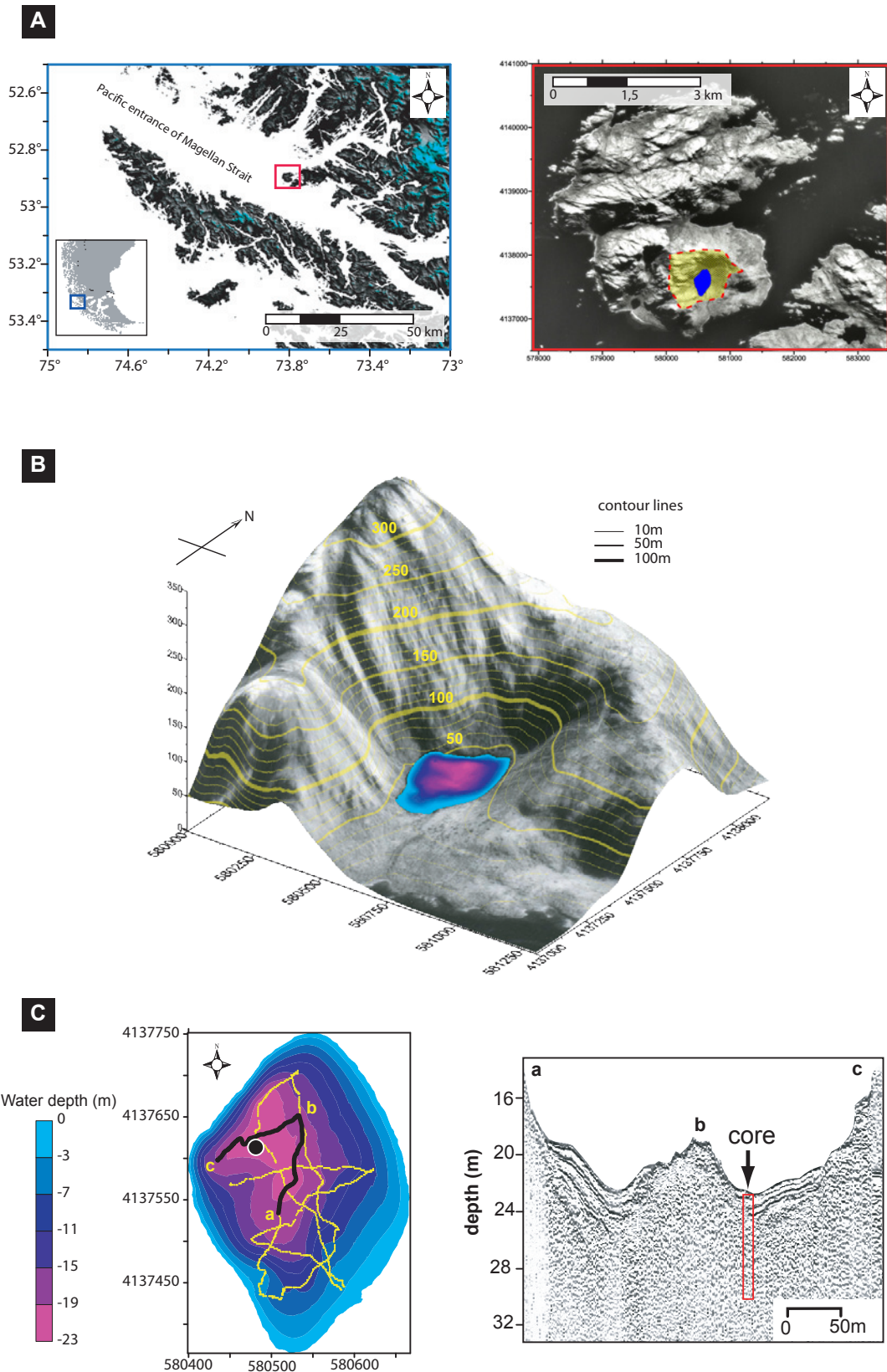


Figure 11. (A) General map of the Southwest Patagonian territories at 53°S (left) indicating the location of the study site at Tamar Island (right). The yellow area in the georeferenced orthophoto denotes the lake catchment. (B) Oblique view (orthophoto+DEM) of the Tamar Lake catchment and elevation contour lines. (C) Bathymetry map of Tamar Lake (left) indicating the location of the piston core (circle) and the performed echosounder tracks. The bold line denotes the track of the seismic profile plotted on the right.

3.2.2. Core analyses

3.2.2.1. Non-destructive analysis, core correlation and geochemical analysis

Macroscopic sediment characteristics such as colour, bed thickness and the deposition of distinctive layers within each sediment core were described in detail by means of visual inspection, to initially identify the main lithological units. Later, the cores were systematically photographed and measured for Magnetic Susceptibility (MS) at 0.2 cm intervals. Gray-scale (GS) analysis was performed for each core photograph using the program ImageJ (Schneider *et al.* 2012). Using this basic information, correlations between the cores were performed in order to develop a composite core without hiatus associated to core breaks.

Geochemical analyses were performed at selected levels along the cores, with a total of 131 samples analyzed. A standard volume of 0.5 cc was used for the analysis of each sample, with which Dry Bulk Density (DBD) and water, Organic Carbon (Corg), Nitrogen and Carbonate content were determined. Geochemical analysis was conducted at the University of Trier's laboratories using a LECO analyzer.

3.2.2.2. Radiocarbon and age model

The chronology of the sediment core was based on sixteen AMS radiocarbon dates performed on plant material (n=14) and bulk sediments (n=2), and two well-known tephra layers occurring on a regional scale (Table 4). The tephra layers present in the Tamar Lake sediment core correspond to two well-dated eruptions from Monte Burney, located around 40 km to north east of the Tamar Lake (Kilian *et al.* 2003) (Figure 9). Radiocarbon dates were calibrated using the Calib program, version 6.1.0 (Stuiver *et al.* 2005). For radiocarbon ages younger than 10,000 years ^{14}C BP the Southern Hemisphere curve was used (SHCal04) (McCormac *et al.* 2004), whilst the Northern Hemisphere calibration curve (IntCal04) (Reimer *et al.* 2004) was used for older dates (>10,000 years ^{14}C BP).

The age model was performed by means of the program MCAgeDepth (Higuera 2008) using the calibrated radiocarbon ages and a corrected depth calculated from the subtraction of all the layers related to events of instantaneous deposition (e.g. tephra, mass flows). The interpolation of the calibrated ages along the core was performed using a cubic spline fit curve, whilst the confidence intervals at 95% was estimated after 1000 Monte Carlo simulations (Higuera 2008).

Table 4. Radiocarbon dates for the Tamar Lake composite core, indicating corrected depths after be subtracted all the layers related to events of instantaneous deposition (e.g. tephra, mass flows). Radiocarbon samples have been calibrated using Calib 6.1.0 and the Southern Hemisphere calibration curve (SHCal04). For ages beyond the SHCal04 calibration curve were used the IntCal04 calibration curve. Median and 1 sigma of distribution for each calibrated radiocarbon date are provided. The age of tephra layers are based on previously reported results (Kilian *et al.* 2003). For more details see the text.

Lab. Code	Core	Composite depth (cm)	Corrected depth (cm)	Material	^{13}C	\pm	Age ^{14}C	\pm	Calendar year BP (median)	Range (1 sigma)
KIA31942	TA1-I	30.5	25.4	Plant macrorest	-30.34	0.17	1075	25	942	928-956
KIA31943	TA1-I	44	38.9	Plant macrorest	-29.61	0.56	1382	41	1257	1185-1296
KIA31944	TA1-I	60	49.4	Plant macrorest	-26.32	0.22	1746	38	1598	1541-1688
KIA31945	TA1-I	77	66.4	Plant macrorest	-27.81	0.20	2295	29	2232	2161-2331
KIA31946	TA1-I	103.5	92.9	Plant macrorest	-29.55	0.18	3003	30	3116	3042-3207
KIA31947	TA1-I	125	114.4	Plant macrorest	-27.34	0.24	3524	41	3745	3689-3827
Burney-T1*	TA1-I	148.5	136.9	--	--	--	3860	50	4198	4090-4288
KIA31948	TA1-I	161	148.8	Plant macrorest	-27.30	0.16	4037	130	4449	4238-4786
KIA31949	TA1-I	183	159.2	Plant macrorest	-29.41	0.10	4750	110	5413	5314-5582
KIA31950	TA1-I	220.5	196.7	Plant macrorest	-28.44	0.43	5715	35	6440	6403-6489
OS-74737	TA 1-I	241.5	217.7	Plant macrorest	-30.06	--	6360	35	7229	7173-7267
KIA31951	TA1-I	252.5	228.7	Plant macrorest	-30.96	0.13	6520	65	7372	7313-7432
KIA31952	TA1-I	282	258.2	Plant macrorest	-31.17	0.17	6730	190	7551	7333-7722
KIA31953	TA1-I	304	280.2	Plant macrorest	-29.62	0.07	7750	50	8484	8425-8538
Burney-T2*	TA1-I	311.5	287.4	--	--	--	7890	45	8620	8546-8697
KIA31954	TA1-I	354	309.9	Plant macrorest	-31.21	0.16	8410	55	9368	9303-9455
KIA31955	TA1-I	461	361.8	Plant macrorest	-42.20	0.14	9640	70	10.935	10.778-11.089
KIA31956	TA1-II	580	442.4	Plant macrorest	-29.70	0.09	11.020	40	12.894	12.770-13.053
COL1943	TA1-II	627.5	489.9	Bulk	-26.60	--	12.422	68	14.499	14.179-14.750
COL1944	TA1-II	639.5	501.9	Bulk	-26.90	--	12.668	70	14.990	14.804-15.184

* Tephra

3.2.2.3. Pollen analyses

Samples of 2 cc were processed following the standard pollen preparation techniques which include HCl (10%, dissolution of carbonates), KOH (10%, deflocculation), sieving (<120 mm), ZnCl₃ (recovery the organic matter by flotation), HF (40%, silica removal), and acetolysis (cellulose removal) (Fægri and Iversen 1989). Tablets of exotic Lycopodium spores were added to allow calculation of pollen and spore concentration (Stockmarr 1971). The residues obtained were mounted on slides and counted under the microscope. A total >300 pollen grains including trees, shrubs, cushion plants and herbs were counted for each sample (terrestrial pollen). The abundance of pteridophytes and paludal/aquatic taxa were calculated in separated sums called: 'total terrestrial pollen and spores' (terrestrial pollen+pteridophytes) and 'total pollen and spores' (terrestrial pollen+pteridophytes+paludal/aquatics). Reference pollen material and specialized literature were consulted for pollen identification (Heusser 1971; Markgraf and D'Antoni 1978).

3.2.3. Numerical analysis

A series of numerical analysis techniques were performed for five pollen records (including Tamar Lake), located along a west-east biogeographic gradient at 53°S. These sites (Table 1 & Figure 12) characterise distinctive ecosystems occurring along the west-east transect and alongside the numerical analysis results, provide of an adequate background to: (i) characterize and summarize intra- and inter sites variations (CONISS and PCA), (ii) obtain a quantitative measure of the changes in the plant community composition (turnover and richness), and (iii) develop quantitative climatic reconstructions (transfer functions). Below the numerical methods used to achieve these goals are described, as well as their paleoecological implications. In addition, the original percentages diagrams for each site are provided (Appendix figures 13-16).

3.2.3.1. Cluster analysis (CONISS) and Principal Component Analysis (PCA)

Pollen zones were defined based on a stratigraphically constrained cluster analysis (CONISS), using square-root transformed data and the Edward and Cavalli-Sforza's chord distance as a dissimilarity coefficient (Grimm 1987). The analysis was performed on all terrestrial pollen taxa (excluding pteridophytes) that reached percentages >5% (27 taxa), after recalculating sums and percentages.

Ordination methods are widely used in paleoenvironmental studies to summarize and reveal correlations among samples and taxonomic composition along one, two or a number of axes (Legendre and Birks 2012). Detrended Correspondence Analysis (DCA) was performed a priori on each of the pollen datasets, in order to estimate the gradient lengths and choose the most adequate algorithm (ter Braak and Šmilauer 2002). The results indicated that maximum gradient lengths of the first axis in all sites do not exceed 2.5 standard deviations, indicating an underlying linear response model (Legendre and Birks 2012). Therefore, Principal Component Analysis (PCA) was chosen as the most adequate statistical tool to summarize the pollen records, in order to develop simple inter-sites comparisons (Figure 12 & Table 1). In all the cases (pollen records), the PCA was performed based on a modified dataset which included only taxa with values exceeding the 5%. This numerical analysis was implemented using CANOCO 4.5 (ter Braak and Šmilauer 2002).

3.2.3.2. Turnover and Richness

The amount of palynological compositional change along the time or turnover can be used as a reliable statistical tool to estimate changes in the β -diversity, namely changes in the diversity between habitats or communities within a landscape (Birks 2007, Birks and Birks 2008). The palynological turnover was calculated for each pollen sites (Figure 12 & Table 1) by means of detrended canonical correspondence analysis (DCCA), using the sample age as an external constraint parameter (Birks 2007, Birks and Birks 2008). The datasets containing the pollen percentages of all the terrestrial taxa were square-root transformed, to stabilize variances, and detrending by segments. Not down-weighted of rare taxa and non-linear scaling was applied. The results are expressed in terms of standard deviation (SD) units of the sample scores (gradient length) on the first time-constrained DCCA axis. The total turnover of each pollen site was calculated as the difference between the highest and lowest values from each sequence (Figure 9). Nevertheless, because of the differences in time covered by the different pollen sites, turnover was also calculated for the interval covered by all four sequences in order to ensure that trends were not affected by using sequences of different duration (Birks 2007). The DCCA was implemented using CANOCO 4.5 (ter Braak and Šmilauer 2002).

Pollen richness or palynological diversity was used as an approximation to examine changes in the total species diversity in a landscape (γ -diversity) or at least within-pollen-source-area diversity (Birks and Birks 2008). Pollen taxonomic richness for each sample was estimated by rarefaction analysis, a method which eliminates the bias in richness caused by different pollen count sizes (Birks and Line 1992). The lowest pollen count [E(Tn)] was used for each sequence in order to standardize the size of the pollen counts at each site. The analysis was conducted using the program Psimpoll (Bennett 2008)

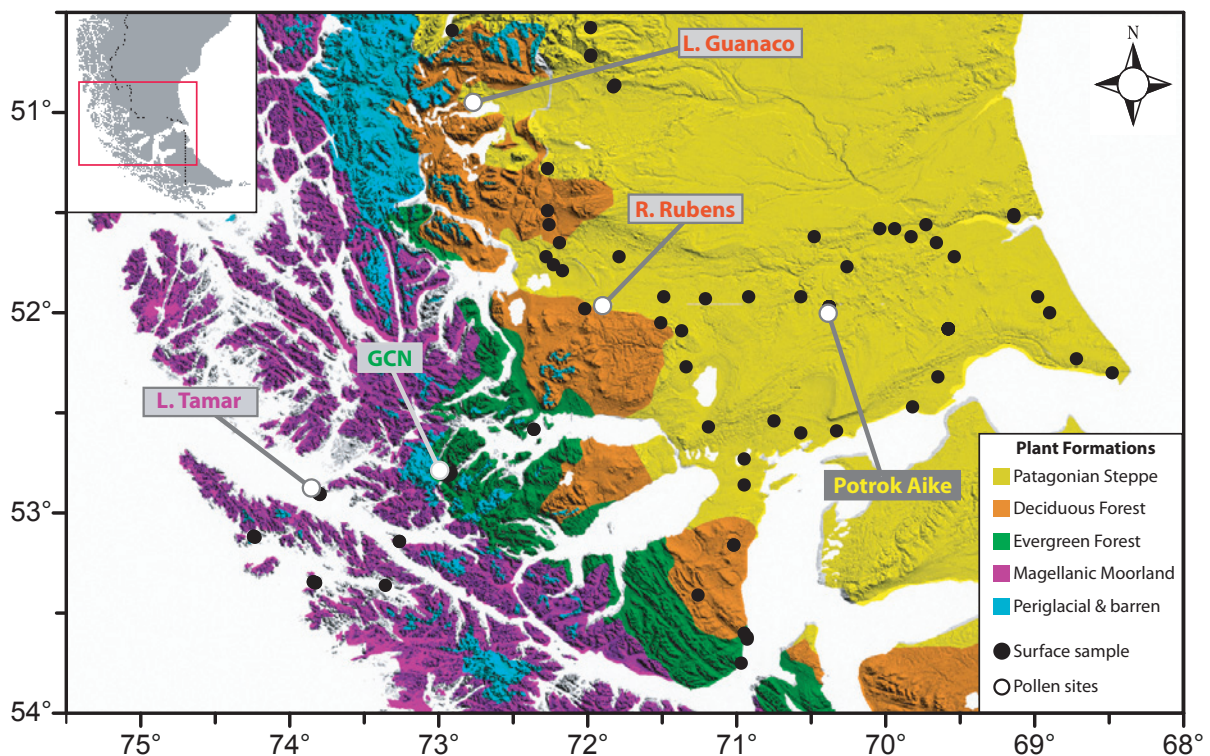


Figure 12. Modern vegetation map (after figure 8) where is indicated the location of pollen sites (rectangles) utilized to (i) examine changes in the plant community composition (turnover and richness) along a west-east gradient (at 53°S) and (ii) develop quantitative climatic reconstructions (transfer functions, see appendix section 8.2) for the postglacial. Locations for modern surface samples (pollen-rain) are also indicated. For more details see the text.

4. RESULTS

4.1. Vegetation and modern pollen-rain

4.1.1. Vegetation and modern pollen-rain in the Southern Patagonian Fjords

Based on the relative abundance of main taxa and information provided by previous studies (Schmithüsen 1956, Oberdorfer 1960, Pisano 1977, Boelcke *et al.* 1985, Gajardo 1994), four main plant communities and ten intra-community associations were identified in the visited locations (Figure 9 & Table 2). Below the main characteristic for each of these main- and intra-community associations (physic environment and dominant taxa) are described, together with the results of the modern pollen-rain which characterize them (Figure 13).

Bogs

Bogs are complex ecosystems characterized by the dominance or co-dominance of sedges, rushes and cushion-plants. In contrast the abundance of woody species (e.g. trees and shrubs) is low.

The pollen assemblage characterizing the bog ecosystems is co-dominated by *Nothofagus dombeyi*-type (mean: 43%; max: 61.1%), *Pilgerodendron uviferum* (mean: 5.5%; max: 14.4%), *Astelia pumila* (mean: 9.2%; max: 20%), Cyperaceae (mean: 12.7%; max: 34.4), Juncaginaceae+Juncaceae (mean: 8.2; max: 14.2%) and *Caltha* (mean: 5.6; max: 12.5%). This assemblage is accompanied by taxa which exceed 5% at least once including *Myrteola nummularia* (max: 11.8%), *Gaultheria* (max: 10.5%), *Luzuriaga marginata* (max: 10.5%), *Empetrum rubrum* (max: 7.8%) and *Donatia fascicularis* (max: 6.3%). Also traces (<5%) of *Lepidothamnus fonkii*, *Podocarpus nubigena*, *Perezia magellanica*, *Drosera uniflora* and *Gaimardia australis* appear as distinctive taxa (Figure 13).

Three different types of bogs were recognized in the visited locations. The most common are the cushion-bog (samples 2, 3, 17, 19) characterized by the dominance of cushion plants such as *Astelia pumila*, *Donatia fascicularis*, *Oreobolus obtusangulus* and *Tetroncium magellanicum* that forms a hard carpet covering the ground. This type of bog occurs normally on flat or very gently sloping terrains (<5 degrees) and/or soils with lower permeability (e.g. rock basement covered by glacial clay). In both cases it is frequent find the water table close to the surface of the bog, resulting in soil stagnation. On the other hand, the Cyperaceous-bog (sample 14) and the Juncaceous-bog (sample 18) are characterized by the dominance of sedges (e.g. *Schoenus antarcticus*) and rushes (e.g. *Marsippospermum grandiflorum* and *Rostkovia magellanica*), respectively. Both types occur in areas of better drainage than cushion-bogs, which allow major development of woody species as *Nothofagus antarctica*, *Nothofagus betuloides*, *Pilgerodendron uviferum*, *Gaultheria mucronata* and *Empetrum rubrum*. All the woody species observed growing in bogs exhibited clear signs of stunted. Pollen samples characterizing the cushion-bogs can be differentiated from the Cyperaceous- and Juncaceous-bogs through relatively high values of typical taxa from bogs (*Astelia pumila*, *Donatia fascicularis*, *Caltha* sp and Juncaginaceae+Juncaceae) and a lack in woody species. On the contrary, the pollen assemblage characterizing the Cyperaceous- and Juncaceous-bog exhibit a mixture of bog and woody taxa (e.g. *Pilgerodendron uviferum*, *Empetrum rubrum*, *Myrteola nummularia*, *Luzuriaga marginata* and *Gaultheria* sp) not observed in cushion-bogs.

Forests

Evergreen Forest communities are predominately characterized by tree species forming closed or semi-closed canopies and a well-developed understory where this occurs. In the studied locations the forest and forest stands were found on moderate to strong slopes (5-20 degrees) with well-drained conditions. These locations were dominated by *Nothofagus betuloides*, nevertheless *Drimys winteri* were the co-dominant taxon of the upper canopy in many locations.

The pollen assemblages characterizing the forest communities are dominated by *Nothofagus dombeyi*-type (mean: 54%; max: 86%), follow by *Misodendrum* sp (mean: 17.1%; max: 42%) and *Drimys winteri* (mean: 5.8; max: 18,6). This assemblage is accompanied by a number of taxa which exceed 5% at least once as: *Gaultheria mucronata* (max: 8.3%), *Desfontainia spinosa* (max: 8.1%), *Maytenus magellanica* (5%) and *Pilgerodendron uviferum* (max: 5%). Relatively high values of ferns spores (Hymenophyllaceae) are also appreciable (Figure 13).

The forest ecosystems studied in this thesis include at least three different types, distinguished by remarkable changes in floristic composition and architectural features (tall and canopy-type). The first is the *Nothofagus betuloides* dwarf Forest (samples 9, 13) characterized by the predominance of *Nothofagus betuloides* forming open to semi-open canopies less than 3 m tall. The trees physiognomy is strongly modified by the wind effect with a large number of broken stems and is deformed in the prevailing wind direction (flag trees). There is a significant infection of *Misodendrum* sp observed in many *Nothofagus* individuals. The understory comprises of a dense scrub that grows as a result of the open canopy and shields the trees against the wind. The dominant species are *Gaultheria* ssp and *Desfontainia spinosa*, accompanied by ferns and herbs. The *Nothofagus betuloides*-*Drimys winteri* Forest (samples 8, 21) occurs in areas protected from the wind, allowing trees to reach up to 10 m tall. As the name suggests, the forest is co-dominated by *Nothofagus betuloides* and *Drimys winteri* in the upper canopy, whereas the understory is characterized by contain a large number of ferns and vines, with decreasing amounts in the scrub elements because the close of the canopy. The Mixed Evergreen Forest (sample 23) occurs in the eastern foot of the Andes (leeward), where precipitation and wind is lower in comparison to the western slopes (windward). These conditions allow the development of a more complex forest ecosystem, where *Nothofagus betuloides* loses its predominance or co-dominates with *Drimys winteri*, *Raukaua laetevirens* and *Maytenus magellanica*. The understory contains several ferns and vines, and scrub elements emerge mostly in the rim of the forest or under canopy gaps. Landslides are a common disturbing factor in western Patagonia ecosystems. In forest ecosystems (sample 20) landslides produce an abrupt opening in the canopy and the input of allochthonous detritus. The result is a return to primary succession stages and the arrival of species with the feasibility to colonize open grounds such as *Gunnera magellanica* and Poaceae.

The pollen-rain characterizing the studied forest ecosystems follows the main characteristics described previously. The *Nothofagus betuloides* dwarf Forest exhibits high values of *Nothofagus dombeyi*-type and *Misodendrum*, whereas the *Nothofagus betuloides*-*Drimys winteri* Forest is co-dominated by *Nothofagus dombeyi*-type and *Drimys winteri*. The latter also exhibits relative high values of Hymenophylliaceae ferns spores. The Mixed Evergreen Forest also exhibits relative high values for *Nothofagus dombeyi*-type and *Misodendrum*, and tree taxa such as *Maytenus magellanica* and *Pilgerodendron uviferum* are also observed.

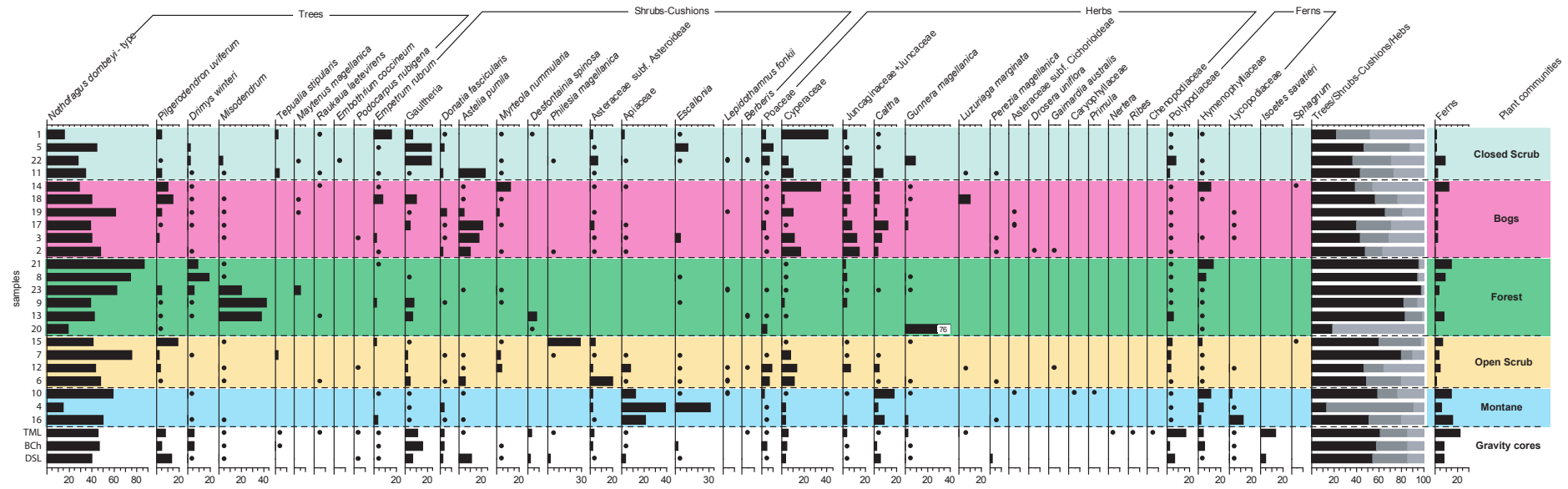


Figure 13. Pollen diagram (relative percentage) from soil samples used to characterize the pollen rain of the dominant plant communities occurring in Southwest Patagonia. Samples are grouped according to main vegetal formations and altitude. In addition, surface sediment samples (gravity cores) from Lake Tamar, Lake Desolacion and Chids Bay are included at the end. The locations of the study sites are indicated in the Table 2 and Figure 9. Black points indicates values <5%.

Shrublands

Shrubland ecosystems are dominated by woody plant communities (small trees and shrubs) less than 2 m tall, occurring on moderate to extreme slopes (5–30°). Its floristic composition is heterogeneous and includes taxa occurring in bogs, forest and montane communities, denoting its ecotonal nature. The pollen assemblages characterizing this community are dominated by *Nothofagus dombeyi*-type (mean: 41.2%; max: 75.2%), Cyperaceae (mean: 11%; max: 40.8%), *Gaultheria* (mean: 8.4%; max: 24.4%), Asteraceae subf. Asteroideae (mean: 5%; max: 20.7%), *Pilgerodendron uviferum* (mean: 4.5%; max: 19.2%) and Poaceae (mean: 4.5%; max: 9.3%). Other taxa which exceed 5% at least once are *Philesia* sp (max: 28%), *Astelia pumila* (max: 23%), *Empetrum rubrum* (max: 15%), *Escallonia* (max: 11%), *Gunnera magellanica* (max: 9.5%), Apiaceae (max: 7.8%) and Juncaginaceae+Juncaceae (max: 7.6%). The presence of Polypodiaceae fern spores is also notable (Figure 13).

Two different types of scrubland were identified in the visited areas: The closed shrublands (samples 1,5,11,22) comprise of ecosystems with mid-to-dense soil cover (30–70%) occurring mostly in low elevations. *Schoenus antarcticus* and *Empetrum rubrum* are the dominant species, accompanied by *Marsippospermum grandiflorum*, *Philesia magellanica*, *Gaultheria pumila*, *Gaultheria mucronata*, *Luzuriaga marginata*, *Geum* sp, *Apium australe*, *Myrteola nummularia*. There are also small populations (tree stands) of *Tepualia stipularis*, *Nothofagus betuloides* and *Pilgerodendron uviferum* in protected areas. The open shrublands (samples 6,7,12,15) comprise of ecosystems with sparse soil cover (20–40%) occurring mostly in mid elevations or wind exposed areas. The most remarkable characteristic of this ecosystem is the presence of stunted and deformed (Krummholz) individuals of *Nothofagus antarctica*, *Escallonia serrata*, *Philesia magellanica* and *Pilgerodendron uviferum*, accompanied by cushion plants as *Bolax* sp and *Caltha* sp.

Montane vegetation

This ecosystem is a treeless landscape, characterized by low soil cover (<20%) and the presence of cushion plants such as *Bolax caespitosa*, *Phyllacne uliginosa*, *Caltha* sp, and *Oreobolus obtusangulus*. The presence of the creeping fern *Lycopodium confertum* is also apparent. This ecosystem is found to occur above 300 m.a.s.l. but its altitudinal limit varies between sites in response to the local topography. The modern pollen-rain which characterizes this ecosystem shows a distinctive pollen assemblage co-dominated by *Nothofagus dombeyi*-type (mean: 41%; max: 59.6%), Apiaceae (mean: 23.9%; max: 38.9%), *Escallonia* (mean: 10.6%; max: 31.8%) and *Caltha* (mean: 9.7%; max: 17.6%). The presence of Lycopodiaceae and Hymenophylliaceae spores is also noted (Figure 13).

4.1.1.1. Cluster analyses and Principal Component Analysis (PCA)

The cluster analyses (Edward & Cavalli-Sforza's chord distance method) performed to obtain a direct measure of degree of similarity/dissimilarity between the samples shows a good differentiation between samples retrieved from forest (clade A) and non-forest ecosystems (clade B)(Figure 14). The clade that defines the non-forest ecosystems (bogs, scrubs, and montane) is complex demonstrating the high heterogeneity of the used pollen dataset. However, it is possible to observe four main clades representing the plant ecosystems of: closed-scrubs (B1), montane (B2) open-scrubs (B3) and bogs (B4). The outliers found into each clade (Figure 14) represent samples with anomalous (high) relative values of some taxa which complicate the cluster analysis. Thus, in the clade B1 which characterizes the closed scrubs it is possible to observe the presence of the samples 18 and 15 (retrieved from bogs and open-scrubs, respectively), which exhibit high values of *Pilgerodendron uviferum* and shrubs. The clade B2 represents the montane vegetation also includes Samples 1 and 14 retrieved from bogs and open scrubs (respectively), both exhibiting relative high values of Cyperaceae and *Empetrum rubrum*. The Clade B3 representing open scrubs includes Sample 19 retrieved from a cushion-bog, which contain high values of *Nothofagus*. In Clade B4 which represents the montane vegetation the sample 11 is also included which was collected from the closed scrub which contain relative high values of *Astelia pumila*. The greatest outlier sample which is the Sample 4, collected from montane vegetation, exhibiting relative high values of *Escallonia* pollen. The surface sediments samples (gravity cores) are grouped into two clades (Figure 14). The samples from Lake Tamar and Chids Bay are into the closed-scrub clade, whereas the sample from Lake Desolacion occurs into the bog clade.

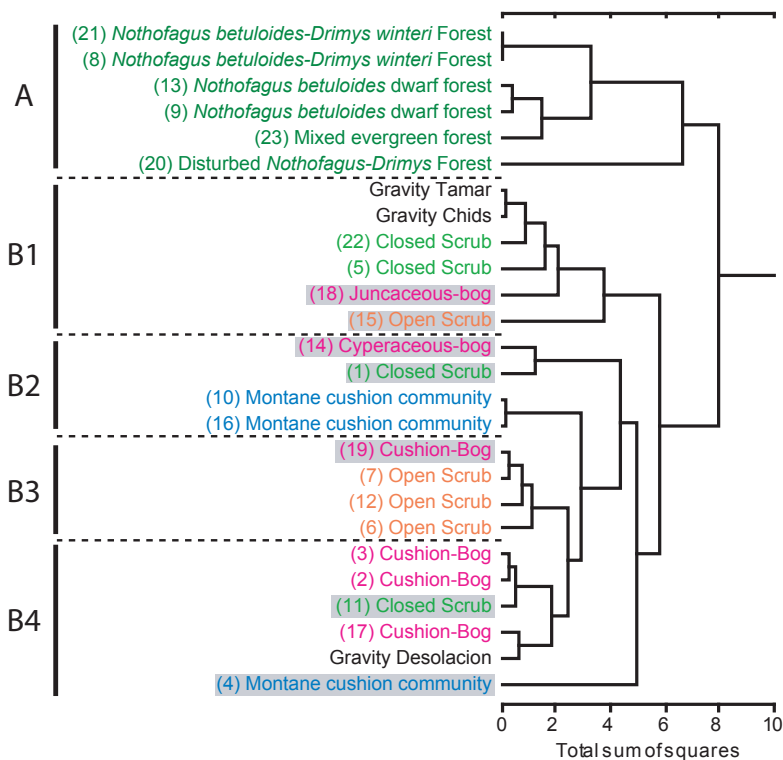


Figure 14. Cluster analysis (Edward & Cavalli-Sforza's chord distance method) of the modern pollen spectra from the Southern Patagonian Fjords. The analysis was performed using the samples obtained from soils and surface sediment (gravity cores). The name and colours indicates the main plant communities previously discussed (Figure 13). Grey rectangles indicate outliers. Sample codes are in parenthesis (Table 2).

The first two axes of the Principal Component Analysis (PCA) explain only 35.5% of the variance, demonstrating (as the cluster analyses did) the high heterogeneity of the used pollen dataset. Nevertheless, the PCA illustrates more clearly the dissimilarity among the samples retrieved from the different ecosystems and its characteristic species (Figure 15). The most distinguished groups are the forest and bog ecosystems, located in the lower right and left corners of the biplot, respectively. Characteristic arboreal taxa (e.g. *Nothofagus dombeyi*-type, *Misodendrum*, *Maytenus magellanica*, *Drimys winteri* and *Desfontainia spinosa*) define the forest group, whereas cushion and herbs species (e.g. *Astelia pumila*, Juncaginaceae+Juncaceae, *Caltha*, Cyperaceae and *Myrteola nummularia*) characterize the bog. The samples from the montane vegetation are located in the upper left corner of the biplot, together with shrub, cushion and herb taxa (e.g. Apiaceae, *Escallonia*, Asteraceae subf. Asteroideae and Poaceae). The samples retrieved from closed-scrubs ecosystems are located in between the previously described groups (forest, bog and montane), whereas the samples from the open-scrubs show a wider distribution (Figure 15). The samples from gravity cores are close to the middle of the graph.

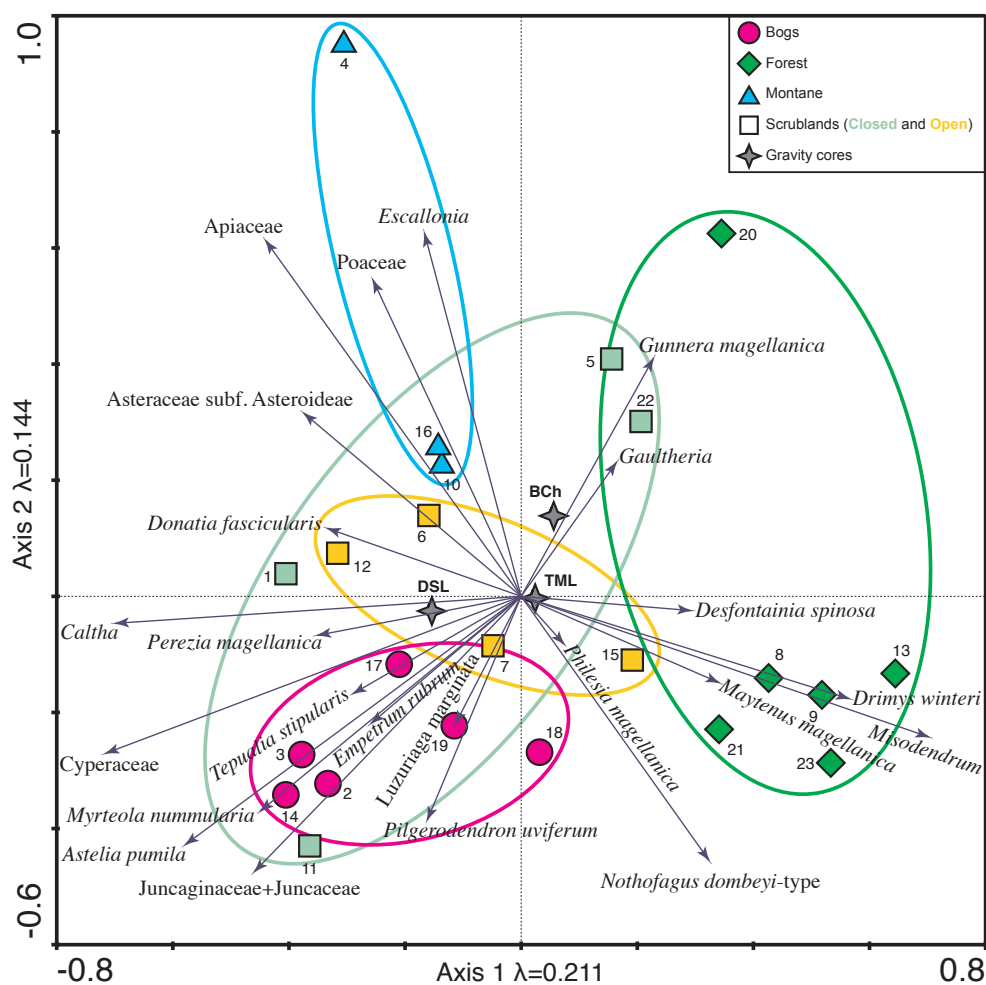


Figure 15. Principal Component Analysis for the main pollen types (>2%) on the first two axes, using the samples obtained from soils and surface sediment (gravity cores) from the Southern Patagonian Fjords.

4.1.2. Pollen rain in a regional context

4.1.2.1. Cluster analysis

Cluster analysis performed on the dataset which contained the samples from western (this thesis) and eastern Patagonia (Quintana 2009), provides of a preliminary overview of the modern pollen-rain along the extent of the west-to-east vegetal gradient which occurs in the region (Figure 16). Based on visual inspection of the cluster analysis, four main groups are identified. The first two groups are comprised of samples collected from the continent (Quintana 2009), whereas the two remaining groups include the previously described plant communities from Fjords (bog, evergreen forest and scrub, and montane vegetation) and some additional samples from the deciduous forest (subgroup 4b).

Below each main group and subgroups are described, indicating in parenthesis the mean or maximum values (relative percentages) reached by particular taxa. The group names follow phytosociological criteria provided by previous studies (Schmithüsen 1956, Godley 1960, Oberdorfer 1960, Pisano 1977, Boelcke *et al.* 1985) based on the dominant vegetation type present in each sampling location (Figure 16).

Group 1: Patagonian Steppe

This pollen assemblage is characterized by high values of Poaceae (mean: 42.9%) associated with *Empetrum rubrum* (mean: 10.2%), Asteraceae subf. Asteroideae (mean: 6.5%), Caryophyllaceae (mean: 6%), Asteraceae subf. Cichorioideae (mean: 4.2%) and Cyperaceae (mean: 3.3%). *Nothofagus dombeyi*-type pollen is also present (mean: 14%) despite the absence of this taxon in the surveyed area. The pollen of the exotic plant *Rumex acetosella* (mean: 4.6%) is frequent in this group. Three further subgroups were identified. Subgroup 1a includes samples located far to the east and near to the Magellan Strait coast (samples u, v), and is characterized by the dominance of Poaceae (mean: 33.2%), along with Asteraceae subf. Asteroideae (mean: 19.4%), Caryophyllaceae (mean: 13.5%) and Brassicaceae (mean: 4.6%). Subgroup 1b shows the highest values of Poaceae (mean: 48.5%) together with Asteraceae subf. Cichorioideae (mean: 7.6%), and consists of samples located inland (samples l, n, o, q, t). Subgroup 1c is characterized by the co-dominance of Poaceae (mean: 40%), *Empetrum rubrum* (mean: 27%) and Apiaceae (mean: 4.2%). These samples were collected in areas severely perturbed by overgrazing (samples p, r, s).

Group 2: Forest-Steppe Ecotone

Co-dominance of Poaceae and *Nothofagus dombeyi*-type pollen (mean: 45.9% and 23% respectively) characterizes this pollen assemblage. The unconstrained cluster analysis suggests the occurrence of two subzones. Subgroup 2a encompasses samples located along the coast (samples b, c) with relative high pollen percentages of *Nothofagus dombeyi*-type along with Poaceae (mean: 40.6% and 34.5%, respectively). The occurrence of *Gaultheria* (mean: 10.6%) and Asteraceae subf. Asteroideae (mean: 5%) pollen is also notable. The Subgroup 2b (samples h, i, j, k, m) contains samples located inland at the forest-steppe border. This subgroup is characterized as the previous one by relative high values of *Nothofagus dombeyi*-type and Poaceae (mean: 48% and 18.4%, respectively) pollen. The occurrence of pollen of others herbs and cushions elements such as *Empetrum rubrum*, Asteraceae subf. Asteroideae, *Acaena*, Caryophyllaceae, Brassicaceae, and *Nassauvia* is also noted. In some samples (h,k) *Rumex* pollen show percentages up 20 % .

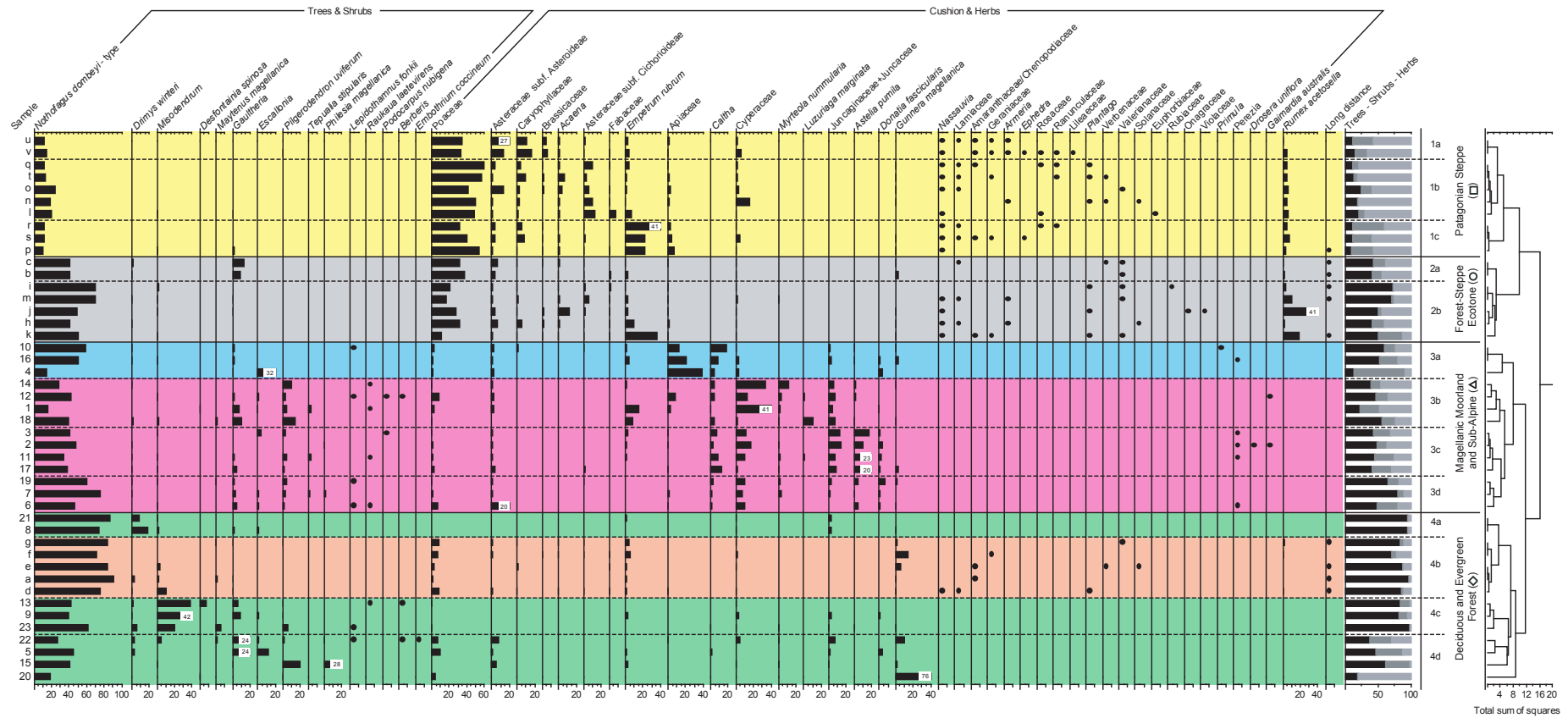


Figure 16. Pollen diagram (relative percentage) from surface samples used to characterize the west-to-east modern pollen-rain along a broad biogeographic gradient (Figure 10 & Table 2). Colors indicate main groups defined by means of cluster analysis. Black points indicates values <5%.

Group 3: Magellanic Moorland

This pollen group shows remarkable fluctuations of *Nothofagus dombeyi*-type from 14.2% to 75.3% (mean: 42.4%). This taxon is accompanied by other taxa which exceed 10% at least once: Cyperaceae (max: 40.7%), Apiaceae (max: 38.9%), *Escallonia* (max: 31.8%), *Astelia pumila* (max: 23%), Asteraceae subf. Asteroideae (max: 20.5%), *Caltha* (max: 17.3%), *Empetrum rubrum* (max: 15.2%), *Pilgerodendron uviferum* (max: 14.4%), Juncaginaceae+Juncaceae (max: 14%), *Myrteola nummularia* (max: 11.7%), *Gaultheria* (max: 10.5%), and *Luzuriaga marginata* (max: 10.5%). Four distinct pollen subgroups can be identified in the dendrogram. The subgroup 3a shows a distinctive pollen assemblage co-dominated by *Nothofagus dombeyi*-type (mean: 41%), Apiaceae (mean: 23.9%) and *Caltha* (mean: 9.7%). This subgroup encompasses samples located upslope (montane plant communities). Subgroup 3b is characterized by the co-dominance of *Nothofagus dombeyi*-type (mean: 31.6%) and Cyperaceae (mean: 22.5%), and accompanied by *Gaultheria*, *Pilgerodendron uviferum*, *Empetrum rubrum*, Poaceae, Apiaceae, *Myrteola nummularia*, *Luzuriaga marginata* and Juncaginaceae+Juncaceae. Samples of this subgroup come from open and swamp environments normally dominated by graminoids and heaths (samples 1, 12, 14, 18). Subgroup 3c includes samples with high relative pollen percentages of *Astelia pumila* (mean: 17.2%), Juncaginaceae+Juncaceae (mean: 10.2%), Cyperaceae (mean: 10%) and *Caltha* (mean: 7.6%) along with *Nothofagus dombeyi*-type (mean: 40.4%). Also traces (<5%) of *Lepidothamnus fonkii*, *Podocarpus nubigena*, *Perezia magellanica*, *Drosera uniflora* and *Gaimardia australis* appear as distinct taxa. The samples from this subgroup (samples 2, 3, 11, 17) come from typical cushion bogs occurring in the Magellanic Moorland. The subgroup 3d is characterized by relative higher pollen percentages of *Nothofagus dombeyi*-type (mean: 61.2%) in comparison to previous subgroups. The diminishing or absence of taxa such as *Empetrum rubrum*, Juncaginaceae+Juncaceae, and *Caltha* is a characteristic of this subgroup. As well as the subgroup 3b; samples from this subgroup represent open environments such as cushion-bogs (sample 19) and open-scrubs (samples 6, 7), but are not graminoid- or heath-dominated.

Group 4: Evergreen and Deciduous Forest

This pollen group is comprised of samples from the *Nothofagus betuloides*-*Drimys winteri* Forest (subgroup 4a) and *Nothofagus betuloides* dwarf Forest and related communities (subgroups 4c and 4d) But also includes samples collected from the deciduous forest or *Nothofagus pumilio* forest (subgroup 4b). This group is characterized by relatively high pollen values of *Nothofagus dombeyi*-type (mean: 59.7%), accompanied by other tree and shrub elements including *Drimys winteri*, *Misodendrum*, *Desfontainia spinosa*, *Maytenus magellanica*, *Gaultheria*, *Escallonia*, *Pilgerodendron uviferum*, and *Philesia magellanica*. Four subgroups were identified based on the clustering results. Subgroups 4a and 4b correspond to pollen assemblages with the highest values of *Nothofagus dombeyi*-type (mean: 80.2% and 80% respectively), differing by the presence of *Drimys winteri* (mean: 13.8%) in Subgroup 4a. This subgroup includes the pollen assemblages with the lowest number of pollen types. Samples from Subgroup 4a were retrieved from evergreen *Nothofagus betuloides*-*Drimys winteri* forest (samples 8, 21), whereas samples from Subgroup 4b encompass samples collected from the deciduous *Nothofagus pumilio* forest (samples d-g) and evergreen *Nothofagus betuloides* forest (sample a). Subgroup 4c is characterized by the co-dominance of *Nothofagus dombeyi*-type and *Misodendrum* (mean: 47.9% and 33.3%, respectively) pollen. This subgroup has significantly low values (<5%) of other trees (e.g. *Drimys winteri*, *Maytenus*, *Desfontainia spinosa*, *Raukaua laetevirens*, *Pilgerodendron uviferum*) and shrubs (e.g. *Gaultheria*, *Escallonia*, *Berberis*, *Lepidothamnus fonkii*). Samples from this subgroup (samples 9, 13, 23) were

obtained from coastal and dwarf *Nothofagus betuloides* forests. Subgroup 4d exhibits a decrease in pollen percentages of *Nothofagus dombeyi*-type (33%), compared to previous subgroups, and a significant increase in percentages of other taxa. Samples 5 and 22 were collected from coastal scrubs and reveal high pollen values of *Gaultheria* (max: 24.1%) and *Escallonia* (max: 11.5%). Sample 15 was retrieved from a *Pilgerodendron uviferum* scrub and display high pollen percentages of *Pilgerodendron uviferum* (max: 20%) and *Philesia magellanica* (max: 28%), whereas Sample 20 was obtained from a natural disturbed (landslide) *Nothofagus betuloides*-*Drimys winteri* forest, and exhibits significant relative pollen percentages of *Gunnera magellanica* (max: 75.8%).

4.1.2.2. Principal Component Analysis (PCA)

The PCA ordination (Figure 17) shows that the first two axes explained ~50% of the total pollen variance, indicating similar groups to those defined by cluster analysis (Figure 16). Samples from the Magellanic Moorland are located in the upper left corner of the biplot alongside characteristic arboreal-scrub (e.g. *Pilgerodendron uviferum*, *Tepualia stipularis* and *Escallonia*) and cushion-herbs (e.g. Juncaginaceae+Juncaceae, Cyperaceae, *Caltha*, *Donatia fascicularis*, *Astelia pumila*, and *Myrteola nummularia*). In the lower left corner is characterized by the occurrence of samples from the Subantarctic Evergreen and Deciduous Forest, characterized by the dominance of arboreal elements (e.g. *Nothofagus dombeyi*-type, *Misodendrum*, *Drimys winteri*, *Maytenus magellanica* and *Desfontainia spinosa*). On the right side of the biplot are the samples from the Patagonian Steppe together with taxa such Poaceae, Asteraceae (subf. Asteroideae and Cichoridae), Caryophyllaceae, Brassicaceae, *Acaena* and *Empetrum rubrum*. Samples from the Forest-Steppe Ecotone are located in an intermediate position between Deciduous Forest and Patagonian Steppe.

4.1.2.3. Canonical ordination

According to the RDA ordination analysis, 46% of the total pollen variance is explained by selected climatic and geographic variables (Table 5). The unrestricted Monte Carlo permutation test identifies two significant (p -value<0.005) variables, explaining 35% of the total variation in the pollen composition (Table 5). The most prominent variable is Pann which explains 26% of the total pollen variance, whereas the variable Tann explains only 4% (Table 6). The first two axis capture 100% of the explained variance (sum of all canonical eigenvalues 0.297), and exhibits a strong species-environment correlation (Table 6). The RDA axis 1 (λ =0.262) explains 88.2% of the variance and is strongly correlated ($r = -0.893$) to the Pann variable, and, to a lesser degree, Tann ($r = -0.067$). The second RDA axis (λ =0.035) explains 11.8% of the residual variance and has a slight correlation to Pann ($r = -0.022$) but is strongly correlated to the Tann ($r = -0.722$) variable (Table 6). Intercorrelations between the environmental variables are not significant (Table 6 & Figure 18). The ordination of samples and species in the RDA biplot follow the mentioned significant climatic variables (Pann and Tann) along both axes. Samples and species characterizing the Magellanic Moorland and the Subantarctic Evergreen Forest are positively correlated to Pann climatic variable and located on the left side of the graph. Samples and species characterizing the Patagonian Steppe and the Forest-Steppe Ecotone are situated to the right side of the plot, and thus negative correlated to the Pann climatic variable (Figure 18). It is also notable that along Axis 2 samples from the Sub-Alpine and the Subantarctic Deciduous Forest, grouped together with Apiaceae and *Gunnera magellanica*, are located in the top of the graph and negatively correlated to Tann. On the other hand, samples from the Evergreen Forest are positioned in the bottom of the graph, together with *Maytenus magellanica*, and positively correlated to Tann (Figure 18).

Table 6. Correlations and inter-correlations between significant climatic variables and RDA axis.

Climatic variable	Axis 1	Axis 2	Pann	p-value	Percentages of explained variance
Pann	-0.893	-0.022	-	0.001	26%
Tann	-0.067	-0.722	0.105	0.0340	4%
Species-environment correlations	0.893	0.724	-	-	Total 30%

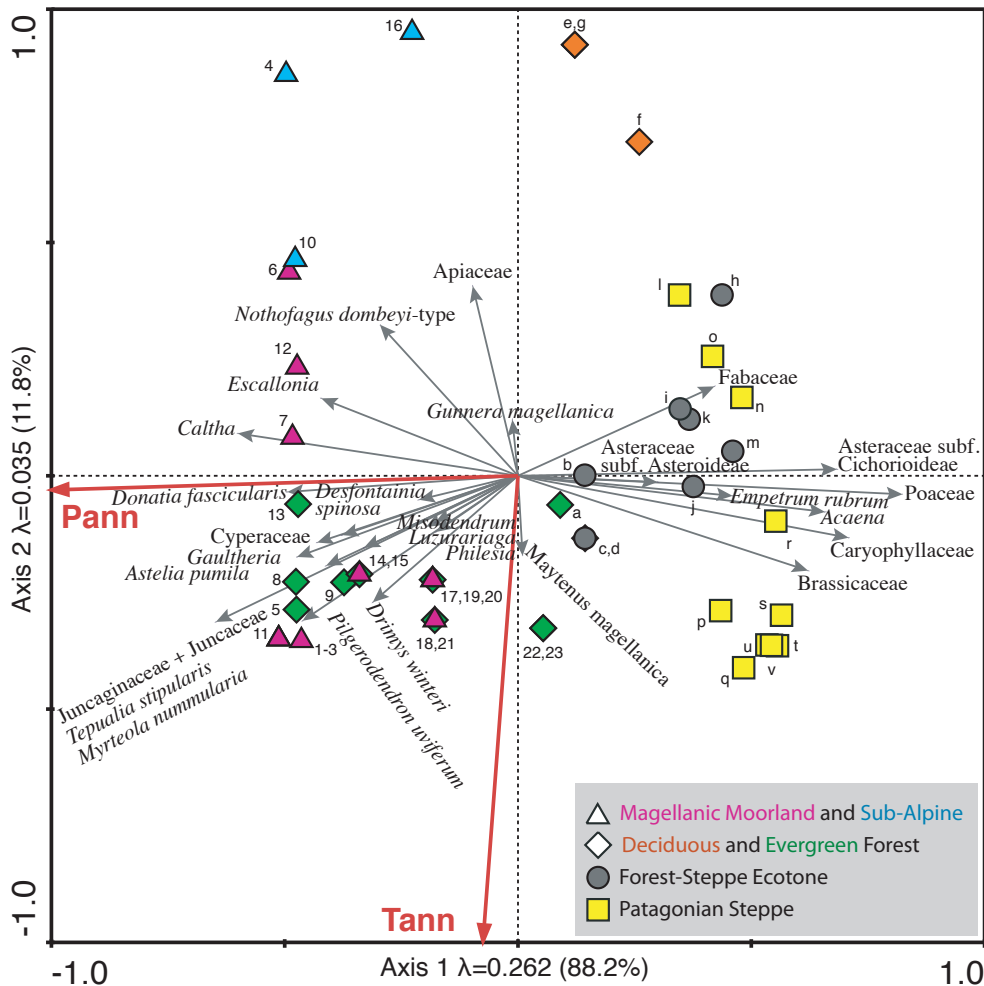


Figure 18. Biplot showing the first two axes of the RDA ordination for modern surface samples and selected taxa. Significant climatic variables Pann and Tann are denoted in red. Correlation and probability values are in the Table 6

4.2. Paleoenvironmental reconstruction of Tamar catchment

4.2.1. Physical environment and vegetation within the Lake Tamar catchment

Lake Tamar covers an area of 75463 m², and its catchment encloses an area of 648079 m² with maximum elevations (334 m.a.s.l.) towards the northwest and minimum to the south-southwest, where the catchment is the open to the sea (Figure 20). This feature (semicircular shape) explains the absence of north and northwest-facing slopes occurring within the catchment, whereas east and southeast-facing slopes are the most frequent (Figure 19). The distribution of the slope classes within the catchment indicates that strong and extreme slopes (10°-30°) are the most frequent. Gentle and moderate slopes occur only in the south area of the catchment, and near to the south shore of the lake, whereas steep slopes (>30°) are more frequent to the northwest and west (Figure 19 & Figure 20).

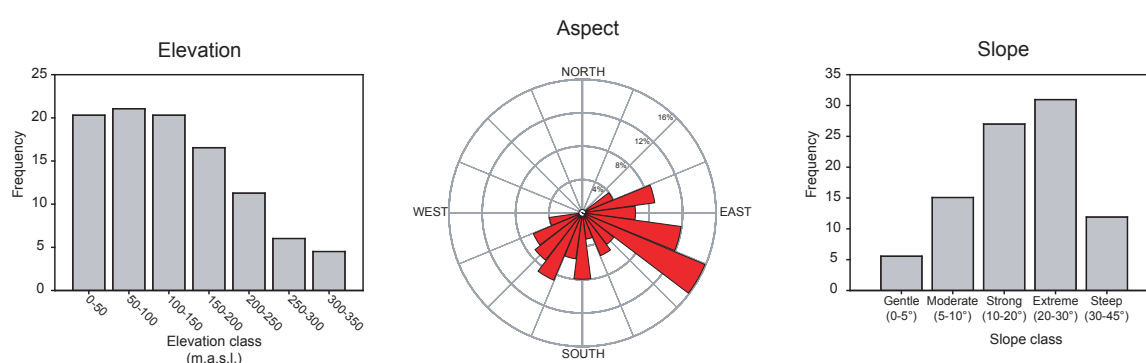


Figure 19. Main physic features (elevation, aspect and slope) from the Tamar Lake catchment

The vegetation survey indicates that four main plant communities occur within the Lake Tamar catchment (Figure 20). Based in performed mapping of the vegetation, the most (cover) frequent plant communities are the scrubs (open 32% and closed 23%) representing around the 55% of the total catchment area (Table 7). Forest represents only the 17% of the total areal cover, whereas bog and montane vegetation exhibit the lowest values (8% and 5% respectively). Unvegetated areas (barren) represent the 15% of relative areal cover within the catchment. The distribution of these plant communities within the catchment follows the altitudinal gradient, with bog dominating at low elevations (<50 m.a.s.l.), forests and closed-scrub at low to mid elevations (50-150 m.a.s.l.), and open-scrub at mid elevations (150-250 m.a.s.l.) and montane communities at high elevations (>250 m.a.s.l.)(Table 7 & Figure 20). In areas with gentle to moderate slopes (<10°) the predominance of bogs communities is observed, situated in the south area of the catchment (Figure 20). In areas with slopes >30°, such as in the southwest of the catchment, open scrubs communities are more frequent and reach low elevations. Nevertheless locations where the slopes exceed 35°, such as in the northwest of the catchment, are unvegetated (Figure 20). The aspect exhibits no clear correspondence with the distribution of the plant communities within the catchment.

Table 7. Total and relative areal cover of the main plant communities identified within the Tamar Lake catchment, and the physical features characterizing the areas where they occur.

Plant communities	Area (m ²)	Area (%)	Elevation average (m.a.s.l.)	Slope average	Aspect average
Bogs	49851	8%	38±5	6°±2	195°±18/S
Forest	108714	17%	101±28	22°±4	170°±13/SE
Closed Scrub	151223	23%	99±29	23°±5	184°±23/S
Open Scrub	207254	32%	175±33	20°±6	127°±22/E
Montane	35289	5%	313±16	18°±7	120°±35/E
Barren	95749	15%	212±51	36°±6	116°±7/E
Total catchment	648079	100%			
Lake	75463				

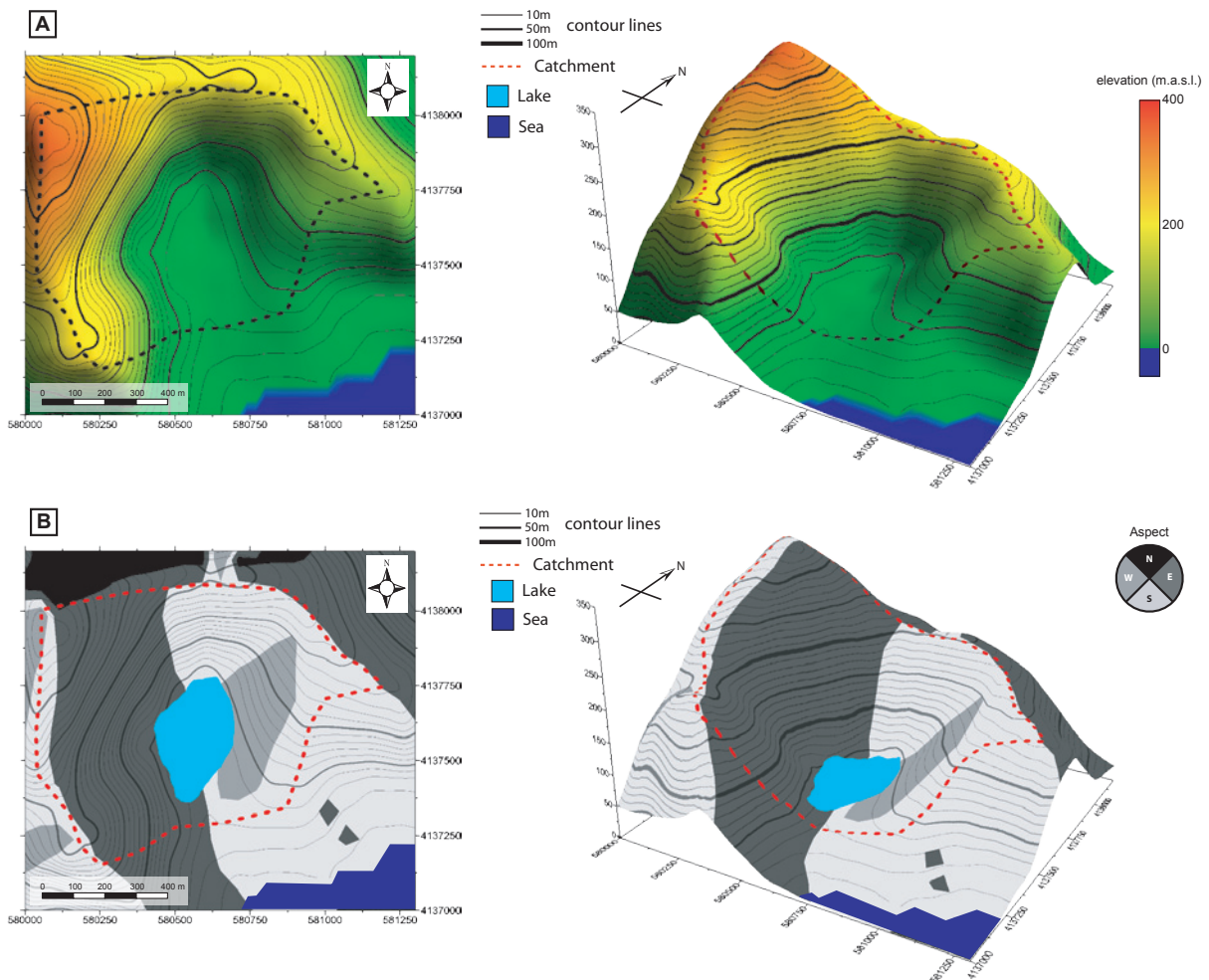


Figure 20. Continue below.

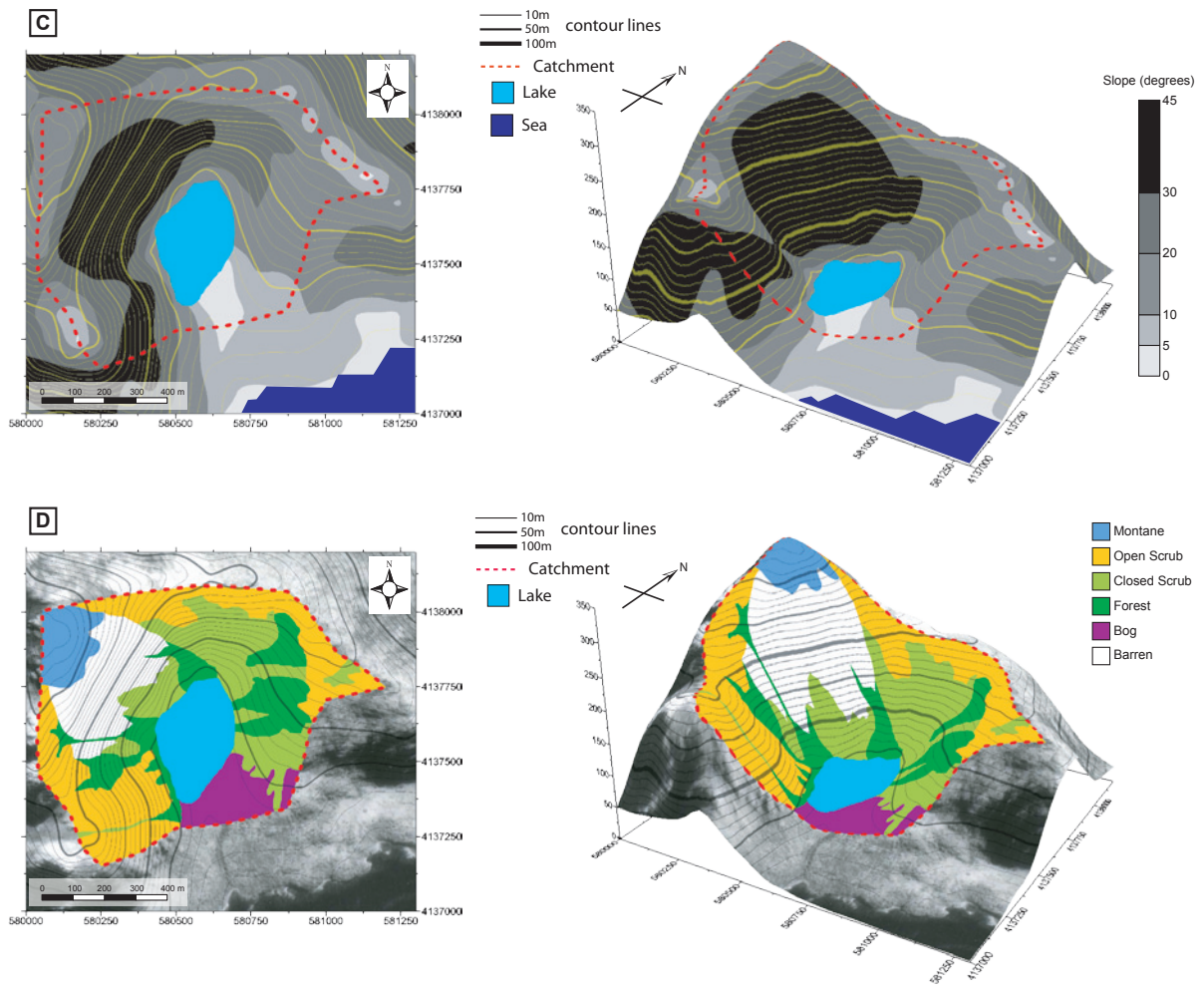


Figure 20. Maps of the most relevant physical features occurring within of Lake Tamar catchment: A) elevation, B) aspect, and C) gradient slope. Below (D), vegetation mapping of Tamar Lake catchment. The images positioned left and right, represent the aerial and 3D perspective (respectively) view for each categorized maps.

4.2.2. Tamar Lake Sediment cores

4.2.2.1. Core stratigraphy and chronology

The sedimentary sequence studied comprise of two long piston cores (LT-I; 0-493 and LT1-II; 400-764 cm) and one gravity-core (LaTM 0-111cm), retrieved from the deepest part of Lake Tamar (22 m water depth)(Figure 11). The composite record consists of a 789 cm long sedimentary sequence characterized by a gradual transition from a basal unit dominated by light-gray sediments towards to lighter brown sediments at the top (Figure 21). Several light-colored deposits (LCD's) that interrupt the pelagic sedimentation are detectable by simple visual core inspection and changes in the grayscale and magnetic susceptibility (Figure 21).

Based on macroscopic attributes (e.g. changes in color and visible textural differences), and changes in the magnetic susceptibility, grayscale and geochemical characteristics, four main lithostratigraphic sections were defined (Figure 21 & Figure 22). The main characteristics of these lithostratigraphic sections are described below, including the results from non-destructive (magnetic susceptibility and grayscale) and geochemical analyses (e.g. DBD, TOC, TIC and C/N ratio).

4.2.2.1.1. Lithological sections

Section I (789-666 cm; ~18,00-15,900 cal yr BP) corresponds to the base of the record and is characterized by the presence of fine-laminated gray-clays with interleaved silty-sand layers. Below 748 cm, the silty-sand layers turn to coarse-sand layers with gravels (Appendix figure 7). High values in the magnetic susceptibility (mean: $9350 \text{ SI } 10^{-6}$) and grayscale (mean: 215) parameters are observable in this section of the core, together with maximum values in the DBD (mean: 1.5 gr/cm^3). The other geochemical parameters show their minimum values for the whole record (Figure 22).

Section II (666-574 cm; 15,900-12,800 cal yr BP) includes the transition from sediments dominated by fine gray silty-clay laminations to sediments interleaved by light-gray and light-brown silty-clay layers. This feature is also clearly identified in continuous decreases in the grayscale values (mean: 135; min-max: 44-203) within the section. The magnetic susceptibility (mean: $1529 \text{ SI } 10^{-6}$) and the DBD (mean: 0.64 gr/cm^3) also experience a decrease in its values, whilst the other geochemical parameters show a slight but significant increase (Figure 22).

Section III (574-312 cm; 12,800-8,700 cal yr BP) is characterized by a change in the matrix now dominated by brown silty-clay sediments, but contains several light-colored deposits. The parameters of grayscale (mean: 63; min-max: 4-150) and magnetic susceptibility (mean: $1529 \text{ SI } 10^{-6}$; min-max: $5\text{-}2760 \text{ SI } 10^{-6}$) record this change in the sediments exhibiting abrupt fluctuations in its values. Maximum values are correlated with the deposition of LCD's whereas minima occur during periods of pelagic sedimentation (Figure 21 & Figure 22). Geochemical parameters also experience significant changes at the beginning of the section, alongside a decrease in the DBD values (mean: 0.21 gr/cm^3) and an increase in the all others. Nevertheless, while the Corg values experience a continuous increase towards the middle of the section, where it reaches its maximum values (mean: 23.7%; max: 31%), the nitrogen values tend to stabilize and remain constant during the rest of the record. Such changes are well represented in the C/N ratio which exhibit higher values towards the middle of the section (mean: 20.9; max: 24.2). The geochemical changes recorded during the occurrence deposition of the LCD's, show an increase in the DBD and C/N values and a decrease in the others parameters (Figure 22).

Section IV (312-0 cm; 8,700 cal yr BP to present) is characterized by significant change in the stratigraphy because the deposition of the massive LCD's ceases. Such a feature is identified by a decrease in the mean values of the grayscale (mean: 46; min-max: 11-198) and magnetic susceptibility (mean: 46 SI 10^{-6} ; min-max: 3-3446 SI 10^{-6}) (Figure 21 & Figure 22). The geochemical parameters of DBD and nitrogen content remain quasi-similar as in the previous section, whilst the Corg and the C/N ratios experience a slight but continuous decline towards the middle of the section (min: 15.6% and 16.3, respectively). Later, both parameters (Corg and C/N ratios) show an increase in their values, coincident with the reappearance of clastic deposits, which remain stable towards to the top of the sequence (mean: 21% and 21.6, respectively). The carbonates also exhibit an increase during the first half of the section, but never exceeds the 5%. Two tephra layers occur within this section, both noticeable by an abrupt increase in the grayscale and magnetic susceptibility values (max: 150 and 3446 SI 10^{-6} , respectively). Geochemical analyses (Kilian pers. comm) indicate that both tephra correspond to eruptions from the Monte Burney, a stratovolcano located around 70 km to the NE from Lake Tamar (Figure 9).

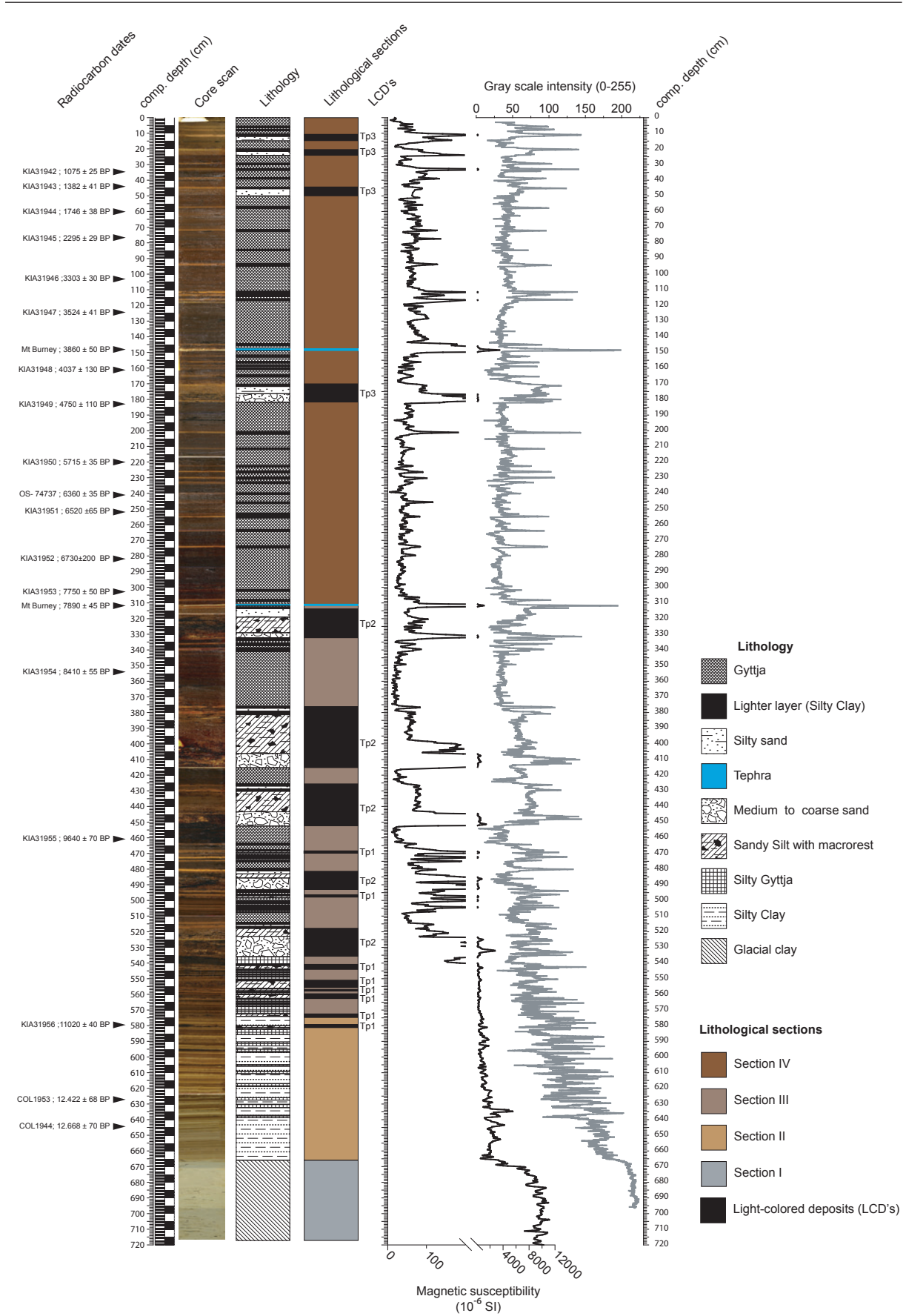


Figure 21. Composite image of the sediment core TML, showing: the position of radiocarbon dates, a descriptive lithology column and the lithological sections discussed in the text, including the position of the different types of light-colored deposits (LCD's). In the right are show the parameters of magnetic susceptibility and gray scale intensity

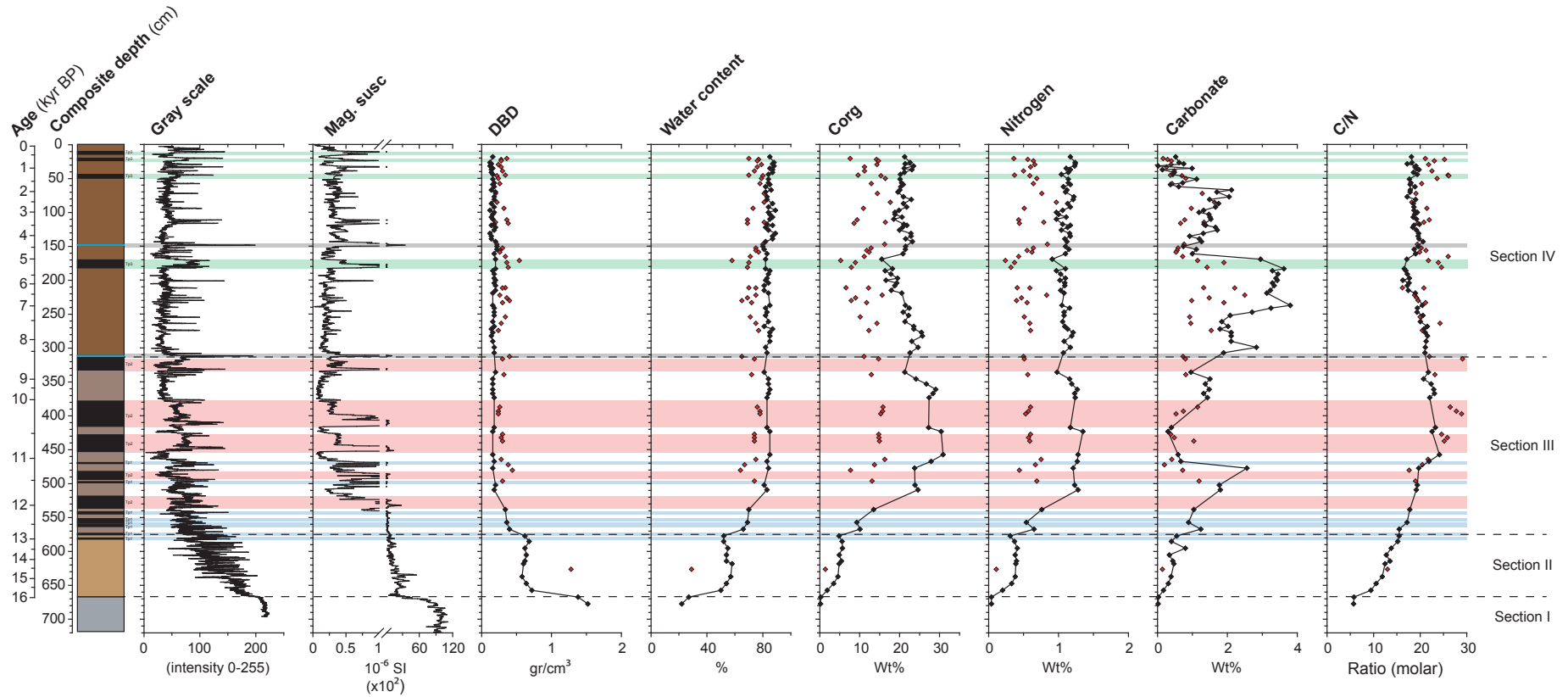


Figure 22. Grayscale, magnetic susceptibility, and geochemical data from core TML1 versus composite core depth (cm) and age (cal. yr BP). Color bars blue, red and green denotes the stratigraphic position of light-colored deposits (LCDs) Types 1-3 (respectively), while grey bars mark the two tephras originating from eruptions of Mt.-Burney. Red diamonds not line-connected on the geochemical parameters, indicates data points retrieved from LCDs.

4.2.2.1.2. Age-depth model

The age-depth model (Figure 23) was performed on the base of a corrected depth, excluding the instantaneous deposition layers (e.g. light-colored deposits and tephra layers), and eighteen AMS radiocarbon dates and two well-known tephra layers (see material and methods). The age model (based in a cubic spline interpolation) indicates a continuous and homogeneous sedimentation rates (mean: $0.3 \pm 0.06 \text{ mm yr}^{-1}$) during the last 16,000 years, the period of pelagic sedimentation in the record (lithological sections II-IV). Below 666 cm (462.8 cm corrected depth) the sediments consist of glacial clays (lithological section I), whereas below 748 cm (544.8 cm corrected depth) several clastic layers and gravels are deposited, evidenced by an increase in the magnetic susceptibility values (Appendix figure 7). Even though the certainty of having reached bedrock is unclear, the presence of these clastic layers suggest at least an important change in the sedimentary environment, and therefore the reliability of age model is constrained until 748 cm, exhibiting an age of $\sim 18,000 \text{ cal yr BP}$.

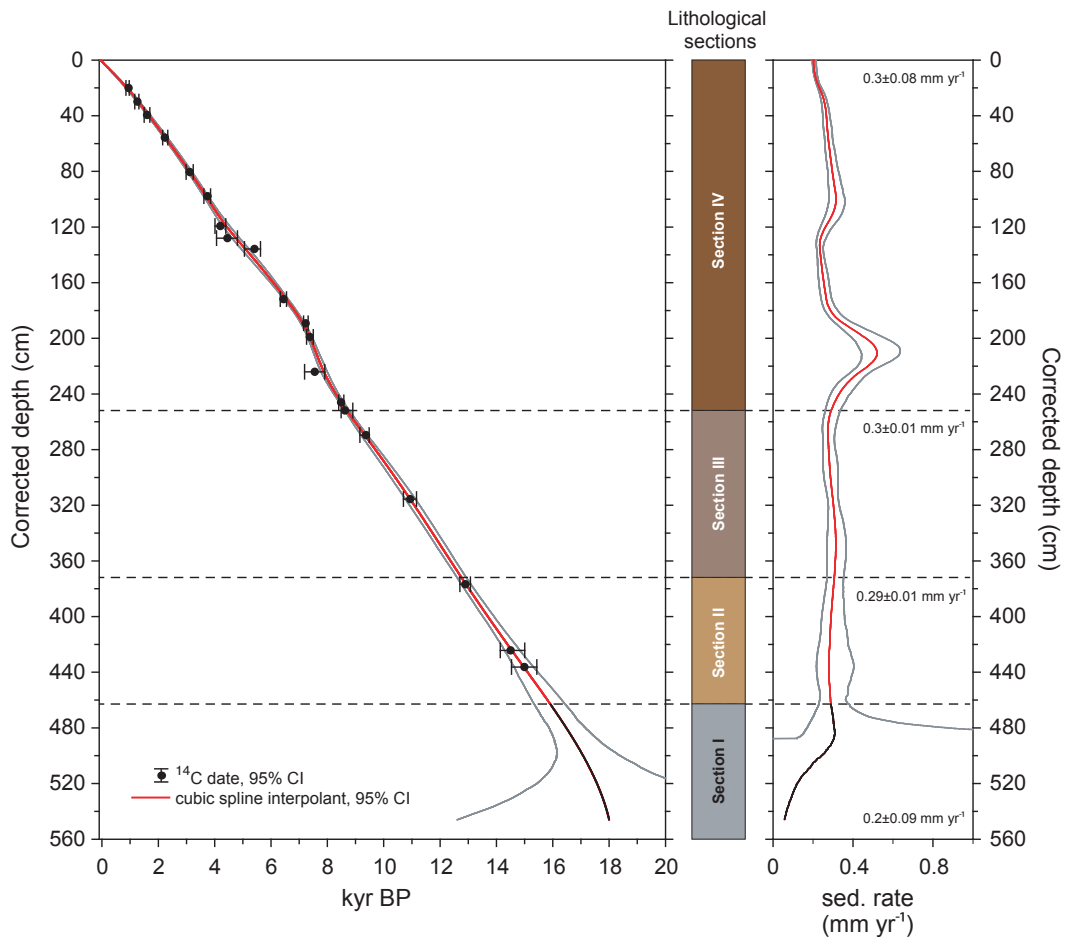


Figure 23. Age-depth model and sedimentation rates (mm yr^{-1}) for the composite sediment core TML. The reliability of the model is constrained to the core sections where organic pelagic sedimentation occurs (lithological section II-IV). Note that the model is plotted against a corrected depth (without light-colored deposits and tephra layers). For more details see the text

4.2.2.1.3. Light-colored deposits (LCD's): main characteristic and event chronology

As was mentioned previously, a remarkable characteristic of the sedimentary record from Tamar Lake (TML) is the presence of several light-colored deposits (LCD's) interrupting the pelagic sedimentary sequence. As the name suggests, light-colored deposits are easily distinguished by visual inspection because of their sharp contrast with the adjacent sediments (matrix). The gray-scale parameter illustrates this feature by means of an abrupt increases in its values during the deposition of light-colored deposits and decreasing during the occurrence of pelagic sedimentation (Figure 21 & Figure 22). Moreover, simultaneous changes in magnetic susceptibility and geochemical parameters denote further differences between the LCD's and adjacent pelagic sediments. In this context, increases (decrease) in magnetic susceptibility and the DBD and C/N ratio (Water, Corg, Nitrogen and Carbonate content) during the deposition of the light-colored layers (pelagic sedimentation) are observed (Figure 22 & Appendix figure 8). In addition, pollen samples retrieved from LCD's do not differs significantly from adjacent samples retrieved from portions where pelagic sedimentation occurs. Nevertheless, a decrease in the percentages of the aquatic fern *Isoetes savatieri* during the deposition of such LCD's clearly is observable (Appendix figure 8).

On the base of these macroscopic features at least four different types of light-colored deposits were identified (Figure 24). Below the main characteristics (e.g. color and texture) are described for each type, indicating the number of occurrences, mean thickness and observations regards geochemical or palynological features when available. Depth, thickness and estimated age of each one of the light-colored deposits found along the core can be found in the appendix section (Appendix table 1)

Type 1 (n=8) is characterized by a simple internal structure, composed by light-brown sandy silt sediments with vegetal macrorest (mostly roots), and capped by a silty-clay layer. Some of them also include a thin basal layer composed of a light-gray silty sand. This type of light-colored deposit occurs at the beginning of Section III, and its thickness does not exceeds 4 cm (mean: 1.9 cm). The parameters of grayscale and magnetic susceptibility tend to show an increase in its values in response to the deposition of the light-gray silty sand basal layer and the upper silty-clay layer. Nevertheless, the sedimentary matrix (silt-gyttja) on which are deposited these light-colored deposit, are also characterized by high fluctuations in the grayscale and magnetic susceptibility parameters. These features make it difficult to identify this kind of light-colored deposit using such parameters. Pollen samples retrieved from within of this type of light-colored deposit do not show a clear tendency of change, nevertheless a slightly increase in the percentages of *Phyllacne uliginosa*, *Escallonia* and *Asteraceae* subf. *Asteroideae* is observable, whereas other pollen types exhibits a slightly decrease in their values (Appendix figure 9). Geochemical analyses were not been performed on this light-colored deposit.

The light-colored deposit **Type 2** (n=5) also occurs in Section III, but towards to the top of the section. This type exhibits thicknesses greater than 10 cm (mean: 21 cm) and a complex internal structure. At least two units are identifiable in this light-colored deposit. The basal unit consists of yellowish grey sands, with normal grading (coarse to medium) and sharp boundaries with the underlying sediments. The upper unit resemble the light-colored deposit (Type 1) described above, but the plants macrorest are more diverse, with the presence of roots, leaves, seeds and wood fragments (Appendix figure 10, Appendix figure 11) . In most of the cases (n=4), a silty-sand unit capped by a fine lighter silty-clay layer (Figure 24) is overlain by the upper unit described previously. Changes in the parameters of grayscale and magnetic susceptibility along the deposition of this light-colored deposit, also denote its internal structure (units). Both parameters show an increase in their values between the deposition of the basal yellowish grey sands and the upper

lighter caps (silty-clay layers). Moreover, the stepwise decrease in magnetic susceptibility, towards the top of the sequence (light-colored deposit), suggests a reduction in the siliciclastic content. As previously mentioned, geochemical data show an increase (decrease) in the DBD and C/N ratio (water, organic carbon, nitrogen and carbonate content) during deposition of this type of light-colored deposit, in comparison to the adjacent sediments from the matrix (interbedded Gytja) (Figure 22). Pollen samples shows a decrease in the percentages of the aquatic fern *Isoetes savatieri* (Appendix figure 9).

The light-colored deposit **Type 3** (n=4) occurs towards the top of the record (in Section IV), and is characterized by a simple lithology composed of a silty-sand unit capped by a fine lighter silty-clay layer (Figure 24), and sharp boundaries with the adjacent sediments. The thickness of the light-colored deposit is variable (mean: 6 cm; min-max: 11.5-3.6 cm), but shows a decreasing trend towards the top of the core. As described previously, changes in the parameters of grayscale and magnetic susceptibility also denote the internal structure (units) of the light-colored deposits. In this case, both parameters show an increase in their values during the occurrence of this light-colored deposit in comparison with the adjacent sediments (matrix), but differ in their trend between the units (Figure 24). Maximum values observed in the grayscale parameter towards the top of the light-colored deposit are a response to the deposition of the lighter silty-clay layer or upper lighter cap. The magnetic susceptibility shows the opposite trend, with maximum values on the bottom and a gradual decrease towards the top of this type of light-colored deposit, suggesting a reduction in the siliciclastic content along the sequence (units). The geochemical parameters replicate the previously mentioned trends of increase (decrease) in the DBD and C/N ratio (water, organic carbon, nitrogen and carbonate content) during the occurrence of the light-colored deposits. Also, the pollen record replicates the previously mentioned trends of a decrease in the percentages of the spores of *Isoetes savatieri* (aquatic fern) during the occurrence of the light-colored deposits. Nevertheless, because of the significant increases experienced by *Isoetes savatieri* since the lithological section IV (8,500 cal yr BP; see pollen section 3.2.2.3), the declines in percentages during the occurrence of the light-colored deposits is more evident (Figure 24, Appendix figure 9). In addition, increases in the percentages of *Nothofagus dombeyi*-type and decreases in the *Gaultheria* are observed (Appendix figure 9).

Type 4 (n=65) is the most frequent and simple light-colored deposit, characterized by a fine (mean: 0.9 cm) lighter silty-clay layer which resembles the previously described lighter caps. The grayscale parameter effectively captures the occurrence of this type of light-colored deposit along the core, whereas magnetic susceptibility fails to detect some of them (Figure 24). The geochemical data indicates, as with the previously described light-colored deposits, opposite trends in the DBD and C/N values versus the water, organic carbon, nitrogen and carbonate contents. Pollen samples were not been analyzed from this type of light-colored deposit.

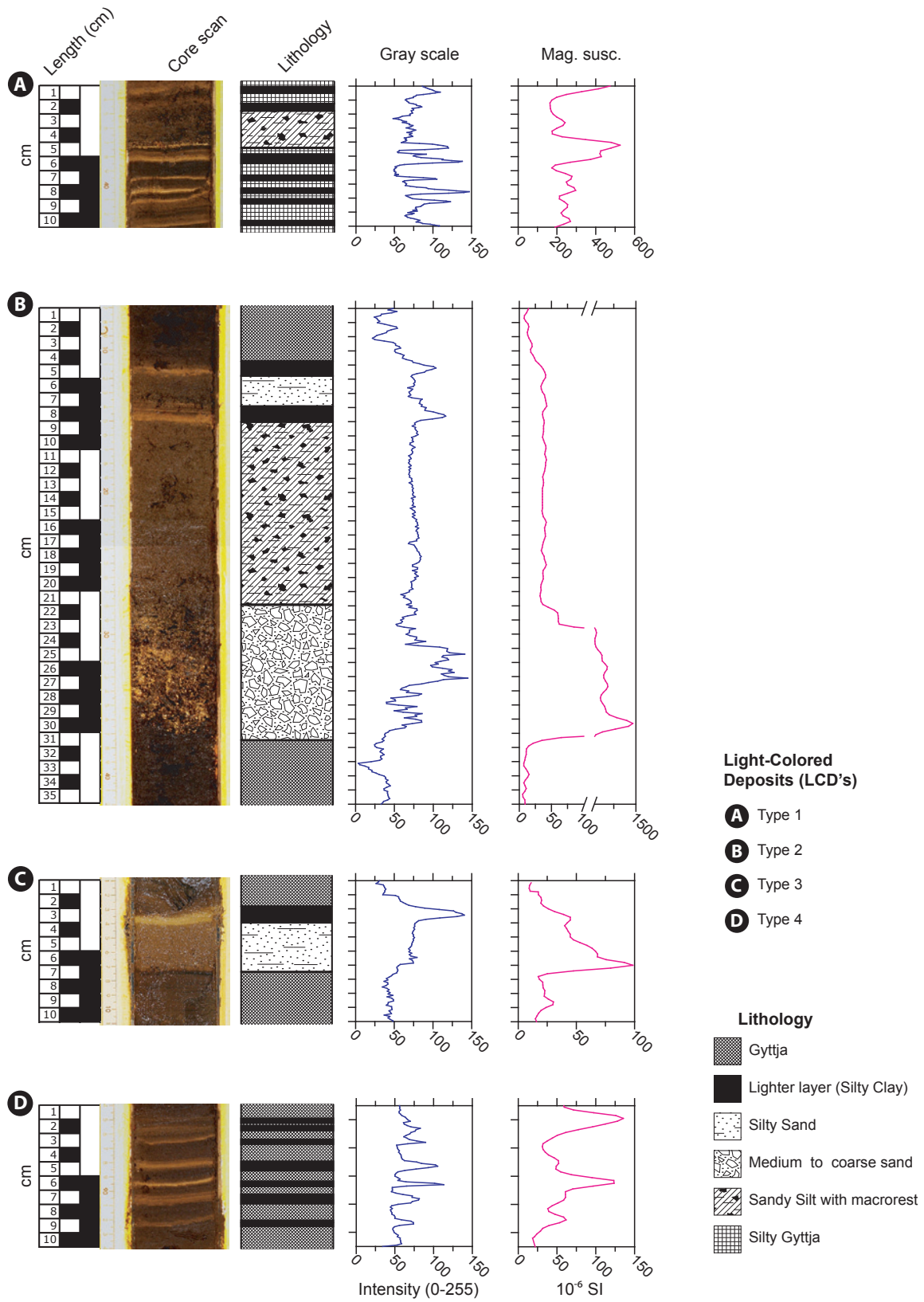


Figure 24. Close-up sections for the four different types of light-colored deposit (LCD's) present in the composite sediment core TML, indicating: length (cm), lithology, and the outcome of the parameters of grayscale and magnetic susceptibility for each one of them.

4.2.2.1.4. Event chronology

Based on the characteristic described above, a total of 74 light-colored deposits were identified as single events in the sediment core of Tamar Lake (Appendix table 1). The event chronology (frequency and recurrence) indicates that events associated with the light-colored deposits Type 4 are the most frequent in the record (mean: 4.4 events per 1000 years), except for the period between ~9000-11,000 cal yr BP when an important decrease in its occurrence is observed (Figure 25b). A noticeable change in event frequency after and before this occurrence gap is observed, with high frequencies before 11,000 cal yr BP (mean: 11 events per 1000 years) and a decrease after 9000 cal yr BP (mean: 3.9 events per 1000 years). The recurrence interval between the events also denote the differences between the period before 11,000 cal yr BP (mean recurrence interval: 80 years) and after 9000 cal yr BP (mean recurrence interval: 250 years). However, the most remarkable feature is the presence of periods with high recurrence time intervals on the order of sub-centennial time scales (<100 years among events) (Figure 25b).

The event chronology exhibited by the remainder of the light-colored deposits (Types 1-3) (Figure 25a) reveal a remarkable succession with regards to the types of events along the core. Events associated with the light-colored deposits 1 and 2 occur only during the late glacial and early Holocene (12,900-11,160 cal yr BP and 11,880-8700 cal yr BP, respectively), whereas events associated with Type 3 only occur during the mid and late Holocene (5050-380 cal yr BP)(Figure 25a).

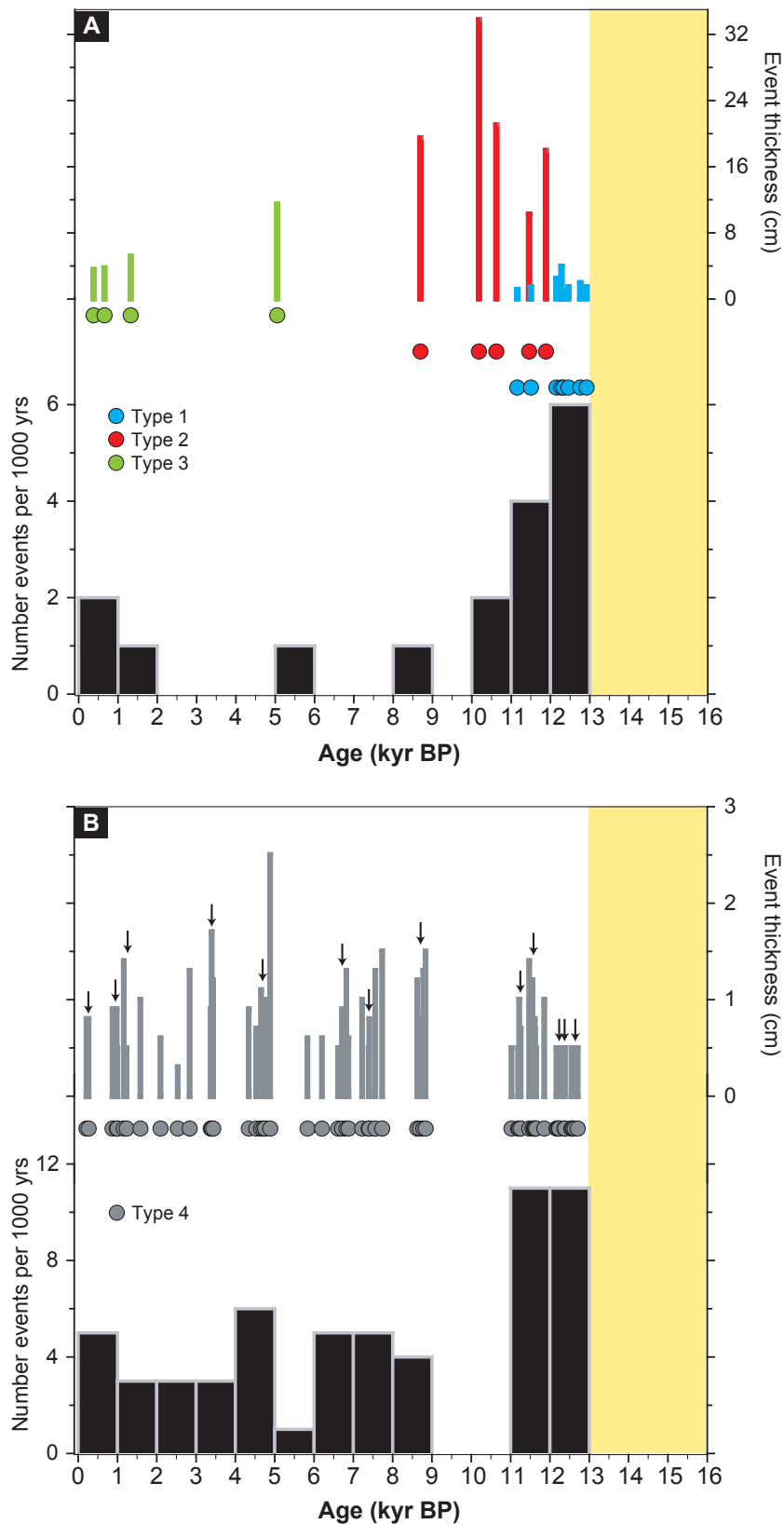


Figure 25. Chronology, thickness and frequency (per 1000 years) of events, based on individualized light-colored deposits (LCD's), present in the TML sedimentary record. Taking into account the differences observed among the LCD's (e.g. internal structure and distribution along the core), in the graph above (A) are plotted only the events corresponding to LCD's types 1-3, while in the graph below (B) are plotted the events associated to the LCD's type 4. Arrows in the graph B indicate periods when the recurrence among events is <100 years (sub-centennial time scales).

4.2.2.2. Pollen record

4.2.2.2.1. Percentages

Four main pollen zones were recognized from the cluster analyses (CONISS)(Grimm 1987)(Figure 26). The main characteristics of these pollen zones are described below, as well as specifications in parenthesis of the some statistical attributes (e.g. mean and min-max values) for the main taxa.

TML1 (665-600 cm; 15,880-13,590 cal yr BP): This pollen zone is characterized by the dominance of herb (mean: 59.8%) and scrub/cushion (mean: 37.6%) pollen. The most important taxa are Poaceae (mean: 14.2%), Asteraceae subf. Asteroideae (mean: 13.7%), *Caltha* (mean: 12.2%), *Gunnera magellanica* (mean: 10.7%), *Empetrum rubrum* (mean: 9.7%), and Cyperaceae (mean: 6%). Other species exceeding 5% at least once are: *Myrteola nummularia*, *Drapetes muscosus*, Apiaceae, Juncaginaceae+Juncaceae, *Perezia*, *Dysopsis glechomoides*, and *Draba*. Also traces (<5%) of Caryophyllaceae, *Acaena*, *Rubus* and Chenopodiaceae are identified. Of particular note is the predominance of Lycopodiaceae spores (mean: 7.3%) during this pollen zone.

TML2 (595-423 cm; 13,420-10,460 cal yr BP): This pollen zone is a transitional phase, characterized by the increase in arboreal pollen (mean: 55%) and a decrease in non-arboreal pollen, scrub/cushion (mean: 28.2%) and herbs (mean: 16.8%), which dominated in the previous zone. Two sub-zones were distinguished from the cluster analysis. The first subzone TML2a (595-508 cm; 13,420-11,670 cal yr BP) exhibits a significant increase in the pollen percentages of *Nothofagus dombeyi*-type (mean: 47.8%; max: 62.4%), and reaches maximum values at the end of this subzone. Other taxa such as *Escallonia* (mean: 5.9%) and *Donatia fascicularis* (mean: 5.7%) also experienced an increase in its relative values during this subzone, whereas *Phyllacne uliginosa* exhibits a peak at the beginning of this. Most of the non-arboreal elements shows a remarkable decreases in their relative percentages through this subzone, including the scrub/cushion taxa Asteraceae subf. Asteroideae (mean: 8.4%) and *Empetrum rubrum* (mean: 3%), and the herbs *Caltha* (mean: 6.9%), *Gunnera magellanica* (mean: 5.1%), Poaceae (mean: 2.6%) and Cyperaceae (mean: 1.3%). A decrease of Lycopodiaceae spores is also identified in this subzone. During the next subzone, TML2b (505-423 cm; 11,610-10,460 cal yr BP), the relative percentages of many non-arboreal taxa continue to decline, reaching minimum values or disappearing altogether from the record. Nevertheless, not all the non-arboreal species experience a decline in their relative percentages. *Escallonia* and *Donatia fascicularis* remain with relative high values, whereas *Gaultheria* (mean: 6%) experience an important increase in its percentages through this subzone. Also *Misodendrum*, a woody-hemiparasite of *Nothofagus*, experience an important increase in its percentages and reaching maximum values (10%) at the end of this subzone. Spores of the terrestrial fern Polypodiaceae and the aquatic fern *Isoetes savatieri* also exhibit an important increase in its relative percentages during this subzone.

TML3 (418-211 cm; 10,280-6200 cal yr BP): The predominance of arboreal pollen (mean: 71.2%), mostly *Nothofagus dombeyi*-type (mean: 57.8%), characterizes this polinic zone. This change occurs at expense of a major decrease in herb pollen (mean: 6.4%) and lesser degree in the pollen from scrub/cushion taxa (mean: 22.4%). Two subzones are identified within this zone. The first subzone, TML3a (418-311 cm; 10,280-8680 cal yr BP), is characterized by the co-dominance of *Nothofagus dombeyi*-type (mean: 56%) and *Misodendrum* (mean: 10.9%). Nevertheless, *Drimys winteri* (min: 2.5%; max: 9.7%) experience an increase in percentages within the subzone reaching maximum values at the end. The other species retain quasi-equal values to the previous zone, only the *Berberis* percentages tend to exhibit more continuity since this period. The second subzone,

TML3b (305-211 cm; 8530-6200 cal yr BP), is co-dominated by *Nothofagus dombeyi*-type (mean: 58.7%) and *Drimys winteri* (mean: 6%; max: 10.6%), whereas the percentages of *Misodendrum* (mean: 4.5%; min: 2.3%) experience a decrease. A slight increase in the percentages of *Gaultheria* (mean: 11%) and the spores from terrestrial ferns (Polypodiaceae & Hymenophyllaceae) are also distinctive features of this subzone. While, the percentages of the aquatic fern *Isoetes savatieri* begin an uninterrupted increasing trend to the present.

TML4 (207-1 cm; 6050 cal yr BP to present): This polinic zone is characterized by successive increases in the percentages of different trees, scrubs/cushions and herbs elements, whereas *Nothofagus dombeyi*-type (mean: 49%) exhibits a gradual decrease in its percentages along the zone (max: 59.4%; min: 36.4%). Three subzones are distinguished through cluster analysis. The first subzone, TML4a (207-116 cm; 6050-3430 cal yr BP), is characterized by increases in percentages of *Pilgerodendron uviferum* (max: 6.4%), Cyperaceae (max: 4.7%) Juncaginaceae+Juncaceae (max: 3.8%), *Astelia pumila* (max: 3.2%) and *Hebe elliptica* (max: 3.2%). Concurrently, *Escallonia* (max: 5.2%), *Donatia fascicularis* (max: 5%) and *Berberis* (max: 3.8%) show a decrease in percentage. In the second subzone, TML4b (109-56 cm; 3300-1550 cal yr BP), additional taxa shows increases in their percentages, including *Raukava laetevirens* (max: 2.8%), *Desfontainia spinosa* (max: 2.3%), *Myrteola nummularia* (max: 2%), *Philesia magellanica* (max: 1.5%) and Apiaceae (max: 1.5%). On the other hand, *Escallonia*-type (max: 9.6%) and *Donatia fascicularis* (max: 5.5%) experience a re-increase in percentages, whilst *Misodendrum* (mean: 1.1%) exhibits a decrease in its percentages. The last subzone, TML4c (35-1 cm; 1020 cal yr BP to present), also exhibits increases or re-increases in the percentages of several taxa including Poaceae (max: 6.1%), *Tepualia stipularis* (max: 5.9%), Empetrum (max: 4.5%), *Berberis* (max: 3.2%) and *Podocarpus nubigena* (max: 1.6%), whilst *Nothofagus dombeyi*-type exhibits a decline (mean: 40%).

4.2.2.2. Concentrations

The pollen concentrations (Figure 27) from the Tamar Lake record follow the trends described previously in percentages, with the predominance of non-arboreal pollen in the basal pollen zone (TML1), followed by a transitional period dominated by scrubs and cushion taxa (TML 2) and later expansion of arboreal elements (TML 3-4) during the mid to late Holocene. Pollen concentrations also offers additional and relevant information concerned with the individual variations or responses of the taxa (Bennett 1983; Fægri and Iversen 1989), because its values are calculated in an independent way which is not affected by the proportionality (sum=100%) exhibited in the percentages (see section 3, material and methods). Therefore, below are described the most remarkable features of the pollen concentration record within the palynological zones previously defined by cluster analysis. The complete pollen concentration record is show in the appendix section (Appendix figure 12).

The basal pollen zone **TML1 (665-600 cm; 15,880-13,590 cal yr BP)** is characterized by low total pollen concentrations (mean: 64,340 grains/cc), and practically the absence of pollen from arboreal and aquatics taxa. Pollen concentrations from grasses and herbs (mean: 32,600 grains/cc) are the most abundant, with *Caltha*, *Gunnera magellanica*, Poaceae, Juncaceae+Juncaginaceae and Cyperaceae as the most predominant taxa. Nevertheless, is also appreciable pollen from some scrub taxa as Asteraceae subf. Asteroideae, *Empetrum rubrum*, *Drapetes muscosus* and Apiaceae. The total concentrations of ferns spores are also low (mean: 7900 spores/cc), however a predominance of Lycopodiaceae over the other types (mean: 4085 spores/cc) is observed. Total pollen concentrations (mean: 221,300 grains/cc) increase considerably during this pollen zone.

TML2 (595-423 cm; 13,420-10,460 cal yr BP), as a result of the expansion of *Nothofagus dombeyi*-type and some scrubs species (e.g. *Gaultheria*, *Escallonia*, *Donatia fascicularis*, *Phyllacne uliginosa*, *Berberis* and *Astelia pumila*). As was mentioned in the previous section (percentages), two subzones were recognized within this pollen zone. During the first subzone, TML2a (595-508 cm; 13,420-11,670 cal yr BP), is observed the increase of *Nothofagus dombeyi*-type concentrations (mean: 74,600 grains/cc) together with *Escallonia* (mean: 8870 grains/cc), *Donatia fascicularis* (mean: 9080 grains/cc), *Phyllacne uliginosa* (mean: 2525 grains/cc) and *Astelia pumila* (mean: 1730 grains/cc). Also observed is an increase in the concentration of Hymenophyllaceae spores (mean: 6812 spores/cc) and a decrease in the Lycopodiaceae (mean: 1230 spores/cc). On the other hand, concentrations of grasses and herbs remains relative high (mean: 32,830 grains/cc), and similar to the previous pollen zone. In the next subzone, TML2b (505-423 cm; 11,610-10,460 cal yr BP), the total pollen concentration continues increasing and reaches maximum values (mean: 254,850 grains/cc). This feature is a result of a rise in the pollen concentration experienced by the tree hemiparasit *Misodendrum* (mean: 11,650 grains/cc), and the scrubs taxa: *Gaultheria* (mean: 12,770 grains/cc), *Escallonia*-type (mean: 17,365 grains/cc) and *Berberis* (mean: 2925 grains/cc). On the other hand, the concentration of grasses and herbs decreases during this subzone (mean: 24,560 grains/cc) because of a decline in the concentrations of Cyperaceae and Juncaginaceae+Juncaceae (mean: 1525 and 835 grains/cc, respectively), and the disappearance of *Perezia* and *Draba* (Appendix figure 12). A remarkable feature that takes place during this pollen subzone is the rise in the concentrations of the ferns and aquatics spores (mean: 41,070 and 5950 spores/cc, respectively). In particular, the abrupt increase experienced by the concentrations of Polypodiaceae spores (mean: 31,000 spores/cc) explains this change.

Total pollen concentrations during the pollen zone **TML3 (418-211 cm; 10,280-6200 cal yr BP)** continue exhibiting high values (mean: 183,890 grains/cc), nevertheless experiences a decrease towards to middle of the zone (or subzone boundary). Thus, during the first subzone TML3a (418-311 cm; 10,280-8680 cal yr BP), the total tree concentrations reach its maximum values (mean: 138,770 grains/cc) in response to the persistent high values exhibited by *Nothofagus dombeyi*-type (mean: 106,230 grains/cc) and a rise in the *Drimys winteri* concentrations (mean: 9500 grains/cc). On the other hand, pollen concentrations of grass-herb and scrub-cushion taxa exhibits a decrease during this subzone (11,044 and 40,290 grains/cc, respectively), nevertheless this change does not affect the total pollen concentrations. Later, during the following subzone TML3b (305-211 cm; 8530-6200 cal yr BP), a decline in the *Nothofagus dombeyi*-type (mean: 66,500 grains/cc), *Misodendrum* (mean: 4980 grains/cc) and *Drimys winteri* (mean: 6740 grains/cc) concentrations lead to a decrease in the total tree concentrations (mean: 79,500 grains/cc). Thus, this feature is the main factor that explains the previously mentioned decline in the total pollen concentrations (mean: 79,500 and 159,580 grains/cc, respectively) at the middle of this pollen zone. Nevertheless, not all the taxa experience a decline during this subzone, being appreciable an increase in the concentration of *Berberis* and the spores of *Isoetes savatieri*.

During the remaining pollen zone, **TML4 (207-1 cm; 6050 cal yr BP to present)**, total pollen concentrations do not change significantly. Nevertheless, as was mentioned in the percentages section, this pollen zone is characterized by the expansion of several trees and scrubs species (Figure 27). The total concentrations of ferns (spores) exhibit an decrease (mean: 19,250 spores/cc) during this zone.

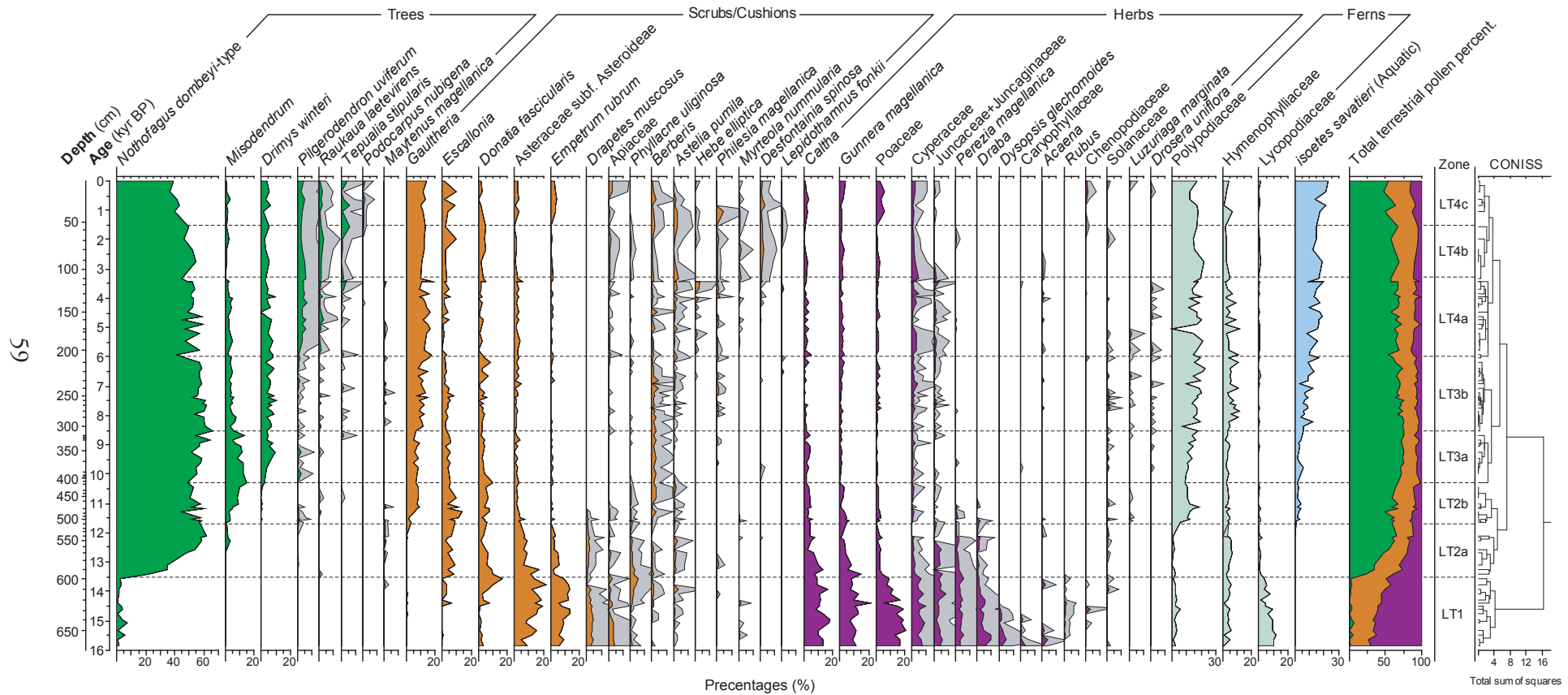


Figure 26. Percentage diagram of selected taxa from Core TML, plotted against the calibrated calendar age. The secondary y-axis displays the composite depth scale (cm). Dashed lines represent the boundaries of pollen zones after the cluster analyses (CONNIS) in the right. Gray area (outside the curves) indicates a exaggeration factor x5.

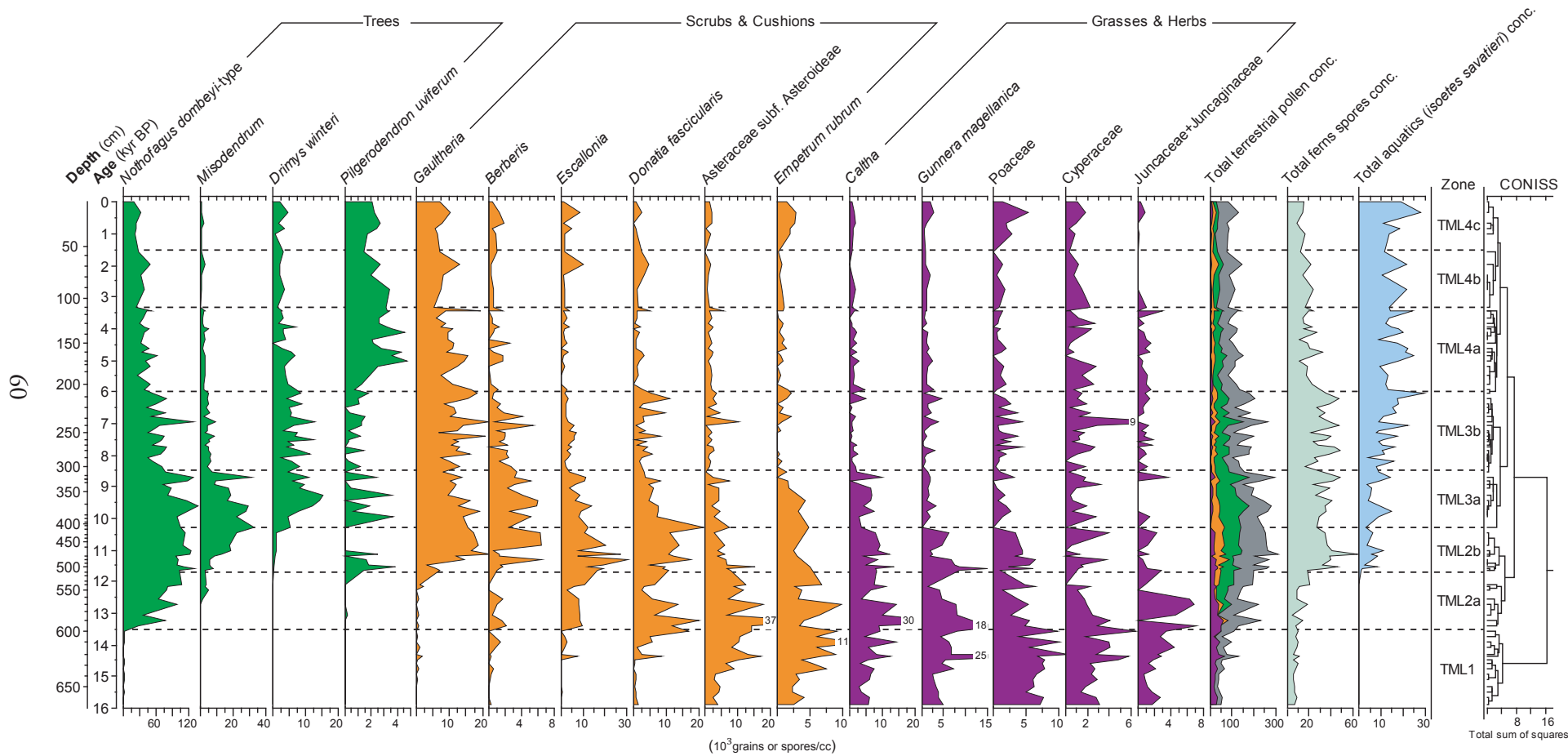


Figure 27. Concentration diagram (grains/cc) of selected taxa from the pollen record of Tamar Lake. On the right of the graph are included the total concentration of terrestrial plants, ferns and aquatics. Please note the differences in the concentration scale among the taxa.

4.2.2.3. Numerical Analyses

4.2.2.3.1. Principal Component Analysis (PCA)

Principal Component Analysis performed over the dataset comprised of taxa which its values exceeds the 5% at least once, indicates that two first axes capture ~78% of the total pollen variance (Figure 28). The most important is Axis 1 which captures 69% of the total variance, whereas the second only captures 9%. In Figure 28 is observable that samples from the basal pollen zone (TML1) are grouped on the right of the biplot together with non-arboreal taxa, which include grasses-herbs (e.g. as Poaceae, Juncaginaceae+Juncaceae, Cyperaceae, *Caltha*, *Gunnera* and *Draba*) and cushion-scrubs taxa (e.g. *Empetrum rubrum* and Asteraceae subf. Asteroideae). On the left side of the biplot are grouped samples from the pollen zones TML3 and TML4 together with arboreal species (e.g. *Nothofagus*, *Misodendrum*, *Drimys winteri*, *Pilgerodendron uviferum* and *Tepualia stipularis*) and scrubs taxa (e.g. *Escallonia* and *Pernettya*). Samples from the pollen zone TML2 are located in an intermediate position, but towards the top of the bitplot, together with *Donatia fascicularis*, *Escallonia* and *Phyllacne uliginosa* (Figure 28).

The sample scores for Axes 1 and 2 (Figure 28) are characterized by different trends of changes along the core, indicating the multivariate nature of the dataset (pollen record). The most remarkable is the monotonic change (from positive to negative values) identified by the sample scores of Axis 1 during the pollen zone TML2 (13,420-10,460 cal yr BP). This change denotes the transition from a pollen record dominated by non-arboreal taxa [pollen zone TML1 (15,880-13,590 cal yr BP)] to one where arboreal and scrubs elements [pollen zones TML3 and TML4 (10,280 cal yr BP to present)] are predominant. Axis 2 also records an important change during this time (pollen zone TML2), showing an abrupt incursion towards positive values in the sample scores (Figure 28) in response to expansion of the scrub-cushion plants (e.g. *Donatia fascicularis* and *Escallonia*) in the pollen record. Previously, during the pollen zone TML1, negative values observed in sample scores of the Axis 2 denotes the dominance non-arboreal pollen in the record. The decrease in the sample scores of the Axis 2 during the pollen zones TML3 and TML4 relates to the expansion of arboreal (e.g. *Drimys winteri*, *Pilgerodendron uviferum* and *Tepualia stipularis*) and scrubs (*Gaultheria*).

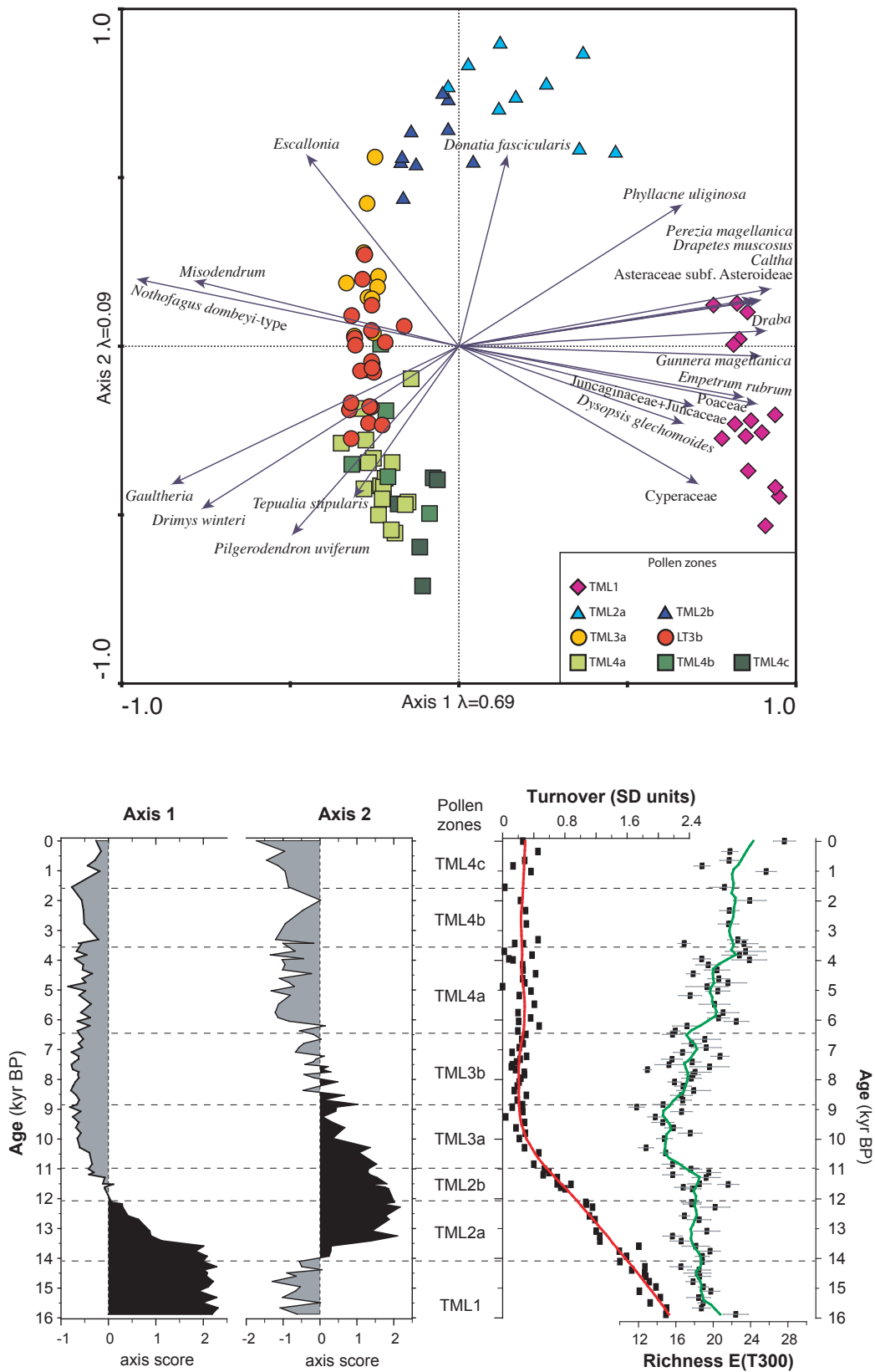


Figure 28. (Above) Biplot of Principal Component Analysis (PCA) for the pollen record TML, performed on a re-calculated dataset containing only taxa >5%. The respective pollen zone for each sample is indicated. (Below) Sample scores for the Axis 1 and 2, plotted against age. Pollen zones are also indicated. Results for the DCCA (Turnover) and the palynological rarefaction analysis (Richness) performed on the pollen record. The estimated palynological richness is based on the minimum number of pollen taxa (T_n). In order to highlight the major trends in the palynological turnover and richness, a Loess smoother (solid lines) has been fitted to the raw data, utilizing a sampling span of 1.5 and rejecting the outliers.

4.2.2.3.2. Palynological Turnover and Richness

The detrended canonical correspondence analyses (DCCA) and the rarefaction analysis performed on the pollen record of Lake Tamar (TML) provide of substantial information about changes in the palynological turnover and richness (respectively) during the last 16,000 years. The DCCA results are expressed in ecologically interpretable units, namely standard deviation (SD) units of compositional turnover, making it possible to perform intra- and inter-sites comparisons (Birks 2007). Moreover, estimation of the total palynological turnover (Table 8), calculated as the difference between the highest and lowest values from each pollen sequence (see section material and methods), provide a statistical parameter to evaluate the amount of compositional change (Birks 2007). A complete turnover of species, with no species in common, would have a total palynological turnover (gradient length) of 4 SD (Hill and Gauch 1980).

The DCCA results from the TML pollen record, indicate a palynological turnover of 2.11 SD for the complete pollen sequence (Table 8). Most of the changes experienced by the DCCA occurs during the pollen zones TML1 and TML2 (15,880-10,460 cal yr BP), where a strong and continuous (linear) decrease (from 2.1 to 0.4 SD) in its values is identified (Figure 28). Later, during the pollen zones TML3 and TML4 (10,280 cal yr BP to present), the DCCA sample scores remains lower and constant (mean: 0.24 SD). This pattern is the result of gradual but sustained decrease, experienced by the non-arboreal taxa along the pollen zones TML1 and TML2 (Figure 28). Furthermore, this denotes the beginning of a pollen assemblage dominated by a new taxonomic composition after the pollen zone TML3 (Figure 28).

The palynological richness (rarefaction analysis) shows relatively high and constant values during the pollen zones TML1 and TML2 (15,880-10,460 cal yr BP), followed by an abrupt decrease at the beginning of the pollen zone TML3 (10,280 cal yr BP)(Figure 28). This decline in the palynological richness is in line with the previously mentioned change in the palynological turnover observed during the pollen zones TML2 and TML3 (10,280 cal yr BP). Therefore, is it likely that such change is a response to the new taxonomic composition which dominates the pollen record after 10,280 cal yr BP to the present (pollen zones TML3 and TML4)(Figure 28). Later, and along the pollen zones TML3 and TML4 (10,280 cal yr BP to present), a stepwise increase in the palynological richness takes place at the beginning of each pollen zone and sub-zone (Figure 28). This pattern is result of succession and consecutive expansion of tree taxa (*Drimys winteri*>*Pilgerodendron uviferum*>*Raukava laetevirens*>*Tepualia stipularis* and *Podocarpus nubigena*) (Figure 26).

4.2.2.4. Numerical Analyses performed in additional pollen record located along a west-east transect

As was mentioned in the introduction, one main objective of this thesis is to examine the ecological implications of the changes experienced by the plant communities along the broad bioclimatic gradient in Southern Patagonia during the postglacial period. To achieve this objective, numerical analyses (CONISS, PCA, DCCA and the rarefaction analysis) were performed on selected pollen records located along a west-east transect at $\sim 53^{\circ}\text{S}$ (see section 3, materials and methods)(Figure 12). The results, and hence this thesis, do not re-interpret these pollen records or, its ecological implications previously described and discussed by the original authors (Huber 2001; Fesq-Martin 2003; Wille *et al.* 2007; Francois 2009). Therefore, the performed analysis must be considered as complementary and in most of the cases only descriptive. Only the in the case of pollen record from Potrok Aike was necessary amend the age model, following recent publications (Kliem *et al.* 2012). The most significant results from the numerical analyses performed on each pollen record are described below. In addition, the main site study characteristics and the most relevant palynological inferences, previously discussed in the original publications, are included.

Table 8. Summary of principal component analysis (PCA) and detrended canonical correspondence analyses (DCCA), measure of trends in turnover (beta-diversity), total inertia (total variance in each sequence), and the first eigenvalue (λ_1) measure of the contribution of the first axis to total variance at the four study sites, using both all samples and only those samples covering the period in common (12,750 cal yr BP to present).

	Sites				
	Tamar	GCN	Rubens	Guanaco	Potrok
PCA					
Eigenvalues Axis 1	0.694	0.508	0.659	0.55	0.49
Eigenvalues Axis 2	0.091	0.285	0.163	0.101	0.175
Accumulative variance (%)	78.4	79.4	82.2	65.1	66.5
DCCA					
All samples					
Inertia (total variance)	1.29	0.53	1.91	0.85	0.52
Turnover (SD)	2.11	1.6	2.3	1.48	1.11
Eigenvalues Axis 1	0,32	0.09	0.31	0.11	0.03
N° samples	91	119	146	278	238
N° species	60	21	65	42	47
Common time scale (<12,750 cal yr BP)					
Inertia (variance)	0.99	0.52	1.60	0.85	0.49
Turnover (SD)	1.7	1.6	1.74	1.48	0.94
Eigenvalues	0.14	0.08	0.27	0.11	0.02
N° samples	73	117	120	278	210
N° species	54	21	61	42	37

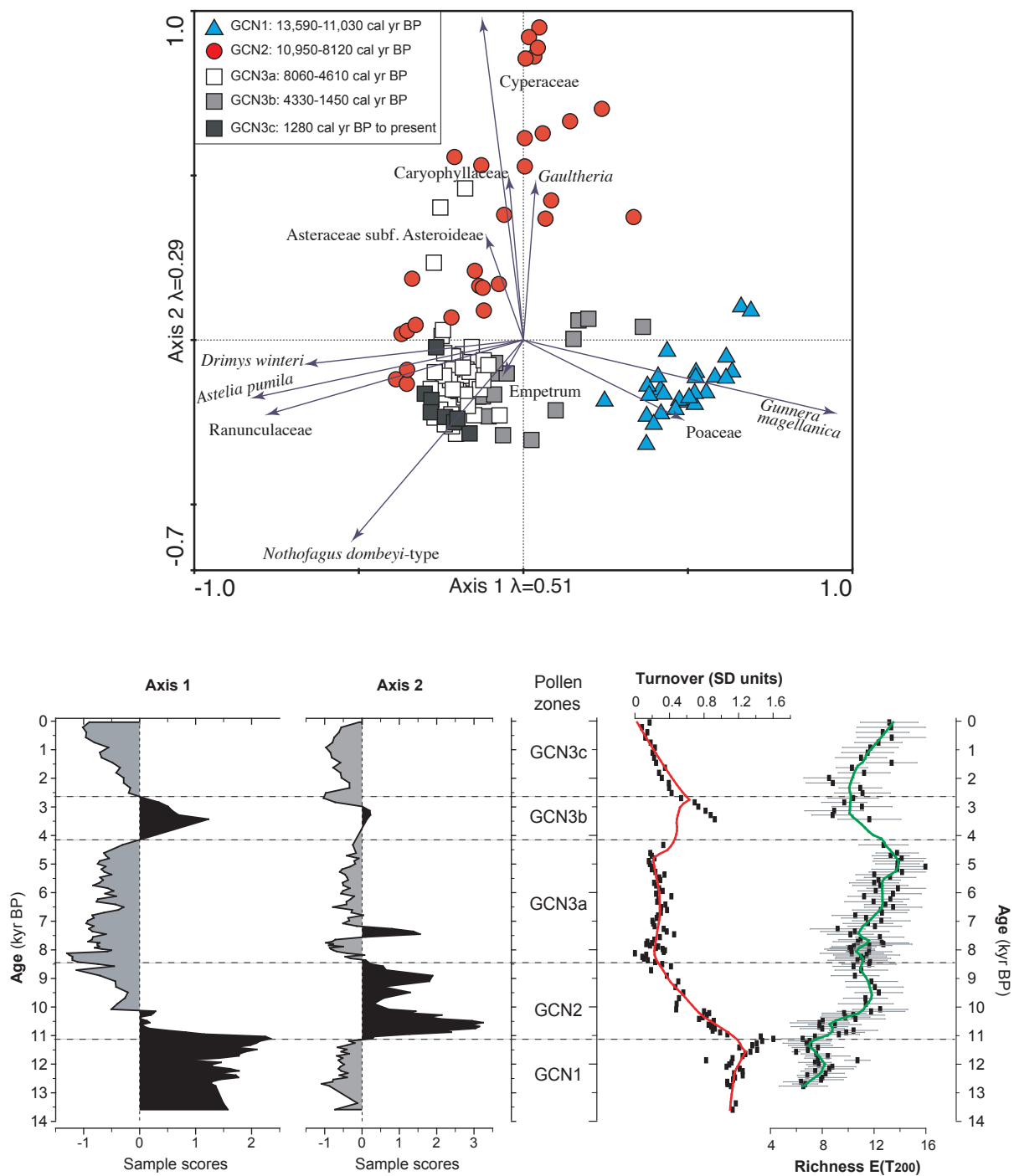


Figure 29. (Above) Biplot of Principal Component Analysis (PCA) for the pollen record GCN, performed on a re-calculated dataset containing only taxa >5%. The respective pollen zone for each sample is indicated. (Below) Sample scores for the Axis 1 and 2, plotted against age. Pollen zones are also indicated. Results for the DCCA (Turnover) and the palynological rarefaction analysis (Richness) performed on the pollen record. The estimated palynological richness is based on the minimum number of pollen taxa (Tn). The results are plotted against age. Pollen zones are indicated on the middle of the graph. In order to highlight the major trends in the palynological turnover and richness, a Loess smoother (solid lines) has been fitted to the raw data, utilizing a sampling span of 1.5 and rejecting the outliers.

4.2.2.4.1. Gran Campo Nevado (GCN) (Fesq-Martin 2003)

The sedimentary record of GCN (52°48.62'S; 72°55.77'W, ~70 m.a.s.l.) was obtained from a peat-bog (i.e. *Marsippospermum grandiflorum*, *Schoenus antarcticus* and *Astelia pumila*) located within the inner Fjords in the vicinity of Canal Gajardo (Peninsula Munoz Gamero) and the Gran Campo Nevado Ice field (Figure 12). The local vegetation comprises communities from the (i) Magellanic Evergreen forest (e.g. *Nothofagus betuloides*, *Drimys winteri*, and *Gaultheria mucronata*) occurring over well-drained areas, and (ii) Magellanic moorlands on flat areas (e.g. Cyperaceae, Juncaceae, *Astelia pumila*, *Donatia fascicularis*, *Gunnera magellanica*, and Ranunculaceae).

The PCA indicates that the first two axes capture 79.4 % of the total variance, with Axis 1 explaining more than 50% of the variation (Figure 29 & Table 8). Three main pollen zones are defined along the pollen record, covering the last 13,590 cal yr BP (Appendix figure 13). The first pollen zone GCN1 (13,590-11,030 cal yr BP), is characterized by show negative (positive) sample scores in the PCA Axis 1 (Axis2), in response to the predominance of *Gunnera magellanica* and Poaceae (Figure 29). This pollen assemblage denotes an early stage of succession dominated by typical pioneer species, similar to the found after severe disturbances or in areas recently ice-free. Later, during the GCN2 pollen zone (10,950-8120 cal yr BP) the PCA values for Axis 1 (Axis 2) shifts towards positive (negative) values in response to the expansion of the several species, which include: herbs (Caryophyllaceae and Ranunculaceae), graminoids and cushion plants (Cyperaceae and *Astelia pumila*), scrubs (Asteraceae subf. Asteroideae and *Gaultheria*) and trees (*Drimys winteri*). This palynological change has been interpreted as the expansion of cushion bog communities in the surrounding areas of the site, and the initial establishment of the Evergreen forests communities in the study area. Finally, during the pollen zone GCN3 (8060 cal yr BP to present), negative values in both PCA axis scores indicate the predominance of *Nothofagus dombeyi*-type pollen in the record, and suggest the definitive establishment of Evergreen forests communities in the study area. This stage is abruptly interrupted around 4330-1450 cal yr BP (GCN3b), when both PCA axes exhibits a shift in their values (towards positive) in response to: (i) the increase and re-expansion of *Gunnera magellanica* and Poaceae pollen and, (ii) the decrease of moorland elements (e.g. Cyperaceae, Juncaceae, *Astelia pumila*, *Donatia fascicularis*, *Gunnera magellanica*, Ranunculaceae). This change (i.e. diminish of moorland communities and re-expansion of pioneer species) denotes a disturbance scenario closely related to the deposition of the Mount Burney ash layer. The ecological mechanism explaining this phenomena is linked to a process of soil acidification caused by the SO₂ released from the tephra layer, and to the low acid-buffering capacity of the soils (Kilian *et al.* 2006).

The DCCA results indicate a total palynological turnover of 2.3 SD for the complete sequence (Table 8). Most of the change occurs abruptly during the pollen zone GCN2 when the values decrease from 1.6 to 0.9 SD (Figure 29). Later, the DCCA values remains low (mean: 0.31 SD), excluding the disturbance interval associated to the deposition of the Mount Burney tephra (pollen sub-zone GCN3b), when the values experience an increase.

The rarefaction analysis is characterized by a stepwise increase of its values during the pollen zones GCN2 and GCN3 (Figure 29). The first of these pulses occurs abruptly at the beginning of the GCN2 pollen zone, while the other occurs gradually along the subzone GCN3. Finally, during the subzone GCN3b (disturbance interval), the rarefaction values experience a decrease, which later exhibits a recovering (increase) along the subzone GCN3c.

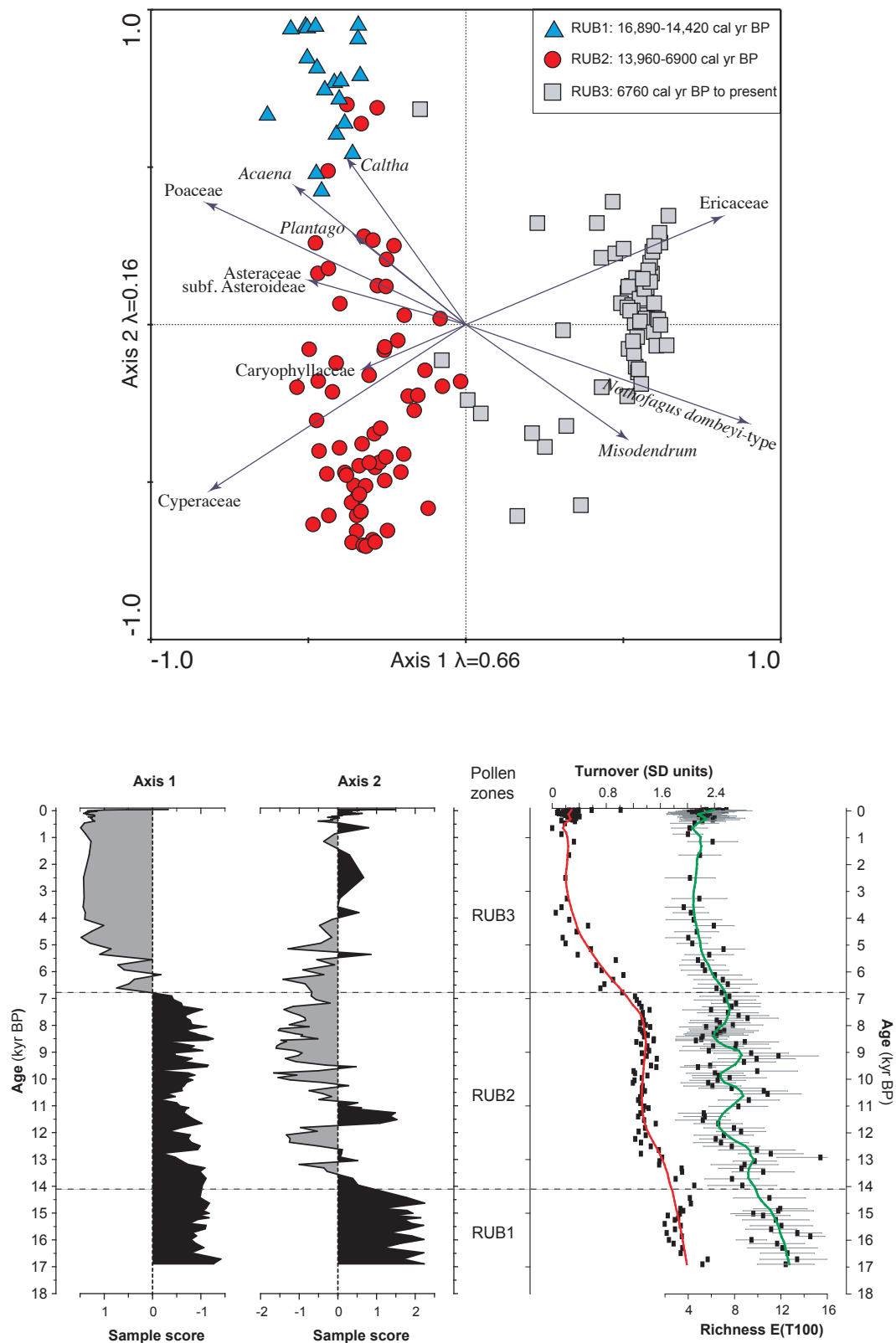


Figure 30. (Above) Biplot of Principal Component Analysis (PCA) for the pollen record Rio Rubens, performed on a re-calculated dataset containing only taxa >5%. The respective pollen zone for each sample is indicated. (Below) Sample scores for the Axis 1 and 2, plotted against age. Pollen zones are also indicated. Results for the DCCA (Turnover) and the palynological rarefaction analysis (Richness) performed on the pollen record. The estimated palynological richness is based on the minimum number of pollen taxa (Tn). The results are plotted against age. Pollen zones are indicated on the middle of the graph. In order to highlight the major trends in the palynological turnover and richness, a Loess smoother (solid lines) has been fitted to the raw data, utilizing a sampling span of 1.5 and rejecting the outliers.

4.2.2.4.2. Rio Rubens (Huber 2001)

The Rio Rubens pollen record (52°48.62'S; 72°55.77'W, 220 m.a.s.l.) was retrieved from a peat-bog (i.e. *Empetrum rubrum* accompanied by *Polytrichum strictum* and *Sphagnum* mosses) and is located on a glacial-age meltwater channel, at ~60 km south of Puerto Natales, Chile (Figure 12). Regional vegetation comprises the contact zone between the deciduous forest and the Patagonian Steppe, whereas the local vegetation comprises thickets and shrubs of *Nothofagus antarctica* and *Chilotrimum diffusum*, which grow around the edges of the bog. Most of the area exhibits clear signs of disturbance (e.g. standing and fallen burnt logs), testimony to the extensive clearing and burn of the deciduous forests (*Nothofagus pumilio*) since the 16th century.

Three main pollen zones were defined along the pollen record, which comprises the last 17,000 years Appendix figure 14, whilst the PCA indicates that first two axes captures more of the 82% the total variance. The most important was Axis 1 which explains ~66% of the variation (Figure 30 & Table 8). Positive (negative) sample scores in the PCA Axis 1 (Axis 2), characterize the first pollen zone (Rub1: 17,000-14,500 cal yr BP), denoting the predominance of herbs and scrubs (e.i. Poaceae, Cyperaceae, *Acaena*, Ericaceae, and Asteraceae subf. Asteroideae) in the pollen record. This initial assemblage suggests the development of an open landscape, dominated by heath-grassland plant communities. During the following pollen zone (Rub: 13,960-6900 cal yr BP), only PCA Axis 2 experiences a significant change in its values, exhibiting negative values all along the pollen zone. This is result of the increase in the Cyperaceae percentages, at expenses of Ericaceae, and initial expansion of *Nothofagus dombeyi*- type (Figure 30). Such palynological changes indicate the expansion and establishment of the shrubby communities along an herbaceous grassland. The gradual transit towards positive values experienced by PCA Axis 2, contrasting with the abrupt change observed in the PCA Axis 1, characterize the last pollen zone (Rub3: 6760 cal yr BP to present). These changes denote the increase in the *Nothofagus dombeyi*- type and Ericaceae percentages, and the decrease of the grasses and herbs taxa (e.i. Poaceae and Cyperaceae) in the pollen record. The ecological implications for this change, is the expansion (at regional scale) of the *Nothofagus* woodland into the shrubby grassland and the establishing of the current ecosystems dominating the forest–steppe ecotone.

The results from the DCCA indicate a total palynological turnover (for the complete studied sequence) of 2.3 SD, which is conducted by means of a stepwise decrease in its values towards the present (Figure 30 & Table 8). The first period of change in the DCCA values, takes place gradually during the transition among the pollen zones Rub1 and Rub2, while the second occurs abruptly (from 1.4 to 0.2 SD) within the pollen zone Rub3.

The rarefaction analysis shows a continuous decrease in the palynological richness toward the present, but including a period of high fluctuations in its values during the pollen zone Rub2 (Figure 30).

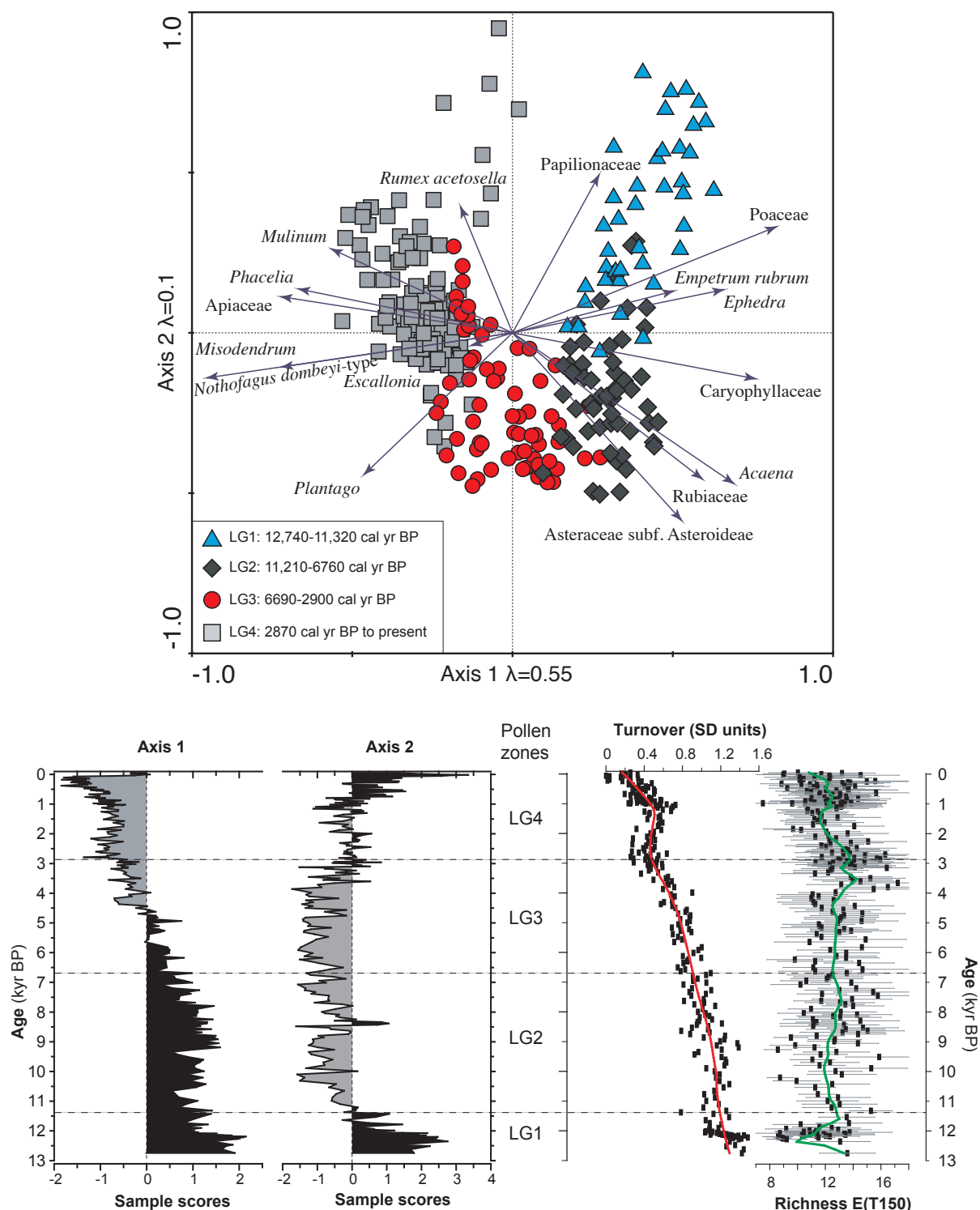


Figure 31. (Above) Biplot of Principal Component Analysis for the pollen record Laguna Guanaco, performed on a re-calculated dataset containing only taxa >5%. The respective pollen zone for each sample is indicated. (Below) Sample scores for the Axis 1 and 2, plotted against age. Pollen zones are also indicated. Results for the DCCA (Turnover) and the palynological rarefaction analysis (Richness) performed on the pollen record. The estimated palynological richness is based on the minimum number of pollen taxa (Tn). The results are plotted against age. Pollen zones are indicated on the middle of the graph. In order to highlight the major trends in the palynological turnover and richness, a Loess smoother (solid lines) has been fitted to the raw data, utilizing a sampling span of 1.5 and rejecting the outliers

4.2.2.4.3. Lago Guanaco (Francois 2009)

Lago Guanaco (51°52'S, 72°52'W, 200 m.a.s.l.) is a small closed-basin lake (~0.13 km²) located ~1.5 km north of Lago Sarmiento, within the Torres del Paine National Park, Chile (Figure 12). The vegetation surrounding the lake is dominated by Patagonian Steppe herbs (i.e. *Mulinum spinosum* and grasses) along with exotic taxa (*Rumex acetosella*, *Salix* sp.) product of the intensive human occupation since the late 19th century. The lake is bordered by a rim of *Carex* sp. up to 2 m water depth, superseded by dense beds of the aquatic *Myriophyllum* sp. at intermediate depths (2-5 m).

The first two PCA axes capture more than 65% of total pollen variance, with Axis 1 explaining 55% of the variance and Axis 2 only 10% (Table 8). Cluster analysis indicates the occurrence of four main pollen zones. The first pollen zone LG1 (12,800-11,500 cal yr BP) is characterized by positive values on both PCA axes, as result of the dominance of grasses (Poaceae), herbs (Caryophyllaceae, *Acaena* and Rubiaceae) and shrubs (*Ephedra*, *Empetrum rubrum*, and Asteraceae subf. Asteroideae) in the pollen record (Figure 31). The pollen assemblage characterizing this pollen zone has been interpreted as the development of a dwarf-shrub steppe in the Lago Guanaco area. Later, during the zone LG2 (11,500-6800 cal yr BP), a shifts towards negative values is identified in the PCA Axis 2 sample scores. This change is related with the appearance (i.e. *Plantago* and *Phacelia*) and disappearance (i.e. *Ephedra*, *Empetrum rubrum* and Rubiaceae) of some herbs and shrubs taxa from the pollen record. These changes, together with the persistent dominance of Poaceae and Asteraceae subf. Asteroideae in the pollen record, suggests the development of a herbaceous grassland during this time. The transition towards negative values experienced by the sample scores of PCA axis 1, characterizes the zone LT3 (6800-2900 cal yr BP) and denoting: (i) the increases in the percentages of *Nothofagus dombeyi*-type and its hemiparasite *Misodendrum* and (ii) the decreases on some grasses and herbs (i.e. Poaceae and Asteraceae subf. Asteroideae) along this pollen zone. These changes suggest the expansion and establishment of stands or patches of *Nothofagus* in the area, together with other shrubby communities. During the last pollen zone LG4 (2900 cal yr BP to present) the PCA Axis 1 shows its minimum values, in response to the tree pollen predominance on the record, while the Axis 2 shows a trend toward positive values in its sample scores, in response to the expansion of several herbs and shrubs taxa in the pollen record (i.e. *Plantago*, *Phacelia*, Apiaceae and *Mulinum spinosum*). The pollen assemblage for this period suggests the development of the deciduous *Nothofagus* woodland in the area.

The DCCA shows a gradual decline in the palynological turnover along the record, and leads to a total turnover of 1.48 SD for the complete sequence (Table 8). Most of the changes in the DCCA occurs during the pollen zones LG1 to LG4 (from 1.48 to 0.26 SD), while during the zone LG4 the DCCA values tend to be more stable (mean: 0.4 SD)(Figure 31).

The rarefaction analysis does not show a clear trend of change along the record (Figure 31), nevertheless several fluctuations are seen which include decreases (around 12,200 cal yr BP) and increases (~3800-2500 cal yr BP and during the last 1100 years) in its values in relation to the mean

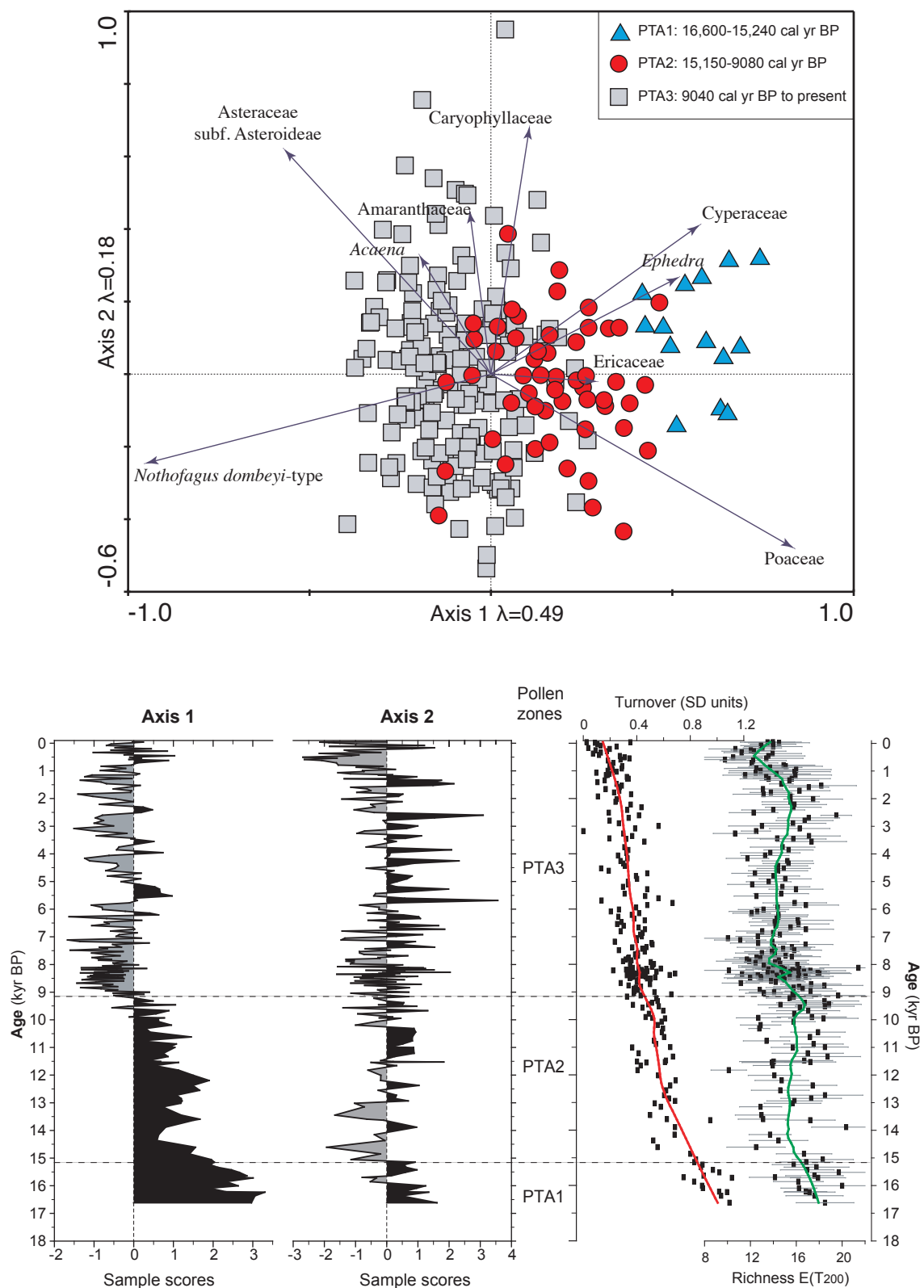


Figure 32. (Above) Biplot of Principal Component Analysis for the pollen record Potrok Aike, performed on a recalculated dataset containing only taxa >5%. The respective pollen zone for each sample is indicated. (Below) Sample scores for the Axis 1 and 2, plotted against age. Pollen zones are also indicated. Results for the DCCA (Turnover) and the palynological rarefaction analysis (Richness) performed on the pollen record. The estimated palynological richness is based on the minimum number of pollen taxa (Tn). The results are plotted against age. Pollen zones are indicated on the middle of the graph. In order to highlight the major trends in the palynological turnover and richness, a Loess smoother (solid lines) has been fitted to the raw data, utilizing a sampling span of 1.5 and rejecting the outliers.

4.2.2.4.4. Potrok Aike (Wille *et al.* 2007).

Laguna Potrok Aike (51°58' S, 70°23' W) is a Maar lake located on the Southernmost Patagonian plains, with a maximum diameter of 3470m and a catchment area of ~200 km² (Zolitschka *et al.* 2006)(Figure 12). The local vegetation comprises of the dry type of the Patagonian Steppe, with several graminoids as the dominant species (i.e. *Festuca gracillima*, *Poa* sp. and *Stipa* sp) accompanied by herbs (i.e. *Acaena* sp, *Adesmia* sp. *Colobanthus subulatus* and *Nardophyllum bryoides*) cushions (i.e. *Empetrum rubrum* and *Perezia recurvata*) and few bushes (*Berberis microphylla* and *Chiliodendron diffusum*).

The pollen record used in this thesis cover the last 16,600 years nevertheless, the complete sequence reaches 51,000 years (Kliem *et al.* 2012). The PCA results indicates that the two first axes captures 66.5% of the total variance, with Axis 1 comprising ~49% of the explained variance of and Axis 2 only 17.5% (Figure 32 & Table 8). Three main pollen zones were defined by means of cluster analysis (Appendix figure 16). The pollen zone PTA1 (16,600-15,240 cal yr BP) is characterized by shows positive values on the sample scores from both axes, in response to the dominance of graminoids (i.e. Poaceae, Cyperaceae) and cushions taxa (i.e. Ericaceae and *Ephedra*). This assemblage suggests the development of a dwarf-shrub steppe during this period. Later, during the pollen zone PTA2 (15.15-9.080 cal yr BP) the PCA Axis 1 shows a decrease in its values but does not reach negative values, in response to the increase of *Nothofagus dombeyi*-type on the pollen record and the decrease of cushions taxa (i.e. Ericaceae and *Ephedra*). Poaceae continues to dominate the pollen record and exhibiting high percentages as in the previous pollen zone (Appendix figure 16). The paleoecological implications for this period is the development of a steppe dominated by grasses, whereas the increases in the *Nothofagus dombeyi*-type pollen have been interpreted as a long distance signal from the ecosystems located to the west (e.g. Andean forest). Finally, during the last pollen zone PTA3 (9040 cal yr BP to present) the co-expansion of Asteraceae subf. Asteroideae and *Nothofagus dombeyi*-type, and the decrease in the percentages of Poaceae lead Axis 1 towards negative values. This change in the pollen record suggests the expansion of scrub and herbs into the grass steppe, leading to the development of a shrubby/herbaceous grassland. The changes experienced by the Andean taxa (i.e. *Nothofagus dombeyi*-type and *Misodendrum*) suggest that Andean forest reached its highest density at this time.

The DCCA indicates a total turnover of the sequence of 1.11 SD, occurring very gradually along the record, and without any significant shifts (Figure 32 & Table 8). On the other hand, the rarefaction analysis shows a stepwise decrease in its values at the beginning of each pollen zone. Thus, high relative values occur during the pollen zone PTA1 whereas during the pollen zone PTA3 the rarefaction analysis exhibits its lower values (Figure 32).

5. DISCUSSION

The one main objective of this thesis is to examine the transformations experienced by the plant communities along the west-east biogeographic gradient of Southern Patagonia during the postglacial, in order to better understand ecological thresholds and responses of distinctive ecosystems to climatic and non-climatic forcing over time and space. To achieve this aim, and provide a minimal framework to address the research questions, it was necessary to develop a number of steps, including: (i) a comprehensive pollen-rain study along the west-east gradient, in order to calibrate the fossil pollen records and understand the environmental variables explaining its variability, and (ii) a new pollen record from the Southern Patagonian Fjords (Tamar Lake) in order to make trans-Andean comparisons and reduce sampling bias.

Each one of these objectives are addressed, as follows: Firstly, in section 5.1 the results from the vegetation and modern pollen-rain surveys from the Southern Patagonian Fjords (section 5.1.1) and along the west-east gradient (section 5.1.3) are discussed, Subsequently, in section 5.2 the paleoenvironmental reconstruction of the Tamar Lake (TML) and its paleoecological and paleoclimatic implications at local scale are discussed. Finally, from the inferences discussed in the previous sections (sections 5.1 and 5.2), and from quantitative results from selected pollen records along the west-east gradient, paleoecological implications at regional scale are discussed in section 5.3.

5.1. Vegetation and modern pollen-rain

5.1.1. Vegetation and modern pollen-rain in the Southern Patagonian Fjords

Botanical and ecological studies of the plant communities occurring in the Southern Patagonian Fjords show are sparse in comparison with other ecosystems occurring in the region (Arroyo *et al.* 2005). Therefore, new information about botanical, ecological or environmental subjects regarding the ecosystems which form the so-called “Magellanic Moorland complex” (Godley 1960; Moore 1979), can be considered as a valuable contribution. In this thesis, vegetation surveys were performed in particular locations within the Fjords and neighboring areas (Figure 9). The results, based on the relative abundance of the main taxa and physiographic criteria, made it possible to identify at least four main plant communities and ten intra-community associations in the examined localities (see section 4.1.1). In order to facilitate the discussion and summarize the results, Figure 33 shows a general schema of distribution for the main plant communities observed in the examined areas. In addition, the most characteristic features of the physical environment where they occur are indicated.

5.1.1.1. Distribution of main plant communities within the Fjords (53°S)

As has been identified throughout this thesis and other studies (Pisano 1983; Roig *et al.* 1985), bogs and scrublands are the predominant plant communities in the western Andean region at 53°S. Their dominance on the landscape denotes the harsh environmental conditions present in the Southern Patagonian Fjords, characterized not by a hyper-humid and cold climate and waterlogged substrates. In addition, prevailing strong winds exert a severe desiccant effect and mechanical stress on the vegetation, which combined with high soil acidity and low supply of essential macro-nutrients seriously limit the development of the plants (Godley 1960; Holgate 1961; Pisano 1977; Moore 1979; Pisano 1983; Roig *et al.* 1985; Luebert and Plissock 2006; Kleinebecker 2007). On the other hand, the complex topography of the area, a result of tectonic

and glacial forces through time (Coronato *et al.* 2008; Glasser and Ghiglione 2009), restricts the development of plant communities. Nevertheless, the heterogeneity of the physical environment makes the development and coexistence of diverse and distinctive plant communities at local spatial scale possible. The findings in this thesis denote the noteworthy changes (in composition and physiognomy) which plant communities experience alongside the physical landscape. In other words, there is a close correlation between the development of certain plant communities and particular features of the physical environment (i.e. the slope, aspect and elevation). Below the most relevant patterns observed in the studied locations discussed.

The main characteristic of the phytogeography of the Southern Patagonian Fjords is the predominance of the bog communities within the “Magellanic Moorland complex” (Godley 1960; Moore 1979). In the studied locations, this plant community is characterized by the dominance of cushion species (e.g. *Donatia fascicularis*, *Bolax caespitosa*, *Astelia pumila*, *Oreobolus obtusangulus*, *Caltha dioneifolia* and *Drapetes muscosus*), which cover the soil surface and form a hard carpet. Field observations indicate that its presence and development is closely associated with the presence of very gentle slopes (<10°) and soils with poor drainage conditions or low permeability (Figure 33). This is also clearly observed in the vegetation mapping performed within the catchment of Tamar Lake (Figure 20, section 4.2.1), and represents a well-known feature discussed in previous studies (Pisano 1983; Roig *et al.* 1985). Other characteristics observed in the studied cushion-bog communities of the visited localities are the lack or low presence of mosses (e.g. *Sphagnum*) that characterize bogs communities (i.e. peat-bogs) occurring inland and to the east of the continent (Pisano 1983). The absence of peat-bogs within the Patagonian Fjords, or the segregation of cushion-bogs in western areas, has been interpreted as a result of the prevalent hyper-humid climatic conditions (Luebert and Plischoff 2006). Nevertheless, recent studies suggest that development and segregation of cushion-bog ecosystems in the western Andes (i.e. Fjords) are also linked to the effect of the sea spray (Kleinebecker 2007). As was previously mentioned, plant communities in western Andean areas are strongly limited by the low supply of essential macro-nutrients because of leaching due to high precipitation (Ruthsatz and Villagrán 1991). Based on geochemical analyses, Kleinebecker and collaborators (2007) suggest that input of base-cations (i.e. Ca, Mg, Na and K) to terrestrial ecosystems via sea spray can play a significant role in the nutrient cycling and trophic conditions of western ecosystems enhancing decomposition. The differences among the vegetation occurring in leeward and windward coastal areas have been identified by previous investigations performed in the region (Pisano 1977; Roig *et al.* 1985), but also in others coastal areas where climate and flora resembles Patagonia as is the case in New Zealand (Meurk *et al.* 1994; Martin and Ogden 2006), Canada (Gignac and Vitt 1990; Vitt *et al.* 1990), and the Isle of Anglesey (Goldsmith 1973). In all these locations, positive correlations between sea spray input and floristic changes have been established. Therefore, addressing the poor knowledge of biogeochemical cycles involved in the terrestrial ecosystems of the Southern Patagonian Fjords should be further investigated.

This thesis corroborates the close correlation between the development of bogs (*sensu lato*) and drainage conditions controlled mainly by the terrain slope, a pattern which is also well-described in previous studies (Pisano 1983; Roig *et al.* 1985; Kleinebecker 2007). Consequently, in the presence of good drainage conditions or moderate slopes (>10°) different species of sedges, dwarf-shrubs and trees find favorable conditions for growing. Although, the slope gradient explains the observed transition or replacement of cushion-bogs communities for communities dominated by woody elements (i.e. shrublands and forests), it does not explain the spatial segregation occurring between the different woody communities (i.e. closed/open shrublands and *Nothofagus betuloides*-*Drimys winteri*/*Nothofagus betuloides* dwarf forests) investigated (Figure 33).

The findings from this thesis suggest that the effect of wind plays an important role in the occurrence of different forest communities. *Nothofagus betuloides*-*Drimys winteri* forests are confined to wind-sheltered locations such as little valleys or depressions, while the *Nothofagus betuloides* dwarf forests occur in unprotected locations (Figure 33). This hypothesis is not only based on the remarkable morphological changes observed in the *Nothofagus betuloides* dwarf forests (i.e. opening in the canopies, the reduction of the height and deformation of branches and trunks), but also on observed changes in the floristic composition of these communities. Such as the replacement of tree species (as *Drimys winteri*) by more wind-tolerant shrub species (e.g. *Gaultheria* sp and *Desfontainia spinosa*). On the other hand, at mid elevations where more extreme slopes (20°-30°) occur, *Nothofagus betuloides* dwarf forests are replaced by an open shrubland community dominated by shrub (i.e. *Escallonia* and *Philesia magellanica*) and cushion species (i.e. *Empetrum rubrum*, *Bolax* and *Caltha*) (Figure 33). A distinctive characteristic of these shrublands is the presence of creeping *Nothofagus antarctica* individuals (krummholz), the only deciduous tree species occurring in the area forming dense patches near the mountain summits. Open shrubland communities dominate in areas with thin soils.

The results (see section 4.1.1) indicate significant differences, in floristic and physiognomic terms, between plant communities occurring near or along the coast and those occurring in higher elevations (Figure 33). More specifically, plant communities occurring in coastal areas (identified in this thesis as closed shrublands) show a high floristic and physiognomic diversity, features also identified by previous studies (Godley 1960; Holgate 1961; Pisano 1977; Moore 1979; Pisano 1983; Roig *et al.* 1985; Luebert and Pliscoff 2006). Additionally, high vegetation cover (>70%) and plant density (i.e. above-ground biomass) are appropriate features to typify this community. The dense shrublands growing in coastal areas are most likely defined by the supply of nutrients via sea spray and the wind-stress.

On the other hand, the vegetation occurring in upland areas is exposed to severe environmental conditions (i.e. high wind velocity and low temperatures). The plant communities identified in this thesis as Sub-Alpine or Montane, are the least studied ecosystems within the Southern Patagonian Fjords (Roig *et al.* 1985; Luebert and Pliscoff 2006). The findings from the thesis suggest that low biodiversity, vegetation cover (<20%) and above-ground biomass are encountered in these ecosystems characterized by cushion plants (e.g. *Bolax caespitosa*, *Phyllacne uliginosa* and *Oreobolus obrusangulus*; Figure 33). Additionally, the presence of unconsolidated and angular fragmentary rock material (regolith), indicates the occurrence of physical weathering processes (e.g. thermal stress or frost weathering) underlying the important role of temperature (Hall *et al.* 2002)(Figure 34).

Sub-Alpine and Montane vegetation are encountered at low elevations (e.g. 300 m.a.s.l.) in coastal areas of the Southern Patagonian Fjords (west), whilst at the same latitude (~53°S) east of the Andes are found at higher elevations (>900 m.a.s.l.; (Boelcke *et al.* 1985). Meteorological studies from Southern Patagonia show that summer temperatures decrease by ~0.6°C with every 100 m increase in elevation (Weischet 1985). Moreover, the mean annual temperature does not experience significant differences along the west-east gradient as found to occur with precipitation (Figure 6 & Figure 7). This is due to the strong oceanic influence on the climate and continental narrowing towards the pole (Coronato *et al.* 2008). Therefore, in order to explain the distribution of these ecosystems across Southern Patagonian, another parameter influencing temperatures should be invoked besides elevation.

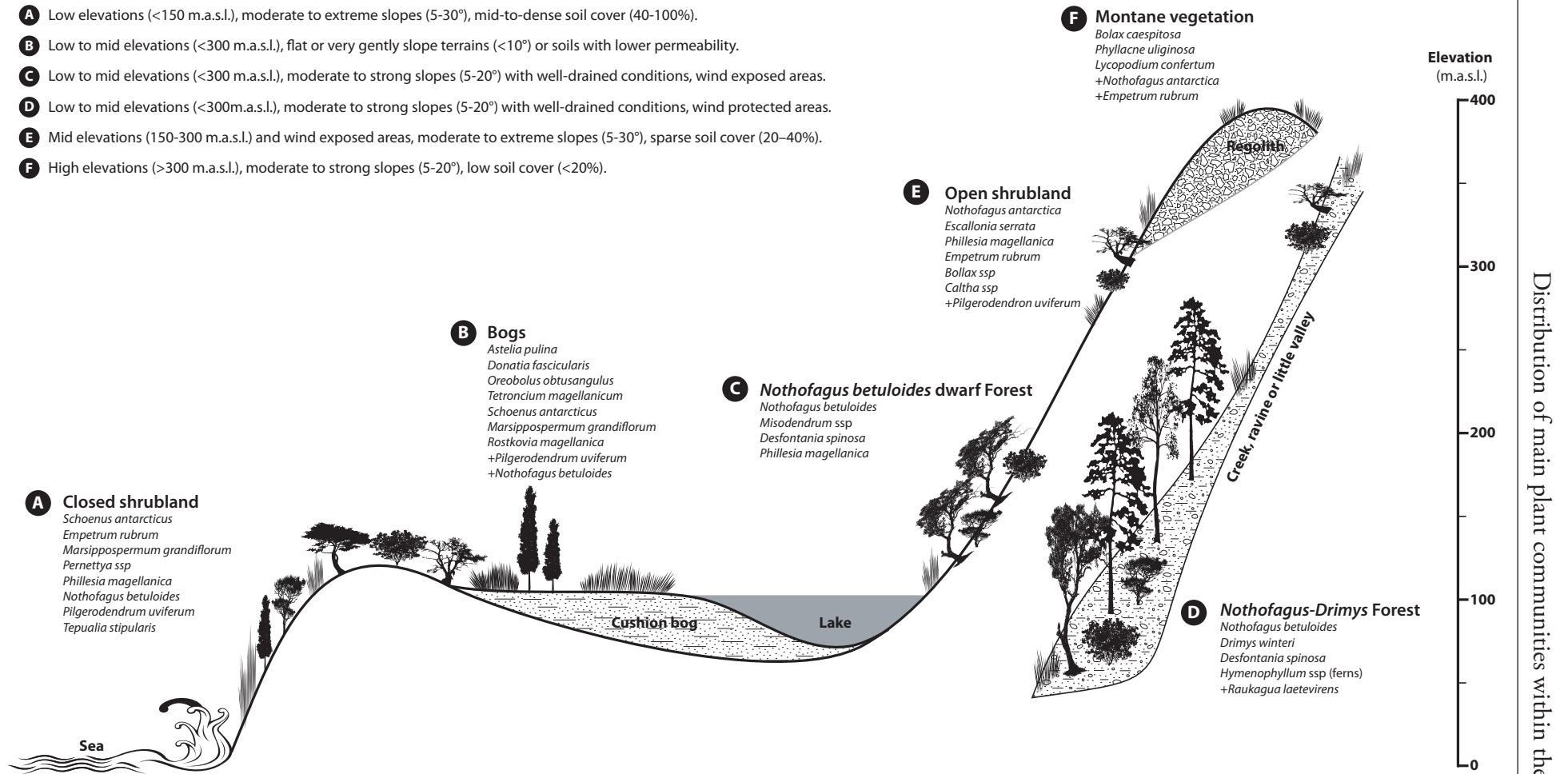


Figure 33. Schematic profile indicating the distribution of main plant communities identified and described in this thesis, as the most characteristic in the Southern Patagonia Fjords (53°S). For each plant community the most representative taxa is indicated, while rare taxa are marked with a “+”. Main characteristics of the physical environment where each plant community occurs are also indicated on the left upper corner of the figure.



Figure 34. Images from Sub-alpine environments present in the Southern Patagonian Fjords at 53°S. Left. General view of the vegetal landscape at ~300 m.a.s.l. Right. Detail of regolith formation in a wind exposed area at ~350 m.a.s.l. The red dashed line indicates the approximate elevation where sub-alpine environments take place. Both photographs from Chids Island (for location see figure 9)

Wind intensity increases with altitude, termed the wind speed gradient (Schroeder and Buck 1970)(Appendix figure 2). The effect of local topography affect wind patterns, as mountains and hills produce the lifting of winds along the Earth's surface, causing an increase in velocity as the wind crosses the ridge (i.e. summit). Therefore, at mountain summits the wind tends to be somewhat stronger than winds in flat areas (Schroeder and Buck 1970)(Appendix figure 2). Furthermore, meteorological studies indicate that strong winds prevent the development of a warm air surface layer leading to a reduction in mean air temperature (Weischet 1985; Schneider *et al.* 2003). In light of the above, the role of wind seems to be critical for the distribution of Sub-Alpine and Montane ecosystems in the Southern Patagonian Fjords, even in the absence of high mountains (e.g. >1000 m.a.s.l.; Figure 2 & Figure 9).

Changes in slope gradient are linked to changes in soil cover, (Holgate 1961; Pisano 1977; Roig *et al.* 1985; Gallart *et al.* 1994; Breuer *et al.* 2013a) showing a close correlation between slope processes (i.e. runoff and mass movement processes) and topography (i.e. slope and altitude; (Coronato *et al.* 2008). For example, in locations with steep slopes (>35°) the presence of soil and vegetation is low or practically absent, suggesting that erosive slope processes limit the establishment of vegetation. While, in flat and gently-sloping areas (0°-20°) located at low elevations soil production rates exceed the erosional rates.

The Southern Patagonian Fjords are characterized by glacial carved landscape with a trough-shape. Mass wasting events (e.g. landslides, snow avalanches, debris and mud flows) occur frequently in these landscapes. Moderate to steep slopes (20°-30°) allow the development of soils, while extremely steep slopes (>35°) can operate as failure zones triggered by strong rainfall or snowmelt episodes (Roig *et al.* 1985) or earthquakes (Breuer *et al.* 2013b). Recent studies indicate that mass movements events can also happen in the absence of an external trigger (climate or tectonic) in ecosystem dominated by bogs and peat, as is the case of Southern Patagonian Fjords (Dykes and Selkirk-Bell 2010). These events occur due to failures within the soil or mineral material below the surface.

Based on the previous observations, a simple conceptual model can be proposed to describe the transition from soil-mantled landscapes to bedrock-dominated landscapes in the Southern Patagonian Fjords. As indicated in Figure 35, the relation between slope and vegetation cover is far from linear, which transforms the mid elevations into locations with the potential to change from soil-dominated and bedrock-dominated areas in response to changes in the temperature, which would influence the ratio among the soil erosion and production rates (Figure 35). This hypothesis is backed up by observations of non-slope related changes in soil cover and the vegetation with elevation. For example, in flat and gentle areas located at mid to high elevations, the presence of thin soils and low soil cover together with a poor development of the vegetation (i.e. sub-alpine communities) indicate that soil erosion rates are higher than soil production rates. Erosion processes are not enhanced by the slope gradient in these locations, and so the most plausible explanation is that an increase in the erosion/production ratio is a consequence of limited soil production at low temperatures. On the contrary, the development of high soil cover and dense vegetation (i.e. closed shrublands) observed in extreme to steep slopes at low to mid elevations (Appendix figure 3), indicates that soil erosion rates are lower than soil production rates. In this case, the decrease in the soil erosion/production ratio is a result of enhanced soil production triggered by increase in temperature at low elevations. The increase in the vegetal cover can also reduce the soil erosion rates, and vice versa (i.e. open vegetation > soil exposure to the prevalent high rainfall and wind conditions > increase in the catchment erosion), suggesting a possible feedback between such parameters (Boelcke *et al.* 1985).

The ecological implications of mass wasting events in the dynamic of the plant communities present in the Southern Patagonian Fjords are practically unknown. In this thesis it has been possible to identify an early succession phase after a disturbance event, generated by a debris flow on a mature mixed Evergreen Forest in the area of Bahia Bahamondes (Appendix figure 4). The presence of a thick (~10 cm) sand and gravel layer covering the soil surface, together with large boulders and fallen trees, highlights the high energy involved in this mass wasting process which affected a relatively large area (~20.000 m²). The affected area was covered by even-aged *Nothofagus betuloides* saplings (~2 m height), a pioneer species capable of growing on open sites with inorganic soils (Pisano 1977; Boelcke *et al.* 1985; Armesto *et al.* 1992). The floor was covered by *Gunnera magellanica*, another typical species seen in primary succession stages, characterized by its symbiotic relationship with a nitrogen-fixing cyanobacteria (Boelcke *et al.* 1985; Osborne *et al.* 1991) (Appendix figure 4).

Forest communities mainly occur in wind-protected locations such as small valleys, which are usually affected by frequent active slope processes (Figure 36). Field observations indicate that presence of talus cones or areas where colluvium accumulates are ideal for the development of woody plant communities (e.g. forests), because they provide a substrate with adequate drainage conditions even for flat and gently sloped areas (Figure 36). The relevance of the colluvium accumulation on the vegetation development is clearly observed in areas where granitic and mylonitic rocks of the Patagonian Batholith outcrop (Appendix figure 3). In these locations, plant colonisation and pedogenesis only take place within wide and open fractures and in areas with a coarse clastic sedimentary substrate such as talus cones (Appendix figure 3; Breuer *et al.* 2013a). The reasons for the lack of plant cover on the granitoid rocks has not been investigated, but it has been proposed that soil formation and the primary stages of plant succession on bare rock surfaces are hampered by an immediate removal of the fine clastic material derived from rock weathering through rapid surface runoff and strong winds (Breuer *et al.* 2013a).

Distribution of main plant communities within the Fjords (53°S)

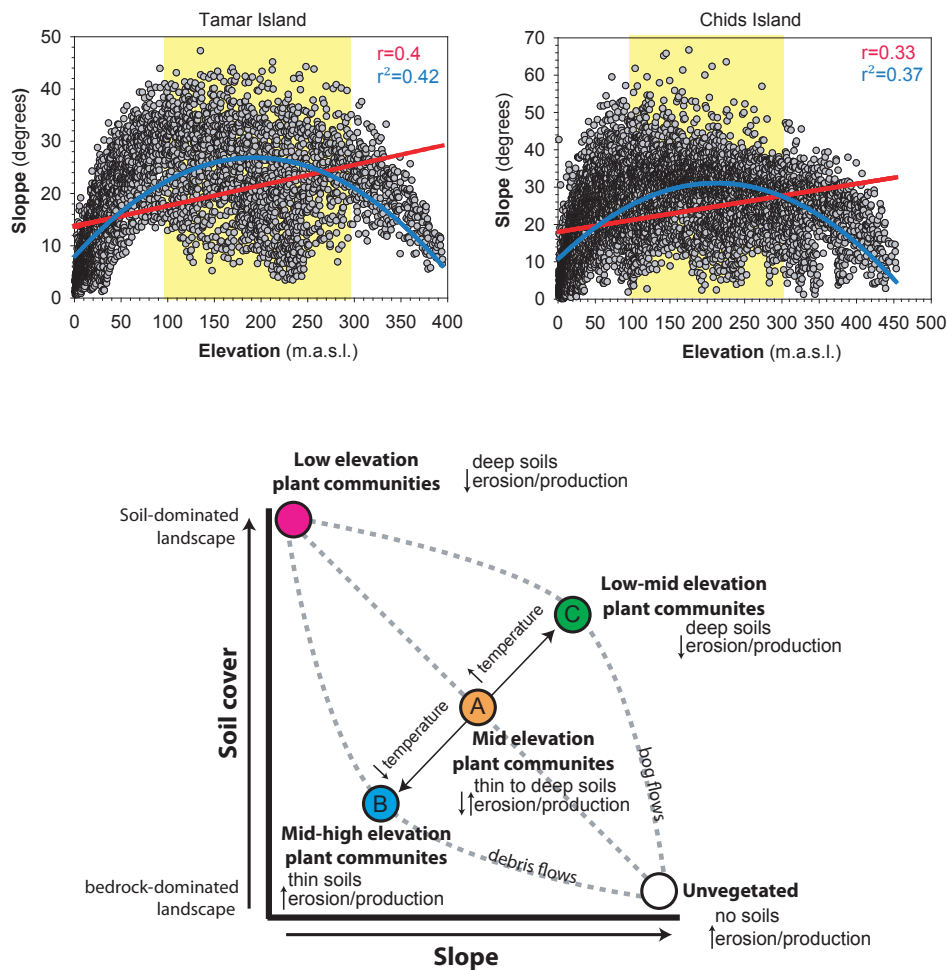


Figure 35. Above. Analysis of the correlation between elevation and slope parameters for two studied locations, Tamar Island and Chids Island (for location see Figure 9). The analysis was performed using GIS, utilizing a grid of 100 m extracted from a DEM (SRTM, 3 arc-sec resolution; 90m). The red line represents the linear regression, and the blue the best fit-curve (quadratic). The yellow bar indicates the mid-elevations. Below. Basic conceptual diagram indicating the main stages and mechanisms involved in the transition from soil-mantled landscapes to bedrock-dominated landscapes in the Southern Patagonian Fjords. For details see text.

Another process resulting into the erosion of soils and disturbance of vegetation observed in the visited areas is the natural process of cushion-bogs destruction. This process takes place in small ponds (<100 m²) located in areas with relatively gentle slopes (<10°), which disrupt the continuity of the vegetation, dominated by cushion-bogs and scrublands communities (Figure 37). It predominantly occurs on a scarp (knickpoint), the zone opposite to where sediments accumulate (Figure 37). In some cases plant communities representing different successional stages replace or invade the pond, suggesting that erosional process occurs at low rates. This observation also highlights the potential role of active slope processes in the regeneration dynamic of these ecosystems.

The processes discussed in this section highlight the complex interactions between the vegetation and environmental factors in the Southern Patagonian Fjords. In addition, it underlines the significant lack of knowledge about several issues on the ecology of these plant communities, the role of topography in the climate and geomorphologic process, and the underlying biogeochemical cycles.

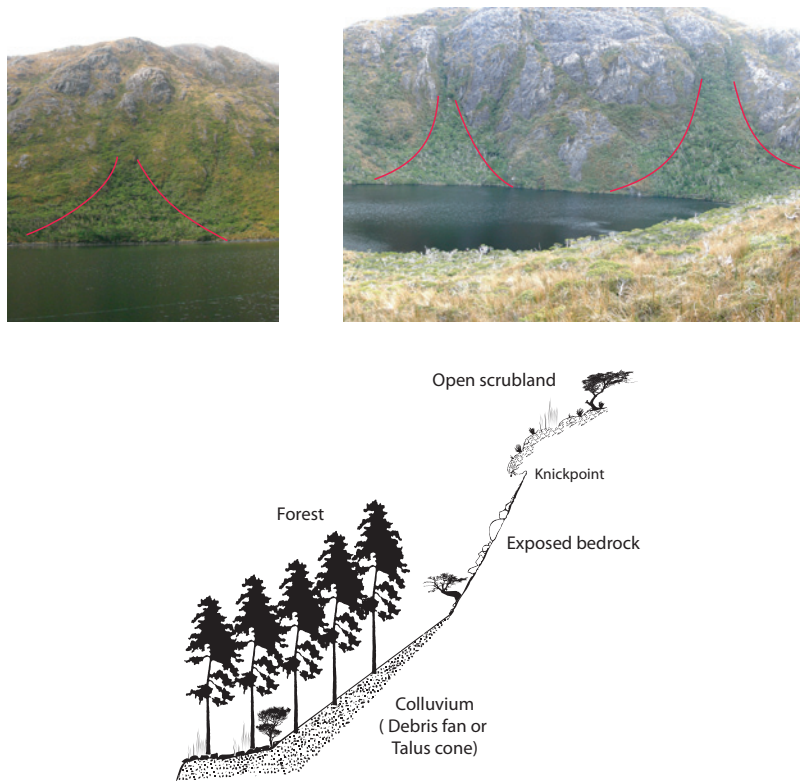


Figure 36. Observed geomorphological context where forest communities occur in the visited areas on the Southern Patagonian Fjords

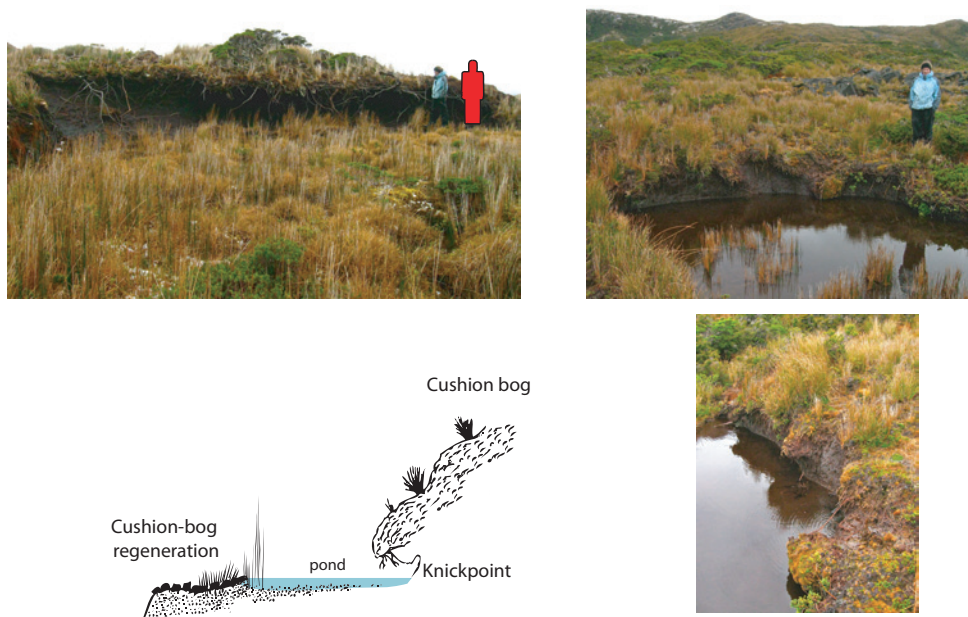


Figure 37. Process of natural destruction of cushion-bogs observed in the visited areas.

5.1.2. Modern pollen-rain within the Fjords and vicinity areas

This is the first comprehensive study of the modern vegetation and modern pollen rain in the Southern Patagonian Fjords (see section 4.1.1). The modern pollen spectra are representative of the distinctive taxa characterizing the different plant communities and correspond well to the described vegetation types (section 4.1.1; Figure 33). For instance, cushion-bogs communities are easily distinguished by the dominance of non-arboreal taxa (e.g. *Astelia pumila*, *Myrteola nummularia*, *Caltha* sp and Juncaceae+Juncaginaceae), whilst forest communities are characterized by arboreal and shrub taxa (e.g. *Drimys winteri*, *Misodendrum* and *Desfontainia spinosa*; Figure 33). Montane or sub-alpine communities have a high Apiaceae percentages, which can be used to distinguish them from shrublands communities characterized by Poaceae and Cyperaceae. Within shrublands communities the presence of *Gaultheria*, *Tepualia stipularis* and Ericaceae defines the closed-shrublands, while *Philesia magellanica* and Asteraceae subf. Asteroideae the open-shrublands (Figure 33). However, the presence of several “outliers-samples” in the cluster analysis and low variance (35.5%) exhibited by the first two PCA axes, highlight the highly heterogeneous nature of the dataset (Figure 14 & Figure 15). Moreover, the cluster analysis shows clearly that only the samples retrieved from forest communities are dissimilar (cluster A) from the all other plant communities (cluster B)(Figure 14). The trend is also observed in the PCA, which shows that samples retrieved from forest communities are located in the right side of the biplot together with tree taxa (*Misodendrum*>*Drimys winteri*>*Maytenus magellanica*>*Nothofagus dombeyi*-type). Whilst the rest of samples are located in the left side of the biplot where non-arboreal taxa are predominant (Cyperaceae>*Caltha*>*Astelia*>Juncaginaceae+Juncaceae>Apiaceae>*Myrteola nummularia*) (Figure 15). The comparison between the cluster and PCA results shows a similarity in the groups identified by both methods, with the samples from cluster A and B1 located to the right side of the biplot and the others (B2-B4) on the left side (Figure 14 & Figure 15). This because the algorithm utilized by PCA (Standardized Euclidean distance or chord distance) is analogous to that used by cluster analyses (Edward & Cavalli-Sforza’s chord distance method; (ter Braak and Prentice 1988; ter Braak and Šmilauer 2002). Therefore, the results from PCA and cluster analyses are comparable and can be summarized by PCA Axis 1 (Figure 38). These findings suggest that main differences between the samples are related to the relative amount of arboreal or non-arboreal taxa, resembling the outcomes from studies performed in areas with similar ecosystems (i.e. Finland, Norway and Alaska). In these studies the arboreal/non-arboreal index was employed in order to distinguish the ecosystem types (i.e. forest, woodland and tundra) and to examine landscape openness and patchiness (Ritchie 1974; Hicks 1977; Prentice 1978; Fægri and Iversen 1989).

In this thesis two different approaches were utilized to characterize and summarize the pollen-rain. The first comprises of a simple modification of the basic arboreal/non-arboreal index by grouping taxa into three categories (i.e. trees/scrubs+cushions/herbs+grasses; sensu Ellenberg and Mueller-Dombois 1967; Heusser 2003), Figure 13 & Figure 38). The second comprises the use of the PCA Axis 1 (sample scores; Figure 15 & Figure 38). These two approaches offer interesting insights into the representation of vegetation in the modern pollen-rain and landscape openness.

As illustrated in Figure 38, most of the samples are characterized by the dominance of tree taxa, mostly *Nothofagus* pollen present in all samples (even when the taxon is not physically present; Figure 13). Ecological studies have shown that most of the species present in the Southern Patagonia Fjords are pollinated by insects, which contrasts the wind-pollination of *Nothofagus* species (Smith-Ramirez and Armesto 1994; Aizen and Ezcurra 1998). Moreover, pollen production in wind-pollinated species is substantially higher than species pollinated by insects (Fægri and Iversen 1989). Therefore, the recorded high percentages of pollen *Nothofagus* in the modern pollen-rain suggest

an overrepresentation of this taxon in the pollen spectra, also noticed in previous studies (Mancini 1998; Prieto *et al.* 1998; Heusser 2003; Trivi *et al.* 2006; Mancini *et al.* 2012).

Samples retrieved from bog sites, record a non-local pollen signal related to the presence of surrounding scrub and forest communities, while bog pollen types are practically absent in pollen spectra from forested sites (Figure 13 & Figure 38).

Forest ecosystems combine the dominance of wind-pollinated plants (*i.e.* *Nothofagus*) which produce and disperse their pollen further and to a greater degree than insect-pollinated plants, and a canopy that probably impedes or limits the incorporation of pollen from the surrounding plant communities. Also, the dominance of soil over moss on the ground and active runoff processes because of the local geomorphological setting where closed ecosystems occur (little valleys and talus cones, see section 5.1.1) can increase the physicochemical corrosion in the pollen and spores, resulting in a subsequent over-representation of more resistant types. Based on the available information, the most susceptible palynomorphs to physicochemical corrosion are Cyperaceae and Juncaginaceae+Juncaceae, both dominant in open areas as bogs (Heusser 1971; Fægri and Iversen 1989). On contrary, open ecosystems (*i.e.* bogs) combine the presence of plant communities dominated by insect-pollinated plants and the absence of a canopy that impedes the incorporation of pollen from the surrounding plant communities. The result is a pollen assemblage containing a local and non-local pollen-signal.

Special attention is required on the discussion of data regarding to the samples from water-sediment interfaces (*i.e.* subaqueous depositional environment) studied in this thesis (Table 2 & Figure 11). As described in section 3.1.1), three undisturbed surface-sediment samples from two lakes (Lake Tamar and Lake Desolacion) and one small bay (Chids Bay) (Table 2 & Figure 11) were utilized to examine the modern pollen rain in aquatic depositional environments. This is the first study in Southern Patagonia which includes surface-sediment samples in the study of modern pollen-rain, providing a unique opportunity to examine and compare samples from different depositional environments.

The results suggest that pollen spectra from aquatic environments show a better representation of the different plant communities (Figure 13). This feature is clearly identified in the PCA biplot, where it is seen that aquatic (and shrubland) samples are located in the middle of the graph (Figure 15). This outcome suggests that shrublands samples include pollen originating from bogs, forest and montane plant communities.

The cluster analysis shows clearly the linkages between surface-sediment (*i.e.* aquatic) samples with the previously discussed groups, which characterize the main plant communities (Figure 14). Lake Tamar and Chids Bay samples are plotted together in the closed-scrubs group (cluster B1), whilst the Desolation Lake samples are into the bogs group (cluster B4). This pattern can be explained based on the main characteristics of the vegetation occurring in the respective sampling areas and the topography of each site. A main characteristic of the phytogeography of the Southern Patagonian Fjords is the coexistence in space of bogs and woody plant communities (“Magellanic Moorland complex” (Godley 1960; Moore 1979). Based on field observations, the woody plant communities (*i.e.* forests and shrublands) are found to be dominant on the Tamar and Chids Islands, rather than in the Desolacion Island where cushion-bogs are the main vegetation. This explains the observed differences between the samples and its segregation/grouping to woody and non-woody plant communities (*i.e.* scrubs vs bogs).

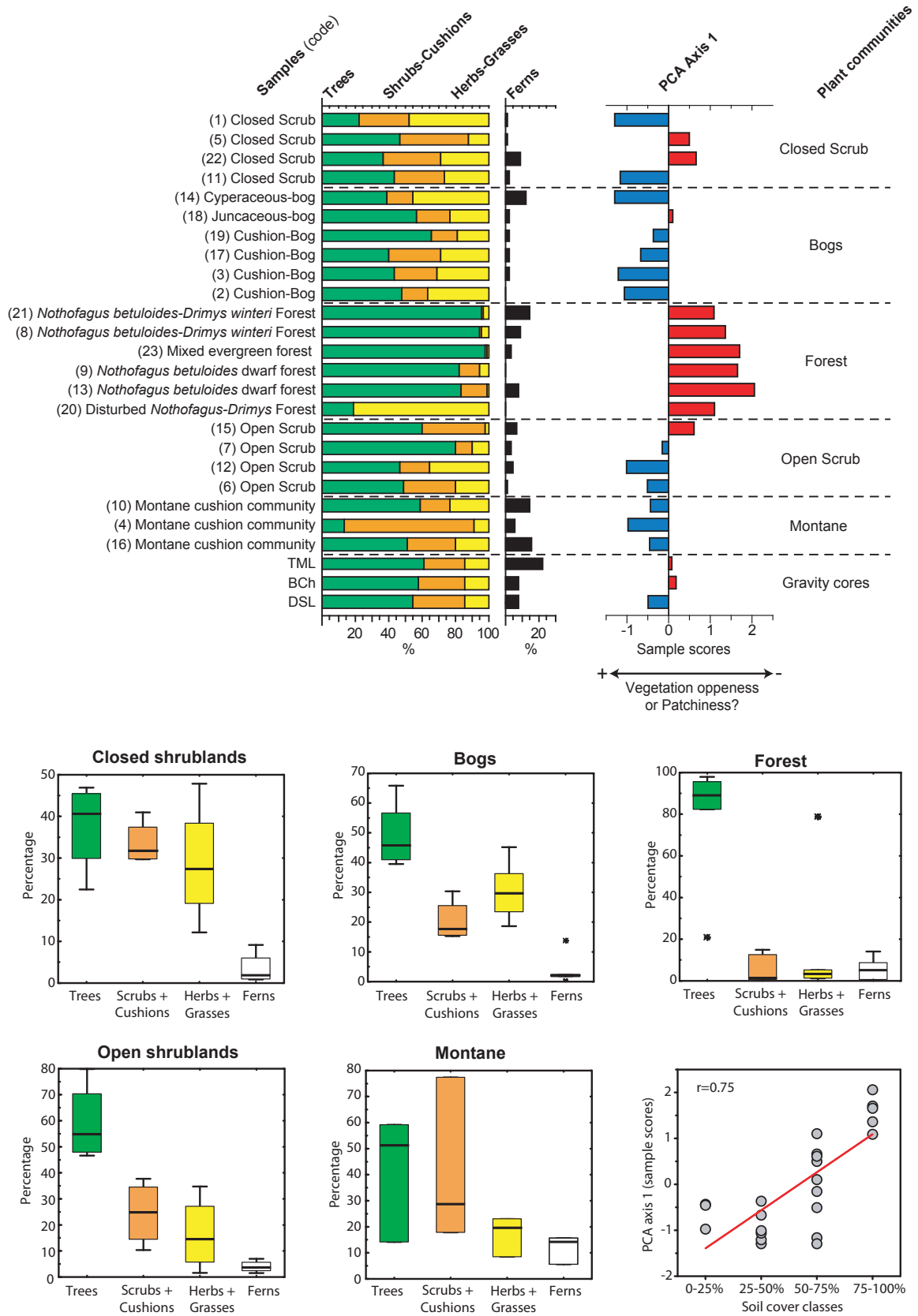


Figure 38. Above. Comparison between summary pollen diagram (left) and PCA Axis 1 (right) from the modern pollen-rain samples retrieved in the Fjords and vicinity areas. Below. Boxplots for percentages corresponding to the different plant communities identified and studied, and linear regression between PCA Axis 1 and soil cover classes. The box encloses the middle half of the data between the first and third quartiles. The central line denotes the value of the median. The horizontal line extending from the top and bottom of the box indicates the range of typical data values. Outliers are displayed as “o” for outside values and “*” for far outside values

Lake Tamar and Bay Chids⁹ are surrounded by a relative large and well-vegetated catchment (64.8 ha and 249.8 ha, respectively), whereas the Lake Desolacion catchment is considerably smaller (26 ha), flatter and less-vegetated. Following the observations provided by studies which examine the role of catchment characteristics in the pollen signal (Jacobson Jr and Bradshaw 1981; Fægri and Iversen 1989), it is expected that the mechanisms involved in the resulting pollen-signal in Tamar and Chids include a combination of pollen transferred by surface runoff and atmospheric precipitation. However, at Desolacion probably the most important input of pollen is by fall-out rather than slope-wash.

In conclusion, a positive correlation is observable between the parameter of soil (i.e. vegetation) cover and the PCA Axis 1, suggesting the feasibility to examine changes in the physical characteristics of the vegetal landscape, such as openness and patchiness, using pollen records.

5.1.3. Modern pollen-rain and vegetation at regional scale (53°S)

The development of a first general overview about the modern pollen-rain along the broad west-east vegetational and climatic gradient of Southern Patagonia, completes the second objective of this thesis. Therefore, results from the modern pollen-rain performed in the Fjords and neighboring areas (discussed in section 5.1.2) were merged with surface samples from the continent (Schäbitz *et al.* 2013; Figure 10 & Table 3). For each sampling location (local or surrounding vegetation, geomorphological characteristics of the area) is described, providing the opportunity to discuss in more detail some aspects regarding the representation of local vegetation in the pollen-signal across different ecosystems in S. Patagonia. Therefore, in order to provide an original contribution to the understanding of the modern pollen-rain along a broad bioclimatic gradient, the most relevant results regarding to the representation of the main plant formations in the pollen-rain are discussed subsequently. Following this, the main features related to disturbance, long-distance and upland pollen transport the correlation of the variance in the pollen assemblages and selected climatic/geographic variables are discussed.

Based on multivariate analyses (i.e cluster and PCA; Figure 16 & Figure 17) four main groups characterizing the main plant formations can be distinguished: (i) the magellanic moorland, (ii) the evergreen and deciduous forests, and (iii) the Patagonian steppe. Additionally, a group associated with the forest-steppe ecotone is identified (Figure 16). The correspondence between pollen groups and vegetation (at the floristic level), is also found in the physiognomic composition (i.e. trees/scrubs+cushions/herbs+grasses) of these pollen groups (Figure 16).

Pollen assemblages characterizing the Patagonian Steppe ecosystems (Figure 16; group 1) reveal high relative pollen percentages of grasses and herbs (i.e. Poaceae, Asteraceae subf. Cichorioideae, Caryophyllaceae, Brassicaceae, *Acaena*), whereas forest dominated ecosystems (Figure 16, Group 4) show high arboreal pollen percentages (i.e. *Nothofagus dombeyi*-type, *Drimys winteri*, *Misodendrum*). Likewise, pollen samples characterizing Magellanic Moorland ecosystems (Figure 16; Group 3) show the co-dominance of graminoids (Juncaginaceae+Juncaceae, Cyperaceae) and shrubs/cushion taxa (i.e. *Astelia pumila* and *Donatia fascicularis*), whereas pollen assemblages from the forest-steppe ecotone (Figure 16; group 2) exhibit a co-dominance of trees (i.e. *Nothofagus dombeyi*-type) and grasses (i.e. Poaceae) and are accompanied by pollen from exotic taxa (i.e. *Rumex*).

The findings above are in line with previous studies (Heusser 1995b; Mancini 1998; Prieto *et al.* 1998; Trivi *et al.* 2006; Schäbitz *et al.* 2013) and confirm the feasibility of using the pollen proxy to identify the main plant formations present in Southern Patagonia. The PCA Axis 1 indicates

⁹ Chids Bay is a well-isolated bay from marine currents, feature that can explain why its pollen assemblage closely resembles with the Tamar Lake.

important changes in floristic composition of the surface pollen samples in relation to its geographic location, namely west or the east of the Andes. This pattern follows the denominated biogeographic subregions, which distinguish a Subantarctic (west) and a Patagonian (east) domain (Morrone 2001; Coronato *et al.* 2008), and indicates an ancient biogeographic history of the region which is related to the progressive uplift of Patagonian Andean during the Neogene, and the subsequent develop of the rain-shadow effect (Hinojosa and Villagrán 1997; Villagrán and Hinojosa 2005; Ortiz-Jaureguizar and Cladera 2006).

In southern Patagonia, disturbed vegetal landscapes are generally related to anthropogenic impact produced by the activity of European settlers in the region during the last century, and associated with the logging and burning of the forest masses and cattle overgrazing (Martinic 1974; Boelcke *et al.* 1985). In this context, the presence of *Rumex acetosella* (an introduced plant during the 19th century from Europe) in the pollen records has been largely utilized as a palynostratigraphic marker to estimate the arrival of European settlers in the region (Veblen and Markgraf 1988; Heusser 2003; Huber and Markgraf 2003a; Moreno *et al.* 2009a). Recent studies in areas affected by fire indicate its presence in early successional stages, suggesting that high percentages of this taxon can be interpreted as an indicator of a recently disturbed landscape (Vidal and Reif 2011). In the modern pollen-rain dataset analyzed (Figure 16) in this thesis, two samples with relatively high values of *Rumex acetosella* occur in the forest-steppe ecotone group (cluster 2b) which today is the area most severally disturbed in Southern Patagonia (Pisano 1977; Boelcke *et al.* 1985). The presence of relatively high values of *Empetrum rubrum* pollen in one of the samples (sample k) is significant, and is also observed in samples retrieved from the Patagonian steppe ecosystems which are severely disturbed and affected by overgrazing (subgroup 1c, Figure 16). Little is known about native plants associated with disturbed landscapes in the region, nevertheless ecological studies indicate an increase in the *Empetrum rubrum* cover in sectors where the soil litter was removed by grazing or aeolian erosion (Pisano 1977; Boelcke *et al.* 1985; Collantes *et al.* 1989; Quintana 2009). Therefore, this taxon can be used as a disturbance indicator (e.g. Puerto del Hambre, Figure 3. Heusser 1995b; McCulloch and Davies 2001).

The pollen surface sample retrieved from Bahia Bahamondes (Figure 9) records relatively high values of *Gunnera magellanica* pollen, which is in line with the abundant presence of *Gunnera magellanica* in the surveyed area (Appendix figure 4). Physiological and ecological studies indicate the presence of symbiotic relationships with a nitrogen-fixing cyanobacteria in many *Gunnera* species (Boelcke *et al.* 1985; Osborne *et al.* 1991). This feature can explain the ability of *Gunnera magellanica* to colonize open ground at primary succession stages, and is also a feature observed in the pollen records from Gran Campo Nevado and Lake Ballena, located at the hyper-humid western Patagonia (Figure 3). Both pollen records show an abrupt vegetation change characterized by an important increase of *Gunnera magellanica* pollen and decrease of moorland elements after the deposition of Mount Burney tephra (MB2) (Fesq-Martin *et al.* 2004; Kilian *et al.* 2006; Fontana and Bennett 2012). The evidence suggests that increase of *Gunnera magellanica* pollen indicates ecosystems in an early successional stage.

The results from the modern pollen-rain in this thesis indicate high percentages of *Misodendrum* occurring mostly in *Nothofagus betuloides* dwarf-forests (subgroup 4c; Figure 16). Field observations are in line with this finding. *Misodendrum* is a hemiparasitic plant encountered in forest stands located in wind-exposed areas (i.e. *Nothofagus betuloides* dwarf forests and open shrublands; (Pisano 1977; Boelcke *et al.* 1985). Studies on the ecology of *Misodendrum* indicate that thin and young branches are more susceptible to be infected (Tercero-Bucardo and Kitzberger 2004), whilst the increase in light availability by the openness of the canopy benefits the mistletoe

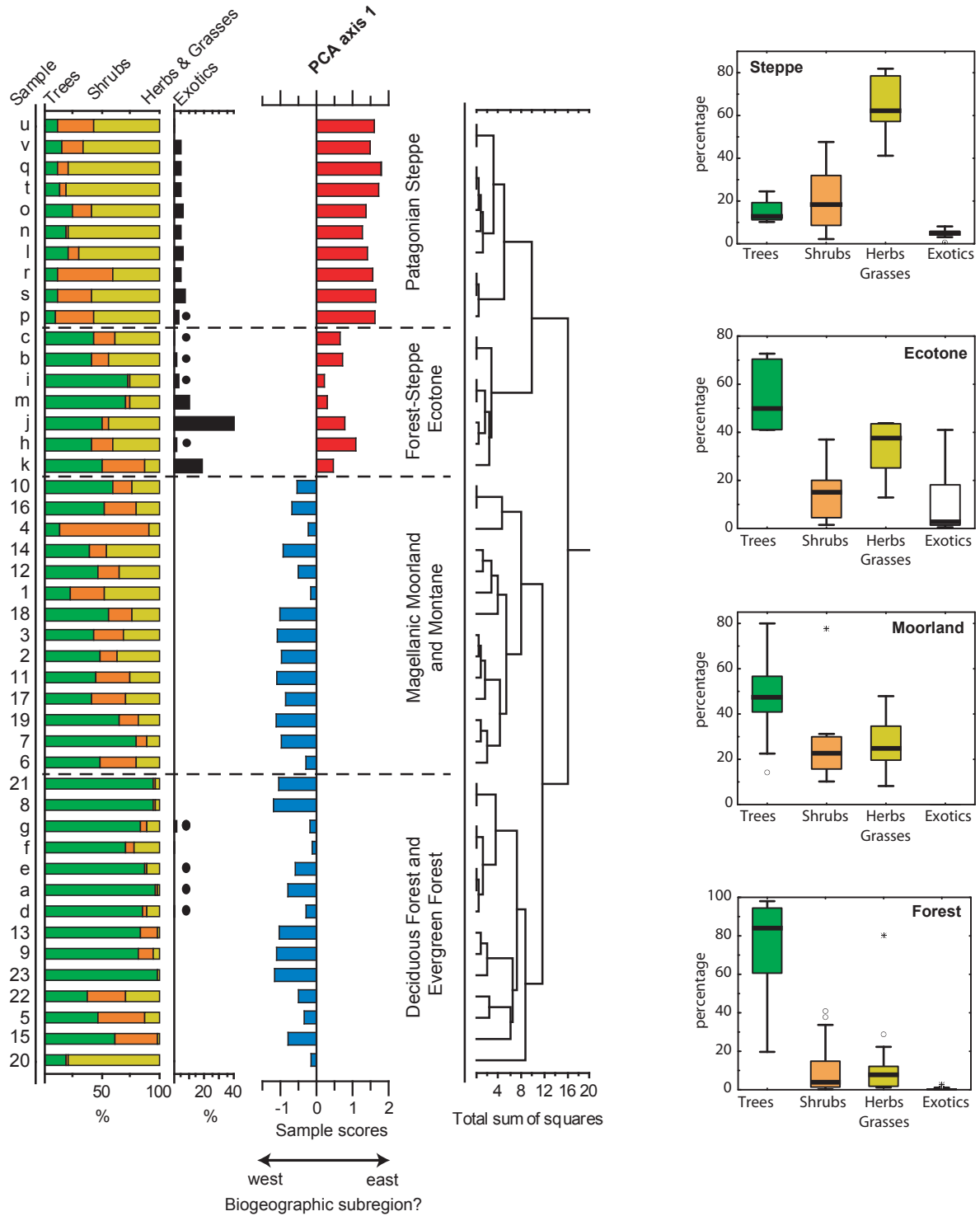


Figure 39. Left. Comparison between summary pollen diagram, PCA Axis 1 and cluster analyses. Right. Boxplots of percentages for the main plant formations studied in this thesis located along the west-east transect. The box encloses the middle half of the data between the first and third quartiles. The central line denotes the value of the median. The horizontal line extending from the top and bottom of the box indicates the range of typical data values. Outliers are displayed as “o” for outside values and “*” for far outside values

aerial shoot production (Soler *et al.* 2013). Seed dispersion of *Misodendrum* (anemochory) is also benefited by strong winds which increase the efficiency of ballistic process (Tercero-Bucardo and Kitzberger 2004). Therefore, and based on previous observations, it is possible to argue for a positive correlation between the degree of infection by *Misodendrum* affecting open forest stands and the severity of the winds. This premise has an important paleoecological implication which will be discussed with more detail later.

Upland and long-distance pollen transport is an important feature which must be taken into account in palynological studies (Fægri and Iversen 1989). In this thesis, this is critical for interpreting the modern pollen-rain of *Nothofagus dombeyi*-type (a wind-pollinated plant with high pollen production, Smith-Ramirez and Armesto 1994; Aizen and Ezcurra 1998). These features contribute to the overrepresentation of this taxon in the modern pollen-rain, resulting in the presence *Nothofagus dombeyi*-type pollen in areas where the taxon is absent, such as the steppe and montane environments (cluster 1 and 3a, respectively; Figure 16).

Based on the values of *Nothofagus dombeyi*-type pollen occurring in the samples from the Patagonian Steppe (Figure 16), it is postulated that values $\leq 20\%$ are not indicative of the presence of *Nothofagus* individuals growing in-situ. Previous studies have also identified the long-distance transport of pollen grains of *Nothofagus dombeyi*-type along the west-east axis (Markgraf *et al.* 1981; Heusser 1995b; Mancini 1998; Prieto *et al.* 1998; Haberle and Bennett 2001; Trivi *et al.* 2006). The modern pollen rain spectra indicate that upland transport of *Nothofagus dombeyi*-type pollen to montane locations in the Fjords is high ($\sim 55\%$; Figure 13).

5.1.4. Pollen assemblages and environmental variables

Canonical analysis (RDA; Figure 18) was performed to modern pollen samples in order to examine the correlation between the variability of pollen assemblages and selected environmental parameters. The results of the analysis show that 46% of the total pollen variance can be explained by the climatic/geographic variables analysed (Table 5). Of the analyzed variables only two are found to be statistically significant the Pann and Tann (Table 6 & Figure 18). The analysis also indicated a high co-linearity between climatic and topographic variables, corroborating the well-known pattern of changes in precipitation along the longitude gradient and in temperature with elevation. Due to this high co-linearity, topographical variables were excluded from successive analysis.

The RDA biplot (Figure 18) shows that the distribution of pollen samples along Axis 1 reproduces the main west-to-east vegetation gradient occurring in the region (Figure 8), and is strongly correlated with annual precipitation (Pann). Meanwhile, the sample distribution along Axis 2 reveals a vegetation gradient occurring with elevation which correlates with mean annual temperature (Figure 18). These results are in agreement with ecological and phytosociological studies performed in the region which identify the precipitation and temperatures as the main environmental factors controlling plant distribution on a regional scale (Schmithüsen 1956; Oberdorfer 1960; Pisano 1977; Boelcke *et al.* 1985; Gajardo 1994).

Based on the underlying climatic signal present on the variation of the pollen assemblages as identified by the RDA, it can be argued that modern pollen can be used to reconstruct the climatic variables of Pann and Tann. Studies undertaken in the tundra-taiga transition in Siberia and the forest-steppe transition in the Tibet made similar findings across wide and strong environmental gradients (Wei *et al.* 2011; Klemm *et al.* 2013).

5.2. Examining the postglacial history of the Southern Patagonian Fjords at 53°S

The deglaciation in the Southern Patagonian Fjords is poorly understood, but it is assumed that the Southern Patagonian Fjords were fully covered by ice during the Last Glacial Maximum (LGM; Coronato *et al.* 2008). Abundant deposits of clastic layers or Ice Rafted Debris (IRDs) between ~30,000 and 18,000 cal yr BP in the marine core MD07-3128 indicate that glaciers reached the continental slope during the LGM (Figure 40; Caniupán *et al.* 2011). Moreover, the abrupt cessation of IRDs deposition is found to coincide with an increase in reconstructed Sea Surface Temperatures (SSTs) from the same core (MD07-3128) ~18,000 cal yr BP (Caniupán *et al.* 2011). Computational models which reconstruct the Patagonian Ice Sheet (PIS) extension during the LGM and the subsequent deglaciation, project a fast ice retreat pattern and reduction in the ice volume (~50% in 300 years and ~80% in 2000 years) as a consequence of the abrupt increase in temperatures since the last termination¹⁰ (Hulton *et al.* 2002).

Geomorphological studies from the Seno Skyring (located to the east of the study area, Figure 40) and the Strait of Magellan partially support the estimations of these models, as glaciers located in these areas lost around 84% to 55% of their length between 17,500-14,500 cal yr BP, respectively (McCulloch *et al.* 2005; Kilian *et al.* 2007b). On the other hand, the deglaciation process was not continuous and a renewal in the glacial activity (i.e. glacier re-advances or standstill in the ice-retreat patterns) was observed in several locations along Southern Patagonia between 14,500-11,500 cal yr BP (McCulloch *et al.* 2005; Kilian *et al.* 2007b; Moreno *et al.* 2009b; Strelin *et al.* 2011). This is also indicated by the SSTs reconstruction from the MD07-3128 core (Figure 41), which show a plateau between ~15,000-12,500 cal yr BP which interrupts the warming trend starting at ~18,000 cal yr BP and peaks into the pronounced early Holocene warming period (Caniupán *et al.* 2011).

Furthermore, the last glacial interglacial transition (LGIT) in Southern Patagonia is in good agreement with the climatic history of west Antarctica, which is registered in several ice cores (WAIS Divide Project Members 2013). Included in this is the initial warm pulse at 18,000 cal yr BP, an interruption in the warming trend at 14,500-12,900 cal yr BP identified as the Antarctic Cold Reversal (ACR), and a further warm period during early Holocene (Figure 41). The Antarctic signature found in the climate of Patagonia highlights the relevance of Southern Patagonia as a key area to perform paleoclimatic studies, particularly when addressing questions regarding the character (magnitude, timing and direction) of the changes related to possible interhemispheric teleconnections and the mechanisms involved.

Geomorphological data from the studied area suggest that glaciers during the LGM were connected to the Gran Campo Nevado (GCN) ice cap, a remnant of the PIS, located to the west of the studied area (Figure 40). The presence of inorganic basal clays with an andesitic composition, observed in neighboring marine cores, was attributed to a high load of glacial sediments (Kilian *et al.* 2007b). The ages of the transition from inorganic basal clays to more organic marine sediments registered in marine records in the Fjord area suggests that ice retreat occurs in a west to east direction (towards the GCN ice cap; Figure 40).

Lake Tamar (TML) is the only available record from this area and offers a unique opportunity to examine the glacial-interglacial transition from a terrestrial environment. The most significant lithological change in the TML core corresponds to an interruption in the deposition of the basal unit (lithological Section 1). Section 1 comprises gray-clays with interleaved sand layers (rhythmites)

¹⁰ The reported ages from Southern Patagonia for the ice retreat from the LGM limits (18,300-17,600 cal yr BP) (McCulloch *et al.* 2005; Kilian *et al.* 2007b), are in general similar to the chronology observed in Northern Patagonia (17,800 cal yr BP; Denton *et al.* 1999) and denotes a synchronous pattern in the beginning of deglaciation of the PIS during the LGM (Denton *et al.* 1999; McCulloch *et al.* 2000). This similar timing for the deglaciation patterns observed in Patagonia (*sensu lato*) resemble chronologically also with global trends for the LGM termination, and together denotes a global rising temperatures since this period (Schaefer *et al.* 2006).

and ends with the sedimentation of dark and organic lake sediments, which dominate toward the top of the core (Figure 21, Figure 22 & Figure 41). The transition can be interpreted as a shift from a sedimentary environment under the direct influence of glacial or periglacial processes to one less influenced by them, and its age of 16,000 cal yr BP indicates the minimum age of ice retreat in the area (Figure 40). This finding is in agreement with the data obtained from neighbouring Cabo Pilar (~50 km; Figure 40), which also shows a sharp transition from light-gray glacial clays to dark-brown organic sediments dated at 16,300 cal yr BP (Wagner 2007). In light of the above, it can be concluded that the northern the Magellan Strait was ice-free around 16,000 cal yr BP.

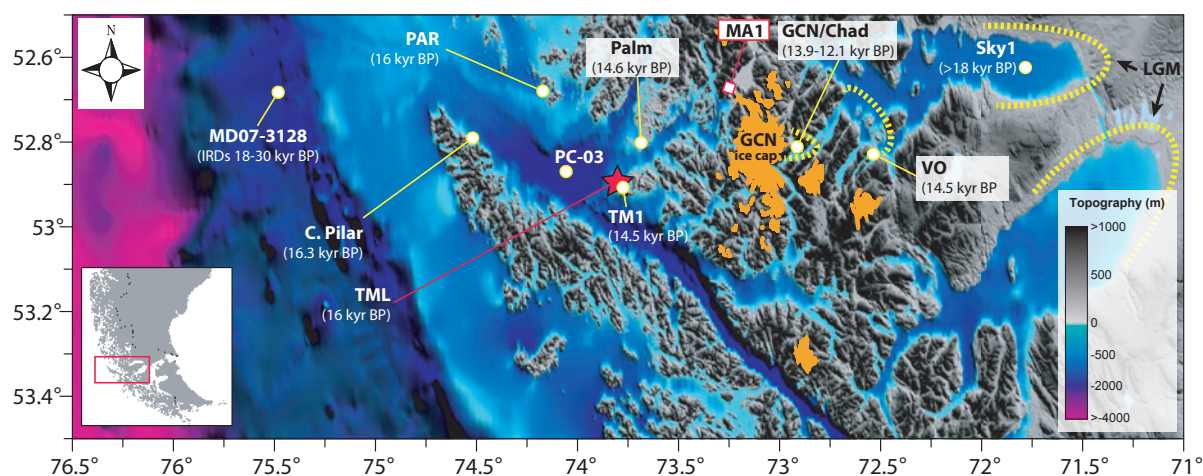


Figure 40. Map of the study area at 53°S indicating the locations of paleoenvironmental proxies discussed in the text. The star shows the location of Tamar Island and TML core. Glaciers are marked in orange and inferred ice limits in yellow. Minimum ages corresponding to ice retreat are also provided.

The late glacial section of the Tamar Lake sequence allows to understand processes occurring in the terrestrial ecosystems of the Southern Patagonian Fjords at 53°S during this important environmental transition. The transition from the basal glacial unit (lithological section I; >16,000 cal yr BP) to the organic lacustrine sediments (Gyttja; lithological sections III-I; from 12,800 cal yr BP to the present) mark a shift from a sedimentary environment glacial or periglacial processes to one which is less influenced by them. This lithological transition is gradual (lithological section II; 16,000-12,800 cal yr BP) and is characterized by the presence of fine laminated sediments from light-gray silty clay to light-brown silty Gyttja (Figure 21, Figure 22 & Figure 41). The gray-scale shows a gradual decrease in its values through the lithological Section II and part of the lithological Section III (until ~10,800 cal yr BP). A similar trend is observed in the C/N ratio, which shows a gradual increase after 16,000 cal yr BP and peaks at ~10,800 cal yr BP (Figure 22 & Figure 41). However, other geochemical parameters such as the dry bulk density (DBD) and organic carbon (Corg) change abruptly at ~16,000 cal yr BP and show a plateau between 16,000 and 12,800 cal yr BP (Figure 22 & Figure 41). These differences in the trends of change suggest that different proxies capture different environmental signals from the Tamar catchment.

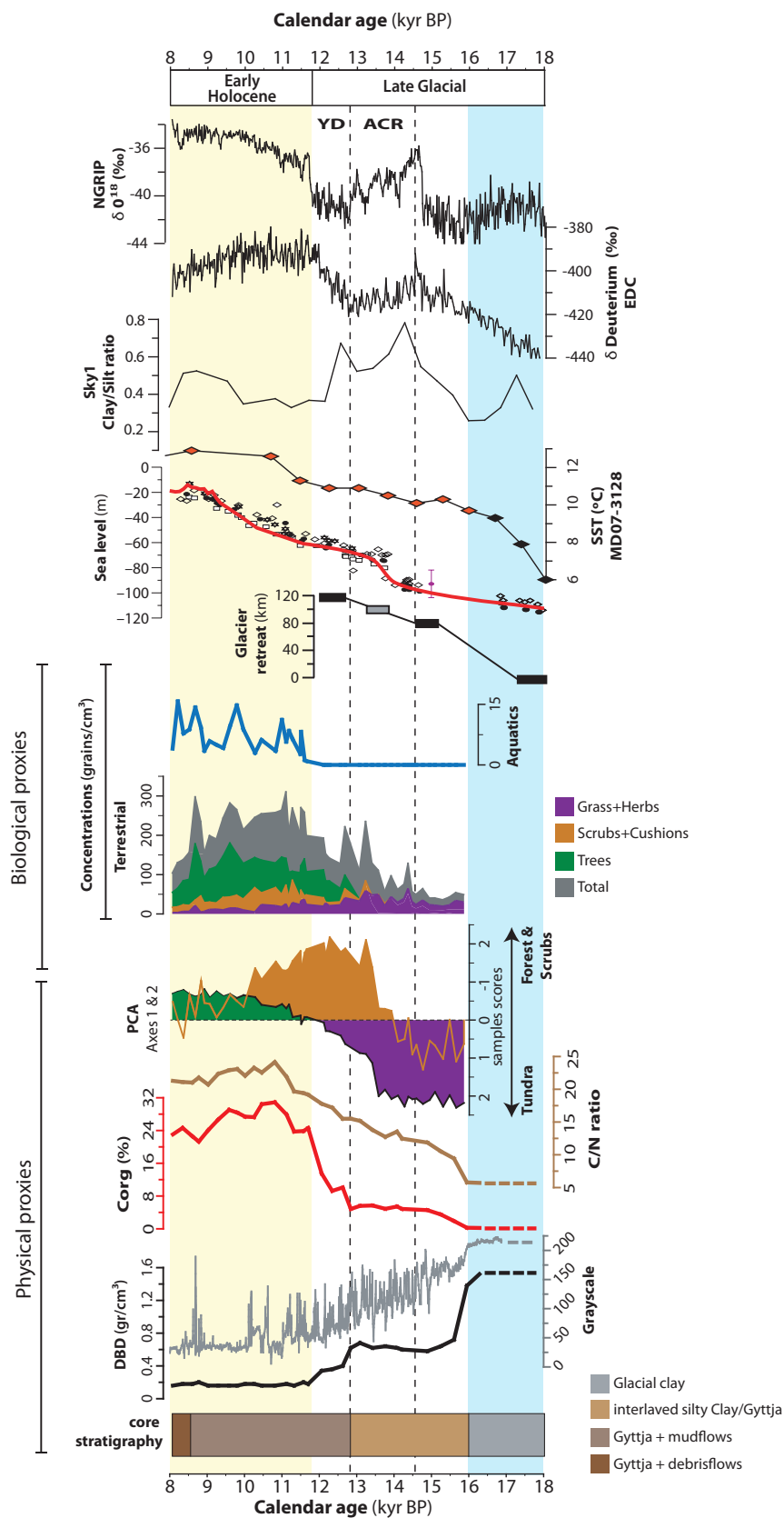


Figure 41. Summary figure for main geochemical and palynological results from the TML core, and selected paleoclimatic proxies

Palynological analyses (see section 4.2.2.2) indicate that the first pollen grains and other palynomorphs appear immediately at the beginning of deposition of organic sediments at ~16,000 cal yr BP, suggesting that the Tamar Lake (i.e. catchment) permitted plant establishment at this time. Hence the sterility¹¹ of the samples from the glacial unit of the TML core may not provide proof for proposing the absence of vegetation within the Tamar catchment or surrounding areas previous to 16,000 cal yr BP.

The pollen diagram from Tamar Lake shows that the basal pollen assemblage (pollen zone TML1: 16,000-13,600 cal yr BP) is dominated by grasses and herbs (e.g. *Caltha*, *Gunnera magellanica* and Poaceae) complemented by some scrub and cushions taxa (e.g. Asteraceae subf. Asteroideae and *Empetrum rubrum*). This assemblage indicates the development of a tundra-like plant community similar to that observed in recently deglaciated areas (Dollenz 1991; Moore and Pisano 1997; Dominguez *et al.* 1999; Dollenz *et al.* 2012). Additionally, low pollen concentrations present in this assemblage suggest a low vegetation cover (Figure 27 & Figure 41), in line with poorly developed soils observed in periglacial and recently deglaciated areas (Dollenz 1991; Moore and Pisano 1997; Dominguez *et al.* 1999; Dollenz *et al.* 2012). Following this, the observed shift in the PCA axes at 13,600 cal yr BP reflects the increase in *Nothofagus dombeyi*-type percentages (Axis 1) and in scrub-cushion plant percentages (Axis 2; e.g. *Escallonia*, *Donatia fascicularis*, and *Phyllacne uliginosa*; Figure 26 & Figure 41). This shift indicates the beginning of a transition towards a landscape co-dominated by bogs and scrubs communities. A gradual but sustained increase in the total pollen concentrations in the pollen zone TML2a (13,600-11,600 cal yr BP), indicates a significant increase in the vegetation cover within the catchment (Figure 41).

The geochemical and palynological findings from the Tamar Lake core suggest that deglaciation at the study area and in its vicinity occurred at ~16,000 cal yr BP, which coincides with the period of rapid and massive retreat of glaciers from the Seno Skyring (>80% length between 18,000-15,000 cal yr BP), and the abrupt increase in the reconstructed SSTs from the MD07-3128 core (Kilian *et al.* 2007b; Caniupán *et al.* 2011; Figure 41). In the Tamar Lake catchment, grass and herbs dominated until 13,600 cal yr BP, when the expansion of woody plant communities (e.g. *Nothofagus*) started (Figure 41).

The change in the vegetation takes place during a period of significant environmental change in the study area, characterized by the marine transgression in the Fjords (14,500-13,500 cal yr BP) and an increase in the intensity of the Southern Westerly Winds (SWWs) (McCulloch *et al.* 2000; Kilian *et al.* 2007b; Caniupán *et al.* 2011). The intensification of the SWWs has been proposed to be the mechanism involved in the glacial advance registered in the Strait of Magellan during the Antarctic Cold Reversal (ACR) (14,500-12,900 cal yr BP). The increase of long-distance (>100 km) transport of clay sediments to the Seno Skyring core (Sky) during this period are thought to also be indicative of an enhancement of wind intensity (Kilian *et al.* 2007a; Figure 41). The increase in woody taxa pollen at 13,600 cal yr BP in the TML core implies an increase in temperature and precipitation. This change coincides with the age of ice retreat and plant colonization in the area of GCN dated at 13,900 cal yr BP (Kilian *et al.* 2007a; Figure 41) and the expansion of cushion plant communities in Santa Ines Island at 13,600 cal yr BP (Fontana and Bennett 2012; Figure 3), suggesting a similar climatic shift.

The C/N ratio and pollen concentrations, show a progressive increase over the late glacial transition and reach maximum values at 10,800 cal yr BP (Figure 41 & Figure 43). These trends

¹¹ The pollen sterility of a sample is a concept utilized in palynology to indicate that pollen concentrations are too low to make possible perform a statistically significant study, understood in this thesis as a minimum count of at least 300 pollen grains of terrestrial taxa. Therefore, the sterility of a sample does not necessarily refer to the total absence of pollen grains.

of increase resemble the reconstructed STTs from the MD07-3128 and suggest a close correlation between temperature, vegetation cover and the development of soils in the study area. In order to obtain a most accurately estimation of the contribution of terrestrial organic carbon in the Late Tamar, the percentage of terrestrial organic carbon content ($C_{org_{terr}}$) was estimated utilizing a mixing equation based on the molar N/C ratios (Perdue and Koprivnjak 2007), and following the methodology utilized by Lamy and collaborators (2010) to estimate the $C_{org_{terr}}$ from marine cores (Figure 43).

The transition from the late glacial to the Holocene is characterized by significant changes in the physical and biotic environments within the Tamar catchment. In the sediment core of Tamar Lake, at $\sim 12,800$ cal yr BP begins the deposition of dark lacustrine sediments Gyttja (lithological sections III-I; Figure 22 & Figure 41). Together with the change in core lithology, the beginning of deposition of several light-colored deposits (LCDs) that interrupt the pelagic sedimentation is observed (Figure 21 & Figure 25). Based on the macroscopic and geochemical characteristics (see section 4.2.2.1.3), four different types of LCDs are distinguished and identified as singles events, allowing the calculation of their occurrence (frequency) over time (Figure 25). LCD Type 1 occurs during the glacial-interglacial transition, Type 2 during the early Holocene, Type 3 during the later Holocene, and Type 4 occur throughout the whole record with the exception of the early Holocene. The calculated frequency of the events indicates a decreasing trend towards the early Holocene, followed by a relative increase during the mid and late Holocene. During the mid and late Holocene, event frequency fluctuates on a millennial scale, with the occurrence of peaks around 8000-6000 cal yr BP, 5000-4000 cal yr BP and during the last 1500 years (Figure 25 & Figure 43).

In order to examine the possible paleoenvironmental implications in the observed pattern of the LCDs deposition, it is necessary to discuss a number of aspects regarding the physical characteristics of the Lake Tamar catchment. As was described in section 4.2.1, one important characteristic of the Lake Tamar catchment is its semicircular shape; open to the sea towards the southwest and closed by hills with steep slopes ($>30^\circ$) to the northwest (Figure 19 & Figure 20). Barren areas observed within the lake catchment occur in locations with steep slopes, which denotes the close correlation between slope gradient and vegetation development (Figure 20). Additionally, the presence of forest communities growing on alluvial fans located in these barren areas with steep slopes highlight the presence of active slope process in this area. The lithological data from the Tamar Lake cores (Figure 42) suggest that the source area of LCD deposits is most likely located at the northwest of the catchment (Figure 20 & Figure 42, details in section 4.2.1). LCDs are recorded in all gravity cores and include types 3 and 4, suggesting a high-energy mechanism associated with their genesis and deposition (Figure 42).

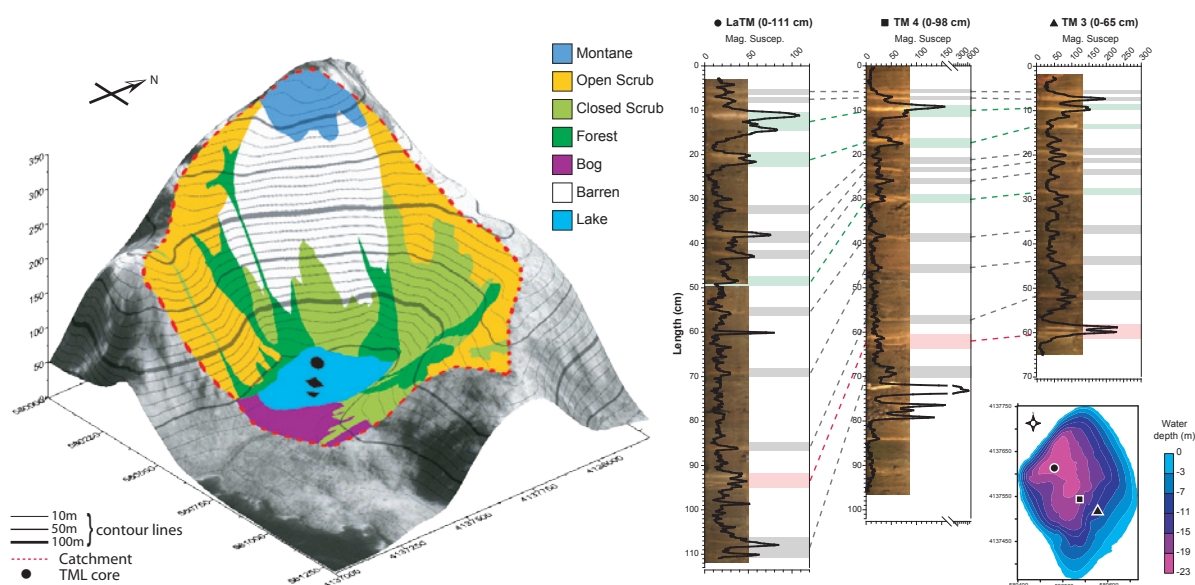


Figure 42. Left. View of the Lake Tamar catchment and surrounding vegetation. Lake bathymetry and lithology of gravity cores are shown

The reconstruction of the vegetational history from the Tamar Lake pollen record reveals two main patterns of change in the vegetation history: (i) the transition and transformation experienced by the ecosystems through time and space and, (ii) the succession of species and the consequent changes in floristic composition.

The palynological turnover analysis obtained from the DCCA approach (see section 3.2.3.2) can be used as an indicator of β -diversity, and thus allows for examination of the transformations experienced by local ecosystems (Birks 2007; Birks and Birks 2008). On the other hand, rarefaction analysis (see section 3.2.3.2 for details), was performed in order to investigate the palynological richness and infer the total species diversity in the landscape (γ -diversity; Birks and Birks 2008).

The continuous decrease in the palynological turnover curve between 16,000 cal yr BP and \sim 10,000 cal yr BP indicates that most of the plant communities present today in the “Magellanic moorland complex” were already present during the early Holocene (Figure 43). Moreover, the slope of the curve suggests that the transition was gradual. A complete species turnover (with no species in common) would have a total palynological turnover (gradient length) of 4 SD (Hill and Gauch 1980). The turnover analysis of the Tamar Lake pollen data revealed a gradient length of 1.7 SD, which implies a moderate change (Figure 43).

On the other hand, the pollen richness curve does not show significant changes during the late-glacial (Figure 43). At \sim 11,000 cal yr BP, the pollen richness decreases, registering the disappearance of pollen taxa (predominantly herbs, see Figure 43) associated with the late-glacial ecosystems. This is most likely related with the increase in the temperatures characterizing the onset of the Holocene. Through the rest of the Holocene, palynological richness increases gradually denoting the succession and expansion of different pollen taxa (Figure 43).

The spread of the arboreal pollen taxa in the record is characterized by an early appearance of *Nothofagus dombeyi*-type (13,600 cal yr BP), followed by *Drimys winteri* (10,300 cal yr BP),

Pilgerodendron uviferum + *Raukautia laetevirens* (6200 cal yr BP), *Tepualia stipularis* (4000 cal yr BP) and *Podocarpus nubigena* (1500 cal yr BP; Figure 26 & Figure 43). Even when it is not possible to distinguish between the different *Nothofagus* species occurring in the area (*Nothofagus antarctica* and *Nothofagus betuloides*) by means of the pollen proxy, leaves of *Nothofagus betuloides* found in the mass wasting deposits (LCD Type 2) indicate the presence of this taxon in the Tamar catchment since 11,800 cal yr BP (Appendix figure 11). Thus, this finding also highlights the potential of plant macrofossils analysis to confirm the occurrence of species at local scale (Jackson and Booth 2007).

The succession of different tree pollen species suggests the occurrence of distinctive forest types through time. *Nothofagus*-dominated forests are inferred between 11,800 and 8500 cal yr BP, followed by *Nothofagus betuloides*-*Drimys winteri* forests between 10,300 and 6200 cal yr BP, and culminating in the establishment of the mixed evergreen forests at ~6200 cal yr BP to present; Figure 26 & Figure 43).

Between 12,800 and 11,000 cal yr BP, the frequency in the deposition of LCDs is found to peak in Types 1 and 4 (characterized to be the most thin and simple; see Section 4.2.2.1.3). The increase of Corg and C/N and of total pollen concentrations indicates the transitional nature of this period. These changes suggest an increase of the vegetation cover and the progressive development of soils in response to the rise in temperature (Figure 44).

During the early Holocene, a decrease in the frequency of events (LCDs) is observed which is related to the end of deposition of the LCDs type 1 and 4. Simultaneous with this change in event frequency, the Corg and C/N reach their maximum values together with the total pollen concentrations. During this period, LCDs type 2 events, which contain vegetal macrorests, occur. These findings indicate that during the early Holocene, when *Nothofagus* forests dominated, a dense vegetation cover occurred at the Lake Tamar catchment related with rising temperatures (Figure 44). The parallel accumulation of soils affected the active slope processes within the catchment reducing surface runoff. Consequently, decreased erosion within the catchment led to the end in deposition of the LCDs types 1 and 4 during this period. However, the increase in the soil thicknesses increased the probability of failures (mechanical stress) within the soil or mineral material below the surface leading to the occurrence of mass wasting events LCDs type 2.

High Corg_{terr} values in the TML core and in the adjacent marine core TM1 during the early Holocene have been interpreted as a result of an increase in the transport of organic terrestrial material associated with high precipitation (Lamy *et al.* 2010, Figure 40 & Figure 44). In this context, the presence of relatively high percentages of *Misodendrum* during the period where the *Nothofagus* forest dominates (~11,800-8500 cal yr BP) supports the paleoclimatic inferences proposed by Lamy and collaborators (2010), namely a wetter and windier early Holocene. The vegetation surveys and the modern pollen rain-data suggest that high values of *Misodendrum* characterize the dwarf *Nothofagus* forest growing under severe wind stress.

Isoetes is susceptible to the content of suspended organic matter which restricts its occurrence to lakes with oligotrophic conditions (Gacia *et al.* 1994). Field observations indicate that Isoetes populations occur only in the shallow margins (<2 m) of Lake Tamar, areas that are seriously impacted during periods of high winds. Thus, the low Isoetes percentages during the Early Holocene are most likely related with high wind-stress and wave activity, as well as high Corg content (Figure 43). The increase of Isoetes values after ~8500 cal yr BP is associated with declining organic content and most likely declining wind stress.

During the mid Holocene, the *Nothofagus*-dominated forests expand and diversify (Figure 43). The succession of several tree species is accompanied by a decrease in the total pollen concentrations and in Corg and C/N values (Figure 43), suggesting a significant decline in vegetation cover and in

soil accumulation. The reappearance and deposition of the LCDs type 4 observed after 8500 cal yr BP (Figure 43), corroborate the decrease in vegetation cover and the consequent exposure of bedrock to surface runoff processes. Most likely these observations in the Tamar Lake record are associated with a decline of wind intensity, precipitation and temperatures. This inference is consistent with the synchronous increase in the surface salinities in marine cores near Tamar Island and (PC-03 and Palm, Figure 40 & Figure 44) suggesting a decrease in precipitation (Lamy *et al.* 2010; Harada *et al.* 2013). Additionally, the reduction in the clay deposition in the Seno Skyring core (Sky, Figure 40 & Figure 44) implies a reduction of the SWW strength (Kilian *et al.* 2007a; Lamy *et al.* 2010). Parallel with changes in the wind and precipitation patterns, the onset of the ENSO activity since the mid Holocene probably affected the climate of the region (Figure 44).

The only speleothem record from the area indicates rather humid intervals at the end of the mid and late Holocene (5000–4000 cal yr BP and during the last 1500 years; (Schimpf *et al.* 2011). Periods of increased precipitation observed in the speleothem record, coincide with the deposition of LCDs Type 3 and an increase in the frequency of events (mostly LCD type 4). As was described in detail in section 4.2.2.1.3, the LCD Type 3 is characterized by a silty-sand unit with no organic material, indicating the occurrence of debris flows in the catchment triggered by strong rainfall or snowmelt episodes.

Changes experienced by plant communities through time are not always in equilibrium with the climate (Webb 1986). A number of factors control changes in species distribution through time, such as intrinsic species characteristics (e.g. dispersal mechanisms, competition, amplitude of response to environmental forcings, etc) and extrinsic characteristics related to the environment (e.g. soil development, distance from spread source, presence of geographical barriers, etc; (Webb 1986; Bennett and Lamb 1988; Wilkinson 1997; Willis *et al.* 1997).

Table 9 summarizes some ecological characteristics of the most important arboreal species encountered in the Southern Patagonian Fjords at present. It should be noted that there are limitations in determining the point at which a particular taxa colonizes an area from pollen records. This is due to differences in pollen production, transport and preservation among the taxa which makes it difficult to define a unique threshold value that can be used as an indicator. Despite of the above, absolute pollen concentrations can be used as a indicator for changes in the abundance of the taxa, allowing to address some aspects related to spread and succession patterns of tree populations (Bennett 1983; Bennett and Lamb 1988).

At Tamar Lake, an increased in floristic diversity of forests inferred by high palynological richness is observed during the Holocene (Figure 43). Shade-intolerant trees (i.e. pioneer species) expand first, followed by semi-tolerant ones, and finally by shade-tolerant species (Figure 45, Table 9). This species succession highlights the important role of ecological mechanisms in determine the floristic composition in the postglacial period. Moreover, geomorphology is another important factor which limits the growth of forest communities (see section 5.1.1.1, Figure 43), increasing species competition for light and nutrients.

Pollen records from the Northern Patagonian Fjords (47°–43°S) show a similar succession of tree species as the Tamar Lake [i.e. *Nothofagus dombeyi*-type (16,000 cal yr BP) > *Drimys winteri* (15,500 cal yr BP) > *Pilgerodendron uviferum*+*Raukaua laetevirens* (14,500 cal yr BP) > *Podocarpus nubigena* (13,000 cal yr BP) > *Tepualia stipularis* (11,500 cal yr BP)], which takes place during the last glacial-interglacial transition (i.e. 16,000–11,500 cal yr BP; (Bennett *et al.* 2000; Haberle and Bennett 2004). However, in the Tamar record this succession occurs within the Holocene. In both cases the underlying mechanism controlling the observed succession of tree species, is most likely intrinsic (i.e. species ecology).

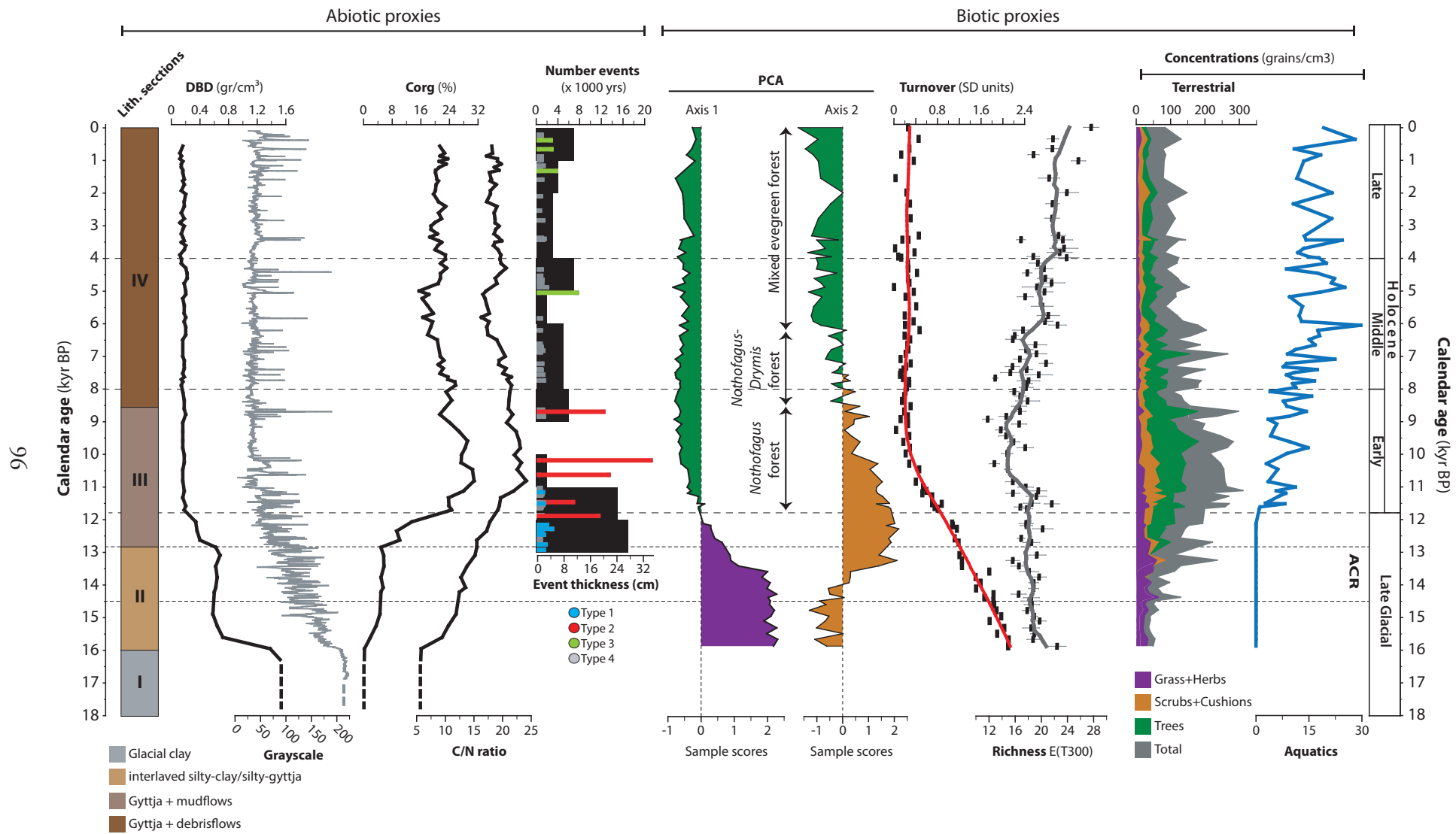


Figure 43. Summary figure of main abiotic and biotic proxies from the TML core

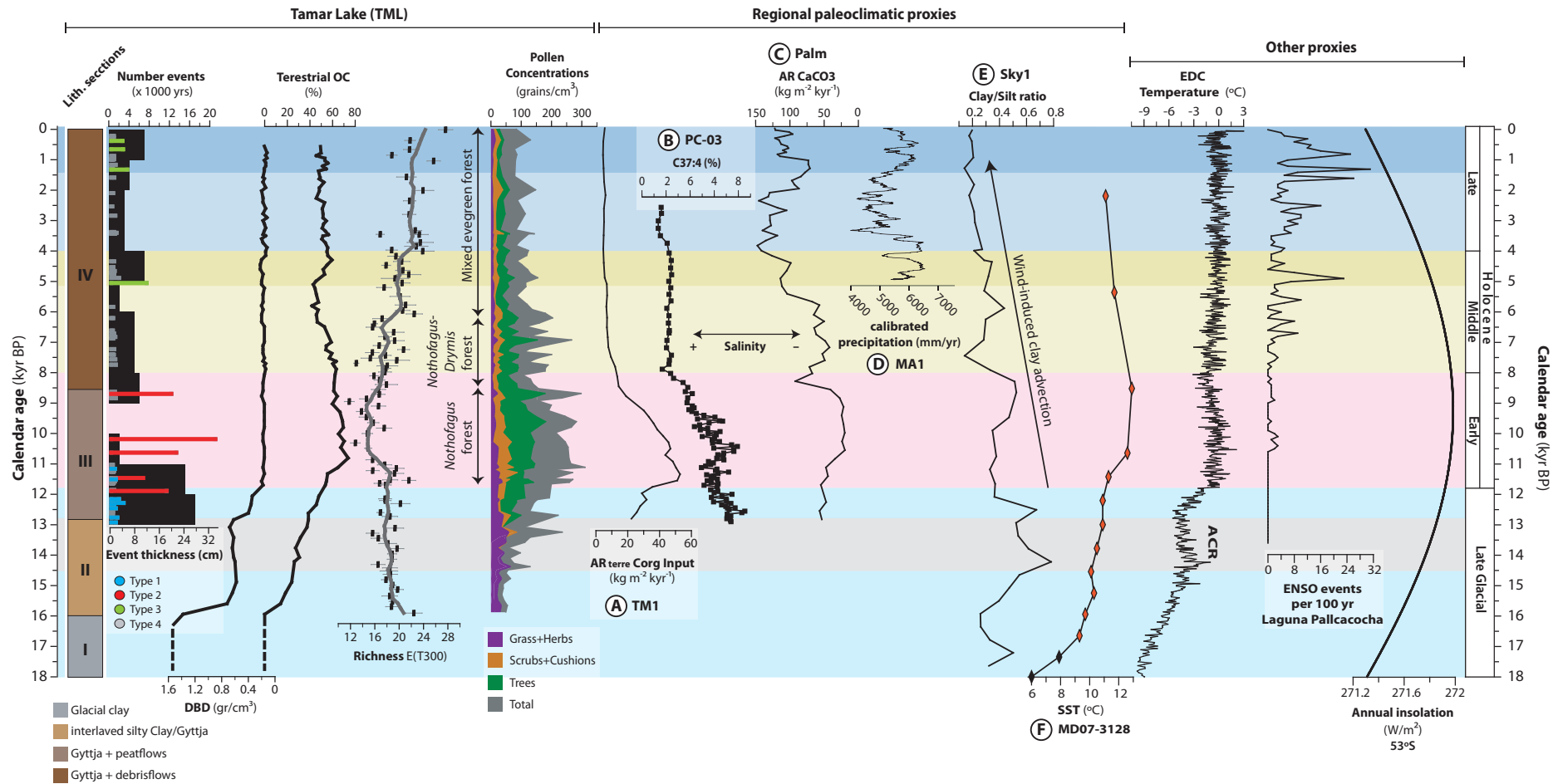


Figure 44. Summary figure for abiotic (geochemical) and biotic (pollen) from TML and selected paleoclimatic proxies. For location see figure 40

The temporal offset of the ecological succession between Northern and Southern Patagonian Fjords (i.e. Tamar Lake) can be attributed to a lag in the migration of species from their refugial location during the LGM, to geographical barriers and/or to climate. The presence of pollen from all tree species (with exception of *Podocarpus nubigena*) since the early Holocene suggests that these trees were present within the Tamar catchment or in its vicinity prior to their expansions (Figure 45, Table 9). Consequently, migration lags most likely can not be invoked to explain the succession of the three tree species (*Nothofagus betuloides*, *Pilgerodendron uviferum*, *Tepualia stipularis*). In the absence of data on threshold concentration values indicating the presence of a certain taxon (e.g. obtained by pollen traps), the most plausible scenario explaining the succession observed is a suppression of interspecific competition by climate or other environmental factors (Prentice 1986).

In light of the above, many questions remain open with regard to the mechanisms involved in the succession of plant communities during the postglacial period in the Southern Patagonian Fjords. In order to address these questions, it is necessary to trace the patterns of migration, colonization and expansion of the different species in the S. Patagonian region. For instance, the analysis of plant macrofossils can confirm the occurrence of a species in the investigated area (Jackson and Booth 2007). Therefore, the presence of *Nothofagus betuloides* leaves found into a mass wasting deposit (LCD Type 2) in the Tamar Lake record show that this species occurred in the Tamar catchment since 11,800 cal yr BP (Appendix figure 11)

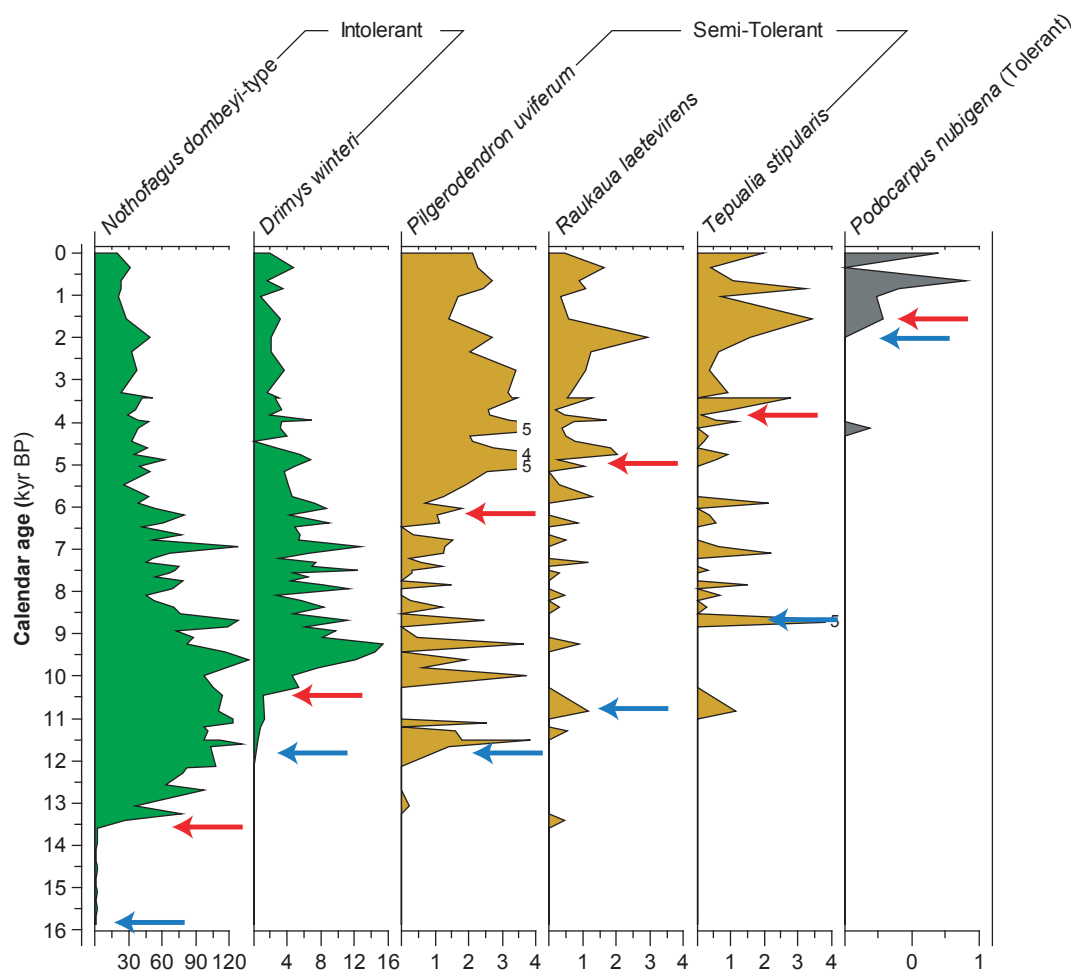


Figure 45. Summarized pollen concentration diagram of tree taxa, indicating its shade tolerance. The red arrow indicates the point when the taxon becomes abundant in the record.

Table 9. Main ecological traits for tree taxa involved in the postglacial forest succession in the Tamar pollen record

Taxa	Shade tolerance ¹	Dispersal mechanism ²	Presence/ Increase ³ (cal yr BP)	Difference ⁴ (years)
<i>Nothofagus spp</i>	Intolerant	Anemochory	>16,000/13,600	3600
<i>Drimys winteri</i>	Intolerant	Zoochory	11,500/10,300	1200
<i>Pilgerodendron uviferum</i>	Intermediate	Anemochory	11,500/6200	5300
<i>Raukautia leatevirens</i>	Intermediate	Zoochory	11,500/5000	5500
<i>Tepualia stipularis</i>	Intermediate	Anemochory	8500/4000	4500
<i>Podocarpus nubigena</i>	Tolerant	Zoochory	4000/1500	3000

1. Gutierrez *et al.* 2009

2. Villagran *et al.* 1986

3. Presence and increase relate to (i) the point when the taxon appears frequently in the record and (ii) when its presence becomes abundant and continuous, respectively. Both were estimated based on concentration curve. Even when not are calibrated these features can be used as a simple approximation to examine the arrival and spread of taxa. See details in text.

4. Relates to the difference between presence and increase values

5.3. Main vegetation changes along a west-east transect in Southern Patagonia at 53°S during the Postglacial

As was enunciated in the introduction, the mechanisms controlling the evolution of the vegetation of Southern Patagonia during the postglacial are poorly understood. For example, it still remains uncertain when the modern phytogeographic gradient in the region was established. The role and timing of environmental forcing (climatic and non-climatic) is also unclear. The multivariate analyses (i.e. PCA, DCCA and rarefaction) and the vegetation survey undertaken in this thesis, allow addressing some of these questions.

Plant ecosystems occurring during the late glacial along the W-E transect at 53°S are adapted to the harsh climatic conditions (i.e. cold and dry) and are characterized by scarce vegetation cover and the absence of trees in both flanks of the Andes (Figure 46). These late glacial ecosystems show significant differences in floristic terms, with dwarf-scrub steppe occurring in the east and a heath-tundra in the west. This finding highlights the strong influence of the Andean massif on the climate (i.e. rain-shadow effect), which can be traced in the biogeography of the flora (also observed in the modern pollen rain) (Hinojosa and Villagrán 1997; Villagrán and Hinojosa 2005; Ortiz-Jaureguizar and Cladera 2006).

During the last glacial interglacial transition (LGIT), the appearance of cushion plants and scrubs in the west in areas formally occupied by the tundra and in the east the expansion of grasses and scrubs in areas formally characterized by dwarf-scrub steppe is inferred (Figure 46). These changes occur in Potrok Aike at ~15,100 cal yr BP, in Tamar and Rubens at ~13,500 cal yr BP and in GCN and Guanaco at ~11,000 cal yr BP (Figure 46). Despite the different chronologies, the inferred increase in the vegetation cover and the emergence of water-demanding taxa in all sites suggest that these changes in vegetation at a regional scale are associated with the increase in temperature and precipitation towards the end of the LGIT in Southern Patagonia (Kilian and Lamy 2012). The ACR reversal to colder and drier conditions does not seem to affect the development of ecosystems characterized by water-demanding species. However, pollen records from Tierra del Fuego register a cold episode that impacted local vegetation during the last glacial interglacial transition, and more specifically between 12,500 and 11,500 cal yr BP (Heusser and

Rabassa 1987; Borromei *et al.* 2007).

In the early Holocene, the PCA suggests the existence of three vegetation types: the moorlands and bogs in the west Andean areas, the extensive grasslands in the eastern plains, and the grass-shrub steppe in between on the eastern flanks of the Andes (Figure 47). These findings suggest that climatic conditions during the early Holocene were probably wetter than today in the west and dryer than today in the east.

After 8500 cal yr BP, the magellanic moorland complex is established in the west (Tamar), at 8200 cal yr BP the evergreen forest expands in GCN in western Andes, and at 9000 cal yr BP the grass-shrub steppe in the eastern plains (Potrok Aike; Figure 47). These changes in the vegetation types are also observed in the turnover curves from western sites (i.e. Tamar and GCN), where the types established at these chronologies remain unchanged to the present day (Figure 46 & Figure 47).

During the late Holocene, the establishment of deciduous forest in the eastern Andean piedmonts (Rubens: 4000 cal yr BP; Guanaco: 2900 cal yr BP) is observed in parallel to the three vegetation types occurring up to this point (Figure 46 & Figure 47). These four vegetational types are also encountered at these locations at present.

Sites located in areas dominated by open woodland and steppe ecosystems (i.e. Lake Guanaco and Potrok Aike, respectively) show a more gradual change, in comparison to forested ecosystems (i.e. Tamar, GCN and Rubens) which show a more step-like change in the turnover gradient (Table 8, Figure 46). On the other hand, the pollen richness suggest an increase of floristic diversity towards present in the records from the west in response to the expansion of taxa associated to the evergreen forest communities, while in eastern sites there are no significant changes observed. This can be associated with a low level of pollen-taxonomical precision or the effect of the over-representation of *Nothofagus*, a prolific pollen producer that can cause serious bias in palynological diversity (Odgaard 2007).

Vegetational changes in Southern Patagonia during the postglacial period are thought to be triggered by climatic parameters (in particular precipitation) (Huber 2001; Fesq-Martin *et al.* 2004; Wille *et al.* 2007; Francois 2009). However, the SWWs affect not only precipitation patterns (Garreaud *et al.* 2013), but also enhance evapotranspiration which, in combination with temperature, produce a moisture availability gradient across the Andes (Lamy *et al.* 2010; Kilian and Lamy 2012). On the other hand, changes in the intensity of the SWWs controls the strengthening/ diminishing of the Foehn Effect (Schneider *et al.* 2003; Garreaud *et al.* 2013). During periods of stronger (weaker) westerlies, an increase (decrease) in the amount of precipitation in western Andes and a decrease (increase) in the east is recorded. This mechanism can be evoked to explain the changes in the biogeographic gradient occurring at Southern Patagonia during the postglacial.

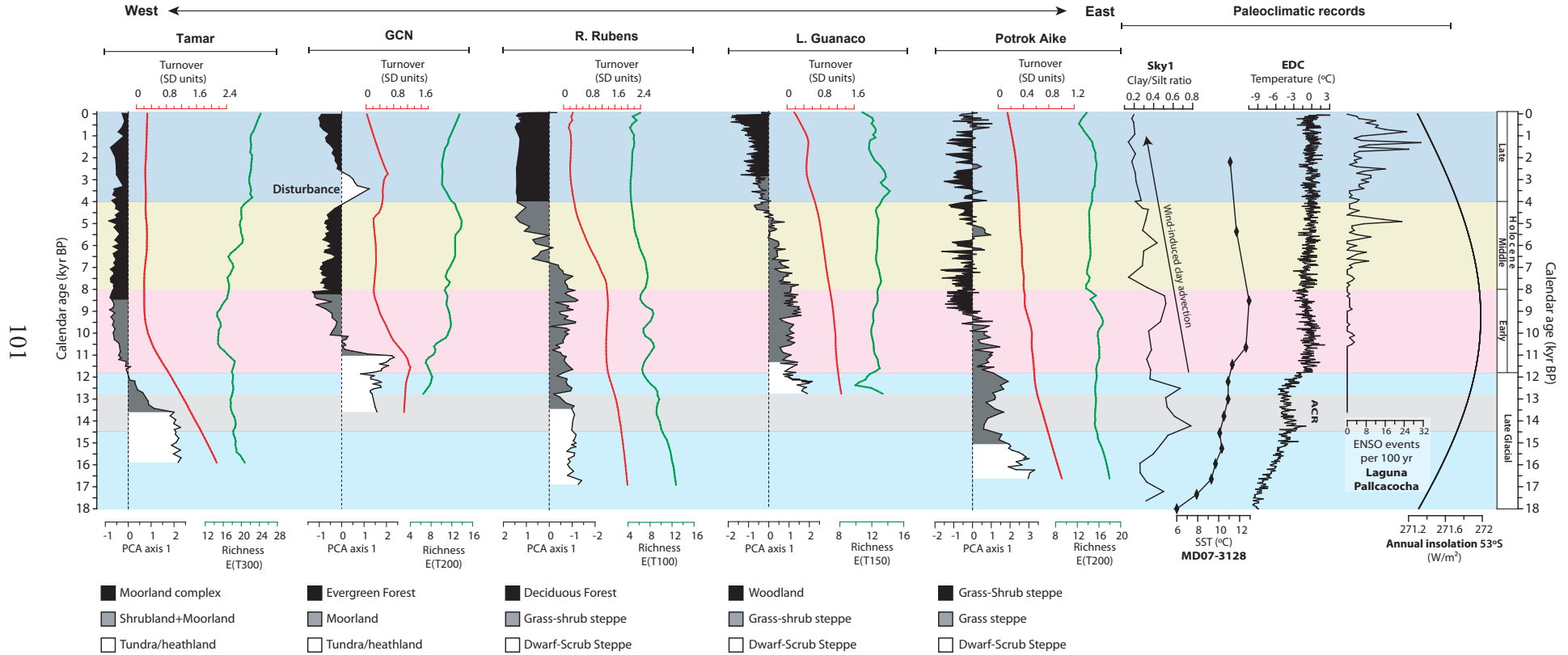


Figure 46. Comparison of the results obtained from the principal component analysis (PCA), detrended canonical correspondence analysis (Turnover) and Rarefaction analysis (Richness) performed at the four additional pollen records located along the west-east transect in Southern Patagonia (Figure 12). In all the cases, the results are plotted against time. The data from Turnover and Richness were smoothed utilizing a 0.2 lowess spline (solid line). The estimated palynological richness was calculated based on the minimum number of pollen taxa (T_n) at each site. Also selected paleoclimatic proxies are provided.

Main vegetation changes along a west-east transect in Southern Patagonia at 53°S during the Postglacial

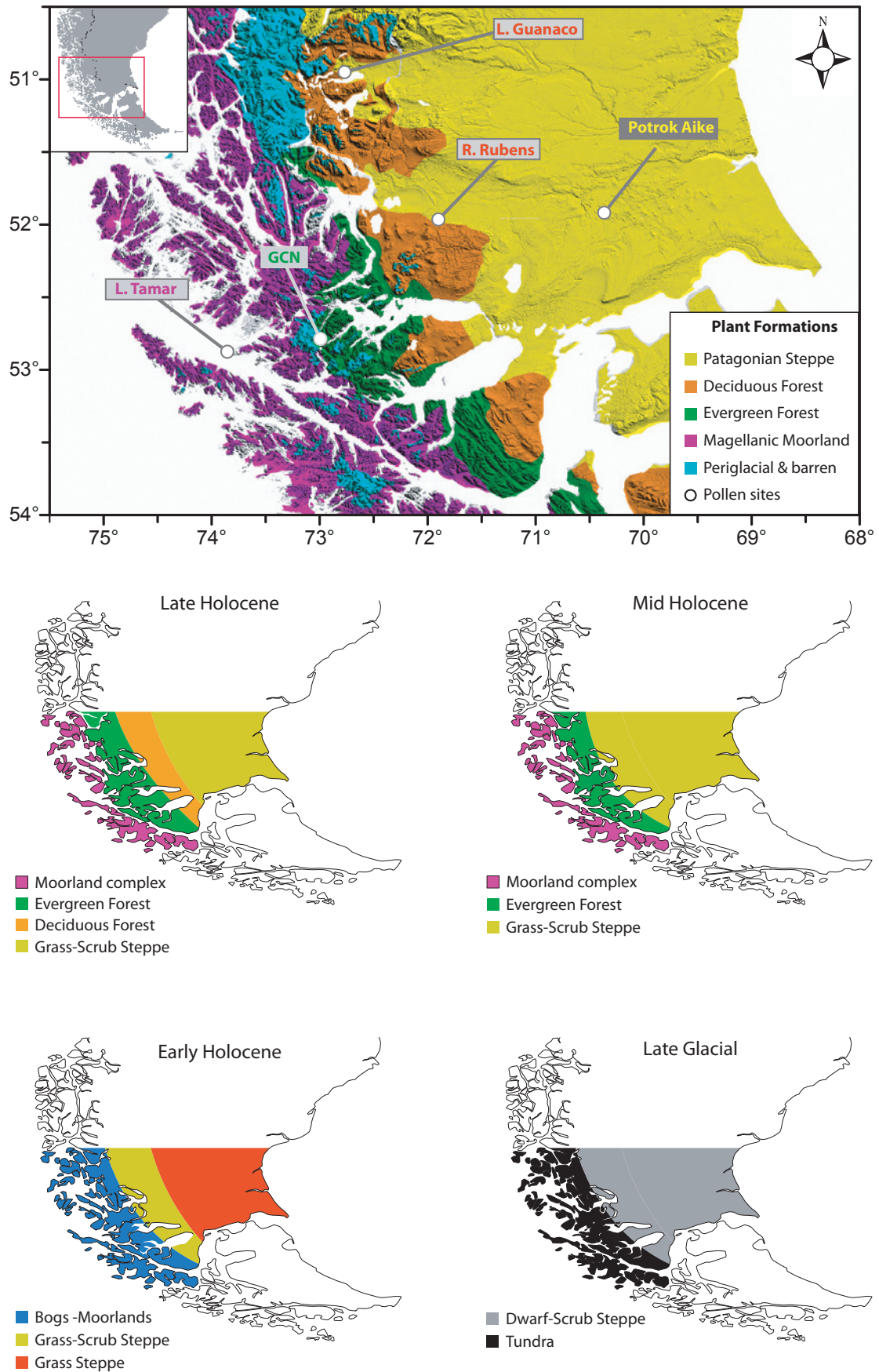


Figure 47. Schematic evolution of the main vegetation types of Southern Patagonia during the Postglacial.

6. CONCLUSIONS

This thesis aims to examine the representation of plant species in the pollen rain, reconstruct the postglacial vegetation history in Southern Patagonia at a local and regional scale, and to infer the climatic and environmental conditions controlling the evolution of these ecosystems.

The vegetation survey performed in this thesis highlights the great heterogeneity characterizing the environments occurring in the Southern Patagonian Fjords that have been poorly investigated to this date. In the areas surveyed, several ecosystems were identified associated to bogs (cushion-bog, Juncaceous-bog and Cyperaceous-bog), forest (*Nothofagus betuloides* dwarf forest and *Nothofagus betuloides-Drimys winteri* forest, Mixed Evergreen Forest), scrublands (closed and open) and montane or sub-alpine plant communities. Their spatial distribution in the region is a function of climatic, topographic and edaphic parameters. Thus, the occurrence of bog or woody communities (*sensu lato*) is closely correlated with the slope gradient that controls the drainage conditions, while the presence of closed-scrublands (coast) and sub-alpine vegetation (hills) is closely correlated to the change of temperature with altitude. The aspect of a location is correlated with wind intensity and controls the occurrence of open scrublands and dwarf forest in areas severely affected by wind (windward) and of forest in sheltered ones (leeward). On the other hand, changes in the vegetation composition and cover are related to changes in the biogeochemical cycle associated with the transport of base-cations via sea spray or with slope-process dynamics (i.e. runoff and mass wasting deposit events). The lack of meteorological stations and associated climate studies in the study area impede the inferences of unequivocal vegetation and climate associations. It is postulated that increases in temperature or decreases in precipitation are the major climate triggers controlling the occurrence of woody (scrublands and forests) or bog ecosystems. Further studies are needed to address in more detail these open questions and to clarify the linkages between physical environment, climate and local vegetation.

The results of the survey of the modern pollen rain show that main vegetation types occurring along the region can be clearly distinguished by their pollen signature. By instance Patagonian Steppe reveals high relative pollen percentages of grasses and herbs (e.g. Poaceae, Asteraceae subf. Cichorioideae, Caryophyllaceae, Brassicaceae, *Acaena*), whereas forest show high arboreal pollen percentages (e.g. *Nothofagus dombeyi*-type, *Drimys winteri*, *Gaultheria*). Likewise, pollen samples characterizing Magellanic Moorland ecosystems show the co-dominance of graminoids (Juncaginaceae, Juncaceae, Cyperaceae) and cushion taxa (e.g. *Astelia pumila*, *Donatia fascicularis*, *Caltha*). Nevertheless, the results from cluster analysis also reveal the high heterogeneity underlying the pollen assembles and the limitation to identify main plant communities obscured by local-vegetation. While, in differences between samples obtained in moss polster and gravity cores denotes the role of the sedimentary environment in the resultant pollen signal (local-regional). On the other hand, multivariate analyses (RDA) indicate a strong and significant correlation between changes (co-variance) in the pollen assemblages and the climatic variables of annual precipitation (Pann) and mean annual temperatures (Tann). As well, changes in the vegetation cover seem to be closely correlated with changes in the complete pollen composition (e.g. arboreal/non-arboreal). These findings highlight the potential of using pollen analysis to reconstruct climatic and physical characteristic of the landscape as the openness. A main subject in the modern pollen-rain of Southern Patagonia is the overrepresentation of *Nothofagus* in the pollen assemblages and its long-distance transport along the region, features that difficult the interpretation of pollen samples with high *Nothofagus* percentages. Therefore, are necessary conduct studies in order to determine how individual taxa are represented in modern pollen spectra (over, even, or under-represented) and how change the production and dispersal of pollen along the region. Only tackling these issues

being possible improve the interpretation of pollen records in Southern Patagonia.

The sedimentary record from Tamar Lake indicates that its catchment was ice-free or less influenced by periglacial processes by ~16,000 cal yr BP. This age, along with others basal ages from marine cores obtained in the vicinities of Tamar Island, indicates that deglaciation of Northern Strait of Magellan occurred between 16,000-14,500 cal yr BP. The chronology also indicates that ice retreat occurs in direction to the Gran Campo Nevado ice cap, denoting its importance as the main source for glacial lobes during the LGM in the study area. The pollen record indicates that after the ice retreat, pioneer species such as grass and herbs established suggesting the existence of harsh (cold/dry) climatic conditions. There are no significant changes observed in vegetation during periods of glacial re-advances (ACR). *Nothofagus* woodland expands at 13,600 cal yr BP following the increase in temperature and precipitation. As the different *Nothofagus* species are not distinguishable by means of pollen, issues related to the migration and succession of *Nothofagus* forest in the region need to be addressed by other type of analyses. In this context, the presence of *Nothofagus betuloides* leaves found into a mass wasting deposit occurring at 11,800 cal yr BP provide the first evidence of unequivocal presence of the taxon within the Tamar catchment. During the Holocene, coeval changes in geochemistry (C/N and Corg) and pollen concentration suggest the close links between vegetation cover and soil development. Maximum vegetation cover and well-developed soils are recorded during the early Holocene and are most probably related to high temperatures registered over this time. The expansion of the mixed evergreen forests since the mid-Holocene is in line with reduced precipitation and progressive cooling inferred by other paleoenvironmental studies in the study area. On the other hand, changes in the characteristics and frequency of the deposition of mass wasting deposit events in the Holocene are associated with changes in vegetation and soil development. In the early Holocene, when maximum vegetation cover and soil development occur, minimum surface runoff is inferred. While, during the late Holocene decrease in the temperatures leading to decreasing vegetation cover and soil development and increasing the surface runoff.

The multivariate analyses (i.e. PCA, DCCA and rarefaction) performed in five pollen records located along a W-E transect and the vegetation and modern pollen-rain surveys undertaken in this thesis elucidate the vegetation history of the region. During the late glacial a tundra-like ecosystem is encountered in the west and a dwarf-shrub steppe in the east, suggesting that even when cold/dry conditions prevail along the region, different ecosystem types are present. In the early Holocene, the PCA suggests the existence of three vegetation types: the moorlands and bogs in the west Andean areas, the extensive grasslands in the eastern plains, and the grass-shrub steppe in between on the eastern flanks of the Andes. These findings suggest a wetter climate regime in the west and a dryer one in the east Andes most likely associated with the strong westerlies that produce a stronger precipitation gradient. In the mid Holocene, the magellanic moorland complex is established in the west, the evergreen forest in western Andes, and the grass-shrub steppe in the eastern plains. During the late Holocene, the establishment of deciduous forest in the eastern Andean piedmonts is observed in parallel to the three vegetation types occurring up to this point. These four vegetational types are also encountered at these locations at present. The changes in vegetation during the mid and late Holocene, indicate a decrease in precipitation in the west and an increase in the east. It can be argued that during periods of stronger (weaker) westerlies, an increase (decrease) in the amount of precipitation in western Andes and a decrease (increase) in the east is recorded. This mechanism can be evoked to explain the changes in the biogeographic gradient occurring at S. Patagonia during the postglacial.

7. BIBLIOGRAPHY

- Adam, D. P. and P. J. Mehringer (1975). "Modern pollen surface samples: an analysis of subsamples." *Journal of Research of the U.S. Geological Survey* 3(6): 733-736.
- Aizen, M. A. and C. Ezcurra (1998). "High incidence of plant-animal mutualisms in the woody flora of the temperate forest of southern South America: biogeographical origin and present ecological significance." *Ecología Austral* 8: 217-236.
- Armesto, J. J., G. Casassa and O. Dollenz (1992). "Age structure and dynamics of Patagonian beech forests in Torres del Paine National Park, Chile." *Vegetatio* 98: 13-22.
- Arroyo, M. T. K., P. Pliscoff and M. Mihoc (2005). "Chapter 12: The Magellanic moorland." *The World's Largest Wetlands: Ecology and Conservation*. L. H. Fraser and P. A. Keddy (eds.): 424.
- Auer, V. (1958). "The Pleistocene of Fuego-Patagonia. Part II. The history of the flora and vegetation." *Annales Academiae Scientiarum Fennicae III. Geologica-Geographica* 50: 1-239.
- Auer, V. (1974). "The isorhythmicity subsequent to the Fuego-Patagonian and Fennoscandian ocean level transgressions and regressions of the latest glaciation." *Annales Academiae Scientiarum Fennicae* 155(A): 1-88.
- Bennett, K. D. (1983). "Devensian Late-Glacial and Flandrian Vegetational History at Hockham Mere, Norfolk, England. I. Pollen Percentages and Concentrations." *New Phytologist* 95(3): 457-487.
- Bennett, K. D. (1997). *Evolution and ecology: the pace of life*, Cambridge University Press.
- Bennett, K. D. (2008). *psimpoll* and *pscomb* programs for plotting and analysis. Available at: <http://chrono.qub.ac.uk/psimpoll/psimpoll.html>.
- Bennett, K. D., S. G. Haberle and S. H. Lumley (2000). "The Last Glacial-Holocene transition in Southern Chile." *Science* 290: 325-328.
- Bennett, K. D. and H. F. Lamb (1988). "Holocene pollen sequences as a record of competitive interactions among tree populations." *Trends in Ecology & Evolution* 3(6): 141-144.
- Birks, H. J. B. (2007). "Estimating the amount of compositional change in late-Quaternary pollen-stratigraphical data." *Vegetation History and Archaeobotany* 16(2-3): 197-202.
- Birks, H. J. B. (2012). "Ecological palaeoecology and conservation biology: controversies, challenges, and compromises." *International Journal of Biodiversity Science, Ecosystem Services & Management* 8(4): 292-304.
- Birks, H. J. B. and H. H. Birks (1980). *Quaternary palaeoecology*. London.
- Birks, H. J. B. and H. H. Birks (2008). "Biological responses to rapid climate change at the Younger Dryas-Holocene transition at Kråkenes, western Norway." *The Holocene* 18(1): 19-30.
- Birks, H. J. B. and J. M. Line (1992). "The use of Rarefaction Analysis for Estimating Palynological Richness from Quaternary Pollen-Analytical Data." *The Holocene* 2(1): 1-10.

- Björck, S., M. Rundgren, K. Ljung, I. Unkel and A. Wallin (2012). "Multi-proxy analyses of a peat bog on Isla de los Estados, easternmost Tierra del Fuego: a unique record of the variable Southern Hemisphere Westerlies since the last deglaciation." *Quaternary Science Reviews* 42(0): 1-14.
- Boelcke, O., D. Moore and F. T. Roig (1985). *Transecta Botánica de la Patagonia Austral*. CONICET, Instituto de la Patagonia & Royal Society. Buenos Aires.
- Bond, W. J., F. I. Woodward and G. F. Midgley (2005). "The global distribution of ecosystems in a world without fire." *New Phytologist* 165(2): 525-538.
- Borromei, A. M., A. Coronato, L. G. Franzen, J. F. Ponce, J. A. L. Saez, N. Maidana, J. Rabassa and M. S. Candel (2010). "Multiproxy record of Holocene paleoenvironmental change, Tierra del Fuego, Argentina." *Palaeogeography, Palaeoclimatology, Palaeoecology* 286(1-2): 1-16.
- Borromei, A. M., A. Coronato, M. Quattrocchio, J. Rabassa, S. Grill and C. Roig (2007). "Late Pleistocene-Holocene environments in Valle Carbajal, Tierra del Fuego, Argentina." *Journal of South American Earth Sciences* 23(4): 321-335.
- Breuer, S., R. Kilian, O. Baeza, F. Lamy and H. Arz (2013a). "Holocene denudation rates from the superhumid southernmost Chilean Patagonian Andes (53S) deduced from lake sediment budgets." *Geomorphology* 187: 135-152.
- Breuer, S., R. Kilian, D. Schörner, W. Weinrebe, J. Behrmann and O. Baeza (2013b). "Glacial and tectonic control on fjord morphology and sediment deposition in the Magellan region (53-∞S), Chile." *Marine Geology* 346(0): 31-46.
- Brewer, S., J. Guiot and D. Barboni (2007). "POLLEN METHODS AND STUDIES | Use of Pollen as Climate Proxies." *Encyclopedia of Quaternary Science*. S. A. Elias (eds.). Oxford, Elsevier: 2497-2508.
- Caldenius, C. (1932). "Las glaciaciones cuaternarias en la Patagonia y Tierra del Fuego." *Geografiska Annaler* 14: 1-164.
- Caniupán, M., F. Lamy, C. B. Lange, J. Kaiser, H. Arz, R. Kilian, O. Baeza Urrea, C. Aracena, D. Hebbeln, C. Kissel, C. Laj, G. Mollenhauer and R. Tiedemann (2011). "Millennial-scale sea surface temperature and Patagonian Ice Sheet changes off southernmost Chile (53°S) over the past 60 kyr." *Paleoceanography* 26(3): PA3221.
- Cárdenas, M. (2006). *Vegetación y clima postglacial en Última Esperanza, Patagonia Sur de Chile*. Department of Ecological Sciences. Santiago de Chile, Universidad de Chile. M.Sc. thesis: 85pp.
- Casassa, G., A. Rivera, W. Haeberlib, G. Jones, G. Kaser, P. Ribstein, A. Rivera and C. Schneider (2007). "Current status of Andean glaciers." *Global and Planetary Change* 59: 1-9.
- Collantes, M. B., J. Anchorena and G. Koremblit (1989). "A soil nutrient gradient in magellanic *Empetrum* heathlands." *Vegetatio* 80: 183-193.
- Coope, G. R. and A. S. Wilkins (1994). "The Response of Insect Faunas to Glacial-Interglacial Climatic Fluctuations [and Discussion]." *Philosophical Transactions: Biological Sciences* 344(1307): 19-26.
- Coronato, A. M. J., F. Coronato, E. Mazzoni, M. Vazquez and J. Rabassa (2008). "The Physical Geography of Patagonia and Tierra del Fuego." in: *The late Cenozoic of Patagonia and Tierra del Fuego*(eds.), Elsevier. *Developments in Quaternary Sciences*, 11: 13-55.

- Coronato, F. and A. Bisigato (1998). "A temperature pattern classification in Patagonia." *International Journal of Climatology* 18(7): 765-773.
- Danowski, J. A. (1993). "Network analysis of message content,." *Progress in communication sciences IV*(eds.). W. D. Richards Jr & G. A. Barnett, eds. Norwood, NJ: 197-221.
- Davies, A. L. and M. J. Bunting (2010). "Applications of Palaeoecology in Conservation." *Open Ecology Journal*: 54-67.
- Delcourt, H. and P. Delcourt (1988). "Quaternary landscape ecology: Relevant scales in space and time." *Landscape Ecology* 2(1): 23-44.
- Delcourt, H. R. and P. A. Delcourt (1991). *Quaternary ecology: a paleoecological perspective*, Springer.
- Delcourt, H. R., P. A. Delcourt and T. Webb Iii (1983). "Dynamic plant ecology: the spectrum of vegetational change in space and time." *Quaternary Science Reviews* 1(3): 153-175.
- Denton, G. H., C. J. Heusser, T. V. Lowell, P. I. Moreno, B. G. Andersen, L. Heusser, C. Schlüchter and D. R. Marchant (1999). "Interhemispheric linkage of paleoclimate during the last glaciacion." *Geografiska Annaler* 81 A: 107-153.
- Dollenz, O. (1991). "Sucesión vegetal en el sistema morrénico del glaciar Dickson, Magallanes, Chile." *Anales Instituto Patagonia, Serie Ciencias, Naturales, Punta Arenas (Chile)* 20(1): 49-60.
- Dollenz, O., J. Henriquez and E. Dominguez (2012). "La vegetacion de las geoformas proglaciares en los glaciares Balmaceda, Tyndall, Taraba y Ema, Magallanes, Chile." *Anales del Instituto de la Patagonia* 40: 7-17.
- Dominguez, E., E. Pisano and O. Dollenz (1999). "Colonización vegetal en el área periglaciaria del glaciar Nueva Zelandia, Cordillera Darwin de Tierra del Fuego, Chile." *Anales del Instituto de la Patagonia* 27: 7-16.
- Dykes, A. P. and J. M. Selkirk-Bell (2010). "Landslides in blanket peat on subantarctic islands: Causes, characteristics and global significance." *Geomorphology* 124(3-4): 215-228.
- Edwards, K. J. and G. M. MacDonald (1991). "Holocene palynology: II human influence and vegetation change." *Progress in Physical Geography* 15(4): 364-391.
- Ellenberg, H. and D. Mueller-Dombois (1967). "Tentative physiognomic-ecological classification of plant formations of the earth." *Ber. geobot. Inst. ETH, Stiftg. Rübel* 6(37): 21-55.
- Endlicher, W. and A. Santana (1988). "El clima del Sur de la Patagonia y sus aspectos Ecológicos." *Anales del Instituto de la Patagonia* 18(Serie Ciencias Naturales): 57-86.
- Fægri, K. and J. Iversen (1989). *Textbook of pollen analysis*. London, United Kingdom, John Wiley & Sons Ltd.
- Fesq-Martin, F. (2003). *Pollenanalytische Untersuchungen zur Rekonstruktion der spät- und postglazialen Vegetationsdynamik des Magellanischen Regenwaldes, Südchile*. Fakultät für Chemie, Pharmazie und Geowissenschaften. Albert-Ludwigs-Universität Freiburg im Breisgau.: PhD Thesis. 160 pages.

- Fesq-Martin, M., A. Friedmann, M. Peters, J. Behrmann and R. Kilian (2004). "Late-glacial and Holocene vegetation history of the Magellanic rain forest in southwestern Patagonia, Chile." *Vegetation History and Archaeobotany* 13(4): 249-255.
- Fontana, S. L. and K. D. Bennett (2012). "Postglacial vegetation dynamics of western Tierra del Fuego." *The Holocene*(Special issue): 1-14.
- Fosdick, J. C., B. W. Romans, A. Fildani, A. Bernhardt, M. Calder and S. A. Graham (2011). "Kinematic evolution of the Patagonian retroarc fold-and-thrust belt and Magallanes foreland basin, Chile and Argentina, 51°30'S." *Geological Society of America Bulletin*.
- Francois, J. P. (2009). Historia paleoambiental del ecotono Bosque-Estepa al interior del Parque Nacional Torres del Paine (Región de Magallanes, Chile) durante los últimos 14.800 años. Department of Ecological Sciences, Universidad de Chile. M.Sc. thesis: 101pp.
- Gacia, E., E. Ballesteros, L. Camarero, O. Delgado, A. Palau, J. L. Riera and J. Catalan (1994). "Macrophytes from lakes in the eastern Pyrenees: community composition and ordination in relation to environmental factors." *Freshwater Biology* 32(1): 73-81.
- Gajardo, R. (1994). La vegetación natural de Chile. Santiago, Editorial Universitaria.
- Gallart, F., N. Clotet-Perarnau, O. Bianciotto and J. Puigdefabregas (1994). "Peat soil flows in Bahía del Buen Suceso, Tierra del Fuego (Argentina)." *Geomorphology* 9(3): 235-241.
- García, J. L., M. R. Kaplan, B. L. Hall, J. M. Schaefer, R. M. Vega, R. Schwartz and R. Finkel (2012). "Glacier expansion in southern Patagonia throughout the Antarctic cold reversal." *Geology* 40(9): 859-862.
- Garreaud, R., P. Lopez, M. Minvielle and M. Rojas (2013). "Large-Scale Control on the Patagonian Climate." *Journal of Climate* 26(1): 215-230.
- Garreaud, R., M. Vuille, R. Compagnucci and J. Marengo (2009). "Present-day South American climate." *Palaeogeography, Palaeoclimatology, Palaeoecology* 281(3-4): 180-195.
- Ghiglione, M. C., F. Suarez, A. Ambrosio, G. Da Poian, E. O. Cristallini, M. F. Pizzio and R. M. Reinoso (2009). "Structure and evolution of the austral basin fold-thrust belt, Southern Patagonian Andes." *Revista de la Asociación Geológica Argentina* 65: 215-226.
- Gibbard, P. L., M. J. Head and M. J. C. Walker (2009). "Formal ratification of the Quaternary System/Period and the Pleistocene Series/Epoch with a base at 2.58 Ma." *Journal of Quaternary Science* 25(2): 96-102.
- Giesecke, T. (2007). "POLLEN METHODS AND STUDIES | Changing Plant Distributions." *Encyclopedia of Quaternary Science*. E. A. Scott and M. J. Cary (eds.). Oxford, Elsevier: 2544-2551.
- Gignac, L. D. and D. H. Vitt (1990). "Habitat Limitations of *Sphagnum* along Climatic, Chemical, and Physical Gradients in Mires of Western Canada." *The Bryologist* 93(1): 7-22.
- Glasser, N. F. and M. C. Ghiglione (2009). "Structural, tectonic and glaciological controls on the evolution of fjord landscapes." *Geomorphology* 105(3-4): 291-302.
- Godley, E. J. (1960). "The Botany of Southern Chile in Relation to New Zealand and the Subantarctic." *Proc. Royal Soc (London)* 152: 457-475.

- Goldsmith, F. B. (1973). "The Vegetation of Exposed Sea Cliffs at South Stack, Anglesey: II. Experimental Studies." *Journal of Ecology* 61(3): 819-829.
- Grimm, E. (1987). "CONISS: A fortran 77 program for stratigraphically constrained cluster analysis by the method of incremental sum of squares." *Computers & Geosciences* 13: 13-35.
- Groffman, P., J. Baron, T. Blett, A. Gold, I. Goodman, L. Gunderson, B. Levinson, M. Palmer, H. Paerl, G. Peterson, N. L. Poff, D. Rejeski, J. Reynolds, M. Turner, K. Weathers and J. Wiens (2006). "Ecological Thresholds: The Key to Successful Environmental Management or an Important Concept with No Practical Application?" *Ecosystems* 9(1): 1-13.
- Gutierrez, A. G., J. J. Armesto, J.-C. Aravena, M. Carmona, N. V. Carrasco, D. A. Christie, M.-P. Peña, C. Perez and A. Huth (2009). "Structural and environmental characterization of old-growth temperate rainforests of northern Chiloe Island, Chile: Regional and global relevance." *Forest Ecology and Management* 258(4): 376-388.
- Haberle, S. and K. Bennett (2004). "Postglacial formation and dynamics of North Patagonian Rainforest in the Chonos Archipelago, Southern Chile." *Quaternary Science Reviews*.
- Haberle, S. G. and K. D. Bennett (2001). "Modern pollen rain and lake mud-water interface geochemistry along environmental gradients in southern Chile." *Review of Palaeobotany and Palynology* 117(1-3): 93-107.
- Hall, K., C. E. Thorn, N. Matsuoka and A. Prick (2002). "Weathering in cold regions: some thoughts and perspectives." *Progress in Physical Geography* 26(4): 577-603.
- Harada, N., U. Ninnemann, C. B. Lange, M. E. Marchant, M. Sato, N. Ahagon and S. Pantoja (2013). "Deglacial-Holocene environmental changes at the Pacific entrance of the Strait of Magellan." *Palaeogeography, Palaeoclimatology, Palaeoecology* 375: 125-135.
- Heusser, C. J. (1971). *Pollen and spores of Chile, Modern types of the Pteridophyta, Gymnospermae, and Angiospermae*. USA.
- Heusser, C. J. (1989). "Late Quaternary vegetation and climate of southern Tierra del Fuego." *Quaternary Research* 31: 396-406.
- Heusser, C. J. (1990). "Late-glacial and Holocene vegetation and climate of subantarctic South America." *Review of Palaeobotany and Palynology* 65: 9-15.
- Heusser, C. J. (1993). "Late quaternary Forest-Steppe contact zone, Isla Grande de Tierra del Fuego, Subantarctic South America." *Quaternary Science Reviews* 12: 169-177.
- Heusser, C. J. (1994). "Paleoindians & fire during the Late Quaternary in southern South América." *Revista Chilena de Historia Natural* 67: 435-443.
- Heusser, C. J. (1995a). "Palaeoecology of a *Donatia-Astelia* cushion bog, Magellanic Moorland-Subantarctic Evergreen Forest transition, southern Tierra del fuego, Argentina." *Review of Palaeobotany and Palynology* 89: 429-440.
- Heusser, C. J. (1995b). "Three Late Quaternary pollen diagrams from southern Patagonia & their palaeoecological implications." *Palaeogeography, Palaeoclimatology, Palaeoecology* 118: 1-24.

- Heusser, C. J. (1998). "Deglacial paleoclimate of the American sector of the Southern Ocean: late glacial-Holocene records from the latitude of Canal Beagle (55°S), Argentine Tierra del Fuego." *Palaeogeography, Palaeoclimatology, Palaeoecology* 141: 277-301.
- Heusser, C. J. (2003). *Ice Age Southern Andes. A chronicle of paleocological events*. Amsterdam, The Netherlands, Elsevier B.V.
- Heusser, C. J., L. E. Heusser, T. V. Lowell, A. Moreira and S. Moreira (2000). "Deglacial palaeoclimate at Puerto del Hambre, subantarctic Patagonia, Chile." *Journal of Quaternary Science* 15: 101-114.
- Heusser, C. J. and J. Rabassa (1987). "Cold climatic episode of Younger Dryas age in Tierra del Fuego." *Nature* 328: 609 - 611.
- Hewitt, G. (2000). "The genetic legacy of the Quaternary ice ages." *Nature* 405(6789): 907-913.
- Hicks, S. (1977). "Modern Pollen Rain in Finnish Lapland Investigated by Analysis of Surface Moss Samples." *New Phytologist* 78(3): 715-734.
- Hicks, S., E. Bozilova, K. Dambach, R. Drescher-Schneider and M. Latalowa (1998). "Sampling methodologies for the collection of modern pollen data and related vegetation and environment." *Paläoklimaforschung* 27(141-144).
- Higuera, P. (2008). CharAnalysis and Monte Carlo Age-Depth programs. <http://charanalysis.googlepages.com/>.
- Hijmans, R. J., S. E. Cameron, J. L. Parra, P. G. Jones and A. Jarvis (2005). "Very high resolution interpolated climate surfaces for global land areas." *International Journal of Climatology* 25(15): 1965-1978.
- Hill, M. O. and H. G. Gauch, Jr. (1980). "Detrended correspondence analysis: An improved ordination technique." *Vegetatio* 42(1-3): 47-58.
- Hinojosa, L. F. and C. Villagrán (1997). "Historia de los bosques del sur de Sudamérica, I: antecedentes paleobotánicos, geológicos y climáticos del Terciario del cono sur de América." *Revista Chilena de Historia Natural* 70(2): 225-240.
- Holdridge, L. R. (1947). "Determination of World Plant Formations From Simple Climatic Data." *Science* 105(2727): 367-368.
- Holgate, M. (1961). "Vegetation and soils in the south Chilean islands." *The Journal of Ecology* 49(3): 559-580.
- Huber, U. and V. Markgraf (2003a). "European impact on fire regimes & vegetation dynamics at the steppe-forest ecotone of southern Patagonia." *The Holocene* 13: 567-579.
- Huber, U. and V. Markgraf (2003b). "Holocene fire frequency and climate change at Rio Rubens Bog, southern Patagonia." *Fire and Climatic Change in Temperate Ecosystems of the Western Americas*. T. Veblen, W. L. Baker, G. Montenegro and T. W. Swetnam (eds.). New York, Springer. 160: 357-380.
- Huber, U., V. Markgraf and F. Schäbitz (2004). "Geographical & temporal trends in Late Quaternary fire histories of Fuego-Patagonia, South America." *Quaternary Science Reviews* 23: 1079-1097.

- Huber, U. M. (2001). Linkage among climate, vegetation and fire in Fuego-Patagonia during the Late-glacial and Holocene, University of Colorado at Boulder, USA. Unpublished PhD thesis.
- Hulton, N. R. J., R. S. Purves, R. D. McCulloch, D. E. Sugden and M. J. Bentley (2002). "The Last Glacial Maximum and deglaciation in southern South America." *Quaternary Science Reviews* 21(1-3): 233-241.
- Huntley, B. (1996). "Quaternary palaeoecology and ecology." *Quaternary Science Reviews* 15(5-6): 591-606.
- INE "Instituto Nacional de Estadísticas." <http://www.ine.cl/>.
- Jackson, S. T. and R. K. Booth (2007). "PLANT MACROFOSSIL METHODS AND STUDIES | Validation of Pollen Studies." *Encyclopedia of Quaternary Science*. E. A. Scott and M. J. Cary (eds.). Oxford, Elsevier: 2413-2422.
- Jacobson Jr, G. L. and R. H. W. Bradshaw (1981). "The selection of sites for paleovegetational studies." *Quaternary Research* 16(1): 80-96.
- Kaplan, M. R., C. J. Fogwill, D. E. Sugden, N. R. J. Hulton, P. W. Kubik and S. P. H. T. Freeman (2008). "Southern Patagonian glacial chronology for the Last Glacial period and implications for Southern Ocean climate." *Quaternary Science Reviews* 27(3-4): 284-294.
- Kilian, R., O. Baeza, T. Steinke, M. Arevalo, C. Rios and C. Schneider (2007a). "Late Pleistocene to Holocene marine transgression and thermohaline control on sediment transport in the western Magellanes fjord system of Chile (53°S)." *Quaternary International* 161(1): 90-107.
- Kilian, R., H. Biester, J. Behrmann, O. Baeza, M. Fesq-Martin, M. Hohner, D. Schimpf, A. Friedmann and A. Mangini (2006). "Millennial-scale volcanic impact on pristine and superhumid ecosystem." *Geology* 34(8): 609-612.
- Kilian, R., H. Hohner, H. Biester, C. Wallrabe-Adams and C. Stern (2003). "Holocene peat and lake sediment tephra record from the southernmost Andes (53-55°S)." *Rev. Geol. de Chile* 30(47-64).
- Kilian, R. and F. Lamy (2012). "A review of Glacial and Holocene paleoclimate records from southernmost Patagonia (49-55°S)." *Quaternary Science Reviews* 53: 1-23.
- Kilian, R., F. Lamy and H. Arz (2013). "Late Quaternary variations of the southern westerly wind belt and its influences on aquatic ecosystems and glacier extent within the southernmost Andes." *Zeitschrift der Deutschen Gesellschaft für Geowissenschaften* 164(2): 279-294.
- Kilian, R., C. Schneider, J. Koch, F. Fesq-Martin, H. Biester, G. Casassa, M. Arévalo, G. Wendt, O. Baeza and J. Behrmann (2007b). "Palaeoecological constraints on late Glacial and Holocene ice retreat in the Southern Andes (53°S)." *Global and Planetary Change* 59: 49-66.
- Kleinebecker, T. (2007). Patterns and gradients in South Patagonian ombrotrophic peatland vegetation. Mathematisch-Naturwissenschaftlichen Fakultät der Westfälischen Wilhelms-Universität Münster. PhD Thesis.: 116 pages.
- Klemm, J., U. Herzsuh, M. F. J. Pisaric, R. J. Telford, B. Heim and L. A. Pestryakova (2013). "A pollen-climate transfer function from the tundra and taiga vegetation in Arctic Siberia and its applicability to a Holocene record." *Palaeogeography, Palaeoclimatology, Palaeoecology* 386(0): 702-713.

- Kliem, P., D. Enters, A. Hahn, C. Ohlendorf, A. Lisé-Pronovost, G. St-Onge, S. Wastegard and B. Zolitschka (2012). "Lithology, radiocarbon chronology and sedimentological interpretation of the lacustrine record from Laguna Potrok Aike, southern Patagonia." *Quaternary Science Reviews* 71(0): 54-69.
- Lamy, F., R. Kilian, H. A. Arz, J. P. Francois, J. Kaiser, M. Prange and T. Steinke (2010). "Holocene changes in the position and intensity of the southern westerly wind belt." *Nature Geoscience* 3: 695-699.
- Legendre, P. and E. Gallagher (2001). "Ecologically meaningful transformations for ordination of species data." *Oecologia* 129(2): 271-280.
- Legendre, P. L. and H. J. B. Birks (2012). "From classical to canonical ordination." *Tracking Environmental Change Using Lake Sediments*. H. J. B. In: Birks, Lotter, A.F., Juggins, S. & Smol, J.P. (eds) (eds.). Dordrecht, Springer, . Volume 5: Data Handling and Numerical Techniques: pp. 201-248.
- León, R., D. Bran, M. Collantes, J. M. Paruelo and A. Soriano (1998). "Grandes unidades de vegetación de la Patagonia extra andina." *Ecología Austral* 8: 125-144.
- Lieberman, B. (2000). "What Is Paleobiogeography?" *Paleobiogeography*(eds.), Springer US. 16: 1-3.
- Linnaeus, C. (1744). "Oratio de Telluris Habitabilis Incremento." *Et Andreae Celsii... Oratio de Mutationibus Generalioribus quae in superficie corporum coelestium contingunt: Cornelium Haak, Lugduni Batavorum*: 17-84.
- Luebert, F. and P. Plischoff (2006). *Sinopsis bioclimática y vegetacional de Chile*. Santiago, Editorial Universitaria.
- Lyell, C. (1837). *Principles of geology: being an inquiry how far the former changes of the earth's surface are referable to causes now in operation*, J. Kay, jun. & brother.
- MacDonald, G. M., K. D. Bennett, S. T. Jackson, L. Parducci, F. A. Smith, J. P. Smol and K. J. Willis (2008). "Impacts of climate change on species, populations and communities: palaeobiogeographical insights and frontiers." *Progress in Physical Geography* 32(2): 139-172.
- MacDonald, G. M. and K. J. Edwards (1991). "Holocene palynology: I principles, population and community ecology, palaeoclimatology." *Progress in Physical Geography* 15(3): 261-289.
- Mancini, M. (2002). "Vegetation and climate during the Holocene in Southwest Patagonia, Argentina." *Review of Palaeobotany and Palynology* 122: 101-115.
- Mancini, M. V. (1998). "Vegetational changes during the Holocene in the Extra-Andean Patagonia, Argentina." *Palaeogeography, Palaeoclimatology, Palaeoecology* 138: 207-219.
- Mancini, M. V. (2009). "Holocene vegetation and climate changes from a peat pollen record of the forest - steppe ecotone, Southwest of Patagonia (Argentina)." *Quaternary Science Reviews* 28(15-16): 1490-1497.
- Mancini, M. V., M. E. de Porras and F. P. Bamonte (2012). "Southernmost South America steppes: vegetation and its modern pollen-assemblages representation." In: *Steppe Ecosystems: Dynamics, Land Use and Conservation*(eds.): 141-156 pp.

- Manten, A. A. (1967). "Lennart Von Post and the foundation of modern palynology." *Review of Palaeobotany and Palynology* 1(1-4): 11-22.
- Markgraf, V. (1983). "Late and Postglacial Vegetational and Paleoclimatic Changes in Subantarctic, Temperate, and Arid Environments in Argentina." *Palynology* 7: 43-70.
- Markgraf, V. (1991). "Younger Dryas in southern South America?" *Boreas* 20: 63-69.
- Markgraf, V. (1993). "Paleoenvironments & paleoclimates in Tierra del Fuego & Southernmost Patagonia, South America." *Palaeogeography, Palaeoclimatology, Palaeoecology* 102: 53-68.
- Markgraf, V. and H. D'Antoni (1978). *Pollen Flora of Argentina*. University of Arizona Press. Tucson, Arizona.
- Markgraf, V., H. D'Antoni and T. Ager (1981). "Modern pollen dispersal in Argentina." *Palynology* 5: 235-254.
- Markgraf, V. and U. M. Huber (2010). "Late and postglacial vegetation and fire history in Southern Patagonia and Tierra del Fuego." *Palaeogeography, Palaeoclimatology, Palaeoecology* 297(2): 351-366.
- Martin, T. J. and J. Ogden (2006). "Wind damage and response in New Zealand forests: a review." *New Zealand Journal of Ecology* 30(3): 295-310.
- Martínez-Harms, M. J. and R. Gajardo (2008). "Ecosystem value in the Western Patagonia protected areas." *Journal for Nature Conservation* 16(2): 72-87.
- Martinic, M. (1974). "Reconocimiento geográfico y colonización de Ultima Esperanza." *Anales del Instituto de la Patagonia* 5: 5-53.
- McCormac, G., A. G. Hogg, P. G. Blackwell, C. E. Buck, T. F. G. T. F. Higham and P. J. Reimer (2004). "SHCal04 Southern Hemisphere Calibration, 0–11.0 cal kyr BP." *Radiocarbon* 3: 1087-1092.
- McCulloch, R. D., M. J. Bentley, R. S. Purves, N. R. J. Hulton, D. E. Sugden and C. M. Clapperton (2000). "Climatic inferences from glacial and palaeoecological evidence at the last glacial termination, southern South America." *Journal of Quaternary Science* 15: 409-417.
- McCulloch, R. D. and S. J. Davies (2001). "Late-glacial and Holocene palaeoenvironmental change in the central Strait of Magellan, Southern Patagonia." *Palaeogeography, Palaeoclimatology, Palaeoecology* 173: 143-173.
- McCulloch, R. D., C. J. Fogwill, D. E. Sugden, M. J. Bentley and P. W. Kubik (2005). "Chronology of the last glaciation in the central Strait of Magellan and Bahía Inútil, southernmost South America." *Geografiska Annaler* 87A(2): 289-312.
- Meurk, C. D., M. N. Foggo, B. M. Thomson, E. T. J. Bathurst and M. B. Crompton (1994). "Ion-Rich Precipitation and Vegetation Pattern on Subantarctic Campbell Island." *Arctic and Alpine Research* 26(3): 281-289.
- Miller, J. (1976). "The climate of Chile." *Climates of Central and South America*. W. Schwerdtfeger (eds.). Amsterdam, Elsevier: 113-145.

- Moore, D. M. (1979). "Southern oceanic wet-heathlands (including Magallanic moorland)." *Heathlands and Related Shrublands of the World*, A. Descriptive Studies. R. L. Specht (eds.), Elsevier Scientific Publishing Company: 489-497.
- Moore, D. M. and E. Pisano (1997). "Biotic colonization of recently deglaciated areas in Fuego-Patagonia: Phytogeographical considerations." *Anales del Instituto de la Patagonia* 25: 21-46.
- Moreno, P. I., J. P. Francois, C. M. Moy and R. Villa-Martínez (2010). "Covariability of the Southern Westerlies and atmospheric CO₂ during the Holocene." *Geology* 38(8): 727-730.
- Moreno, P. I., J. P. Francois, R. P. Villa-Martinez and C. M. Moy (2009a). "Millennial-scale variability in Southern Hemisphere westerly wind activity over the last 5000 years in SW Patagonia." *Quaternary Science Reviews* 28(1-2): 25-38.
- Moreno, P. I., M. R. Kaplan, J. P. Francois, R. Villa-Martinez, C. M. Moy, C. R. Stern and P. W. Kubik (2009b). "Renewed glacial activity during the Antarctic cold reversal and persistence of cold conditions until 11.5 ka in southwestern Patagonia." *Geology* 37(4): 375-378.
- Moreno, P. I., R. Villa-Martinez, M. L. Cardenas and E. A. Sagredo (2012). "Deglacial changes of the southern margin of the southern westerly winds revealed by terrestrial records from SW Patagonia (52S)." *Quaternary Science Reviews* 41(0): 1-21.
- Morrone, J. J. (2001). "Biogeografía de América Latina y el Caribe." *M&T—Manuales & Tesis SEA*, vol. 3. Zaragoza. 148 pp.
- Mueller-Dombois, D. and H. Ellenberg (1974). *Aims and methods of vegetation ecology*. Nueva York, John Wiley.
- Oberdorfer, E. (1960). "Pflanzensoziologische Studien in Chile - Ein Vergleich mit Europa." *Flora et Vegetatio Mundi* 2: 1-208.
- Odgaard, B. V. (2007). "POLLEN METHODS AND STUDIES | Reconstructing Past Biodiversity Development." *Encyclopedia of Quaternary Science*. E. A. Scott and M. J. Cary (eds.). Oxford, Elsevier: 2508-2514.
- Ortiz-Jaureguizar, E. and G. Cladera (2006). "Paleoenvironmental evolution of southern South America during the Cenozoic." *Journal of Arid Environments* 66(3): 498-532.
- Osborne, B., F. Doris, A. Cullen, R. McDonald, G. Campbell and M. Steer (1991). "*Gunnera tinctoria*: An Unusual Nitrogen-Fixing Invader." *BioScience* 41(4): 224-234.
- Overpeck, J. T., I. T. Webb and I. C. Prentice (1985). "Quantitative interpretation of fossil pollen spectra: dissimilarity coefficients and the method of modern analogs." *Quaternary Research* 23: 87-108.
- Pennington, W. (1986). "Lags in adjustment of vegetation to climate caused by the pace of soil development. Evidence from Britain." *Vegetatio* 67(2): 105-118.
- Perdue, E. M. and J.-F. β. Koprivnjak (2007). "Using the C/N ratio to estimate terrigenous inputs of organic matter to aquatic environments." *Estuarine, Coastal and Shelf Science* 73(1-2): 65-72.
- Pillans, B. and T. Naish (2004). "Defining the Quaternary." *Quaternary Science Reviews* 23: 2271-2282.

- Pisano, E. (1973). "Fitogeografía de la Península de Brunswick. Magallanes. Comunidades mesohigromórficas e higromórficas." *Anales Instituto Patagonia (Chile)* 4: 141-206.
- Pisano, E. (1977). "Fitogeografía de Fuego-Patagonia Chilena. 1: Comunidades vegetales entre las latitudes 52° y 56°S." *Anales del Instituto de la Patagonia* 8: 121-250.
- Pisano, E. (1982). "Comunidades vegetales vasculares de la Isla Hornos." *Anales Instituto Patagonia (Chile)* 13: 125-143.
- Pisano, E. (1983). "The Magellanic Tundra Complex." *Ecosystems of the World. Mires: Swamp, Bog, Fen and Moor-Regional Studies*. A. J. P. e. Gore (eds.). Amsterdam, Elsevier: 295-329.
- Ponce, J. F., A. M. Borromei, J. O. Rabassa and O. Martinez (2011). "Late Quaternary palaeoenvironmental change in western Staaten Island (54.5°S, 64°W), Fuegian Archipelago." *Quaternary International* 233(2): 89-100.
- Prentice, C. I. (1986). "Vegetation responses to past climatic variation." *Vegetatio* 67(2): 131-141.
- Prentice, L. C. (1978). "Modern pollen spectra from lake sediments in Finland and Finnmark, north Norway." *Boreas* 7(3): 131-153.
- Prieto, A. R., S. Stutz and S. Pastorino (1998). "Vegetación del Holoceno en la cueva Las Buitreras, Santa Cruz, Argentina." *Revista Chilena de Historia Natural* 71: 277-290.
- Quintana, F. A. (2009). "Paleoambientes del extremo sur de Santa Cruz: análisis polínico de sedimentos lacustres del Cuaternario Tardío." *Fac. Cienc. Exactas y Nat., Univ. Nac. de Mar del Plata, Argentina PhD Thesis*: 146 pp.
- Ramos, V. and M. C. Ghiglione (2008). "Tectonic Evolution of the Patagonian Andes." in: *The late Cenozoic of Patagonia and Tierra del Fuego*(eds.), Elsevier. *Developments in Quaternary Sciences*, 11: 57-71.
- Razik, S., C. M. Chiessi, O. E. Romero and T. von Dobeneck (2013). "Interaction of the South American Monsoon System and the Southern Westerly Wind Belt during the last 14 kyr." *Palaeogeography, Palaeoclimatology, Palaeoecology* 374(0): 28-40.
- Reimer, P. J., M. G. Baillie, E. Bard, A. Bayliss, J. W. Beck, C. J. Bertrand, P. G. Blackwell, C. E. Buck, G. S. Burr, K. B. Cutler, P. E. Damon, R. L. Edwards, R. G. Fairbanks, M. F. Friedrich, T. P. Guilderson, A. G. Hogg, K. A. Hughen, B. K. Kromer, G. McCormac, S. Manning, C. B. Ramsey, R. W. Reimer, S. Remmele, J. R. Southon, M. Stuiver, S. Talamo, F. W. Taylor, J. van der Plicht and C. E. Weyhenmeyer (2004). "IntCal04 Terrestrial Radiocarbon Age Calibration, 0–26 cal kyr BP." *Radiocarbon* 3: 1029-1058.
- Ritchie, J. C. (1974). "Modern pollen assemblages near the arctic tree line, Mackenzie Delta region, Northwest Territories." *Canadian Journal of Botany* 52(2): 381-396.
- Roig, F. A., J. Anchorena, O. Dollenz, A. M. Faggi and E. Méndez (1985a). "Las comunidades vegetales de la Transecta Botánica de la Patagonia Austral. Primera parte: Área continental." *Transecta Botánica de la Patagonia Austral*. O. Boelcke, Moore, D. M., & Roig, F. A. (eds.) (eds.). Buenos Aires, Conicet, Royal Society, Instituto de la Patagonia: 350-456.
- Roig, F. A., O. Dollenz and E. Méndez (1985b). "La vegetación en los canales." *Transecta botánica de la Patagonia Austral*. O. Boelcke, D. Moore and F. A. Roig (eds.). Buenos Aires, Argentina, Consejo Nacional de Investigaciones Científicas y Técnicas: 457-519.

- Rull, V. (2010). "Ecology and Palaeoecology: Two Approaches, One Objective." *The Open Ecology Journal* 5: 1-5.
- Ruthsatz, B. and C. Villagrán (1991). "Vegetation pattern and soil nutrients of a Magellanic moorland on the Cordillera de Piuchué, Chiloë Island, Chile." *Revista Chilena de Historia Natural* 64: 461-478.
- Sagredo, E. A., P. I. Moreno, R. Villa-Martinez, M. R. Kaplan, P. W. Kubik and C. R. Stern (2011). "Fluctuations of the Ultima Esperanza ice lobe (52 degrees S), Chilean Patagonia, during the last glacial maximum and termination 1." *Geomorphology* 125(1): 92-108.
- Schäbitz, F., M. Wille, J.-P. Francois, T. Haberzettl, F. Quintana, C. Mayr, A. Lücke, C. Ohlendorf, V. Mancini, M. M. Paez, A. R. Prieto and B. Zolitschka (2013). "Reconstruction of palaeoprecipitation based on pollen transfer functions – the record of the last 16 ka from Laguna Potrok Aike, southern Patagonia." *Quaternary Science Reviews* 71: 175-190.
- Schaefer, J. M., G. H. Denton, D. A. Barrell, S. Ivy-Ochs, P. W. Kubik, B. G. Andersen, F. M. Phillips, T. V. Lowell and C. Schlüchter (2006). "Near-Synchronous Interhemispheric Termination of the Last Glacial Maximum in Mid-Latitudes." *Science* 312: 1510-1513.
- Schimpf, D., R. Kilian, A. Kronz, K. Simon, C. Spötl, G. Wörner, M. Deininger and A. Mangini (2011). "The significance of chemical, isotopic, and detrital components in three coeval stalagmites from the superhumid southernmost Andes (53°) as high-resolution palaeo-climate proxies." *Quaternary Science Reviews* 30(3-4): 443-459.
- Schmithüsen, J. (1956). "Die raumliche Ordnung der chilenischen Vegetation." *Boner Geogr. Abh* 17: 3-86.
- Schneider, C. and D. Gies (2004). "Effects of El Niño-Southern Oscillation on Southernmost South America precipitation at 53°S revealed from NCEP-NCAR reanalyses & Weather Station Data." *International Journal of Climatology* 24: 1057- 10765.
- Schneider, C., M. Glaser, R. Kilian, A. Santana, N. Butorovic and G. Casassa (2003). "Weather observations across the southern Andes at 53°S." *Physical Geography* 24: 97-119.
- Schneider, C. A., W. S. Rasband and K. W. Eliceiri (2012). "NIH Image to ImageJ: 25 years of image analysis." *Nat Meth* 9(7): 671-675.
- Schroeder, M. J. and C. C. Buck (1970). Chapter 6: General winds. *Fire weather: a guide for application of meteorological information to forest fire control operations.*, U.S. Department of agriculture-Forest service. *Agriculture Handbook* (360): 229.
- Seppä, H. and K. D. Bennett (2003). "Quaternary pollen analysis: recent progress in palaeoecology and palaeoclimatology." *Progress in Physical Geography* 27(4): 548-579.
- SERNAGEOMIN (2003). *Mapa Geológico de Chile: versión digital*. Santiago, Servicio Nacional de Geología y Minería, *Publicación Geológica Digital*, No. 4.
- Shulmeister, J., I. Godwin, J. Renwick, K. Harle, L. Armond, M. S. McGlone, E. Cook, J. Dodson, P. P. Hesse, P. Mayewski and M. Curran (2004). "Southern Hemisphere Westerlies in the Australasian sector over the last glacial cycle: a synthesis." *Quaternary International* 118-119: 23-53.

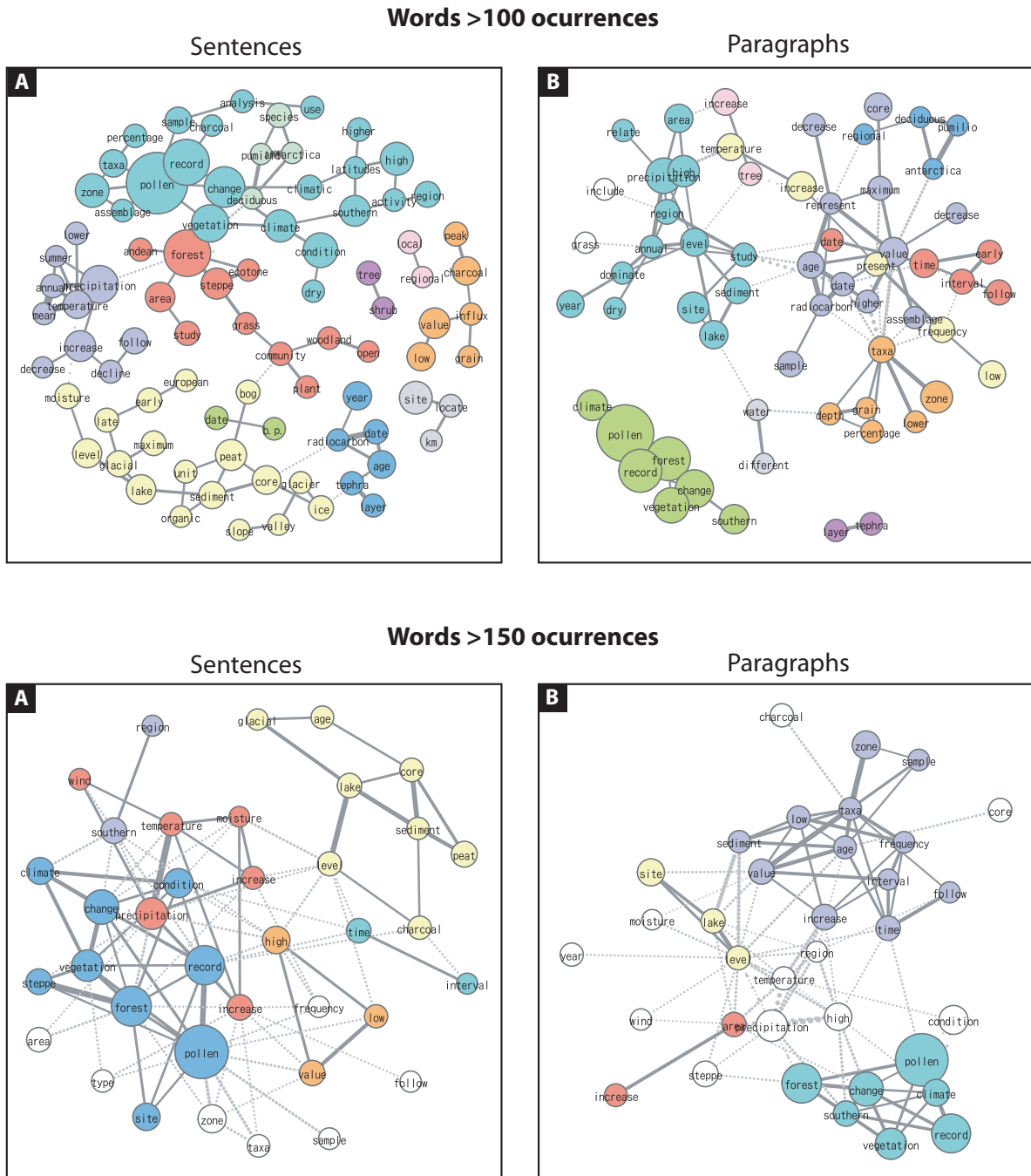
- Smith-Ramirez, C. and J. J. Armesto (1994). "Flowering and Fruiting Patterns in the Temperate Rainforest of Chiloe, Chile--Ecologies and Climatic Constraints." *Journal of Ecology* 82(2): 353-365.
- Soler, R., G. Martinez Pastur, M. V. Lencinas and M. Rosenfeld (2013). "Variable retention management influences biomass of *Misodendrum* and *Usnea* in *Nothofagus pumilio* southern Patagonian forests." *New Zealand Journal of Botany*: 1-12.
- Stockmarr, J. (1971). "Tablets with spores used in absolute pollen analysis." *Pollen et Spores* 13(4): 615-621.
- Strelin, J. A., G. H. Denton, M. J. Vandergoes, U. S. Ninnemann and A. E. Putnam (2011). "Radiocarbon chronology of the late-glacial Puerto Bandera moraines, Southern Patagonian Icefield, Argentina." *Quaternary Science Reviews* 30(19-20): 2551-2569.
- Stuiver, M., P. J. Reimer and R. W. Reimer (2005). CALIB 6.0. <http://intcal.qub.ac.uk/calib/>.
- Sugden, D. E., M. J. Bentley, C. J. Fogwill, N. R. J. Hulton, R. D. McCulloch and R. S. Purves (2005). "Late-glacial glacier events in southernmost South America: a blend of 'northern' and 'southern' hemispheric climatic signals?" *Geografiska Annaler* 87A(2): 273-288.
- ter Braak, C. J. F. and I. C. Prentice (1988). "A theory of gradient analysis." *Advances in Ecological Research* 18: 272-317.
- ter Braak, C. J. F. and P. Šmilauer (2002). "CANOCO Reference Manual and CanoDraw for Windows User's Guide: software for canonical community ordination (version 4.5). Microcomputer Power."
- Tercero-Bucardo, N. and T. Kitzberger (2004). "Establishment and life history characteristics of the southern South American mistletoe *Misodendrum punctulatum* (Misodendraceae)." *Revista Chilena de Historia Natural* 77: 509-521.
- Thompson, D. W. J. and S. Solomon (2002). "Interpretation of Recent Southern Hemisphere Climate Change." *Science* 296(5569): 895-899.
- Thompson, D. W. J. and J. M. Wallace (2000). "Annular modes in the Extratropical Circulation. Part I: Month-to-Month Variability." *Journal of Climate* 13: 1000-1016.
- Tonello, M. S., M. V. Mancini and H. Seppä (2009). "Quantitative reconstruction of Holocene precipitation changes in southern Patagonia." *Quaternary Research* 72(3): 410-420.
- Trivi, M., L. S. Burry and H. L. D'Antoni (2006). "Modelo de dispersión – depositación del polen actual en Tierra del Fuego, Argentina." *Revista Mexicana de Biodiversidad* 77(89-95).
- Varma, V., M. Prange, U. Merkel, T. Kleinen, G. Lohmann, M. Pfeiffer, H. Renssen, A. Wagner, S. Wagner and M. Schulz (2012). "Holocene evolution of the Southern Hemisphere westerly winds in transient simulations with global climate models." *Clim. Past* 8(2): 391-402.
- Veblen, T. and V. Markgraf (1988). "Steepe expansion in Patagonia?" *Quaternary Research* 30: 331-338.
- Vegas-Vilarrubia, T., V. Rull, E. Montoya and E. Safont (2011). "Quaternary palaeoecology and nature conservation: a general review with examples from the neotropics." *Quaternary Science Reviews* 30(19-20): 2361-2388.

- Vidal, O. and A. Reif (2011). "Effect of a tourist-ignited wildfire on *Nothofagus pumilio* forests at Torres del Paine biosphere reserve, Chile (Southern Patagonia)." *BOSQUE* 32(1): 64-76.
- Villa-Martinez, R. and P. I. Moreno (2007). "Pollen evidence for variations in the southern margin of the westerly winds in SW Patagonia over the last 12,600 years." *Quaternary Research* 68(3): 400-409.
- Villagran, C., J. J. Armesto and R. Leiva (1986). "Recolonizacion postglacial de Chiloe insular: evidencias basadas en la distribucion geografica y los modos de dispersion de la flora." *Revista Chilena de Historia Natural* 59(1): 19-28.
- Villagrán, C. and L. F. Hinojosa (2005). "Esquema biogeográfico de Chile." *Regionalización Biogeográfica en Iberoamérica y Tópicos Afines: Primeras Jornadas Biogeográficas de la Red Iberoamericana de Biogeografía y Entomología Sistemática*. J. Llorente-Bousquets and J. J. Morrone (eds.), Las Prensas de Ciencias, UNAM, Mexico City: 551-557.
- Villalba, R., A. Lara, M. H. Masiokas, R. Urrutia, B. H. Luckman, G. J. Marshall, I. A. Mundo, D. A. Christie, E. R. Cook, R. Neukom, K. Allen, P. Fenwick, J. A. Boninsegna, A. M. Srur, M. S. Morales, D. Araneo, J. G. Palmer, E. Cuq, J. C. Aravena, A. Holz and C. LeQuesne (2013). "Unusual Southern Hemisphere tree growth patterns induced by changes in the Southern Annular Mode." *Nature Geosci* 5(11): 793-798.
- Vitt, D. H., D. G. Horton, N. G. Slack and N. Malmer (1990). "Sphagnum-dominated peatlands of the hyperoceanic British Columbia coast: patterns in surface water chemistry and vegetation." *Canadian Journal of Forest Research* 20(6): 696-711.
- Wagner, A. (2007). Fjord sediments as Late Glacial to Holocene climate archives of the southernmost Andes Chile, 52°S. Geochemical and geophysical analysis of sediment cores. Geology Department, University of Trier. Diploma Thesis: 203 pages.
- WAIS Divide Project Members (2013). "Onset of deglacial warming in West Antarctica driven by local orbital forcing." *Nature* 500(7463): 440-444.
- Waller, M. (2013). "Drought, disease, defoliation and death: forest pathogens as agents of past vegetation change." *Journal of Quaternary Science* 28(4): 336-342.
- Webb, T., III (1986). "Is vegetation in equilibrium with climate? How to interpret late-Quaternary pollen data." *Vegetatio* 67(2): 75-91.
- Wei, H.-c., H.-z. Ma, Z. Zheng, A.-d. Pan and K.-y. Huang (2011). "Modern pollen assemblages of surface samples and their relationships to vegetation and climate in the northeastern Qinghai-Tibetan Plateau, China." *Review of Palaeobotany and Palynology* 163(3-4): 237-246.
- Weischet, W. (1985). "Climatic constraints for the development of the far South of Latin America." *GeoJournal* 11(1): 79-87.
- Whittaker, R. H. (1975). *Communities and ecosystems*. London, Collier Macmillan.
- Whittaker, R. J., K. J. Willis and R. Field (2001). "Scale and species richness: towards a general, hierarchical theory of species diversity." *Journal of Biogeography* 28(4): 453-470.
- Wilkinson, D. M. (1997). "Plant Colonization: Are Wind Dispersed Seeds Really Dispersed by Birds at Larger Spatial and Temporal Scales?" *Journal of Biogeography* 24(1): 61-65.

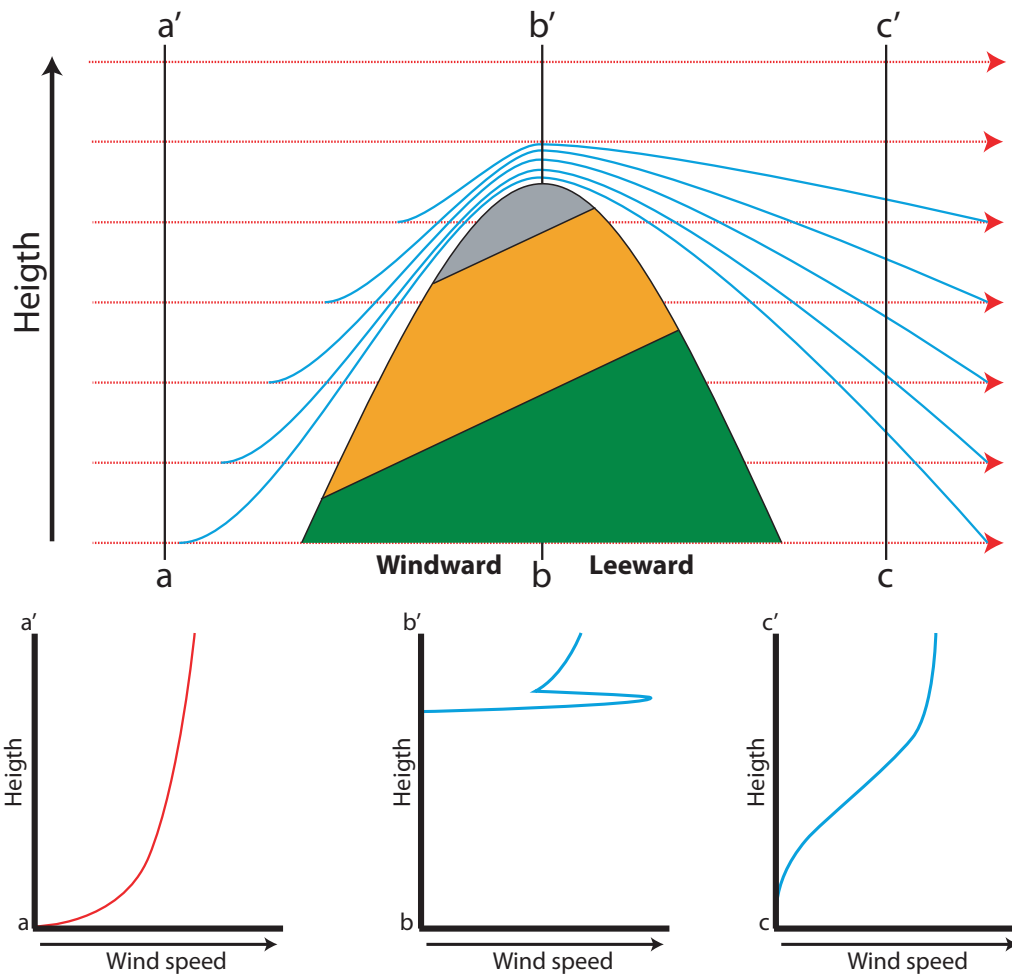
- Wille, M., N. I. Maidana, F. Schäbitz, M. Fey, T. Haberzettl, S. Janssen, A. Lücke, C. Mayr, C. Ohlendorf, G. H. Schleser and B. Zolitschka (2007). "Vegetation and climate dynamics in southern South America: The microfossil record of Laguna Potrok Aike, Santa Cruz, Argentina." *Review of Palaeobotany and Palynology* 146(1-4): 234-246.
- Wille, M. and F. Schäbitz (2009). "Late-glacial and Holocene climate dynamics at the steppe/forest ecotone in southernmost Patagonia, Argentina: the pollen record from a fen near Brazo Sur, Lago Argentino." *Vegetation History and Archaeobotany* 18: 225-234.
- Willis, K. J., R. M. Bailey, S. A. Bhagwat and H. J. B. Birks (2010). "Biodiversity baselines, thresholds and resilience: testing predictions and assumptions using palaeoecological data." *Trends in Ecology & Evolution* 25(10): 583-591.
- Willis, K. J., K. D. Bennett and D. Walker (2004). "Introduction." *Philosophical Transactions of the Royal Society of London. Series B: Biological Sciences* 359(1442): 157-158.
- Willis, K. J. and H. J. B. Birks (2006). "What Is Natural? The Need for a Long-Term Perspective in Biodiversity Conservation." *Science* 314(5803): 1261-1265.
- Willis, K. J., M. Braun, P. Sümegei and A. Tóth (1997). "Does soil change cause vegetation change or vice versa? A temporal perspective from Hungary." *Ecology* 78(3): 740-750.
- Woodward, F. I. (1987). *Climate and Plant Distribution*. Cambridge University Press, London, England.
- Wunderlich, J. and S. Mueller (2003). "High-resolution sub-bottom profiling using parametric acoustics." *International Ocean Systems* 7: 6-11.
- Zolitschka, B., F. Schäbitz, A. Lücke, H. Corbella, B. Ercolano, M. Fey, T. Haberzettl, S. Janssen, N. Maidana, C. Mayr, C. Ohlendorf, G. Oliva, M. M. Paez, G. H. Schleser, J. Soto, P. Tiberi and M. Wille (2006). "Crater lakes of the Pali Aike Volcanic Field as key sites for paleoclimatic and paleoecological reconstructions in southern Patagonia, Argentina." *Journal of South American Earth Sciences* 21(3): 294-309.

8. APPENDIX

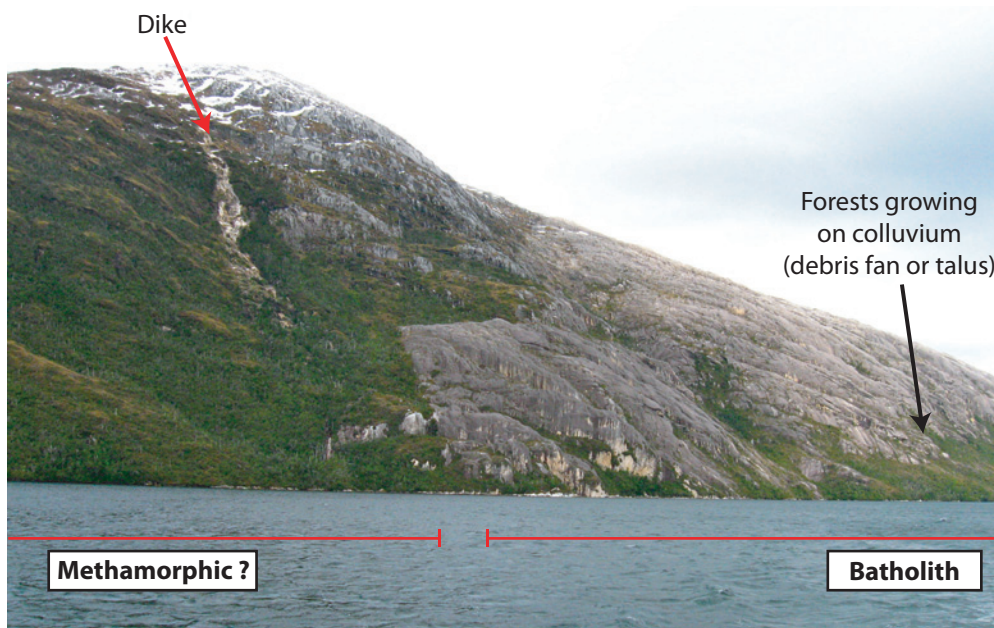
8.1. Appendix A. Figures and Tables



Appendix figure 1. Co-occurrence network from the quantitative content analysis performed on a dataset that include only scientific publications (n=29) related with Quaternary palynological issues of Southern Patagonia (see table 1 for references). The results (co-occurrence networks) are representing words (nodes) from the texts (excluding the bibliography) from the analysed pollen publications-dataset. Two methods and analysed in terms of: sentences (left) and paragraphs (right). The resulting co-occurrence network was measured utilizing a community-modularity clustering method (Clauset *et al.* 2004). The position of the nodes was calculated use Fruchterman-Reingold algorithm (Fruchterman and Reingold)



Appendix figure 2. Idealized wind behaviour scenarios in a landscape with and without topography. Above. Cross section along the landscape in where is indicated with red lines the wind behaviour in a scenario without topography, and with blue lines the wind behaviour in the presence of a mountain (grey). Below. Graph for wind speed versus height along three profiles (a,b,c). The first (a) characterizes the idealized behaviour of the wind speed along the height in the absence of topography. On the contrary the profiles a and b denotes the effect of the topography. Notice the increase of the flow (wind speeds) in response to the topography because the compression of the flux in the top of the hill, and the presence of a wind-sheltered zone on the leeward (Modified from several sources).



Appendix figure 3. (Above) Hanging vegetation occurring in coastal areas and, (Below) an example of the observed absence of vegetation probably related to characteristics of rock type.

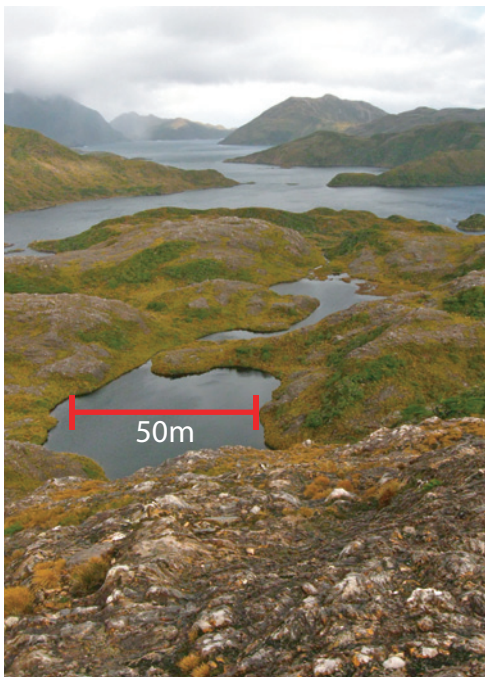
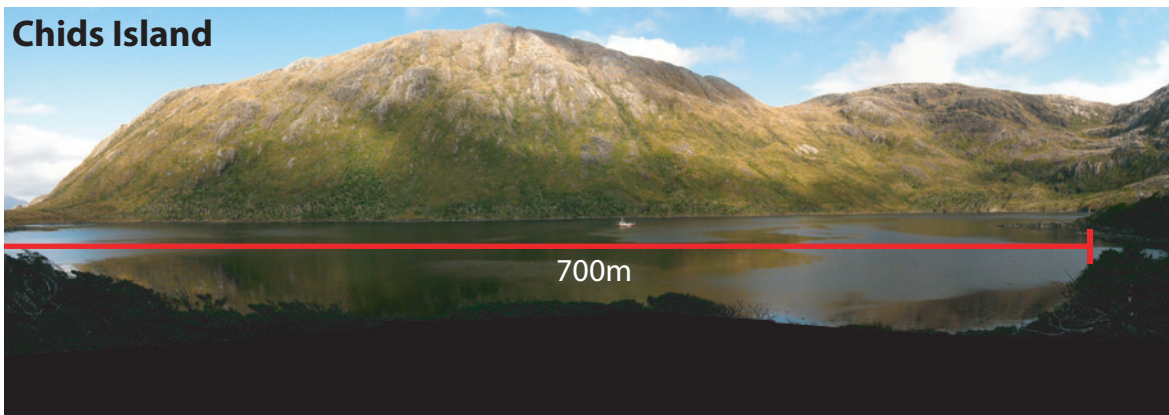


Appendix figure 4. Images showing the area affected by a recent landslide in the area of Bahia Bahamondes, being appreciable the soil covered by *Gunnera magellanica*.

Tamar Island



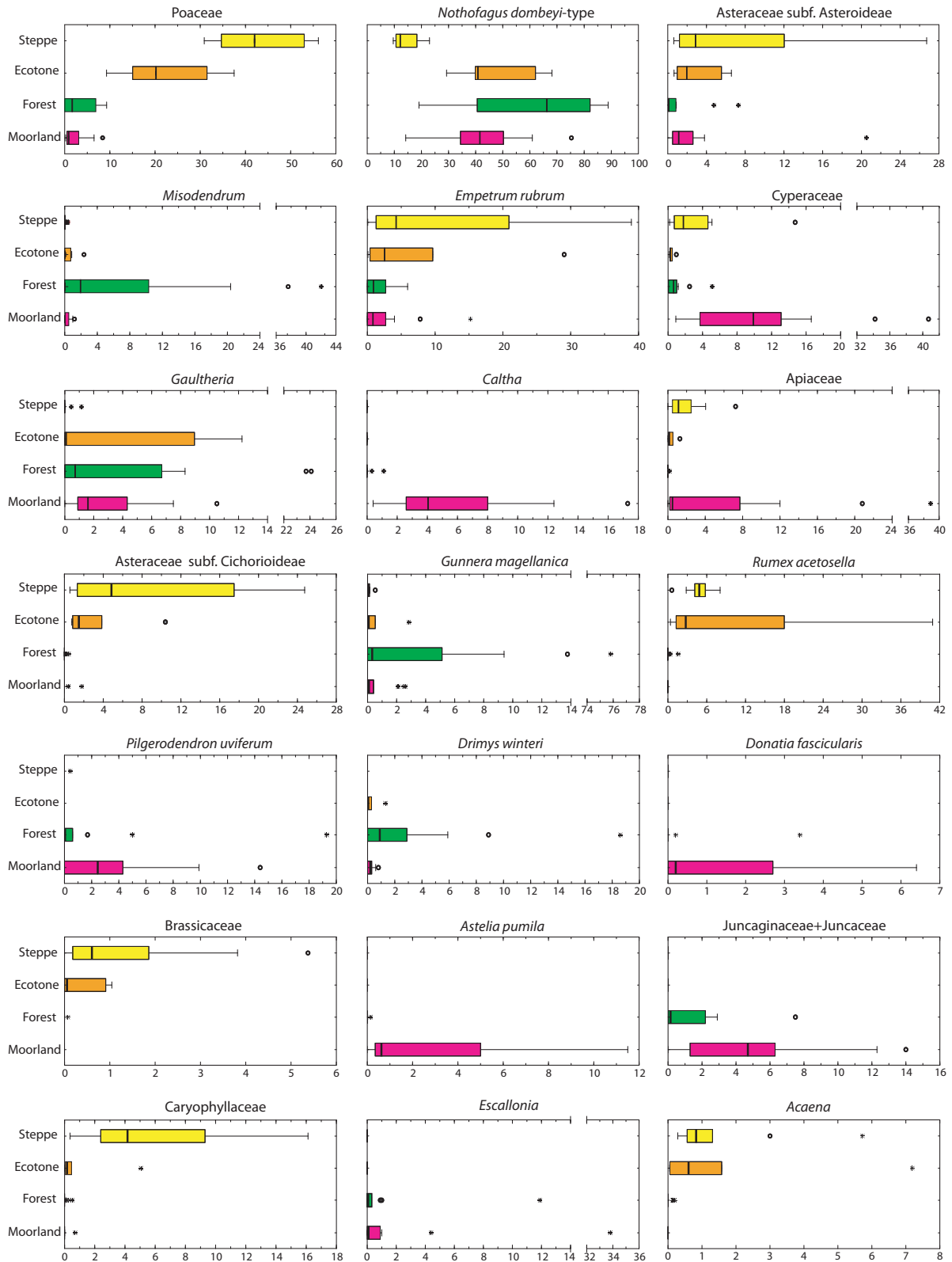
Chids Island



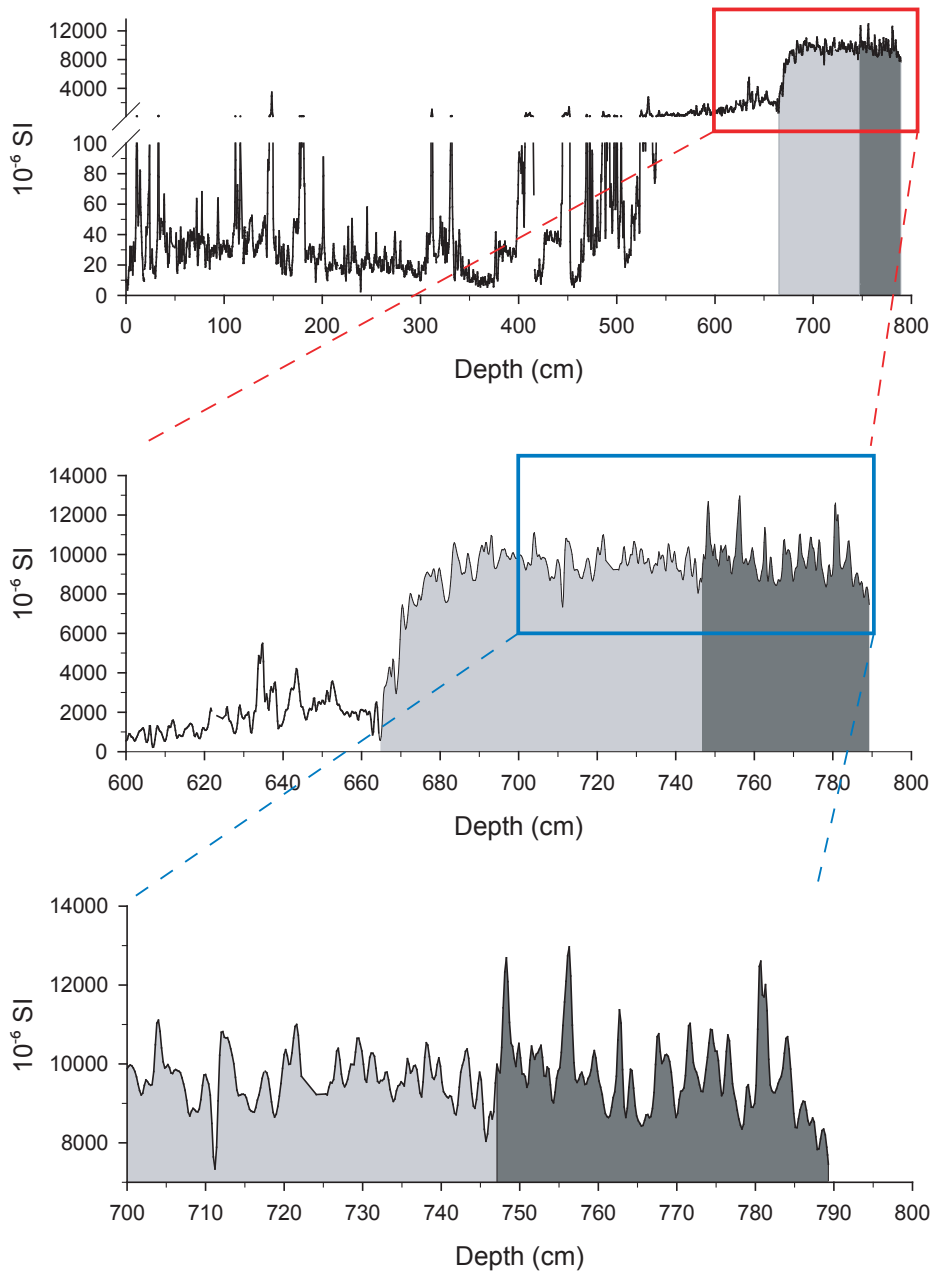
Desolacion Island



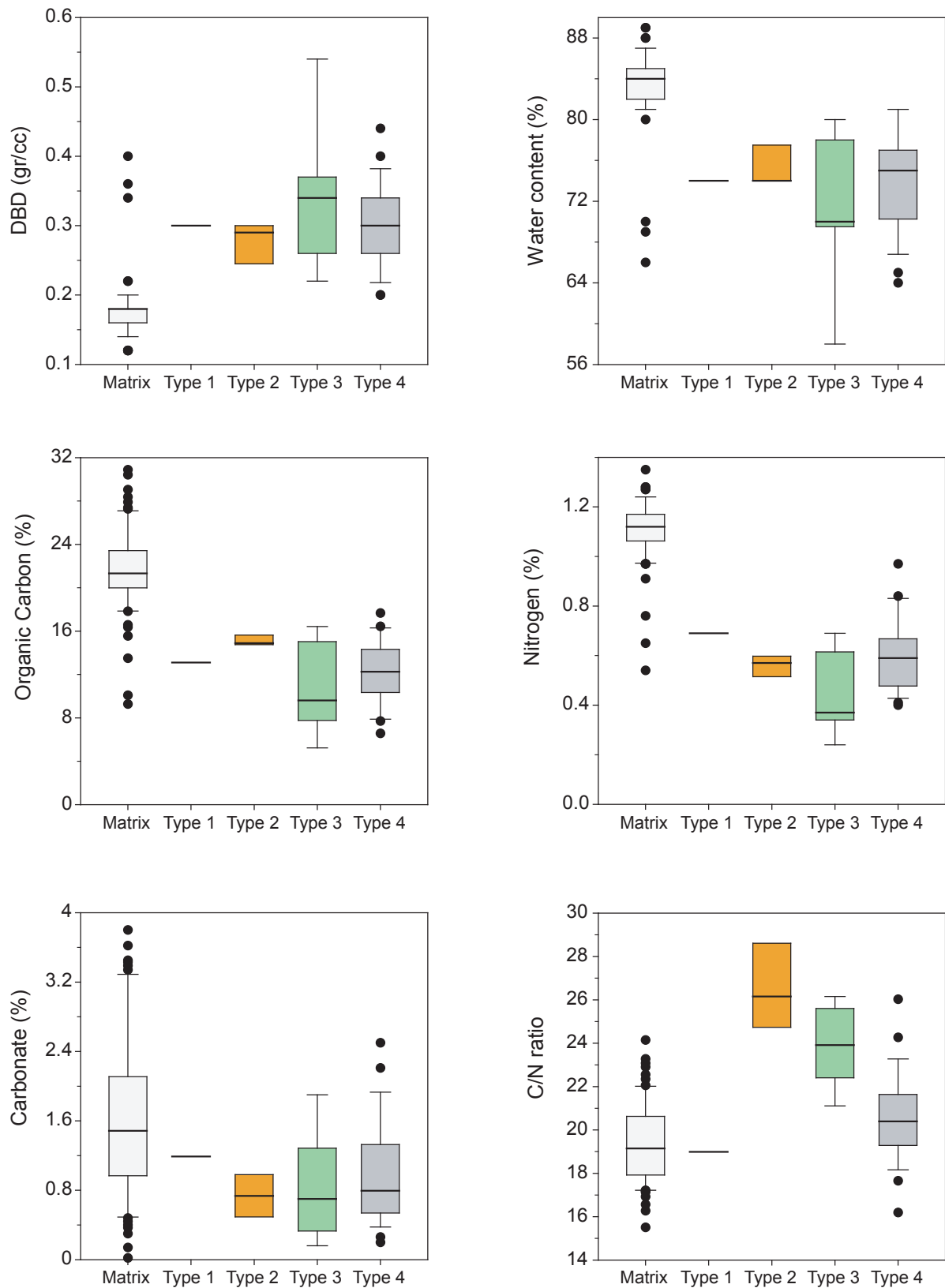
Appendix figure 5. Panoramic view of Tamar lake, Chids bay and Desolacion lake.



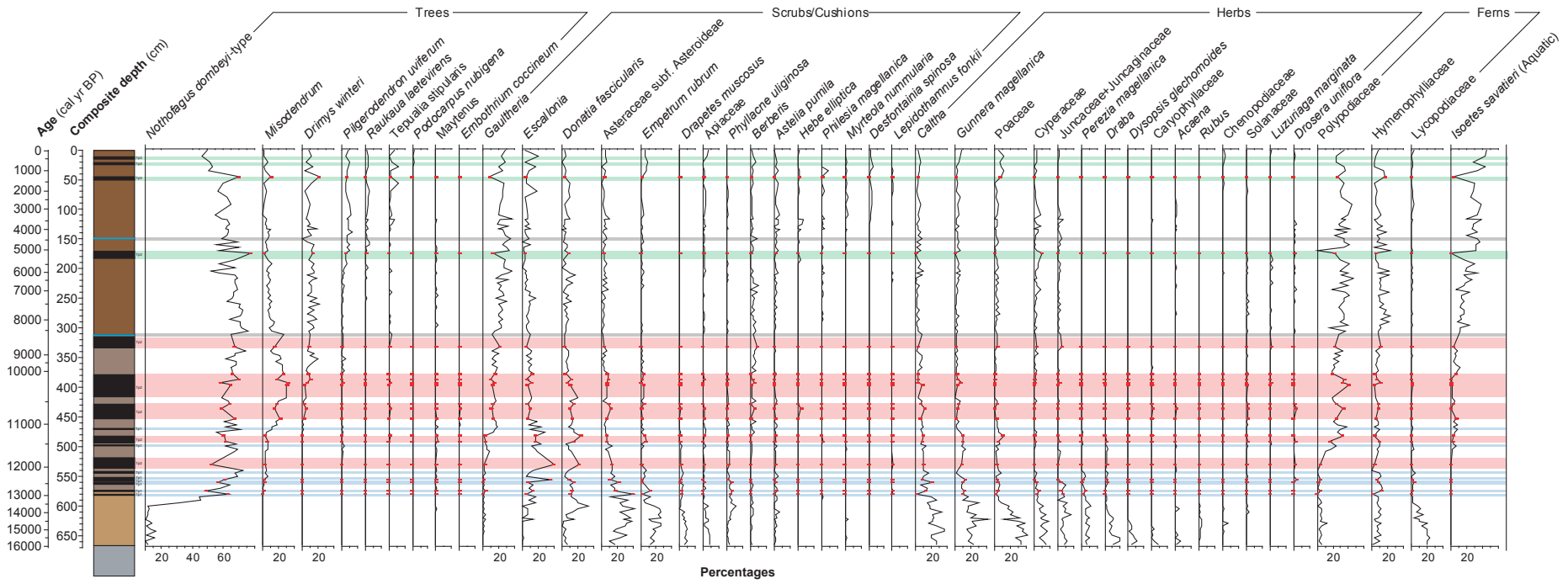
Appendix figure 6. Boxplots of modern pollen rain percentages for selected taxa arranged by dominant plant formations occurring in Southern Patagonia. The box encloses the middle half of the data between the first and third quartiles. The central line denotes the value of the median. The horizontal line extending from the top and bottom of the box indicates the range of typical data values. Outliers are displayed as “o” for outside values and “*” for far outside values. Note changes in scale.



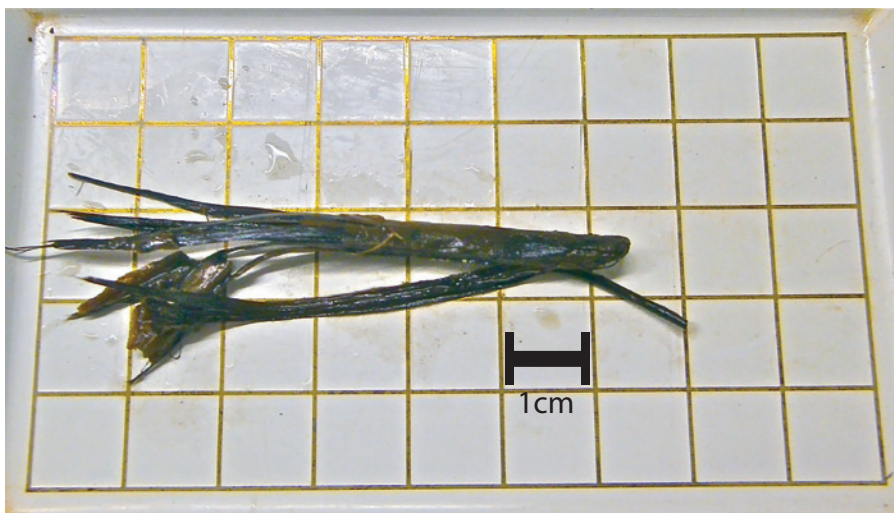
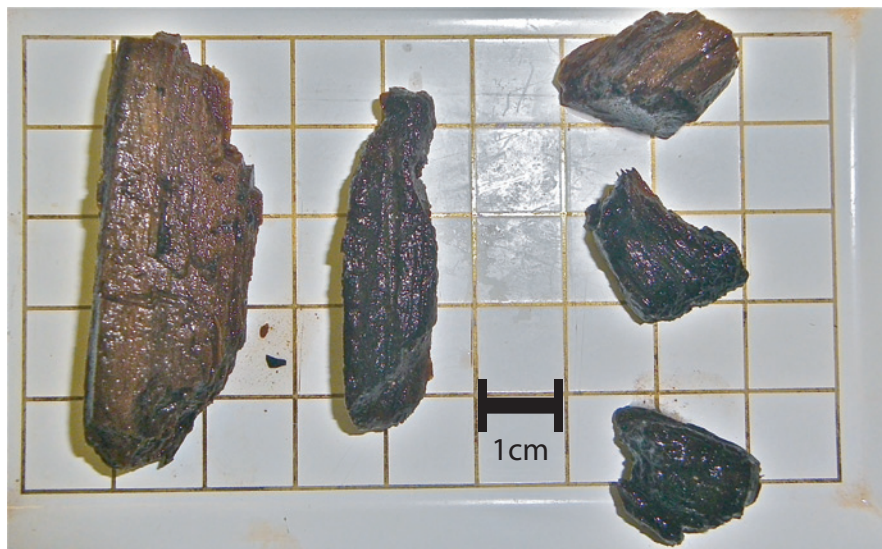
Appendix figure 7. Detail of the magnetic susceptibility results from the Tamar lake sediment core indicating in gray the basal section of the record where predominates clays (light gray) and sandy layers (dark gray).



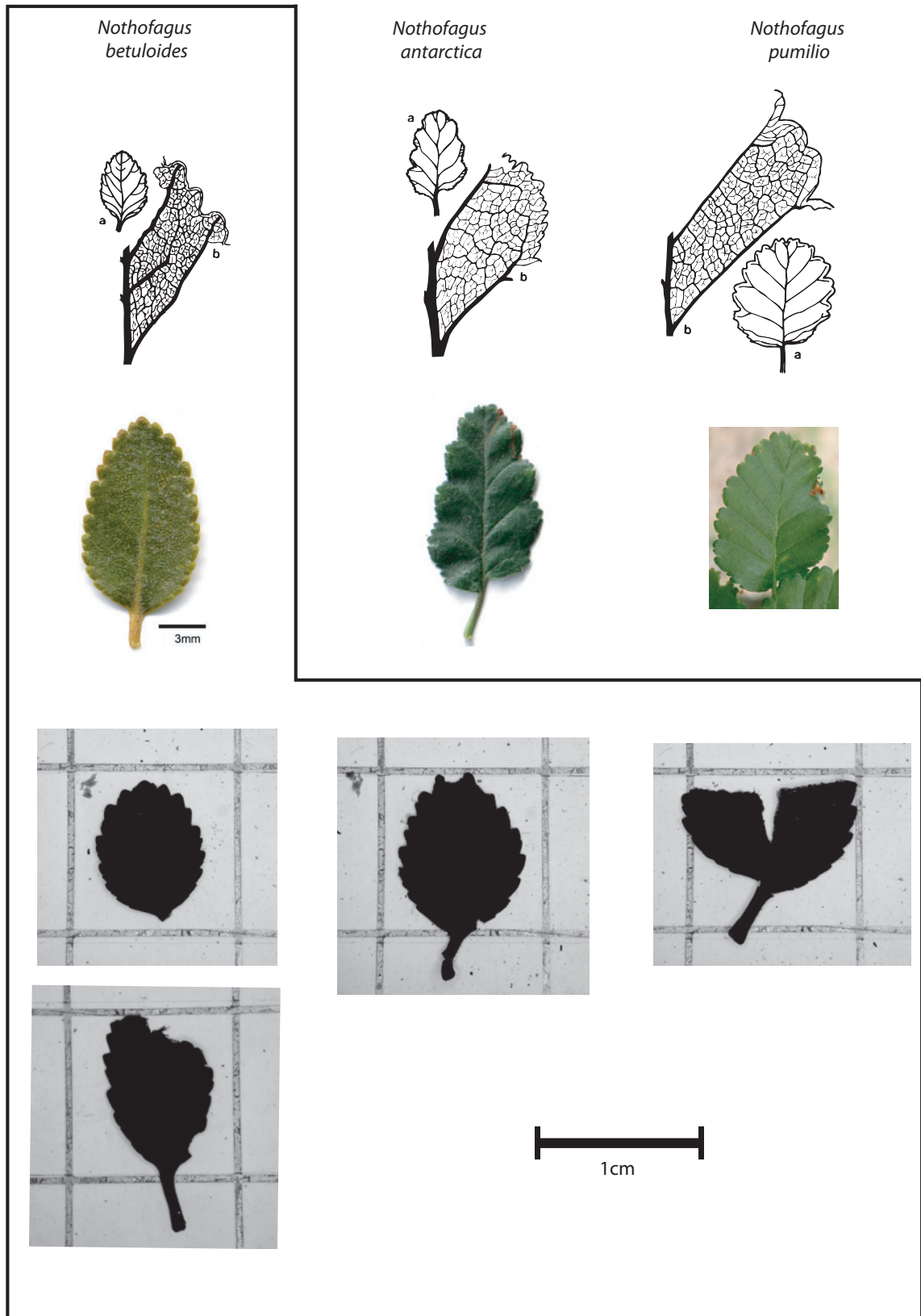
Appendix figure 8. Boxplots of selected geochemical parameters for pelagic sediments (matrix) and LCD's (types 2-4) present within of the sediment core from Tamar lake . The box encloses the middle half of the data between the first and third quartiles. The central line denotes the value of the median. The vertical line extending from the top and bottom of the box indicates the range of typical data values. Outliers are displayed as "o".



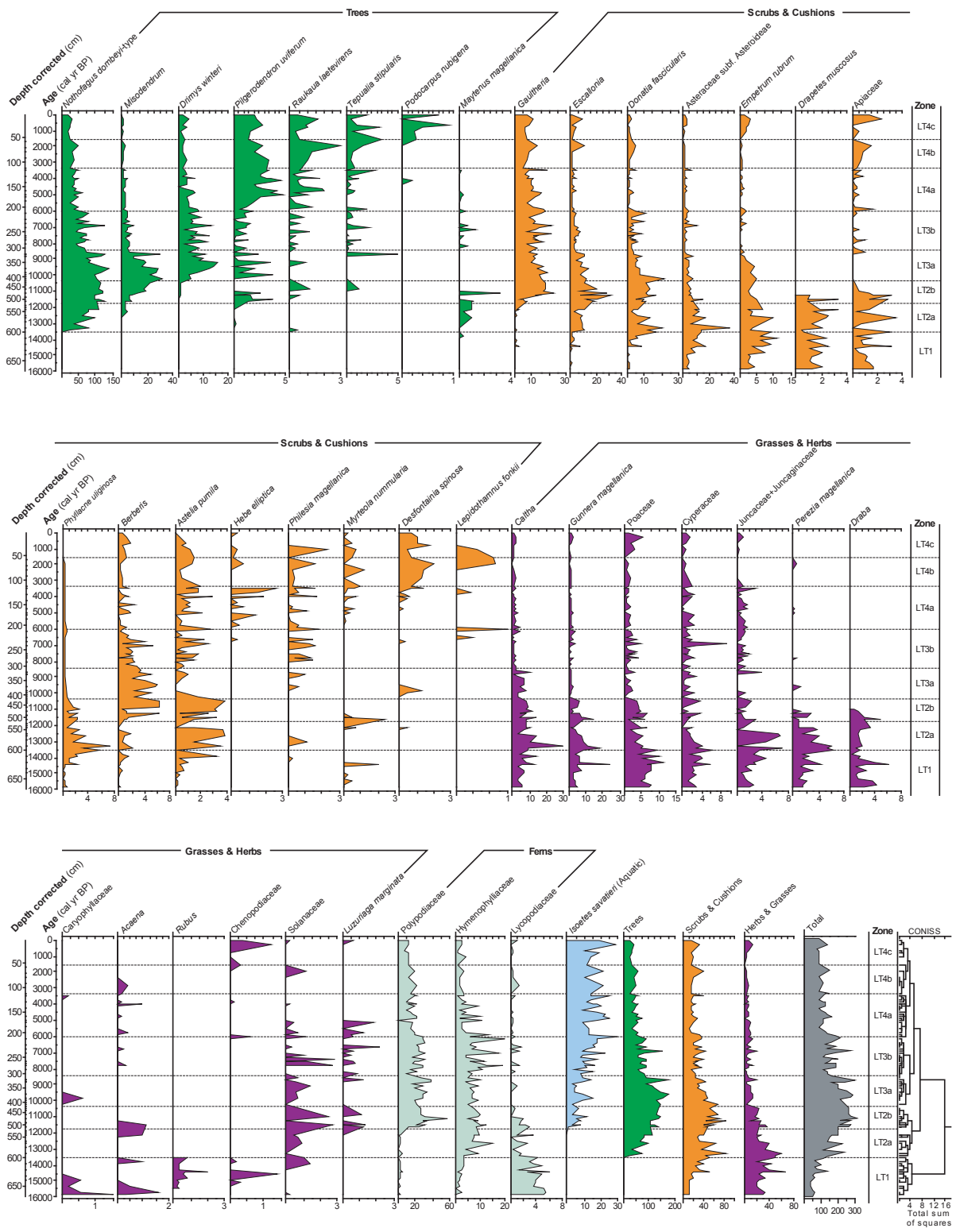
Appendix figure 9. Percentage diagram of the pollen record from Tamar of lake, where are included the samples (in red) associated to mass wasting deposits or light-colored deposits (LCDs). Colour bars blue, red and green denotes the stratigraphic position of LCDs Types 1-3 (respectively).



Appendix figure 10. Plant macrorest found in the mass wasting deposits of Tamar lake sediment core.

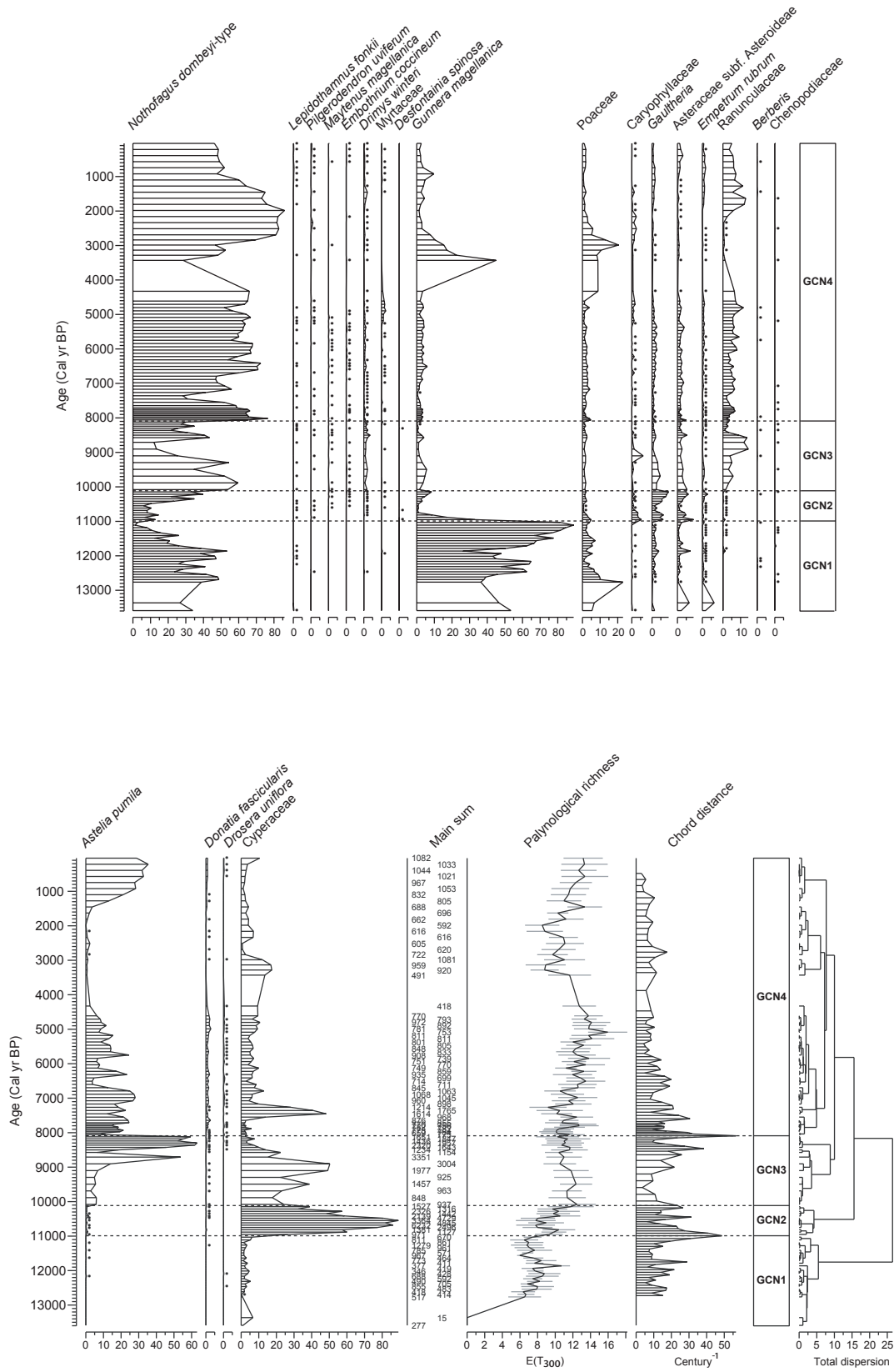


Appendix figure 11. Leaves of *Nothofagus betuloides* found in the mass wasting deposits of Tamar lake sediment core.



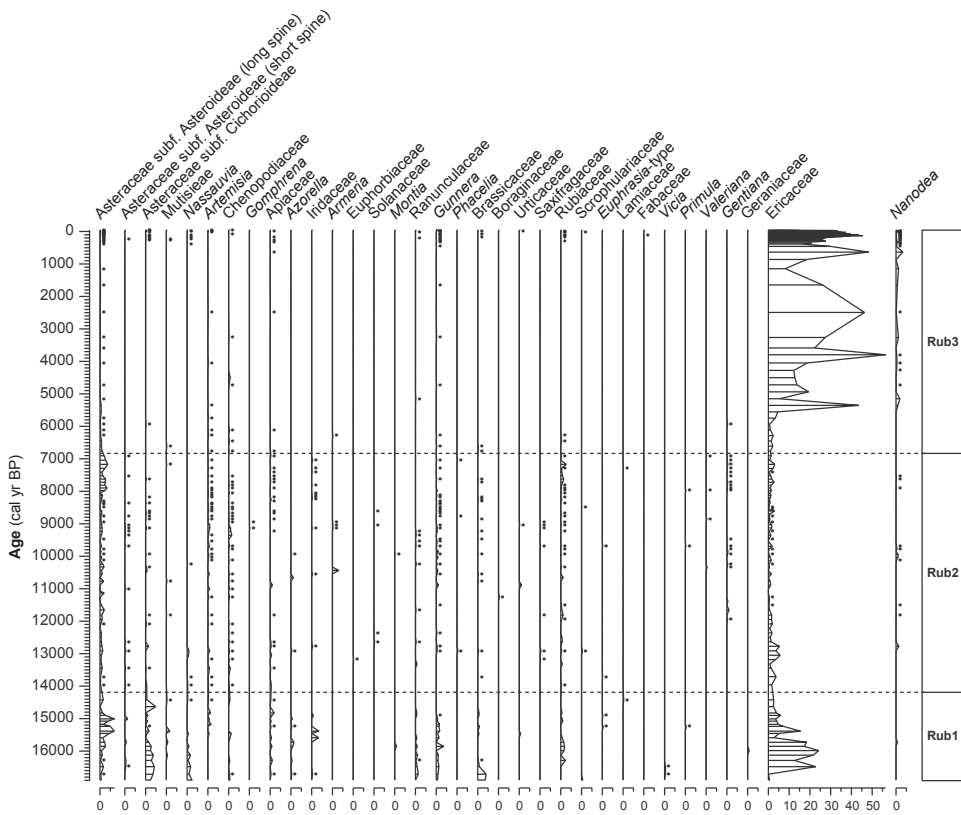
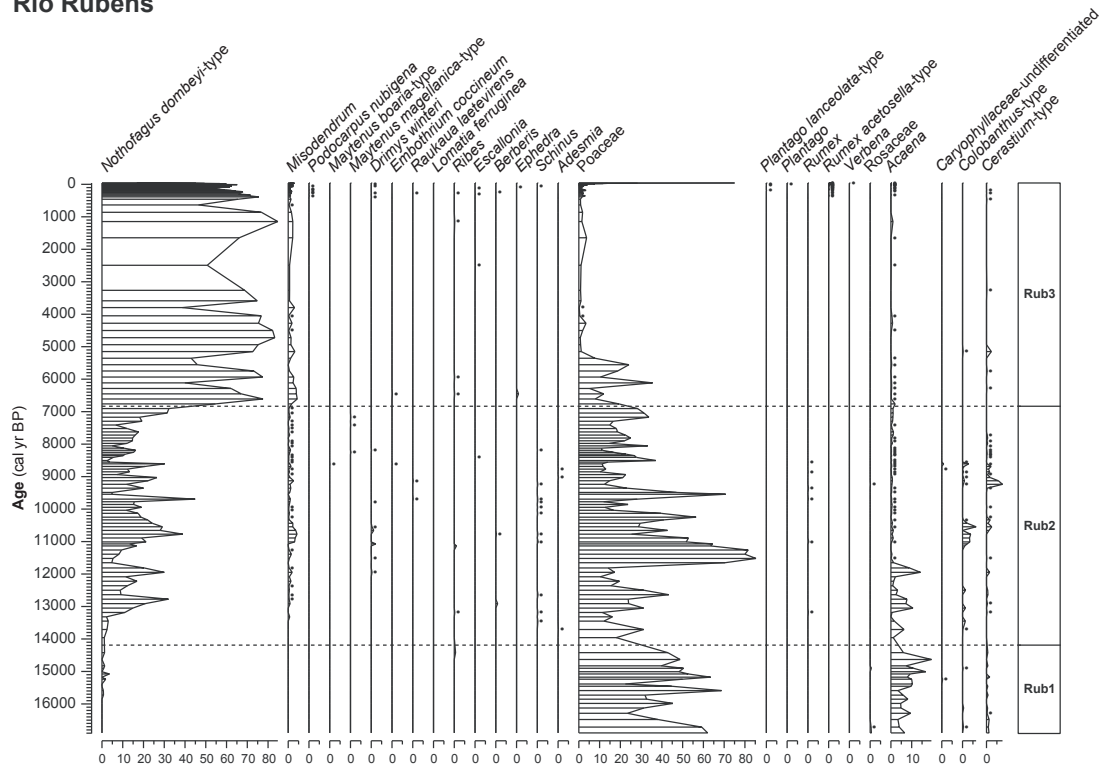
Appendix figure 12. Concentration diagram (grains/cc) including all the taxa from the pollen record of Tamar Lake.

Gran Campo Nevado



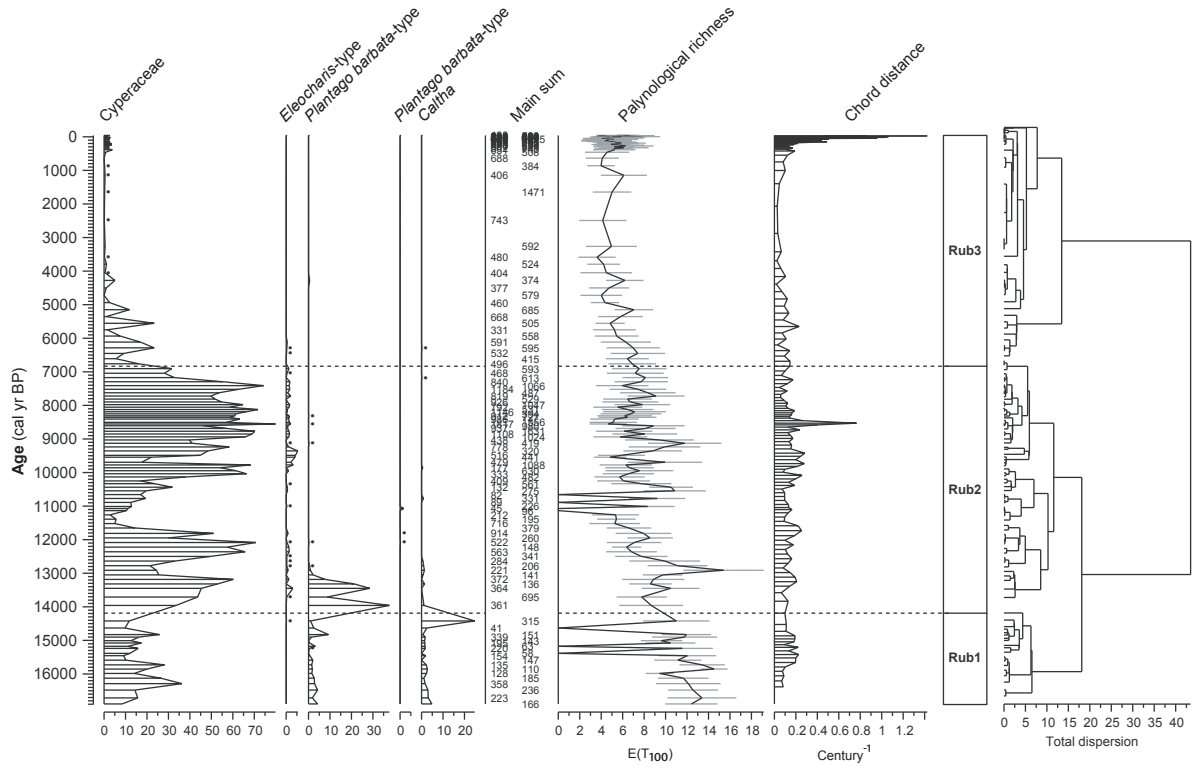
Appendix figure 13. Percentages pollen diagram from Gran Campo Nevado sediment core.

Rio Rubens



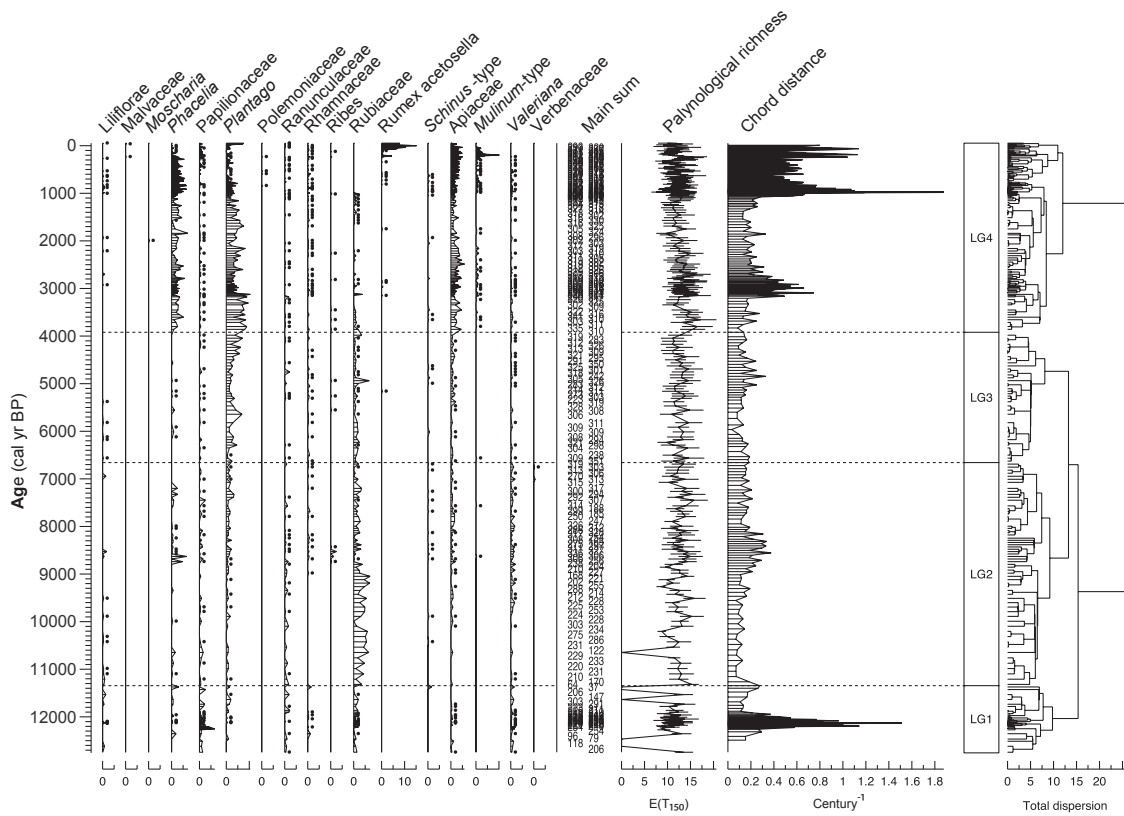
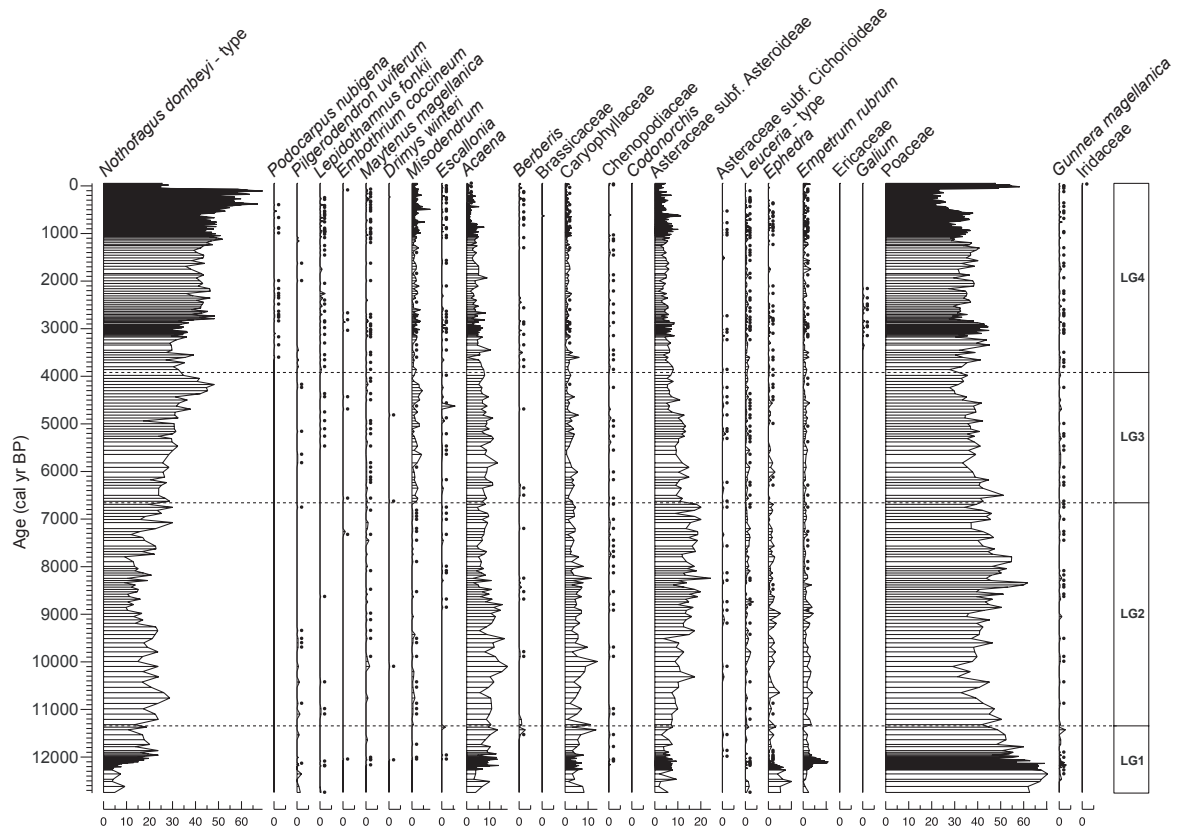
Appendix figure 14. Percentages pollen diagram from Rio Rubens sediment core.

Rio Rubens



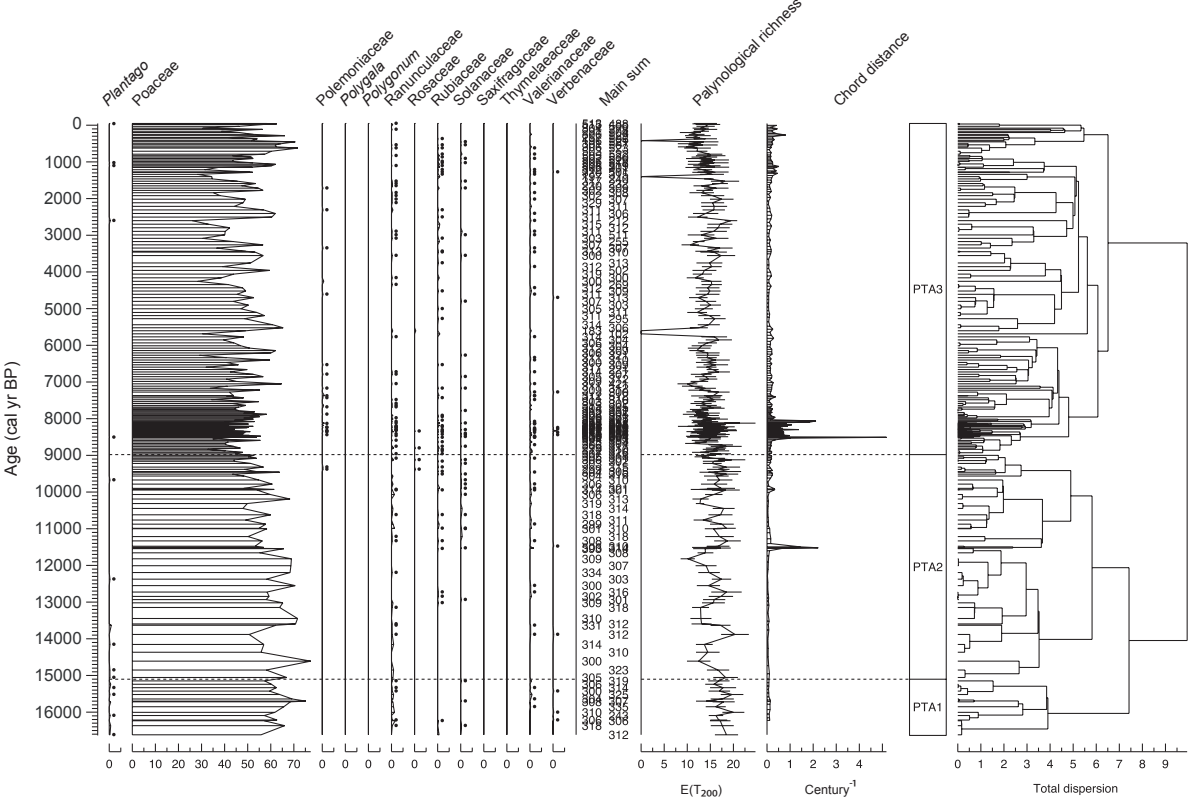
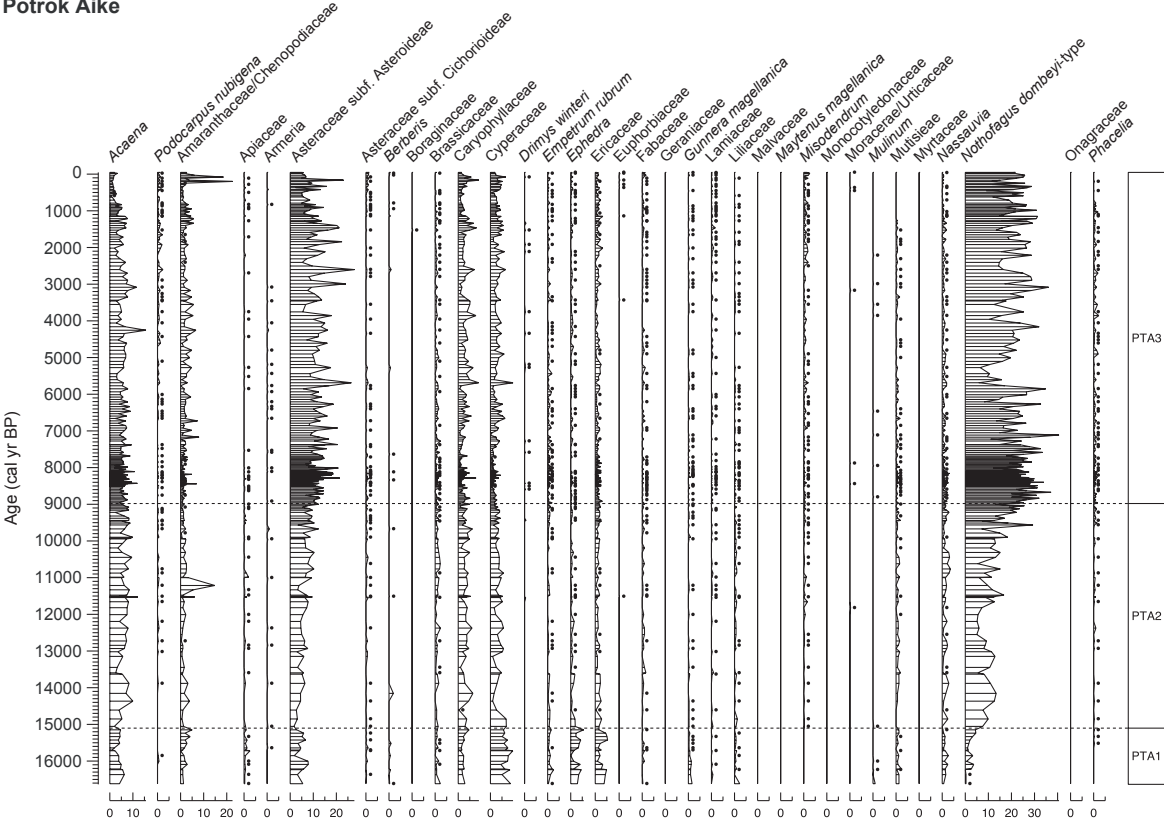
Appendix figure 14. (continue)

Lago Guanaco



Appendix figure 15. Percentages pollen diagram from Lago Guanaco sediment core.

Potrok Aike



Appendix figure 16. Percentages pollen diagram from Potrok Aike sediment core.

Appendix table 1. Chronology of events associated to light-colored deposits (LCDs) present in the sediment core of Tamar Lake

LCDs	Composite depth (cm)	Thickness (cm)	Age (calendar yr BP)
Type I			
1	469.4	1.2	11,156
2	498.5	1.5	11,501
3	543.5	2.5	12,151
4	554.0	4.0	12,280
5	556.8	1.0	12,334
6	562.0	1.5	12,456
7	574.5	2.0	12,757
8	581.0	1.5	12,917
Type II			
1	332.5	19.5	8692
2	415.0	33.8	10,181
3	451.6	21.1	10,624
4	492.8	10.3	11,456
5	535.5	18.0	11,883
Type III			
1	12.6	3.6	380
2	22.2	3.8	655
3	47.4	5.2	1321
4	176.3	11.5	5050
Type IV			
1	6.3	0.8	212
2	8.3	0.8	266
3	30	0.9	875
4	33.5	0.9	981
5	34.5	0.5	997
6	40	1.4	1160
7	42.4	0.5	1232
8	58	1	1583
9	72.6	0.6	2096
10	85.1	0.3	2532
11	95.1	1.3	2835
12	111.9	0.9	3371
13	114.5	1.7	3397
14	116.9	1.2	3434
15	145.4	0.9	4339
16	152.8	0.7	4529

Appendix A. Figures and Tables

17	157.1	1.1	4652
18	158.9	0.3	4710
19	161	1	4752
20	166.5	2.5	4883
21	201.6	0.6	5834
22	211.6	0.6	6201
23	223	0.5	6613
24	226.7	0.9	6711
25	231.2	1.3	6822
26	233.4	0.6	6874
27	246	1	7221
28	253.7	0.5	7387
29	255.4	0.8	7405
30	264.5	1.3	7559
31	275	1.5	7731
32	309.2	1.2	8627
33	333.3	0.8	8693
34	337.2	1.3	8778
35	340.5	1.5	8838
36	464.1	0.5	11,023
37	471.1	0.5	11,192
38	473	1	11,218
39	475	0.7	11,257
40	494.8	1.4	11,472
41	501.5	1.2	11,556
42	503.5	0.7	11,594
43	505	0.8	11,614
44	506	0.7	11,620
45	507.5	0.5	11,649
46	515	1	11,854
47	544.5	0.5	12,164
48	546	0.5	12,193
49	547.5	0.5	12,222
50	548.5	0.5	12,234
51	558.5	0.5	12,369
52	559.5	0.5	12,382
53	563.5	0.5	12,546
54	564.5	0.5	12,559
55	566	0.5	12,588
56	567.8	0.5	12,627
57	570.8	0.5	12,705

8.2. Appendix B. Transfer functions

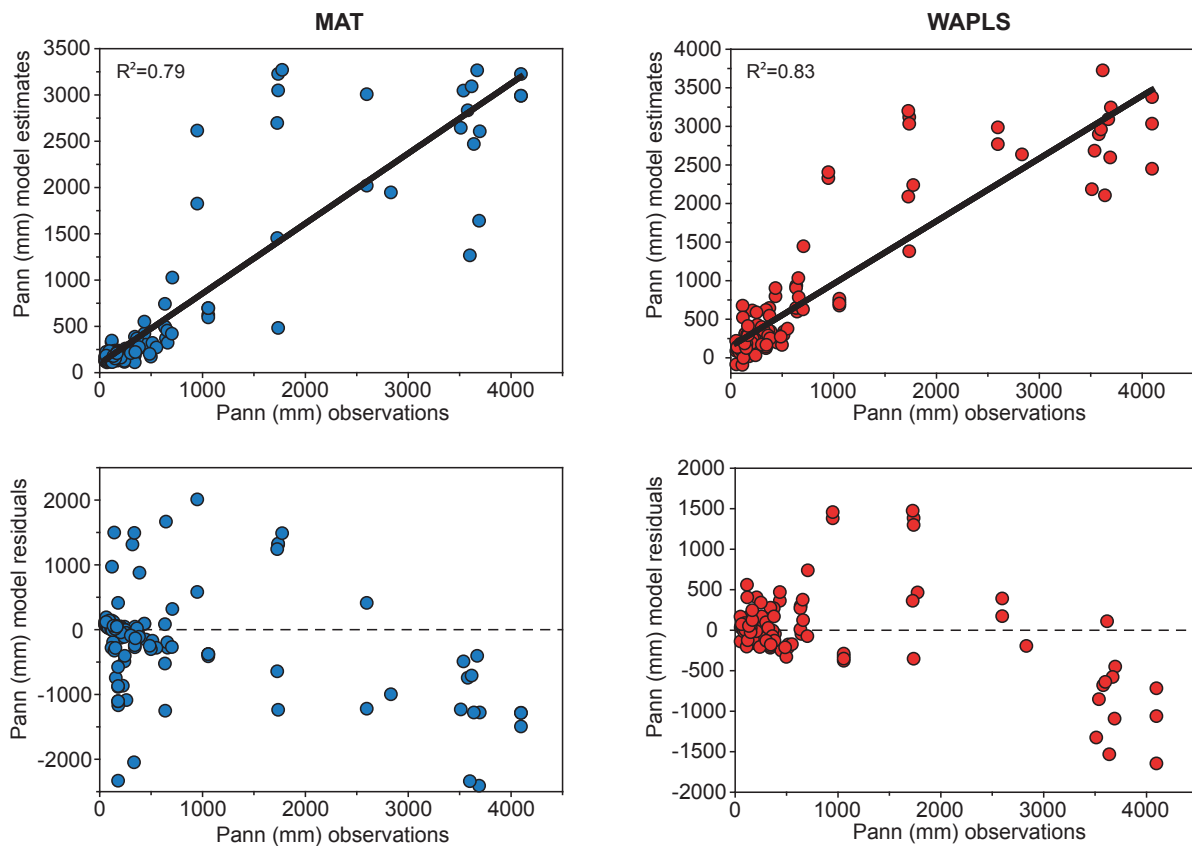
Transfer functions were developed in order to perform quantitative palaeoclimatic reconstructions from selected pollen sites occurring along the west-to-east transect (Figure 12). The dataset used for the development of the transfer function models consists of a modified dataset from Schäbitz *et al.* 2013, within which a new modern pollen-rain samples from the Fjords ($n=23$) is included, as discussed in this thesis, reaching a total of 124 soil surface samples and 41 pollen taxa. The climatic variables of annual Precipitation (Pann) and mean annual Temperatures (Tann), obtained from the WorldClim dataset (Hijmans *et al.* 2005), were used to run the models. A logarithmic transformation was performed on all pollen percentages before developing the transfer functions, in order to stabilize the variance and to reduce the statistical noise. Different transfer function algorithms were tested (MAT = Modern Analogue Technique, WA = Weighted Average and WAPLS = Weighted Average Partial Least Square) in order to find the most appropriate calibration model in a leave-one-out cross-validation procedure. For the MAT the Squared Chord Distance (SCD) and the Squared-Chi-Squared (SCS) algorithms were used for estimating the climate variable, including the incorporation of 10 closest surface samples into the calculation. For determination of the statistically reliable components of each model, the performance data were compared (Appendix table 2). The chosen model shows a high R^2 (coefficient of determination between predicted and observed climate values), low RMSEP (Root Mean Square Error of Prediction) and a low maximum bias. For the regression models the smallest number of useful components were chosen. This was determined by a decrease of less than 2% towards the lower number of components (Birks 1998). Transfer functions were implemented using the program C2 version 1.7.2 (Juggins 2003).

As shown in Appendix table 2, the Modern Analogue Technique (MAT), Weighted Average (WA) and Weighted Average Partial Least Square (WAPLS) algorithms reach good statistical performances for the climatic variable of annual precipitation (Pann). Within these, the best results are displayed by the MAT-SCD ($R^2 = 0.79$), WA-Inv ($R^2 = 0.83$), and WAPLS-C1 ($R^2 = 0.83$). However, the last two models have similar R^2 and RMSEP values, differing only with a slight increase in the maximum values of bias in the WA-Inv approach (Appendix table 2). Therefore, the later results and comparisons are based only on MAT-SCD and WAPLS-C1. On the other hand, the results for the annual temperature (Tann) estimations not reach good statistical performances. The best result was exhibited by the WAPLS-C1 model ($R^2: 0.37$, RMSEP: 0.5 and Max. bias 1.2), but it is clear that its performance is much worse than for the estimation of precipitation. Therefore, because of these statistical uncertainties, the temperature estimates will be not used and discussed in this thesis.

Appendix figure 17 indicates that WAPLS and MAT models have a tendency to underestimate the precipitation at higher ranges (>2500 mm/year), whereas at mid to lower ranges (<2000 mm/year) both models overestimate the precipitation. This feature is clearly observed in the respective residuals for both models (Appendix figure 17), and highlights possible limits and complexities in the performed reconstructions of precipitation based on pollen records. Nevertheless, as was mentioned previously, both models (WAPLS and MAT) reach an adequate statistical performance to develop this kind of quantitative reconstruction.

Appendix table 2. Performance of the reconstruction models, indicating: the coefficient of determination between predicted and observed climate values (R^2), the maximum bias (Max. bias), root mean square error of prediction (RMSEP) and the percentage of change among the components (%Change). The best model within each set of algorithms are indicated in color, namely: MAT (Modern analogue technique), WA (weighted averaging) and WAPLS (Weighted averaging partial least squares regression). For more details see the text.

Model	R^2	Max bias	RMSEP	%Change
MAT				
Squared Chi-squared Distance	0.74	1336	590.7	
Squared Chord Distance	0.79	1072	548.4	
WA				
Classical deshrinking	0.83	1171	556.4	
Inverse deshrinking	0.83	969	513.8	
WAPLS				
Component 1	0.83	931	513.1	...
Component 2	0.88	502	510.8	0.6
Component 3	0.89	541	599.7	-17.4
Component 4	0.90	525	831.0	-38.6
Component 5	0.90	506	1113.2	-33.9



Appendix figure 17. Scatter plot of the predicted precipitation values versus the observations (upper panel) and its respective residuals (lower panel), for the WAPLS and MAT models

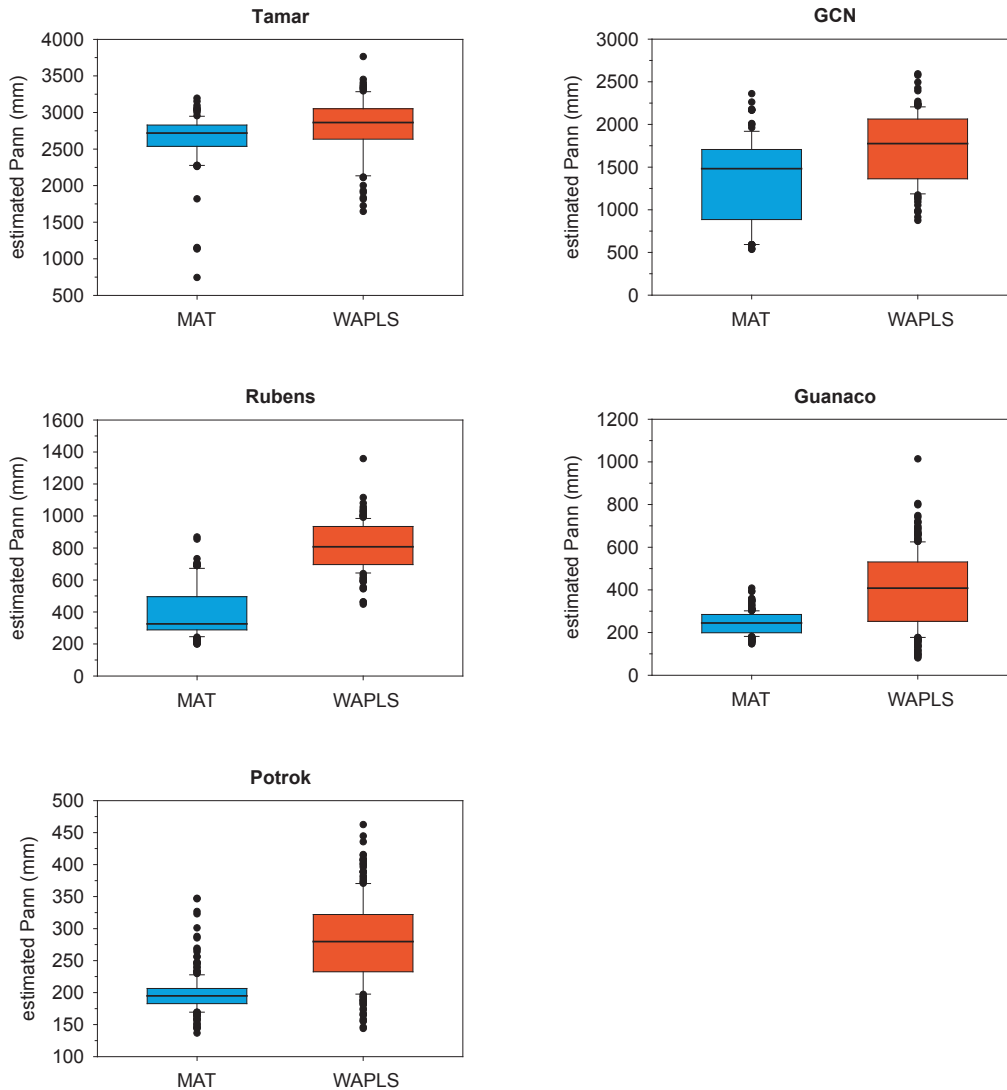
Quantitative climate reconstruction along a west-to-east transect at 53°S

Paleoprecipitation was estimated on selected pollen records located along a west-east transect at ~53°S (Figure 12), using the transfer function models with the best statistical performances: WAPLS and MAT (for details about the models performances, see previous section). The results indicate that estimated precipitation using the MAT algorithm exhibits lower values in comparison with WAPLS (Appendix table 3 & Appendix figure 18). This feature becomes more noticeable in the reconstructions performed on pollen records located in the forest-steppe ecotone (i.e. Rio Rubens and L. Guanaco) and the steppe (i.e. Potrok Aike), where the differences between the models' outcomes (expressed as function of the mean and median) are double (Appendix table 3 & Appendix figure 18). On the other hand, reconstructions using the WAPLS algorithm in L. Guanaco and Potrok Aike show a major dispersion of the data (noticed as function of SD and CV) in comparison with the MAT model (Appendix table 3 & Appendix figure 18). The contrary (higher dispersion of the data in the MAT model than the WAPLS) is observed in the reconstruction performed from GCN and R. Rubens, whereas in the L. Tamar reconstruction the dispersion of the data is similar (Appendix table 3 & Appendix figure 18). Despite these differences between the models, the reconstructed Pann shows an increase in the precipitation towards the present in all the reconstructions (Appendix figure 19-23).

Appendix table 3. Basic statistic parameters for each of the reconstructions (WAPLS and MAT) performed on selected pollen records located along a west-east transect at ~53°S.

	WAPLS			MAT		
	Min/Max	Mean/Median	SD/CV (%)	Min/Max	Mean/Median	SD/CV (%)
Tamar	1647/3764	2792/2862	409/14%	744/3194	2612/2718	407/15%
GCN	874/2592	1717/1775	402/23%	536/2359	1343/1481	503/37%
Rubens	448/1358	814/807	148/18%	199/868	405/325	161/39%
Guanaco	80/1014	402/408	169/42%	147/408	243/244	51/21%
Potrok	144/462	279/279	64/22%	136/347	198/194	30/15%

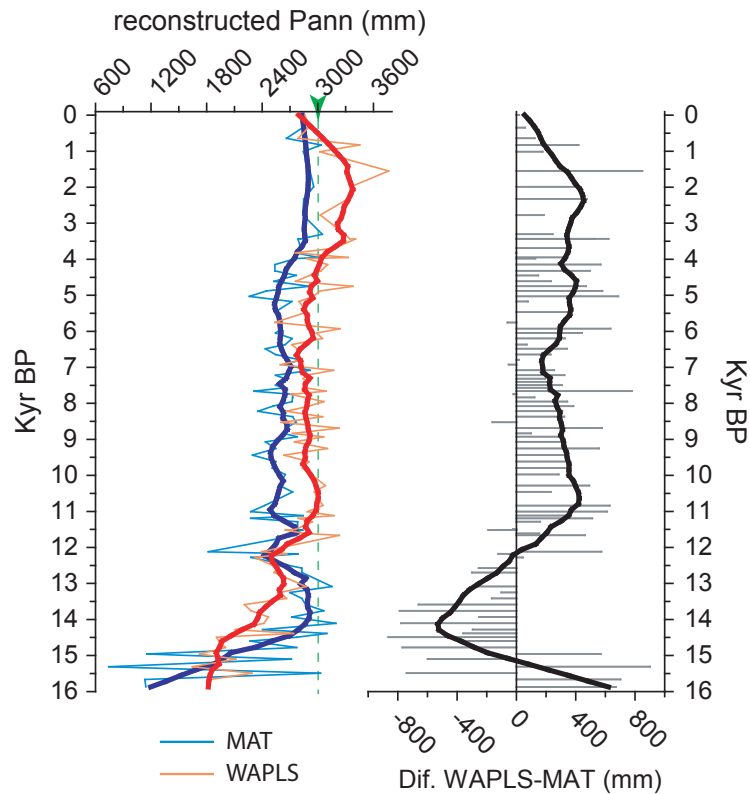
The most significant results from the transfer functions (Pann reconstructions) are described below, performed on each of the pollen record used, also indicating the main differences among the models.



Appendix figure 18. Boxplots of estimated precipitation (Pann) from the transfer function models (MAT and WAPLS) for each of the pollen records utilized in this thesis in order to perform quantitative paleoprecipitation reconstructions along a west-east transect at $\sim 53^{\circ}\text{S}$ (Figure 12). The box encloses the middle half of the data between the first and third quartiles. The central line denotes the value of the median. The vertical line extending from the top and bottom of the box indicates the range of typical data values. Outliers are displayed as “o”.

Tamar Lake (modern Pann 3000 mm/yr)

The reconstructed annual precipitation (Pann) from Tamar Lake are found to show highest Pann values in the studied transect, with values ranging between 744 to 3194 mm in the MAT reconstruction and between 1647 to 3764 mm in the WAPLS (Appendix table 3 & Appendix figure 18). As mentioned previously, the Pann reconstruction performed with the MAT algorithm shows relatively low values in comparison to the WAPLS (Appendix table 3 & Appendix figure 18), nevertheless the data dispersion (i.e. SD and CV, Appendix table 3) is similar in both models. The absolute differences between the reconstructions with the time indicate that observed divergences (MAT-WAPLS mean: +400 mm, Appendix figure 19) remain relatively constant along the record. Only two periods, at 12,000-15000 cal yr BP and during the last 1000 years, show differences between the reconstructions, where the MAT reconstruction exceeds the WAPLS reconstruction, and when the WAPLS decreases (Appendix figure 19).



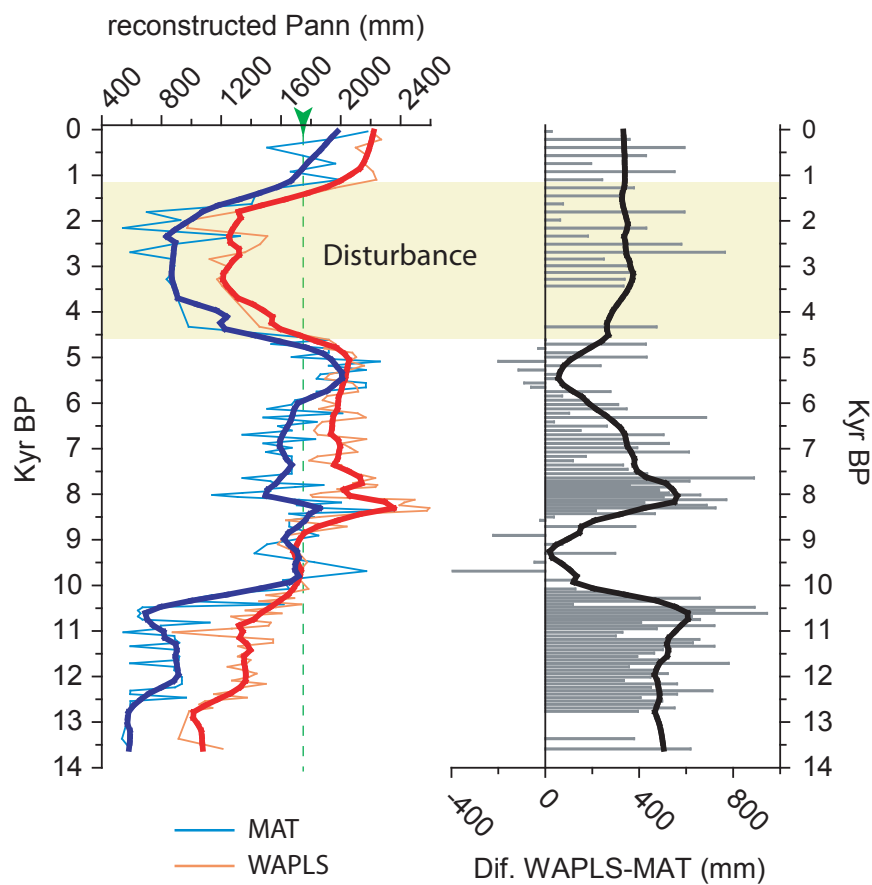
Appendix figure 19. (Left) Reconstructed annual precipitation (Pann) parameter from the pollen record of Tamar lake, utilizing the transfer functions WAPLS (red) and MAT (blue). The green arrow and dashed line indicate the modern Pann at the study site. (Right) Results from a simple subtraction operation (expressed in mm) performed among the transfer functions, in order to visualize more easily divergences between the curves. The solid-hard line on the graphs correspond to a Loess smoother, have been fitted to the raw data in order to highlight the major trends, utilizing a sampling span of 1.5 and rejecting the outliers.

The Pann reconstruction using the MAT model shows a fluctuating but sustained increase at the beginning the record (from 16,000 to 14,500 cal yr BP), leading the values from 1100 mm to 3000 mm (mean: 1870 mm) (Appendix figure 19). After this distinctive increase, the values remain high (mean: 2680 mm) and relatively stable, nevertheless during the late glacial (14,5000-12,300 cal yr BP) and the last 4000 cal yr BP a slight increase in the values (mean: 2870 and 2860 mm, respectively) is identified.

The WAPLS reconstruction also shows an important increase in the Pann values at the beginning of the record, specifically during the late glacial (16,000 to 11,500 cal yr BP) (Appendix figure 19). Nevertheless, and contrary to the unidirectional and monotonic increase described previously on the MAT reconstruction, this increase in the Pann occurs in a stepwise pattern that take place in two pulses between 14,500-13,400 cal yr BP (Pann from 1900 to 2600 mm) and 12,100-11,500 cal yr BP (Pann from 2600 to 2900 mm), and is interrupted by a plateau between 13,400-12,100 cal yr BP (Pann mean: 2580 mm). Later, and during most of the Holocene, the Pann values remain steady (mean: 2970 mm). Around 3500 cal yr BP is observable a slight increase (mean: 3320 mm) in the Pann values followed by a decrease during the last 600 years (mean: 2850 mm).

GCN (modern Pann 1730 mm/yr)

The Pann reconstructions performed on the GCN pollen record show a relatively wide dispersion of the data in both models (Appendix table 3 & Appendix figure 18), with values ranging between 536 to 2359 mm in the MAT reconstruction and between 874 to 2592 mm in the WAPLS. The differences between the models (MAT-WAPLS mean: +375 mm) are relative constant for the whole record, except between 10,400-8300 cal yr BP and 6000-4500 cal yr BP when both reconstructions reach similar values (Appendix figure 20). There is an abrupt decrease in the estimated Pann in both models around 4300-1800 cal yr BP. This feature is closely related with the disturbance event associated with the deposition of the tephra layer from Mount Burney that takes place during the pollen zone GCN3b.



Appendix figure 20. (Left) Reconstructed annual precipitation (Pann) parameter from the pollen record of GCN, utilizing the transfer functions WAPLS (red) and MAT (blue). The green arrow and dashed line indicate the modern Pann at the study site. (Right) Results from a simple subtraction operation (expressed in mm) performed among the transfer functions, in order to visualize more easily divergences between the curves. The solid-hard line on the graphs correspond to a Loess smoother, have been fitted to the raw data in order to highlight the major trends, utilizing a sampling span of 1.5 and rejecting the outliers.

The MAT reconstruction shows relatively low values (mean: 580 mm) at the bottom of the sequence (13,590 to 12,500 cal yr) follow by a slightly increase around 12,400 cal yr BP (mean: 840 mm) that occurs until ~10,400 cal yr BP when an abrupt increase in the Pann values is observed, which leads to the high values of the Holocene (mean: 1700 mm). During this period

the reconstructed values for the Pann are relatively constant (not considering the abrupt decrease associated with the disturbance event, previously mentioned), exhibiting only a slightly increase between 5700 to 5000 cal yr BP (mean: 2055 mm)(Appendix figure 20).

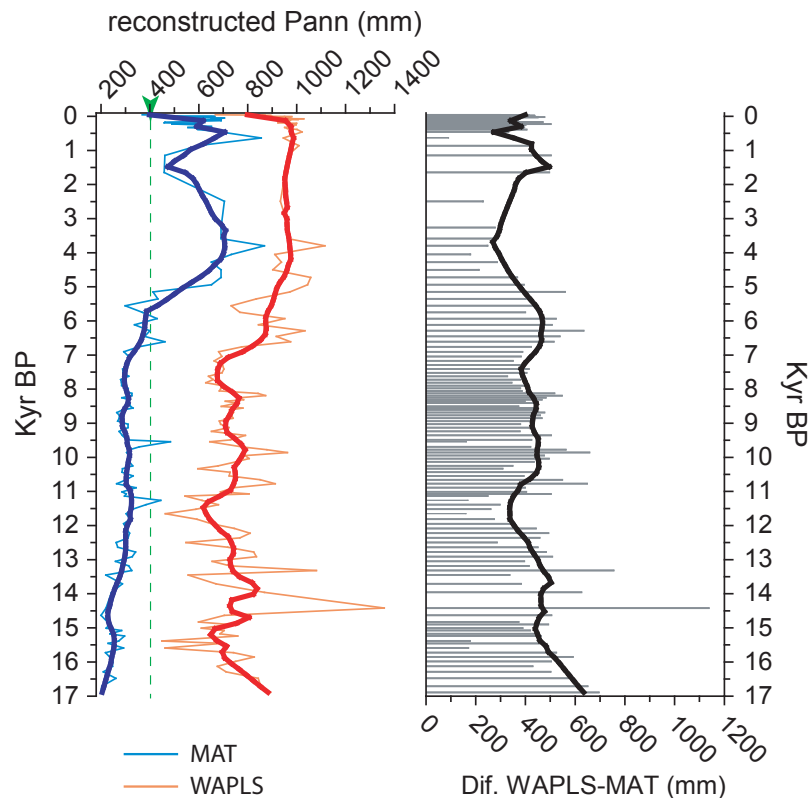
The Pann reconstruction performed by means the WAPLS model shows a stepwise increase in the values that lead to the rise in the Pann from low values present in the bottom (13,590 to 12,600 cal yr BP; mean: 1065 mm) to relative high values at the top of the record (<8500 cal yr BP; mean: 2050 mm). This pattern takes place by means of three particular rises (centered at 12,500, 10,500 and 8500 cal yr BP) that form distinctive plateaus in the Pann values at 12,400 to 10,600 cal yr BP (mean: 1340 mm), 10,400 to 8600 cal yr BP (mean: 1670 mm) and during the last < 8500 cal yr BP (mean: 2050 mm)(Appendix figure 20). During the Holocene, and more specifically during the last 8500 years, the Pann values keep relatively constant (mean: 2050 mm). Only at around at 8200 cal yr BP (mean: 2500 mm) is an increase observed, whereas between 4300-1800 cal yr BP an abrupt decrease is observed, related to the previously mentioned disturbance event (Appendix figure 20).

Rio Rubens (modern Pann 407 mm/yr)

The Pann reconstructions (MAT and WAPLS) performed in the pollen record from Rio Rubens exhibit, as in the rest of the sites, lower values in the MAT reconstruction in comparison with WAPLS (Appendix table 3 & Appendix figure 18). Nevertheless, and contrary to the trends observed in the rest of the sites, the differences between the used algorithms (MAT-WAPLS mean: +409 mm) remain relatively constant along the record (Appendix figure 21).

The MAT reconstruction shows low Pann values (mean: 300 mm) during most of the record, specifically between 16,300 to 5150 cal yr BP. Within this period, three different stages related with slight increases in the Pann levels are identified at 16,900 to 13,450 cal yr BP (mean: 240 mm), around 13,300 to 6900 cal yr BP (mean: 310) and between 6800 to 5150 cal yr BP (mean: 390 mm) (Appendix figure 21). Later, around 5000 cal yr BP, the Pann experience an abrupt increase reaching relative high values (mean: 600 mm) that continue until the present, a trend that is interrupted at around 1645 to 860 cal yr BP by a decrease (mean: 505 mm) in the reconstructed Pann.

The Pann reconstruction resulting from the WAPLS model shows low values during most of the first half of the record (16,900-6900 cal yr BP, mean: 730 mm), conditions that resemble with the MAT reconstruction previously described. Nevertheless the Pann reconstruction from WAPLS shows more variability and particularly a presence of periods below the mean (centered at ~15,500, ~11,600 and 7500 cal yr BP)(Appendix figure 21). An abrupt increase in the Pann takes place at around 6800 cal yr BP (mean: 915 mm), followed by a brief decrease at ~5500 cal yr BP (mean: 780 mm), and a later return to high values (mean: 945 mm) after 5100 cal yr BP (Appendix figure 21).



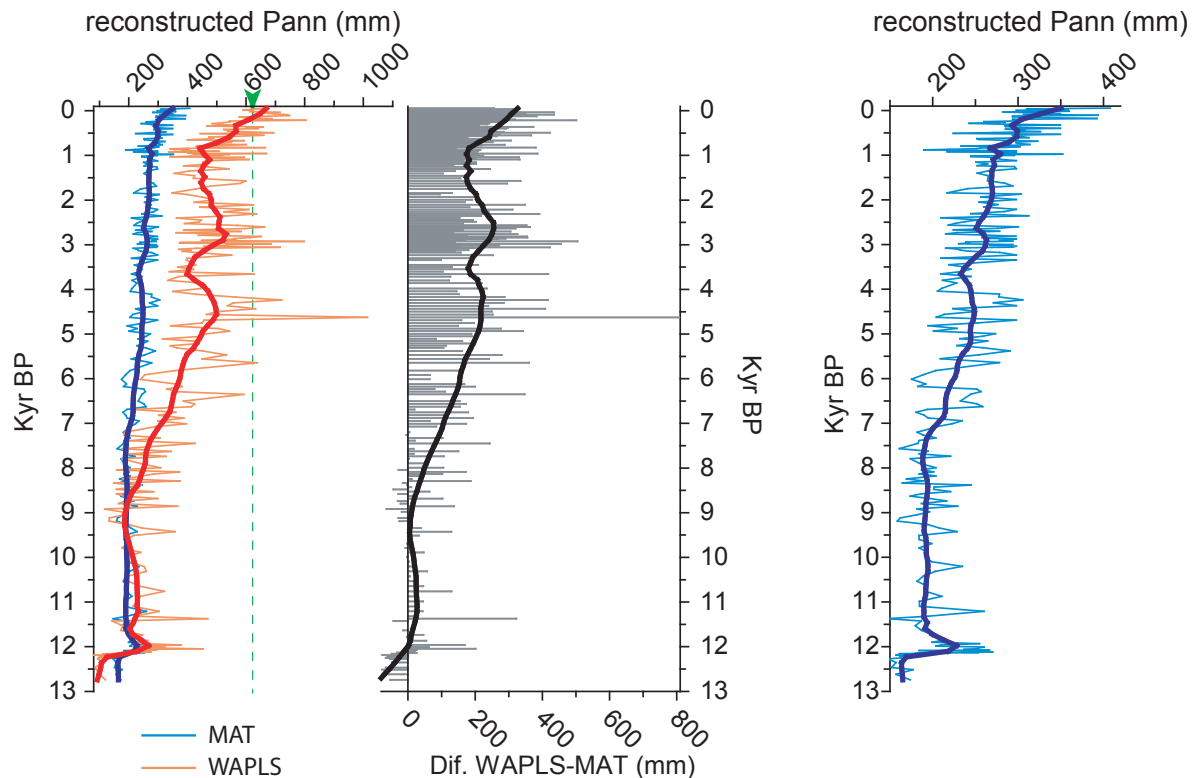
Appendix figure 21. (Left) Reconstructed annual precipitation (Pann) parameter from the pollen record of Rio Rubens, utilizing the transfer functions WAPLS (red) and MAT (blue). The green arrow and dashed line indicate the modern Pann at the study site. (Right) Results from a simple subtraction operation (expressed in mm) performed among the transfer functions, in order to visualize more easily divergences between the curves. The solid-hard line on the graphs correspond to a Loess smoother, have been fitted to the raw data in order to highlight the major trends, utilizing a sampling span of 1.5 and rejecting the outliers.

Lago Guanaco (modern Pann 635 mm/yr)

The Pann reconstructions derived from the pollen record of Lago Guanaco show apparently substantial differences among the models (Appendix figure 22). In particular, the MAT reconstruction exhibits values for the data range and dispersion more than three and two times (respectively) lower than the observed in the WAPLS model (Appendix table 3 & Appendix figure 18). Nevertheless, such differences are not constant along the record, being appreciable that previous to ~8800 cal yr BP the estimated Pann is relatively similar in both models ((Appendix figure 22). Since ~8800 cal yr BP the difference among the models (MAT-WAPLS mean: +150 mm) experiences a significant change as result of the major magnitude in the variation experienced in the WAPLS model than in the MAT.

As previously mentioned, one characteristic of the MAT reconstruction is the small internal variation of the data (i.e. range and dispersion) and hence magnitude of changes, in comparison with the trends observed in the WAPLS model (Appendix table 3 & Appendix figure 18). As consequence, when both models are plotted against each other it seems to be that MAT reconstruction does not contains important changes (Appendix figure 22). Nevertheless, if the model (MAT) is plotted by separate it is possible to recognize significant changes (Appendix figure 22, right). From this, it is possible to observe that the Pann reconstruction derived from the MAT model is characterized to

show very low (12,750 to 12,150 cal yr BP; mean: 168 mm) and low values (12,150 to 7200 cal yr BP; mean: 202 mm), during the first-half of the record. Later, since ~7200 cal yr BP, the Pann values experience a sustained increase and reaching relative steady values around 5500 cal yr BP (mean: 253 mm) that continue until ~850 cal yr BP. Within this period (~7200 to 850 cal yr BP), the occurrence of particular decreases in the reconstructed Pann at ~6000 and between 4000-3500 cal yr BP (Appendix figure 22) is identified. Finally, during the last 850 years a new sustained increase in the Pann takes place (mean: 300 mm), reaching maximum values at the present.



Appendix figure 22. (Left) Reconstructed annual precipitation (Pann) parameter from the pollen record of Lago Guanaco, utilizing the transfer functions WAPLS (red) and MAT (blue). The green arrow and dashed line indicate the modern Pann at the study site. (Middle) Results from a simple subtraction operation (expressed in mm) performed among the transfer functions, in order to visualize more easily divergences between the curves. The solid-hard line on the graphs correspond to a Loess smoother, have been fitted to the raw data in order to highlight the major trends, utilizing a sampling span of 1.5 and rejecting the outliers. Notice that reconstructed annual precipitation (Pann) utilizing the MAT transfer functions is plotted as single graph in the right of the figure.

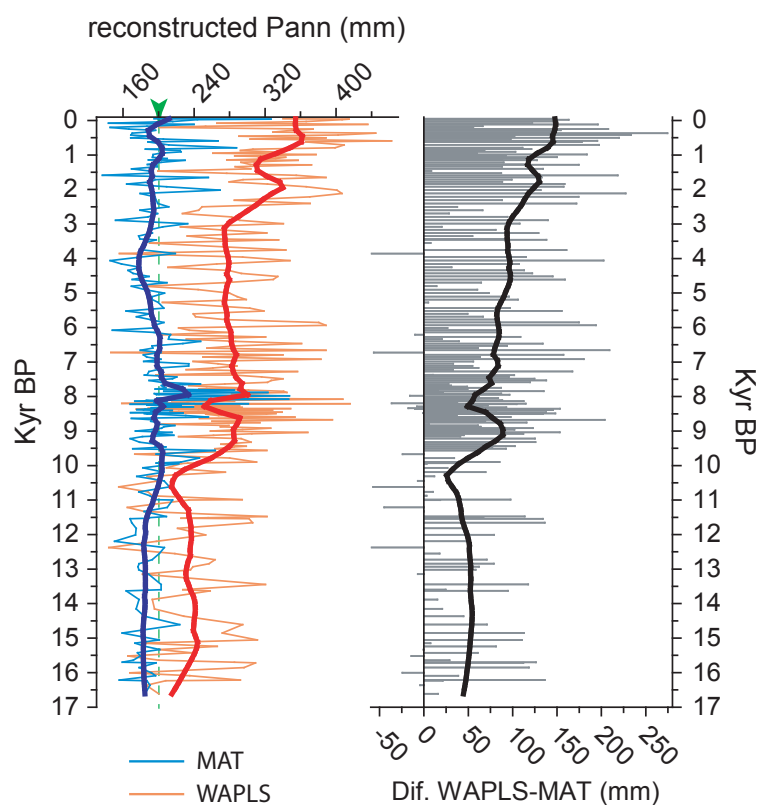
The WAPLS reconstruction shows similar trends to the MAT reconstruction, with very low (mean: 118 mm) and low Pann values (mean: 237 mm) in the bottom of the record (12,750-12,150 cal yr BP and 12,150-8900 cal yr BP, respectively), followed by a period of sustained increase between ~8900 to 4500 cal yr BP (Appendix figure 22). During this period, a decrease in the Pann is observable at ~6000 cal yr BP which resembles the MAT reconstruction. Also similar is the decrease observed between 4000-3500 cal yr BP, and the sustained increase in the Pann after ~850 cal yr BP (Appendix figure 22). Only a minor decrease around 2000-1200 cal yr BP in the Pann, not observable in the MAT reconstruction, seems to be a characteristic from the WAPLS reconstruction.

Potrok Aike (modern Pann 203 mm/yr)

The outcomes from the models (MAT and WAPLS) used to reconstruct the annual precipitation (Pann) in the Potrok Aike pollen record, are characterized to show substantial dissimilarities not only in the range and dispersion of data (Appendix table 3 & Appendix figure 18), but also in its trends along the time (Appendix figure 23). In particular, and as was previously mentioned, the MAT reconstruction is characterized to show low values and data dispersion (SD and CV) in comparison with the WAPLS (Appendix table 3 & Appendix figure 18). The differences among the models are not continuous along the record (MAT-WAPLS mean: +81 mm). Relatively stable values occur before to ~10,200 cal yr BP (MAT-WAPLS mean: +46 mm), whereas after ~10,200 cal yr BP the differences between the models exhibit an increase towards the present (MAT-WAPLS mean: +90 mm)(Appendix figure 23).

The MAT reconstruction shows relative low and variable values at the bottom of the record, particularly between 16,600 to 11,550 cal yr BP (mean: 182 mm), followed by an increase in the Pann between 11,500 to 6200 cal yr BP (mean: 207 mm)(Appendix figure 23). Within this period a conspicuous peak between 8200 to 7800 cal yr BP (mean: 232 mm) and a slightly decrease between 9450 to 8300 cal yr BP (197 mm) is identified. After 6200 cal yr BP, the Pann shows relatively stable values (mean: 195 mm), condition only disrupted by a gradual decrease between at 4900 to 3170 cal yr BP (mean: 181 mm; minimum at 4200 cal yr BP) and a small increase in the Pann values between 800-900 cal yr BP (mean: 214 mm)(Appendix figure 23). Finally during the last 500 years the reconstructed Pann show a decrease in its values (mean: 178 mm).

The WAPLS reconstruction shows three different stages of Pann (low-middle-high) along the record, which take place in stepwise increases at 10,200 and 2500 cal yr BP (Appendix figure 23). In specific, the first stage occurs in the bottom of the sequence (16,600 to 10,200 cal yr BP) and corresponds to the lower Pann reconstruction (mean: 233 mm). The next occurs between 10,100 to 2500 cal yr BP and is characterized by show intermediate Pann values (mean: 276 mm). Within this period an important decrease in the Pann (mean: 258 mm) between 8500 to 8100 cal yr BP is identified. Finally during the last 2400 years the Pann show maximum values (mean: 338 mm), trend that is interrupted by a small decrease between 1500 to 830 cal yr BP (mean: 305 mm) (Appendix figure 23).



Appendix figure 23. (Left) Reconstructed annual precipitation (Pann) parameter from the pollen record of Potrok Aike, utilizing the transfer functions WAPLS (red) and MAT (blue). The green arrow and dashed line indicate the modern Pann at the study site. (Right) Results from a simple subtraction operation (expressed in mm) performed among the transfer functions, in order to visualize more easily divergences between the curves. The solid-hard line on the graphs correspond to a Loess smoother, have been fitted to the raw data in order to highlight the major trends, utilizing a sampling span of 1.5 and rejecting the outliers.

8.3. Bibliography appendix A & B

Birks, H. J. B. (1998). "Numerical tools in palaeolimnology - Progress, potentialities, and problems." *Journal of Paleolimnology* 20(4): 307-332.

Clauset, A., M. E. J. Newman and C. Moore (2004). "Finding community structure in very large networks." *Physical Review E*: 1-6.

Fruchterman, T. M. J. and E. M. Reingold (1991). "Graph Drawing by Force-directed Placement." *Softw., Pract. Exper.* 21(11): 1129-1164.

Hijmans, R. J., S. E. Cameron, J. L. Parra, P. G. Jones and A. Jarvis (2005). "Very high resolution interpolated climate surfaces for global land areas." *International Journal of Climatology* 25(15): 1965-1978.

Juggins, S., Ed. (2003). *C2 User guide. Software for ecological and palaeoecological data analysis and visualisation.* University of Newcastle, Newcastle upon Tyne, UK. 69 pages.

Relethford, J. (1984). *Cluster analysis for researchers.* Belmont, CA, Lifetime Learning Publications.

Schäbitz, F., M. Wille, J.-P. Francois, T. Haberzettl, F. Quintana, C. Mayr, A. Lücke, C. Ohlendorf, V. Mancini, M. M. Paez, A. R. Prieto and B. Zolitschka (2013). "Reconstruction of palaeoprecipitation based on pollen transfer functions – the record of the last 16 ka from Laguna Potrok Aike, southern Patagonia." *Quaternary Science Reviews* 71: 175-190.

Erklärung

Ich versichere, dass ich die von mir vorgelegte Dissertation selbständig angefertigt, die benutzten Quellen und Hilfsmittel vollständig angegeben und die Stellen der Arbeit –einschließlich Tabellen, Karten und Abbildungen–, die anderen Werken im Wortlaut oder dem Sinn nach entnommen sind, in jedem Einzelfall als Entlehnung kenntlich gemacht habe; dass diese Dissertation noch keiner anderen Fakultät oder Universität zur Prüfung vorgelegen hat; dass sie –abgesehen von unten angegebenen Teilpublikationen– noch nicht veröffentlicht worden ist, sowie, dass ich eine solche Veröffentlichung vor Abschluss des Promotionsverfahrens nicht vornehmen werde.

Die Bestimmungen der Promotionsordnung sind mir bekannt. Die von mir vorgelegte Dissertation ist von Prof. Dr. Frank Schäbitz betreut worden.

Nachfolgend genannte Teilpublikationen liegen vor:

- Lamy, F., R. Kilian, H. A. Arz, J. P. Francois, J. Kaiser, M. Prange and T. Steinke (2010). "Holocene changes in the position and intensity of the southern westerly wind belt." *Nature Geoscience* 3: 695-699.

Jean P. Francois S.

Köln, den 05.05.2014

Lebenslauf

Name: Francois Sepúlveda
Vorname: Jean-Pierre
Anschrift: Vincenzstr 24, 51065 Köln
Geburtsdatum: 02. 07. 1976
Staatsangehörigkeit: Chilenisch

Ausbildung

Seit 2008

- Promotion Studenten im Seminar für Geographie und ihre Didaktik, Universität zu Köln.

2003-2007

- Master Studium (M.Sc.) Programa de Ecología y Biología Evolutiva (IEB). Universidad de Chile. Chile.
- Auslandsaufenthalt: Macro-Charcoal analyses course. Oregon University, USA.

1996-2001

- Diplom-Studium: Licenciatura en Biología, Pontificia Universidad Católica de Valparaíso, Chile.

Beruf

2006-2007

- Wissenschaftlicher Mitarbeiter im Laboratorio Botánica, Universidad Nacional Andrés Bello, Chile.

2003-2005

- Wissenschaftlicher Mitarbeiter. Centro de Estudios del Cuaternario (CEQUA), Universidad de Magallanes, Punta Arenas, Chile.

Teilnahme an Forschungsprojek

2005-2007

- Wissenschaftlicher Assistent. Proyecto FONDECYT # 1050139, Cazadores-Recolectores Esteparios en la diversidad ambiental del Norte de Aysén Continental durante el Holoceno Tardío (Valle del Río Cisnes, ~44°S).

2004-2007

- Wissenschaftlicher Assistent: Proyecto FONDECYT # 1040204, "Historia vegetacional y

climática postglacial de Patagonia Centro-Sur (45°-53°S)”

- Wissenschaftlicher Assistent: Proyecto FONDECYT # 1030766, “Variabilidad vegetacional y climática postglacial en los ecosistemas templados del sur de Chile”.

Stipendien zum Studium

2008-2012

- Stipendium zur Promotion. Deutscher Akademischer Austausch Dienst and Comisión Nacional de Ciencia y Tecnología (DAAD-CONICYT)

2006

- Stipendium zum “Master Studium”. Beca de estudios de Postgrado. Instituto de Ecología y Biodiversidad (IEB). Universidad de Chile. Chile

Awards

2007. Top student poster award, International Quaternary Association (INQUA) Congress.

Publikationen (ISI)

Schäbitz, F., M. Wille, J.-P. Francois, T. Haberzettl, F. Quintana, C. Mayr, A. Lücke, C. Ohlendorf, V. Mancini, M. M. Paez, A. R. Prieto and B. Zolitschka (2013). "Reconstruction of palaeoprecipitation based on pollen transfer functions – the record of the last 16 ka from Laguna Potrok Aike, southern Patagonia." *Quaternary Science Reviews* 71: 175-190.

de Porras, M. a. E., A. Maldonado, A. M. Abarzua, M. L. Cardenas, J. P. Francois, A. Martel-Cea, C. R. Stern, C. Mendez and O. Reyes "Postglacial vegetation, fire and climate dynamics at Central Chilean Patagonia (Lake Shaman, 44–∞S)." *Quaternary Science Reviews* 50 : 71-85.

Lamy, F., R. Kilian, H. A. Arz, J. P. Francois, J. Kaiser, M. Prange and T. Steinke (2010). "Holocene changes in the position and intensity of the southern westerly wind belt." *Nature Geoscience* 3: 695-699.

Moreno, P. I., J. P. Francois, C. M. Moy and R. Villa-Martínez (2010). "Covariability of the Southern Westerlies and atmospheric CO₂ during the Holocene." *Geology* 38(8): 727-730.

Moreno, P. I., J. P. Francois, R. P. Villa-Martinez and C. M. Moy (2009a). "Millennial-scale variability in Southern Hemisphere westerly wind activity over the last 5000 years in SW Patagonia." *Quaternary Science Reviews* 28(1-2): 25-38.

Moreno, P. I., M. R. Kaplan, J. P. Francois, R. Villa-Martinez, C. M. Moy, C. R. Stern and P. W. Kubik (2009b). "Renewed glacial activity during the Antarctic cold reversal and persistence of cold conditions until 11.5 ka in southwestern Patagonia." *Geology* 37(4): 375-378.

Moy, C. M., R. B. Dunbar, P. I. Moreno, J. P. Francois, R. Villa-Martinez, D. M. Mucciarone, T. P. Guilderson and R. D. Garreaud (2008). "Isotopic evidence for hydrologic change related to the westerlies in SW Patagonia, Chile, during the last millennium." *Quaternary Science Reviews* 27(13-14): 1335-1349.

Buchkapitel

Moy, C. M., P. I. Moreno, R. Dunbar, M. R. Kaplan, J. P. Francois, R. Villalba and T. Haberzettl (2009). *Climate Change in Southern South America During the Last Two Millennia Past Climate Variability in South America and Surrounding Regions*. F. Vimeux, F. Sylvestre and M. Khodri, Springer Netherlands. 14: 353-393.

Mendez, C., O. Reyes, A. Maldonado and J. P. Francois (2009). "Ser humano y medio ambiente durante la transición Pleistoceno-Holoceno en las cabeceras del río Cisnes (~44° S, Aisén Norte)." In: *Arqueología de Patagonia: una mirada desde el último confín*, editado por M. Salemme, F. Santiago, M. Álvarez, E. Piana, M. Vázquez y M. E. Mansur. Editorial Utopías, Ushuaia.

Francois, J. P. (2004). "Eslabones de una cadena rota: el caso del bosque relicto de Santa Inés." In: *Historia Natural del Parque Nacional Bosque Fray Jorge* (F.A. Squeo, J.R. Gutiérrez & I.R. Hernández, Eds.) Ediciones Universidad de La Serena, La Serena, Chile (2004) 11: 205-218.